REPORT NO. DOT-TSC-OST-77-23, III

REFERENCE USE ONLY

HYBRID VEHICLE TECHNOLOGY CONSTRAINTS AND APPLICATION ASSESSMENT STUDY

Volume III: Sections 5 through 9

D. E. Lapedes et al.

The Aerospace Corporation
Environment and Energy Conservation Division
El Segundo CA 90245

NOVEMBER 1977

FINAL REPORT

Prepared for
U.S. DEPARTMENT OF TRANSPORTATION
OFFICE OF THE SECRETARY
Office of the Assistant Secretary for Systems Development and Technology
Office of Systems Engineering
Washington DC 20590

Technical Report Documentation Page

Report No. DT-TSC-OST-77-23, III	2. Government Accession No.	3. Recipient's Catalog No.
Title and Subtitle YBRID VEHICLE TECHNOLOGY CONSTRAINTS ND APPLICATION ASSESSMENT STUDY olume III: Sections 5 - 9		5. Report Date November 1977
		6. Performing Organization Code
Author(s) D. E. Lapedes, M. G. Hinton, L. Forrest, J. Kohlenberger, T. Ryan, H. Sampson, W. Smalley, C. Speisman, H. White.		8. Performing Organization Report No. DOT-TSC-OST-77-23, III
Performing Organization Name and Address he Aerospace Corporation* nvironment and Energy Conservation Division l Segundo, CA 90245		10. Work Unit No. (TRAIS) OS714/R7508
		11. Contract or Grant No. F04701-76-C-0077
Sponsoring Agency Name and Address .S. Department of Transportation, Office of the ecretary, Office of the Asst. Sec. for Sys. Dev. & ec., Office of Systems Engineering ashington, DC 20590		13. Type of Report and Period Covered Final Report April 1975 - June 1976
		14. Sponsoring Agency Code

Supplementary Notes

*Jnder contract to: U.S. Department of Transportation, Transportation Systems Center, Kendall Square, Cambridge, MA 02142

Abstract

his four-volume report presents analyses and assessments of both heat engine/ ttery- and heat engine/flywheel-powered hybrid vehicles to determine if they ould contribute to near-term (1980-1990) reductions in transportation energy con- imption under several sets of operational conditions: urban driving, highway riving, and stop-start, low-speed delivery service conditions. In addition, the npact of such hybrid vehicle use on vehicle-related exhaust emissions is deter- ined, and the ability to accommodate a different energy resource base in the nger term is evaluated; i.e., by permitting a portion of the recharge energy r the on-board energy storage device (battery or flywheel) to be provided by wall- ug electric power from the utility industry instead of from the on-board heat ngine. Alternative paths for power transmission from the heat engine to the ehicle drive wheels are considered along with the potential of regenerative brak- g to reduce vehicle energy consumption.

his third of four volumes contains five sections. Sections 5 and 6 discuss the ehicle powertrain characteristics and the characteristics of the stationary enerating plants. Section 7 describes physical and performance characteristics nposed on the hybrid vehicle. Section 8 describes computer programs developed r the analysis and Section 9 discusses results of the powertrain component sizing nalysis.

Key Words Hybrid Automotive Vehicles, ransportation Energy Consumption, utomotive Vehicle Exhaust Emissions, atteries, Flywheels, Motors- enerators, Heat Engines, Transmis- ons, Regenerative Braking.	18. Distribution Statement DOCUMENT IS AVAILABLE TO THE U.S. PUBLIC THROUGH THE NATIONAL TECHNICAL INFORMATION SERVICE, SPRINGFIELD, VIRGINIA 22161

Security Classif. (of this report)	20. Security Classif. (of this page)	21. No. of Pages	22. Price
nclassified	Unclassified	190	

n DOT F 1700.7 (8-72) Reproduction of completed page authorized

PREFACE

This four-volume report presents the results of an analysis conducted by The Aerospace Corporation for the U.S. Department of Transportation, Transportation Systems Center, as part of the Automotive Energy Efficiency Project, sponsored by the Energy and Environment Division of the Office of the Secretary, U.S. Department of Transportation.

Appreciation is hereby extended to the Technical Monitor at the Transportation Systems Center, Mr. Joseph Abbas, whose guidance and suggestions were most helpful to the conduct of the study.

METRIC CONVERSION FACTORS

Approximate Conversions to Metric Measures

Symbol	When You Know	Multiply by	To Find	Symbol
		LENGTH		
in	inches	*2.5	centimeters	cm
ft	feet	30	centimeters	cm
yd	yards	0.9	meters	m
mi	miles	1.6	kilometers	km
		AREA		
in^2	square inches	6.5	square centimeters	cm^2
ft^2	square feet	0.09	square meters	m^2
yd^2	square yards	0.8	square meters	m^2
mi^2	square miles	2.6	square kilometers	km^2
	acres	0.4	hectares	ha
		MASS (weight)		
oz	ounces	28	grams	g
lb	pounds	0.45	kilograms	kg
	short tons (2000 lb)	0.9	tonnes	t
		VOLUME		
tsp	teaspoons	5	milliliters	ml
Tbsp	tablespoons	15	milliliters	ml
fl oz	fluid ounces	30	milliliters	ml
c	cups	0.24	liters	l
pt	pints	0.47	liters	l
qt	quarts	0.95	liters	l
gal	gallons	3.8	liters	l
ft^3	cubic feet	0.03	cubic meters	m^3
yd^3	cubic yards	0.76	cubic meters	m^3
		TEMPERATURE (exact)		
°F	Fahrenheit temperature	5/9 (after subtracting 32)	Celsius temperature	°C

*1 in = 2.54 (exactly). For other exact conversions and more detailed tables, see NBS Misc. Publ. 286, Units of Weights and Measures, Price $2.25, SD Catalog No. C13.10:286.

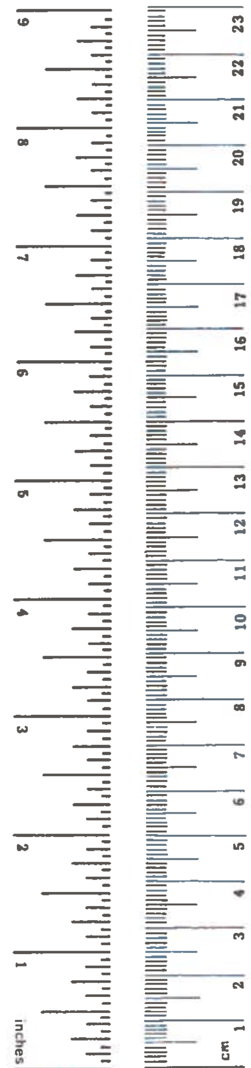

Approximate Conversions from Metric Measures

Symbol	When You Know	Multiply by	To Find	Symbol
		LENGTH		
mm	millimeters	0.04	inches	in
cm	centimeters	0.4	inches	in
m	meters	3.3	feet	ft
m	meters	1.1	yards	yd
km	kilometers	0.6	miles	mi
		AREA		
cm^2	square centimeters	0.16	square inches	in^2
m^2	square meters	1.2	square yards	yd^2
km^2	square kilometers	0.4	square miles	mi^2
ha	hectares (10,000 m^2)	2.5	acres	
		MASS (weight)		
g	grams	0.035	ounces	oz
kg	kilograms	2.2	pounds	lb
t	tonnes (1000 kg)	1.1	short tons	
		VOLUME		
ml	milliliters	0.03	fluid ounces	fl oz
l	liters	2.1	pints	pt
l	liters	1.06	quarts	qt
l	liters	0.26	gallons	gal
m^3	cubic meters	35	cubic feet	ft^3
m^3	cubic meters	1.3	cubic yards	yd^3
		TEMPERATURE (exact)		
°C	Celsius temperature	9/5 (then add 32)	Fahrenheit temperature	°F

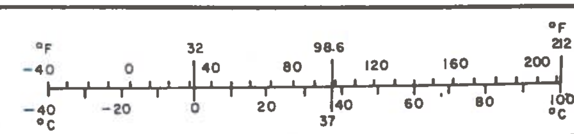

TABLE OF CONTENTS

TABLE OF CONTENTS (Continued)

LIST OF ILLUSTRATIONS

LIST OF ILLUSTRATIONS (Continued)

LIST OF ILLUSTRATIONS (Continued)

LIST OF ILLUSTRATIONS (Continued)

LIST OF ILLUSTRATIONS (Continued)

LIST OF TABLES

LIST OF TABLES (Continued)

LIST OF TABLES (Continued)

5. SELECTED CHARACTERISTICS FOR POWERTRAIN COMPONENTS

From the general characteristics presented in Section 4 for each of the powertrain components, specific characteristics were formulated for use in the powertrain simulation computer program. In addition to these specific characteristics, the rationale for the choice of characteristics and the limitations inherent in data validity are noted wherever possible.

5.1 HEAT ENGINE PERFORMANCE CHARACTERISTICS

The heat engine selected for use in this study is an internal combustion, spark ignition, reciprocating piston, gasoline-fueled powerplant. Considering the horsepower requirements for the size range of hybrid vehicles under investigation (commuter car, family car, and delivery van) a suitable engine for portraying performance characteristics is the General Motors 4-cylinder, 140-cubic inch displacement (CID) engine used in the 1975 model year Chevrolet Vega and Monza and Pontiac Astre automobiles. The engine is rated at 87 hp at 4400 rpm. It has a 2-barrel carburetor, a compression ratio of 8 to 1, a bore-stroke ratio of 3.5/3.625 inches, and an oxidizing catalytic converter with air injection in the exhaust system for control of hydrocarbons (HC) and carbon monoxide (CO). Exhaust gas recirculation (EGR) is used for control of oxides of nitrogen (NO_x).

Data for brake specific fuel consumption (BSFC) (pounds per horsepower-hour) and brake specific exhaust emissions (grams per horsepower-hour) of HC, CO, and NO_x are presented in Figures 5-1 through 5-4; the computer-generated curves were produced by the Department of Transportation (DOT) Transportation Systems Center. Not shown in these figures are the idle conditions, which are as follows:

Shaft speed	650 rpm
Fuel flow	2.2 lb/hr
Emissions	
HC	0.9 gm/hr
CO	0.4 gm/hr
NO_x	0.8 gm/hr

It should be noted that the data for specific exhaust emissions are for a warmed-up engine. Use of these data is considered to be somewhat at variance with procedures required by the Environmental Protection Agency (EPA) for vehicle emission tests that require a cold soak period prior to emission measurements. In particular, engine choking during cold start has a marked effect on exhaust emissions during the first 60 seconds of the test cycle. Hence, ultimately some correction may be necessary to the calculated values for hybrid vehicle emissions, although the incremental gram correction might be reasonably small. First, modern engines with shortened choke periods, fuel mixture preheating, and rapid heating of catalytic converters are less affected by cold-start phenomena. Secondly, engine choking required for conventional powertrains may be reduced or eliminated for hybrid powertrains, because (a) the engine is not required to supply rapid changes in high power levels for acceleration, (b) the vehicle can be operated as an all-electric system until the engine warms up, and (c) the engine starting and initial motoring might be provided by delivery of power from the energy storage system without the introduction of fuel-rich mixtures.

Operation of the engine was constrained to follow a curve of near-minimum BSFC. Thus, for each level of engine total horsepower* required during computer simulation of hybrid vehicle operation, the engine speed was uniquely determined. This relationship between power and speed is given in Table 5-1. Because other elements in the powertrain are affected by this constraint, it represents only a first approximation to an energy-optimized form of powertrain operation. For example, the accessory loads are a strong function of engine rpm, and speeds lower than those given in Table 5-1 could result in reduced overall fuel consumption, depending on the tradeoff between increased BSFC and decreased engine power required. Furthermore, the specific relationship shown in Table 5-1 was selected to allow the engine to operate at both low exhaust emissions and low fuel consumption. This means that a compromise must be used in each case; thus,

---

*Total horsepower includes the power for propulsion plus the power to run vehicle accessories and engine auxiliaries.

neither the lowest emissions nor the lowest fuel consumption available with the engine could actually be used. Hence, the BSFC was generally closer to a value of 0.6 than to the minimum value of 0.5. This effect implies that an engine designed or modified specifically for hybrid vehicle operation might be capable of performance superior to the stock engine used in this study. Possible changes in engine maintenance and durability would be major concerns of the designer in either case.

With regard to sizing of the heat engine, data presented in Section 4.1 for spark ignition engines were used in the analyses. Curves depicting specific weight (lb/hp) and specific volume (ft^3/hp) as a function of maximum engine horsepower are given in Figures 5-5 and 5-6. The maximum engine horsepower refers to the maximum shaft power plus power for engine auxiliaries, and it is this total power requirement (plus vehicle accessory power) that is determined in the sizing analysis.

5.2 PERFORMANCE CHARACTERISTICS FOR ELECTRIC MOTOR, GENERATOR, AND CONTROL SYSTEM

5.2.1 Electric Motor

The motor used to provide torque to the vehicle drive wheels is a dc, series-wound, brush-commutator system supplied with chopped dc power from the battery and with rectified ac power from the generator. Motor output power passes through a gear reduction system and a differential gear train before reaching the vehicle drive wheels. The power conversion efficiency for the reduction gears and the differential gears was fixed for each at 98 percent.

For vehicle operation over the Federal Emissions Test Driving Cycle, the series-wound motor is expected to provide power conversion efficiencies of about the same magnitude as compound or shunt-wound motors. Permanent magnet motors could provide approximately a 4 to 5 percent increase in efficiency, but, because they have been built only in small sizes to date and are expensive, no major effort was expended to uncover data characterizing their performance.

Characteristics for the dc series-wound motor are expressed by equations based on physical principles. Well-behaved scaling laws were relied on for establishing part-load characteristics. Effects produced by possible saturation of the magnetic field were not considered in this analysis. Motor loss coefficients are empirically derived from rated power and speed, and the associated per unit loss factors were obtained from Ref. 5-2. (These per unit loss factors could increase substantially for motors designed for minimum weight and volume.) Stray losses were neglected because they are generally of concern only for large motors rated in excess of 200 hp.

5.2.1.1 Performance Characteristics for the Motor

The basic relationships defining applied motor voltage and armature current as a function of motor output torque, speed, and loss coefficients are shown in the following equations.

The applied motor voltage is

$$V_{app} = V_{BL} + \left[1 + \frac{R_a}{K'\left(\frac{2\pi}{60}\right)N_m}\right]\left\{\frac{T_m N_m^2 + \left(\frac{5252}{746}\right)\left(K_{ML} N_m^4\right)}{\frac{0.737\,K'}{\left[\left(\frac{2\pi}{60}\right)K'\right]^2} - \frac{5252}{746}\left(K_{HL} + K_{EL} N_m\right)}\right\}^{1/2} \qquad (5\text{-}1)$$

The armature current is

$$I_a = \left[\frac{T_m + \left(\frac{5252}{746}\right)K_{ML} N_m^2}{0.737\,K' - \frac{5252}{746}\left(K_{HL} + K_{EL} N_m\right)\left(\frac{K'\,2\pi}{60}\right)^2}\right]^{1/2} \qquad (5\text{-}2)$$

where T_m is motor output torque in ft-lb and N_m is motor speed in rpm, and the other terms are defined in the succeeding discussion.

The motor efficiency is then given by

$$\eta_m = \frac{C\,T_m\,N_m}{V_{app}\,I_a} \qquad (5\text{-}3)$$

where C is a units conversion factor.

The motor losses expressed in Eqs. (5-1) and (5-2) are obtained by the following equations.

Armature resistance is

$$R_a = \frac{(pu)_{cpl} \; V_R}{I_R} \;, \qquad \text{ohms} \tag{5-4}$$

Mechanical loss coefficient is

$$K_{ML} = \frac{(pu)_{ml} \; I_R \; V_R}{N_R^3} \;, \qquad \frac{\text{watts}}{(\text{rpm})^3} \tag{5-5}$$

Core loss coefficients are*

$$K_{HL} = \frac{(pu)_{cl} \; I_R \; V_R}{2(V_R^2/N_R)} \;, \qquad \frac{\text{watts}}{(\text{volts}^2/\text{rpm})} \tag{5-6}$$

$$K_{EL} = \frac{(pu)_{cl} \; I_R \; V_R}{2 \; V_R^2} \;, \qquad \frac{\text{watts}}{(\text{volts})^2} \tag{5-7}$$

Brush contact loss is

$$V_{BL} = 2.0 \;, \qquad \text{volts} \tag{5-8}$$

The machine constant is given by

$$K' = \frac{V_R - V_{BL} - V_R \; (pu)_{cpl}}{\left(\frac{2\pi}{60}\right) I_R \; N_R} \tag{5-9}$$

*Per unit core losses are evenly split between hysteresis losses and eddy current losses.

In the preceding equations, N_R refers to the motor rated speed. For a given system voltage delivering a rated voltage V_R to the motor, the rated current I_R is determined by

$$I_R = \frac{746\ P_m^R}{V_R\left[1 - (pu)_{cpl} - (pu)_{ml} - (pu)_{cl}\right] - V_{BL}}, \qquad \text{amps} \qquad (5\text{-}10)$$

The motor rated power P_m^R, in horsepower, is established by the more severe of two conditions:

a. Power required at the vehicle peak design cruise speed

b. One third of the power required during vehicle peak design acceleration

The value of one third permits a brief overload of the motor by a factor of 3. This is considered to be a valid performance characteristic, and, with adequate cooling provisions, motor lifetime should not be strongly affected. Maximum motor current was set at 1600/3 amperes. Motor rated voltage was set initially at 36 volts and increased by 12-volt increments, if needed, to avoid exceeding maximum motor current.

An upper bound for the motor rated speed was set at 12,000 rpm, corresponding to vehicle peak design cruise speed. Should this not prove to be an achievable operating condition, a manual gear shift can be used in the drivetrain to reduce the motor speed.

Lastly, reasonable data for per-unit losses in a motor of 20 to 30 hp are given as follows:

Copper loss	$(pu)_{cpl} = 0.0585$
Mechanical loss	$(pu)_{ml} = 0.027$
Core loss	$(pu)_{cl} = 0.0255$

It should be noted that the per-unit losses of a motor of any given size may vary over a wide range, depending on speed, weight, and cost.

5.2.1.2 Sizing Data for the Motor

The induced electromotive force in a dc machine is proportional to the number of conductors, the total flux, and the rate at which the conductors cut the flux. Thus, one may write

$$V_{emf} \sim Z \Phi N \tag{5-11}$$

where V_{emf} is the induced voltage, Z is the total number of conductors, Φ is the flux, and N is the speed. The flux in the air gap between the rotor and stator is given by the product of the air gap flux density and the area of the air gap:

$$\Phi = B_g \pi DL \tag{5-12}$$

The power that is converted from electrical to mechanical form or vice versa is the product of the conductor current I_c and the induced electromotive force. Thus, it is seen that

$$P = V_{emf} \cdot I_c \tag{5-13}$$

Substitute the relations (5-11) and (5-12) into (5-13) and multiply and divide by the armature diameter:

$$P \sim B_g (D^2 L) N \frac{ZI_c}{\pi D} \tag{5-14}$$

The quantity $ZI_c/\pi D$ is the total ampere-conductors per unit of armature circumference and is denoted by σ. The armature heating and commutation are proportional to the total ampere-conductors per unit of armature circumference, i.e., the armature loading.

One figure of merit for a dc machine is the so-called output constant. The output constant is the ratio of the converted power to the product (D^2L) N. In explicit terms, the output constant becomes

$$\text{Output Constant} = \frac{P}{(D^2 L)\,N} = kB_g\,\sigma \tag{5-15}$$

The constant k has the value 0.11×10^{-8} when σ is in ampere-conductors per inch and B_g is in lines per square inch. P is in watts. D and L are in inches, and N is in revolutions per minute. Depending on the particular nature of the machine design, the armature loading is between 100 and several thousand ampere conductors per inch, while flux densities may vary from 20,000 to 60,000 lines per square inch. The corresponding range in the value of the machine constant is a function of the machine rating. Figure 5-7 illustrates the variation of the output constant for typical design practice.

The specific weight sizing curve shown in Figure 5-8 is calculated from the dc machine data of Figure 5-7. The following sample calculation illustrates the procedure. For a machine rating of 10 W/rpm, the corresponding value of the machine constant is 0.019 W/rpm-in^3. The D^2L value for the armature is calculated to be

$$D^2L = \frac{10 \text{ W/rpm}}{0.019 \text{ W/rpm-in}^3} = 526 \text{ in}^3 \tag{5-16}$$

For a rated speed that is assumed to be 4000 rpm, the power rating of the machine is

$$\text{Power} = \frac{(10 \text{ W/rpm})\ (4000 \text{ rpm})}{746 \text{ W/hp}} = 53.6 \text{ hp} \tag{5-17}$$

The estimate of the machine weight is made by multiplying the D^2L value by the factor 0.705 pound of total machine weight per cubic inch of D^2L. The numerical value 0.705 lb/in.^{3} is representative of a dc machine design that has been optimized for weight. The optimized weight design depends on the rated speed, the rated power, and the thermal design. The specific power is the ratio of the machine weight to the rated power:

$$\text{Specific Power} = \frac{(526 \text{ in}^3)\ (0.705 \text{ lb/in}^3)}{53.6 \text{ hp}} = 6.9 \text{ lb/hp} \tag{5-18}$$

For comparative purposes, manufacturer's data on dc motors are also presented in Figure 5-8. These data represent a variety of thermal designs and a range of rated speeds. Consequently, the variation among the data and the diversity between the data and the sizing curve reflect these two differences. It should be noted in passing that the data from Refs. 5-4 through 5-6, and 5-19 represent motors currently in use in electric or hybrid vehicles.

The specific volume sizing curve displayed in Figure 5-9 is calculated from the dc machine data of Figure 5-7. The D^2L product represents 21 percent of the total machine volume for a design optimized at 4000 rpm. Under these circumstances, the specific volume corresponding to the value of 10 W/rpm is determined to be

$$\text{Specific Volume} = \frac{\left(\dfrac{10\ \text{W/rpm}}{0.019\ \text{W/rpm-in}^3}\right)\left(\dfrac{21\%}{100\%}\right)^{-1}}{(1728\ \text{in}^3/\text{ft}^3)\ (53.6\ \text{hp})} = 0.027\ \text{ft}^3/\text{hp} \qquad (5\text{-}19)$$

Again, for comparative purposes, standard manufacturer's data are displayed in Figure 5-9.

5.2.2 Electric Generator

5.2.2.1 Performance Characteristics for the Generator

An electric generator is used to provide input power to the vehicle drive motor and to provide recharge power for the battery system. The type of generator selected for this use is a salient pole, permanent magnet, 3-phase synchronous machine. It has a design operating speed of 12,000 rpm and is mechanically connected to the heat engine by a set of gears.

With an engine operation philosophy that relies on a variable, but limited, range for power output and speed output (Section 2.3), a direct mechanical link with the generator would result in the same type of operation for this electrical element in the powertrain. Hence, although the generator could be modeled in a manner similar to that for the drive motor, it is not subjected to wide-ranging rapid power and speed changes, and a constant efficiency was chosen to characterize the transfer of mechanical to electrical energy. The value selected for efficiency was 80 percent for generator part-load simulation in analyses establishing energy consumption and exhaust emissions. For component sizing purposes (i.e., for sizing the heat engine), a value of 92.6 percent was used, corresponding to generator output at vehicle peak design cruise speed. These values are considered consonant with current hardware characteristics.

5.2.2.2 Sizing Data for the Generator

The data on the weight sizing curves for the dc and ac generators were obtained from earlier works (Refs. 5-15 through 5-18, and 5-21). This data is displayed in Figure 5-10. The 12,000 rpm curve is used for the weight sizing of the generator in the current hybrid vehicle study. The density of rotating electrical machinery varies between 200 and 300 lb/ft^3. The volume sizing curve of Figure 5-11 was obtained by dividing the weight sizing curve for both the 6000 rpm and 12,000 rpm ac generator by an assumed density of 250 lb/ft^3.

5.2.3 Electric Power Control System

5.2.3.1 Performance Characteristics for the Power Control System

For purposes of this study, both electric power conditioning and control are referred to as the control system. No detailed modeling of system characteristics was attempted. Instead, a fixed value for power transfer efficiency of 95 percent was used. This value of efficiency was then applied to power flow between (a) the generator and the motor, (b) the generator and the battery, and (c) the battery and the motor.

5.2.3.2 Sizing Data for the Power Control System

It is the function of the motor controller to supply the applied armature voltage to provide current required by the torque demand on the motor. The three general types of motor control are as follows:

a. Variable resistance in the armature circuit
b. Step voltage change with and without field control
c. Thyristor modulation of the armature voltage

For electric-type vehicles, efficient energy utilization is critical. The variable resistance in the armature circuit is an inefficient means for controlling the motor. Consequently, it is not considered in this study.

Motor control can also be accomplished by a switching network. The switching network combines the individual battery cells into groups of series and parallel combinations in order to match the applied armature voltage to the motor back electromotive force (emf). The disadvantage of this scheme for series motors is that many levels are required in the switching voltages in order to provide smooth acceleration of the vehicle.

Control techniques based on the thyristor concept are finding increasing application in the field of motor control. The two main solid-state elements that are used in electronic motor controllers are the power transistor and the silicon-controlled rectifier (SCR). At the present time the power controlling capabilities of the SCR are higher than those of the power transistor. Although the basic principles of modulating a voltage source with a thyristor are well known, no uniform designs have emerged. There is a definite dependence of the weight and volume of a thyristor control element with the voltage of the system. At the present time, most of the solid-state motor controllers have been designed for fixed-base operation and are not optimized for weight and volume as the data of Figures 5-12 and 5-13 show. The weight sizing curve in Figure 5-12 was obtained from an earlier study on electric vehicles (Ref. 5-14). The volume sizing curve in Figure 5-13 was calculated on the basis of an assumed packaging density of 40 lb/ft^3 for the electronic controller.

5.3 BATTERY CHARACTERISTICS

A set of battery characteristics for state-of-the-art technology was derived from data acquired during the battery technology review (Section 4.3). The batteries portrayed herein are the lead-acid and nickel-zinc systems. Other battery systems are either too costly or are not sufficiently well characterized to be used in a computerized model at the present time. As noted in Section 4.3, the lead-acid battery is not satisfactory for application to hybrid vehicles. It was included in the overall analysis merely for purposes of comparison.

Figure 5-14 shows current-voltage (I-V) curves for a typical lead-acid battery. The voltage values represent single-cell voltages and the current I is normalized by dividing by the rated battery capacity C in ampere-hours. Figure 5-15 is a similar set of curves for a typical nickel-zinc battery.

Additional data needed to complete the battery model are presented in Table 5-2. These data define the limits of battery operation and consist of IBMAX/C (normalized maximum available battery charge and discharge current), VMA (maximum allowable cell voltage) and VMC (minimum allowable cell voltage). Values for VMA and VMC are based on suggestions of the respective battery manufacturers (Refs. 5-23 and 24) and are set at a level to minimize the chance of cell damage resulting from either overcharge or overdischarge. For hybrid vehicle applications, control of minimum and maximum battery voltages is important because most of the charging and discharging is done at high rates.

The efficiency of energy conversion was set at the same fixed value for both types of batteries. When recharging was accomplished by the on-board heat engine, the battery charge-discharge watt-hour efficiency was taken to be 70 percent; when this recharging was performed at a stationary power source, the efficiency was assumed to be 80 percent. It is recognized that the efficiency is markedly dependent on such factors as charging current, discharge current, current waveform, and battery state-of-charge. The scope of this study did not warrant additional sophistication in analytical treatment of this subject, and the selected values are considered to be reasonable reflections of what could be achieved with actual hardware.

5.4 FLYWHEEL CHARACTERISTICS

Characteristics of two types of flywheels for hybrid vehicles were examined by contractors in studies funded by EPA: a conventional steel disc flywheel as developed by Lockheed Missiles and Space Co. (LMSC) and a higher energy "superflywheel" as designed by Johns Hopkins University (JHU). These are presented in Table 5-3. Based on information contained in these two studies (Refs. 5-25 and 5-26), a steel, disc-shaped flywheel system was selected as the primary system for use in this study. Although the information shown in Table 5-3 indicates a superior specific energy for the reinforced plastic composite flywheel system, the test data were not considered sufficiently conclusive to verify the figures shown. Much of the difference in specific energy is attributable to the use of a safety containment guard ring in the steel flywheel system and the elimination of this ring for the reinforced plastic composite system. The effect of this difference is two-fold: (a) The containment guard ring weight is removed from the calculation for energy density; and (b) within the confines of the automobile chassis, a larger flywheel radius can be used when the guard ring is removed. In addition, the JHU system is mounted in the car with a vertical wheel axis, whereas the LMSC system is mounted with a horizontal wheel axis which results in a smaller wheel radius in order to have effective road clearance. The LMSC choice of mounting appeared to be dictated by design simplicity and cost in electing to use a wheel axis concentric with (rather than perpendicular to) the heat engine power output shaft.

If JHU had used the same design philosophy as LMSC (including the need for a guard ring), then, for equivalent energy storage, the reinforced plastic composite wheel would have had to turn at almost 80,000 rpm. This would pose obvious problems in bearing design. However, as a projection to future potential, the JHU type of design was included in the energy consumption analysis for a 4000-lb car.

The transfer of power from the heat engine to the flywheel and from the flywheel to the vehicle drive wheels must be accomplished through the continuously variable transmissions whose power losses are defined by the efficiencies for each unit at a given operating condition. In addition, the flywheel system itself is subject to parasitic losses whether or not power is being transferred into or out of the system. These losses are accounted for by modifications to the flywheel stored energy and not by affecting the power flow into and out of the flywheel.

Flywheel horsepower losses as a function of flywheel speed are given by the following equation:

$$HPL = \left[2.65 \times 10^{-13} (FWN)^{2.8} \left(\frac{FWR}{0.544}\right)^{4.6} \left(\frac{P}{5}\right)^{0.8}\right]$$
$$+ \left[2.5 \times 10^{-10} (FWN)^{1.9} \left(\frac{FWR}{0.544}\right)^{3}\right]$$
$$+ \left[3.4 \times 10^{-4} (FWN)^{0.72} \left(\frac{FWR}{0.544}\right)^{2}\right] + \left[0.331 \left(\frac{FWR}{0.544}\right)^{2} \left(\frac{5}{P}\right)\right] \quad (5\text{-}20)$$

where

HPL = flywheel subsystem power loss, hp
FWN = flywheel rotor speed, rpm
FWR = flywheel rotor radius, ft
P = ambient pressure of air within flywheel housing, mmHg

The horsepower losses include windage losses (first term), bearing losses (second term), seal losses (third term), and vacuum pump power required (fourth term). These data are considered applicable to all sizes of flywheel systems in this study but are based on the losses utilized in the flywheel feasibility study conducted by LMSC (Ref. 5-27) for a 13.06-inch-diameter, disc flywheel weighing 86 pounds and operating in a pressure environment of 5 mmHg. Scaling for windage losses was based primarily on the relationships evolved by JHU (Ref. 5-26).

At any given time, the effective flywheel efficiency can be expressed as

$$\eta_{FW} = \frac{\text{power out}}{\text{power in}} = \frac{\text{power in - HPL}}{\text{power in}} \quad (5\text{-}21)$$

Hence, at low power levels, the effective efficiency is low, and the system would be penalized most severely for operation on a vehicle driving cycle that involved considerable loiter time (i.e., energy is being extracted whether the flywheel is used or not). This is a deficiency not shared by the battery system. Because the energy storage capability of the flywheel is quite small, the loss of energy during overnight rundown was not considered in the analysis, and no energy was expended in bringing the rotor up to design speed. But as flywheel designs advance to greater energy storage capability, the parasitic losses will have to be minimized to avoid a source of undesirable energy consumption.

The basic philosophy established for flywheel operation is that it be permitted to rotate at the maximum possible speed, governed first by rotor material strength considerations and secondarily by estimated maximum speed capability for support bearings. For a given rotor radius, the maximum rotor speed can be expressed by the equation:

$$N_{dm} = \frac{60}{\pi \cdot r} \sqrt{K_1 \cdot g \cdot \left(\frac{\sigma_w}{\rho}\right)} \tag{5-22}$$

and

$$E_d = \frac{3.766 \times 10^{-4} \cdot \pi^3 \cdot N_d^2 \cdot \rho \cdot r^5 \cdot \left(\frac{h}{r}\right)}{3600g} \tag{5-23}$$

$$E_{dm} = 3.766 \times 10^{-4} \cdot \pi \cdot K_1 \cdot \rho \cdot \left(\frac{\sigma_w}{\rho}\right) \cdot r^3 \cdot \left(\frac{h}{r}\right) \tag{5-24}$$

where

N_d = design speed of rotor, rpm
N_{dm} = maximum design speed of rotor, rpm
E_d = design energy stored in rotor, W-hr
E_{dm} = maximum design energy stored in rotor, W-hr
r = rotor radius, ft
h = thickness of rotor, ft
σ_w = allowable working stress of rotor material, lb/ft^2
ρ = density of rotor material, lb/ft^3
K_1 = rotor inertial shape factor
g = gravitational constant = 32.174 ft/sec^2

Based on the data presented in Ref. 5-25 through 5-28, the following physical characteristics for the rotor were selected:

$$h = 0.425\ r$$
$$K_1 = 0.61 \text{ for a disc-shaped rotor}$$

for maraging steel:

$$\sigma_w = 1.225 \times 10^7\ \text{lb/ft}^2$$
$$\rho = 489.0\ \text{lb/ft}^3$$

and for Kevlar:

$$\sigma_w = 2.085 \times 10^7\ \text{lb/ft}^2$$
$$\rho = 84.6\ \text{lb/ft}^3$$

Scaling of weight in pounds and volume in cubic feet for each component in the flywheel subsystem was based on data given in Refs. 5-25 through 5-28 and was calculated from the following equations for the case of rotor speed governed only by material strength considerations:

$$W_R = \frac{E_{dm}/3.766 \times 10^{-4}}{K_1 \cdot \left(\frac{\sigma_w}{\rho}\right)} \tag{5-25}$$

$$V_R = \pi \cdot r^3 \cdot \left(\frac{h}{r}\right) \tag{5-26}$$

The results were as follows:

Steel Rotor*	Kevlar Rotor*
$W_H = 229.6\ V_R$	$W_H = 229.6\ V_R$
$W_B = 0.012\ W_R$	$W_B = 0.0672\ W_R$
$W_S = 0.0028\ W_R$	$W_S = 0.016\ W_R$
$W_P = 0.0058\ W_R$	$W_P = 0.034\ W_R$

*It was assumed that the housing was made of steel for both steel and Kevlar rotors. It was also assumed that the Kevlar rotor did not require a containment ring.

Steel Rotor	Kevlar Rotor
$W_{CR} = 0.067\ E_d$	$W_{CR} = 0$
$W_M = 0.006\ E_d$	$W_M = 0.006\ E_d$

and

$$W_{FWSS} = W_R + W_H + W_B + W_S + W_P + W_{CR} + W_M \tag{5-27}$$

$$V_{FWSS} = V_R \left(\frac{W_{FWSS}}{W_R}\right)^{0.61} \tag{5-28}$$

where

W_R = rotor weight, lb
W_H = housing weight, lb
W_B = bearing weight, lb
W_S = seal weight, lb
W_P = vacuum pump weight, lb
W_{CR} = containment ring weight, lb
W_M = miscellaneous subsystems weight, lb
W_{FWSS} = flywheel subsystem weight, lb
V_R = rotor volume, ft^3
V_{FWSS} = flywheel subsystem volume, ft^3

Table 5-4 provides a summary of the flywheel subsystem characteristics for each type of vehicle analyzed in this study. These calculations were performed for flywheel rotor speeds limited only by strength considerations. Under these conditions and with the scaling equations that were selected, the specific energy (watt-hours per pound) and energy density (watt-hours per cubic foot) are invariant for a given type of rotor material. Hence, the size of rotor doesn't improve its ability to store energy more efficiently within a given space or weight restriction. Of course, size does have a marked effect on energy stored. The JHU type of installation offers almost three times the energy storage capacity as the LMSC engine shaft in-line design. (Whether the JHU approach is practical from an overall cost and installation viewpoint is not known at this time.)

The use of a composite-reinforced plastic rotor, when compared to a steel rotor, resulted in an increase in flywheel system specific energy by a factor greater than 4. About half of the increase is attributable to the elimination of the containment ring, and the other half of the increase is attributable to the improved material strength properties. It can also be seen that while the basic flywheel unit (rotor only) has a high specific energy, inclusion of subsystem weights reduces this factor to values about equal to those attributed to lead-acid batteries.

An additional factor of great import is the parasitic loss HPL shown for each flywheel. The larger composite wheels show marked increases in this loss as is most evident when expressed as a ratio with the wheel design energy. (However, in the ratio form, the parasitic percent loss is less for the larger rotors for each material.) Better than 90 percent of the parasitic loss is attributable to windage loss. The windage loss is based on the flywheel housing atmospheric pressure level of 5 mmHg, which LMSC selected for the lower speed, smaller size, steel rotors. Reducing this loss for the larger composite wheels to the comparable percent values for steel would entail decreasing the pressure to less than 1 mmHg.

The inverse relationship of pump power and flywheel housing pressure in Eq. (5-20) assumes that sealing of the flywheel shaft is not improved over that for steel rotors. Hence, as pressure decreases, the windage loss decreases, but the pump power increases and can rapidly become the dominant loss (offsetting the advantage of the high-speed plastic rotor). One computer run was made at very low pressure (Table 5-4) but with no increase in pump power over that required to hold 5 mmHg to observe the effect on vehicle performance. The use of Eq. (5-20) over a wide range of pressure definitely needs verification if the performance of plastic and steel rotors are to be accurately compared.

5.5 CONTINUOUSLY VARIABLE TRANSMISSION CHARACTERISTICS

Data were received from the Orshansky Transmission Corp. (Refs. 5-29 and 5-30) on the operating characteristics of the dual-range hydromechanical transmission being developed under a contract from the Advanced Automotive Power Systems Division (AAPSD) of the Energy Research and Development Administration (ERDA).

The power-carrying components of this transmission are shown in Figure 5-16. The configuration is characterized by a variable-ratio simple planetary to provide the front power flow split, a pair of transfer gears to provide the rear power flow split in high range, and a counter shaft by which the low-range speed reduction is obtained and on which a hydraulic unit is mounted to provide the rear power split in low range. The input shaft is directly coupled to the planet carrier, and the input power is split between the ring gear 1 and the sum gear 3.

In the low range (Figure 5-17), most of the input power passes through the sun gear, the counter shaft, and out to the drive shaft via the engaged low clutch. The power passing to the ring is transmitted from hydraulic unit B to hydraulic unit A, acting as pump and motor, respectively. Both hydraulic units are of variable displacement, and the control system maintains one unit at the maximum displacement while adjusting the displacement of the other unit. The ratio of the displacements determines the reactive torque provided by ring 1 and also determines the overall transmission ratio.

With the transmission in low range, as the sun and output increase in speed, the ring decreases in speed until an overall transmission speed ratio is reached, when the speed of the ring equals the speed of the output shaft. For the gear ratios chosen, the synchronism of plates in the high-range clutch occurs when the transmission output speed equals 0.55 times the input speed. The high-range clutch is engaged (Figure 5-18) and, when fully pressurized, causes the low-range clutch to be released. Most of the input power now flows mechanically through the ring and directly out to the drive shaft. The remaining input power is split off at the planet and flows through the reaction sun to hydraulic unit A, hydraulic unit B, and through transfer gears to the output.

The operating characteristics of the transmission are presented in Table 5-5, in a form suitable for use in the computer simulation. Here, the TR ratio of shaft output torque TO to shaft input torque TI is given as a function of the speed ratio NO/NI = NR (rpm out/rpm in), for three different input speeds NI. The efficiency is determined by computing the product of NR and TR.

For the transmission located between the flywheel and the vehicle drive wheels, the output speed is determined by vehicle speed, and the input speed is determined by flywheel speed (accounting for gear ratios of interposed gear system G). With the output torque specified by torque required at the drive wheels (again accounting for interposed gear ratios G), the input torque and, hence, torque required out of the flywheel are then calculated from the quotient of TO divided by TR.

A similar procedure is followed for the transmission located between the heat engine and the flywheel, but, in addition, a double iterative loop is required to arrive at the transmission operating point. Referring to Figure 5-19, the iterative procedure can be seen diagramatically. Horsepower out of the transmission HPT2-0 is set at a baseline value and will change in response to certain vehicle speeds as described in Section 2.3. In any event, it is a known quantity as is the flywheel speed NFW. The first step in the iteration is to guess at a reasonable value for transmission efficiency ETAT 2. This then gives a value for horsepower put out by the heat engine for propulsion purposes only (HPE). As noted in Section 5.1, the engine speed NE is a function of the total engine power output BHP, including accessory/auxiliary power HPAC, which in turn is a function of NE (Section 5.6). Hence, in the next step, a subloop is required to close on a solution for HPAC, BHP, and NE, with HPE held fixed. With NE determined and combined with NFW, the transmission speed ratio NR is established and, in turn, the torque ratio TR. A new transmission efficiency is calculated, and the procedure is repeated until a final solution is reached.

Transmission weight and volume are determined by the factors 2.2 lb/hp and 0.02 ft^3/hp, respectively. These factors were derived from data in Refs. 5-25 through 5-27, 5-29, and 5-32 and are based on transmission power output.

5.6 VEHICLE ACCESSORY AND ENGINE AUXILIARY POWER REQUIREMENTS

Vehicle accessory power requirements covering air conditioning and power steering have been reviewed and characterized, along with engine auxiliary power requirements for water pump, fan, and alternator/generator, in Figures 5-20 through 5-26 as a function of engine speed. These are based on the data of Refs. 5-27 and 5-31 through 5-35, which give the power required as a function of engine speed (rpm). The operation of these units is in accordance with the needs of conventional automobiles. It has been assumed, for purposes of the present study, that such design and operation is consistent with the needs of hybrid vehicles. However, because of the unique means of engine operation in hybrid vehicles, revised designs and operating schemes might eventually evolve. For the present analysis, a gear ratio of 0.7 was selected to connect the engine to the accessory and auxiliary system in order to reduce the system speed and power required. Hence, the power required was determined by entering the independent axis labeled "engine speed" with 0.7 times engine speed rather than with engine speed.

The air conditioning power requirements, shown in Figure 5-20, are based on data from Refs. 5-31 through 5-35. The upper limit is based on air conditioning for a 100°F ambient day (Ref. 5-34), while the lower limit is indicative of the lower individual values measured on a test fleet of six 1973 model year full-size automobiles (Ref. 5-33). The values selected are those that were provided to LMSC by EPA for use in the flywheel feasibility study (Ref. 5-27).

The selected power steering load shown in Figure 5-21 is based essentially on pumping losses during normal driving (Refs. 5-31 and 5-33 through 5-35). The higher loads occur only at low engine and vehicle speeds during a parking maneuver. The value selected is based on the average measured on the test vehicles reported in Ref. 5-33.

The water pump loads reported in Refs. 5-31 and 5-33 through 5-35 are in generally good agreement, as indicated in Figure 5-22. The selected level is based on the average of values reported in Refs. 5-31 and 5-35.

The loads imposed by the radiator cooling fan are shown in Figure 5-23, as reported in Refs. 5-27, 5-31, and 5-33 through 5-35 with the selected value based on Refs. 5-27 and 5-33.

The alternator-generator loads shown in Figure 5-24 vary with the rated capacity of the alternator (Refs. 5-31 and 5-33 through 5-35). The selected value is based on the average value reported in Ref. 5-33 for six full-size cars equipped with a 30-amp alternator.

The total accessory power requirements are summarized in Figures 5-25 and 5-26, together with the range of values given in Refs. 5-31 through 5-35. Figure 5-25 shows the total load without air conditioning; Figure 5-26 includes the air conditioning load.

5.7 GEAR SYSTEM CHARACTERISTICS

Both the hybrid heat engine-battery and heat engine/flywheel powertrain require the use of gears (in addition to transmissions) to match input and output speeds of coupled rotating elements in the powertrain. Although the various gear sets have a wide range in gear ratio, it was assumed that such variations have a small effect on gear efficiency. In addition, the efficiencies selected for each gear set were held constant regardless of shaft speed or torque being transmitted and were assumed to adequately represent average values over the driving cycle. The efficiencies and gear ratios used in the computer program are shown in Tables 5-6 and 5-7 (refer to Section 2.1 for powertrain schematics that show gear locations).

The variation shown in motor output gear ratio is the result of modifications necessary to comply with the designated vehicle design parameters. The gear ratio is basically determined by the motor torque multiplication necessary to achieve a given vehicle acceleration or cruise speed, whichever is the more severe requirement. An additional influencing factor is that the peak motor speed may not exceed 12,000 rpm. Because, for the 4000-lb car, the gear ratio for an 11-second acceleration causes the motor to overspeed at 80 mph, the acceleration time for this cruise speed had to be markedly relaxed from 11.0 to 17.5 seconds. A similar effect relaxes the acceleration time for the 2500-pound vehicle to 18.5 seconds. This result implies that a means of shifting gears is a requirement for high-performance vehicles that combine high acceleration with high cruise speed.

However, the specific gear ratio specified in Table 5-7 permits the vehicle to negotiate the EPA Urban Driving Cycle without shifting gears.

The gear ratio has a small effect on motor efficiency as the vehicle operates over a given driving cycle. The scope of this study did not permit an evaluation of each and every design condition on the vehicle energy expenditure and exhaust emissions. Instead, the effect of simple changes in vehicle powertrain efficiency is covered in the discussion of parametric analyses in Section 10.

The weight of each gear set in pounds was taken to be 0.5 percent of the vehicle loaded weight; the volume of each gear set in cubic feet was taken to be 0.005 percent of the vehicle loaded weight (based on Ref. 5-21).

5.8 REFERENCES

5-1. K. R. Stamper, W. F. Marshall, and R. Colello, Engine Performance Test Report: 1975 GM 140 CID, 2V, EPT-75-3, U.S. Department of Transportation, Washington, D. C. (November 1975) (ERDA-DOT Interagency Agreement No. RA-75-10).

5-2. H. Pender and W. A. Del Mar, eds., Electrical Engineers Handbook: Electric Power, 4th ed., John Wiley & Sons, Inc., New York (November 1958).

5-3. D. A. Dengler, Westinghouse Electric Corporation, West Mifflin, Penna. (Personal Communication, 8 August 1975).

5-4. M. A. Thompson and L. A. Walters, "The Design of D-C Commutator Motors for High Performance Electric Vehicles," SAE Paper No. 740169, presented at the Automotive Engineering Congress, Detroit, Mich., 25 February - 1 March 1974.

5-5. M. Inagaki, "Electric Vehicle Development in Japan," Proceedings of the First International Electric Vehicle Symposium, Phoenix, Ariz., 5-7 November 1969.

5-6. G. Baumann, "Propulsion-Systems for Electric Vehicles," Bosch Techn. Ber., Vol. 3, p. 6, December 1971.

5-7. J. N. Kersey, Lawnel Corporation, Bluefield, Va. (Personal Communication, 14 July 1975).

5-8. K. F. Nauerz, The Imperial Electric Company, Akron, Ohio (Personal Communication, 17 July 1975).

5-9. Motors and Generators, NEMA Standards, NEMA Standards Publication, MG 1-1972, National Electrical Manufacturers Association, New York (1972).

5-10. A. Kusko, Solid-State DC Motor Drives, Massachusetts Institute of Technology Press, Cambridge, Mass. (1969).

5-11. J. Monda, Westamp, Inc., Santa Monica, Calif. (Personal Communication, 17 July 1975).

5-12. E. A. Rishavy, W. D. Bond, and T. A. Zechin, "Electrovair -- A Battery Electric Car," SAE Paper No. 670175 presented at Automotive Engineering Congress and Exposition, Detroit, Mich., 9-13 January 1967.

5-13. R. P. Putkovich and F. J. Prines, "Solid-State DC Controllers for Electric Vehicles," Proceedings of the First International Electric Vehicle Symposium, Phoenix, Ariz., 5-7 November 1967.

5-14. Prospects for Electric Vehicles, A Study of Low-Pollution-Potential Vehicles-Electric, National Air Pollution Control Administration and Arthur D. Little, Inc., Raleigh, N. C. (October 1969) (Contract No. PH 68-67-108).

5-15. Space Power Systems, North Atlantic Treaty Organization Advisory Group for Aerospace Research and Development (November 1969).

5-16. A Study of Advanced Auxiliary Power Unit (APU) Systems, WADDR-TR-60-626, The Garrett Corporation, AiResearch Manufacturing Company Division, Los Angeles, Calif. (1 June 1960) (ASTIA AD247200).

5-17. Aircraft Electrical Power Equipment, Bendix Aviation Corporation, Eatontown, N.J.

5-18. Product Data, Lear Siegler, Inc., Power Equipment Division, Cleveland, Ohio.

5-19. F. Loram, CAV Limited, London, England (Personal Communication, 4 August 1975).

5-20. Product Brochure, RPM Industries, Los Angeles, Calif.

5-21. Final Report Hybrid Heat Engine/Electric Systems Study, Vol. I, TOR-0059(6769-01)-2, The Aerospace Corporation, El Segundo, Calif. (1 June 1971).

5-22. D. F. Taylor, and E. G. Siwek, "The Dynamic Characterization of Lead-Acid Batteries for Vehicle Applications," SAE Paper No. 730252, 8-12 January 1973.

5-23. F. L. Marsh, Gould, Inc. (Personal Communication, 23 June 1975).

5-24. L. R. Erisman, Eagle-Picher Industries (Personal Communication, 1 July 1975).

5-25. R.R. Gilbert, et al., Flywheel Drive System Study, LMSC D246393, Lockheed Missiles and Space Co., Inc., Sunnyvale, Calif. (31 July 1972)

5-26. G.L. Dugger, et al., Heat-Engine/Mechanical Energy Storage, Hybrid Propulsion Systems for Vehicles, CP011, John Hopkins University, Bethesda, Md. (March 1972).

5-27. Flywheel Feasibility Study and Demonstration, LMSC-DOO7915, Lockheed Missiles and Space Co., Sunnyvale, Calif. (30 April 1971).

5-28. R. L. Fullman, Energy Storage by Flywheels, 75CRD051, General Electric Company, Corporate Research and Development, Schenectady, N.Y. (April 1975).

5-29. Design and Development of a Continuously Variable Ratio Transmission for an Automotive Vehicle, Orshansky Transmission Corporation, New York (18 November 1975).

5-30. P. Huntley, Orshansky Transmission Corporation, New York (Private Communication, 3 July 1975).

5-31. Automotive Accessory Drive System Study, 74-310772, Air Research Manufacturing Company of Arizona, Phoenix, Ariz.

5-32. Hybrid Propulsion System Evaluation, Phase I, Final Report, AER640, Sundstrand Aviation (25 February 1972).

5-33. C. W. Coon, et al., Technological Improvements to Automobile Fuel Consumption, Vol. IIA, DOT-TSC-OST-74-39.IIA, for U.S. Dept. of Transportation, Washington, D.C. (December 1974) (Southwest Research Institute).

5-34. C. Marks, Which Way to Achieve Better Fuel Economy, General Motors Engineering Staff, Detroit, Mich. (3 December 1973)

5-35. P. A. Lundy, American Motors Corporation, Detroit, Mich. (Unpublished drawings, Personal Communication, 18 August 1970).

TABLE 5-1. ENGINE TOTAL POWER AND SPEED RELATIONSHIP FOR NEAR-MINIMUM BSFC: 1975 GM 140-CID-2V

Speed (rpm)	Total Power (bhp)
650	0
820	6.5
990	10.5
1159	12.3
1323	14.1
1490	15.8
1655	17.6
1820	19.3
1985	21.1
2315	24.6
2645	28.1
2978	31.6
3310	35.2
3640	38.7
3970	42.0
4400	63.0
4400	87.0

TABLE 5-2. BATTERY CELL MODELS

Lead-Acid

$\overline{W} = 0.093$ lb/amp-hr

VMC = 1.30

VMA = 2.40

$\overline{E} = 12.7 \frac{\text{W-hr}}{\text{lb}}$[a]

$\overline{V} = 1.31\ \text{in}^3$/amp-hr

State-of-Charge, %	0	5	12	15	25	38	50	68	88	100
IBMAX/C (discharge)	0.15	0.17	0.18	0.23	0.31	0.48	1.61	2.16	4.5	5.2
IBMAX/C (charge)	0.99	0.93	0.86	0.77	0.73	0.60	0.50	0.43	0.16	0.08

Nickel-Zinc

$\overline{W} = 0.06$ lb/amp-hr

VMC = 1.45

VMA = 1.96

$\overline{E} = 22.0 \frac{\text{W-hr}}{\text{lb}}$[a]

$\overline{V} = 0.7\ \text{in}^3$/amp-hr

State-of-Charge, %	0	5	10	17	25	35	50	67	85	100
IBMAX/C (discharge)	0	0.4	1.4	3.0	4.8	5.7	7.1	8.0	9.0	22.0
IBMAX/C (charge)	12.7	11.3	9.9	6.9	5.5	4.8	3.9	3.0	2.1	1.0

[a]E, specific energy for multicell battery based on $\overline{W}$, VMC, and 10 percent weight added for cell packaging.

TABLE 5-3. HYBRID VEHICLE FLYWHEEL CHARACTERISTICS ESTABLISHED BY EPA CONTRACTORS (Refs. 5-25 and 5-26)

Characteristic	Steel Flywheel (LMSC)	Reinforced Plastic Composite "Super-Flywheel" (JHU)
Flywheel System Weight (lb)	187	255
Rated (rpm)	24,000	32,000
Flywheel System Specific Energy (W-hr/lb)	2.7	20.5
Flywheel Weight (lb)	86	162

TABLE 5-4. SUMMARY OF FLYWHEEL SUBSYSTEM CHARACTERISTICS: OPERATION AT MAXIMUM ROTOR DESIGN SPEED

Characteristic[a]	Vehicle Loaded Weight (lb)				
	Steel Rotor			Kevlar Rotor	
				LMSC	JHU
	2500	4000	6000	4000	4000
r (ft)	0.493	0.544	0.593	0.718	1.0
$N_d (= N_{dm})$ (rpm)	27,151.5	24,599.6	22,591.7	58,480.8	42,003.6
$E_d (= E_{dm})$ (W-hr)	449.9	604.9	781.0	2369.6	6395.2
W_R (lb)	78.2	105.2	135.8	41.85	113.0
V_R (ft^3)	0.160	0.215	0.278	0.495	1.335
W_{FWSS} (lb)	149.4	200.9	259.4	174.6	470.5
V_{FWSS} (ft^3)	0.237	0.319	0.411	1.182	3.188
E_d/W_R (W-hr/lb)	5.75	5.75	5.75	56.62	56.62
E_d/V_R (W-hr/ft^3)	2810.0	2810.0	2810.0	4790.0	4790.0
E_d/W_{FWSS} (W-hr/lb)	3.01	3.01	3.01	13.58	13.58
E_d/V_{FWSS} (W-hr/ft^3)	1898.0	1898.0	1898.0	2005.0	2005.0
HPL @ N_d (hp)	1.194	1.403	1.613	10.72	4.56[b]
E_d/HPL (hr)	0.5053	0.5782	0.6493	0.2964	1.877[b]
P (mmHg)	5.0	5.0	5.0	0.765	0.001

[a] See Section 5.4 for definition of terms.
[b] Pump power assumed same as for holding 5 mmHg.

TABLE 5-5. TORQUE RATIO VS SPEED RATIO FOR ORSHANSKY CONTINUOUSLY VARIABLE TRANSMISSION (Refs. 5-29 and 5-30)

Speed Ratio NR	Torque Ratio TR (Torque Out/Torque In)		
	NI = 1051[a]	NI = 1315[a]	NI = 1751[a]
0.05	8.96	9.16	9.26
0.10	6.35	6.39	6.44
0.15	4.87	4.91	4.94
0.20	3.89	3.98	3.99
0.30	2.67	2.85	2.88
0.40	2.02	2.16	2.17
0.50	1.62	1.72	1.72
0.60	1.32	1.37	1.35
0.70	1.16	1.23	1.23
0.80	1.03	1.11	1.11
0.90	0.92	0.997	1.02
1.0	0.84	0.91	0.92
1.2	0.71	0.76	0.77
1.4	0.61	0.66	0.66
1.6	0.53	0.57	0.57
1.8	0.44	0.48	0.49
2.0	0.37	0.42	0.42

[a]NI = input speed, rpm

TABLE 5-6. SELECTED CHARACTERISTICS FOR GEAR SETS

Powertrain	Gear Set Location	Efficiency (%)	Gear Ratio
Heat Engine/ Battery	Heat Engine Out - Accessories/ Auxiliaries In	99	1.43 (R)[a]
Heat Engine/ Battery	Heat Engine Out - Generator In	98	2.61 (I)[a]
Heat Engine/ Battery	Motor Out - Differential In	98	GR_m (R)[b]
Heat Engine/ Battery	Differential Rear End	98	2.73 (R)
Heat Engine/ Flywheel	Heat Engine Out - Accessories/ Auxiliaries In	99	1.43 (R)
Heat Engine/ Flywheel	Heat Engine Out - Transmission 2 In	98	1.2 (R)
Heat Engine/ Flywheel	Transmission 2 Out - Flywheel In	98	20.0 (I)
Heat Engine/ Flywheel	Flywheel Out - Tranmission 1 In	98	15.1 (R)
Heat Engine/ Flywheel	Differential Rear End	98	2.73 (R)

[a] I = speed increaser; R = speed reducer.

[b] See Table 5-7.

TABLE 5-7. GR_m RATIO

Vehicle Design Weight (lb)	Vehicle Design Peak Cruise Speed (mph)	Vehicle Design Peak Acceleration Time, 0-60 mph (sec)	GR_m
4000	80	17.5	4.278
4000	65	11.0	5.102
4000	55	11.0	5.102
2500	65	18.5	4.734
6000	65	25.0	4.473

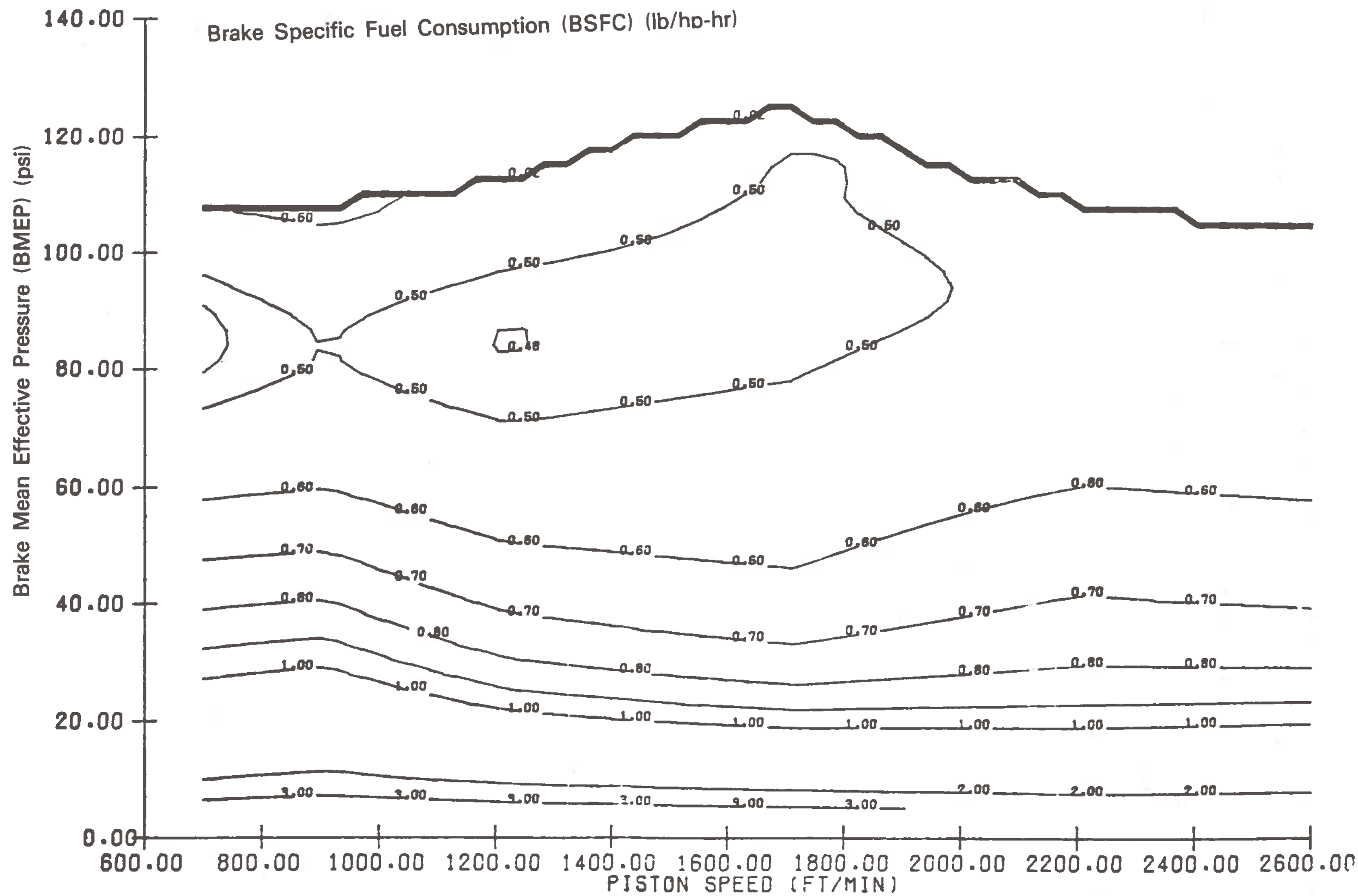

FIGURE 5-1. GM 140-CID ENGINE: BRAKE SPECIFIC FUEL CONSUMPTION (Ref. 5-1)

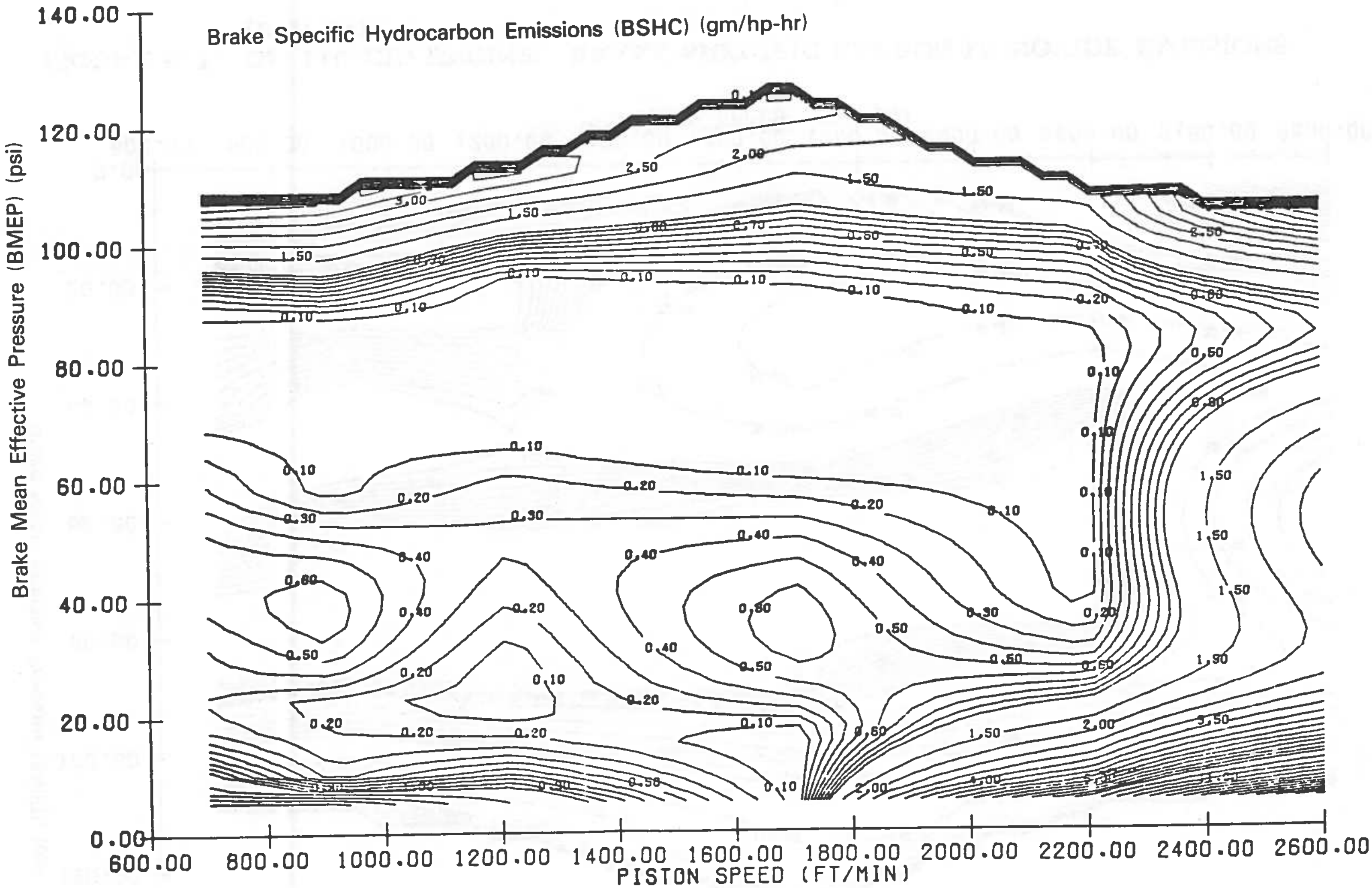

FIGURE 5-2. GM 140-CID ENGINE: BRAKE SPECIFIC HYDROCARBON EMISSIONS (Ref. 5-1)

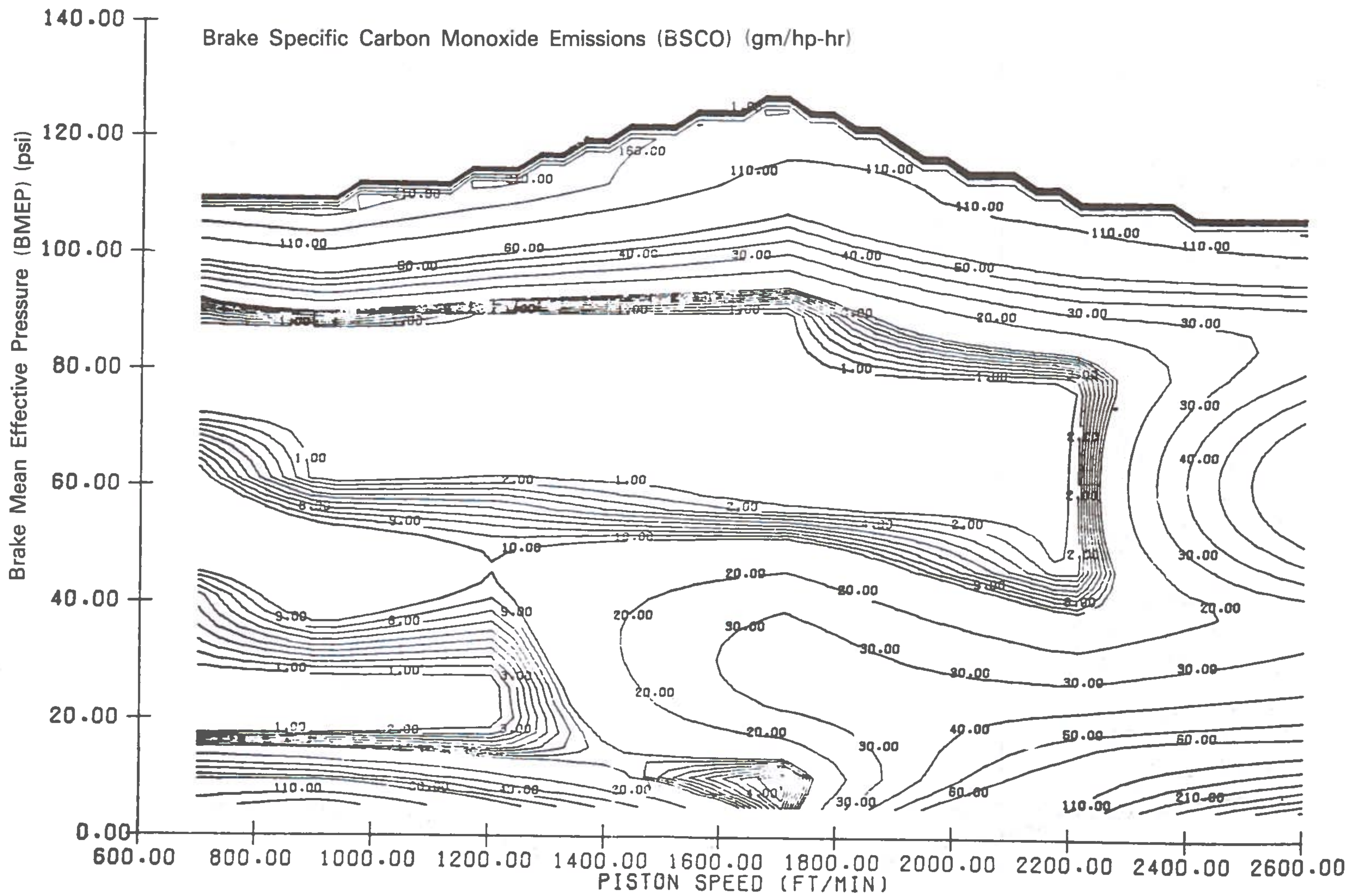

FIGURE 5-3. GM 140-CID ENGINE: BRAKE SPECIFIC CARBON MONOXIDE EMISSIONS (Ref. 5-1)

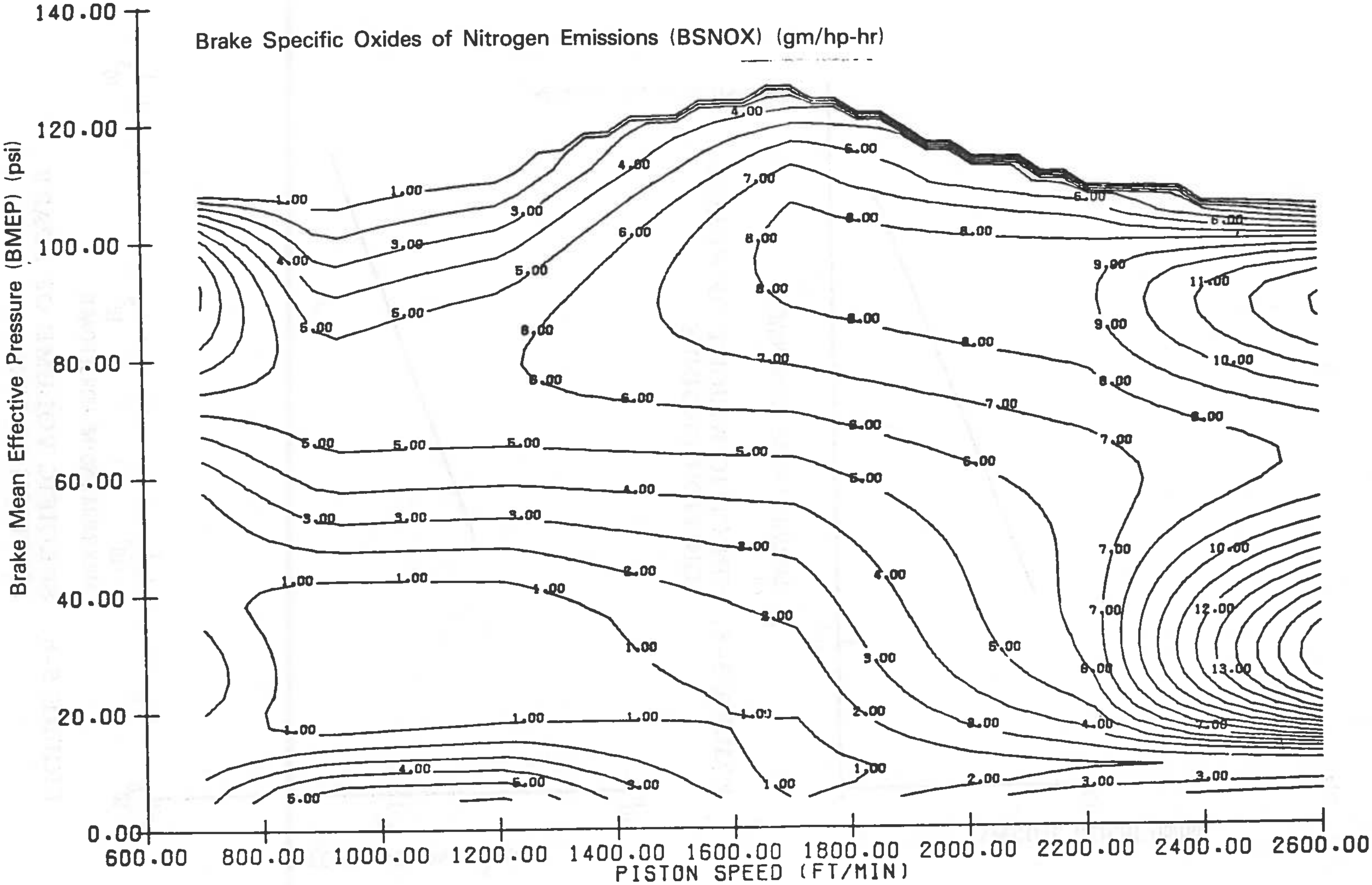

FIGURE 5-4. GM 140-CID ENGINE: BRAKE SPECIFIC OXIDES OF NITROGEN EMISSIONS (Ref. 5-1)

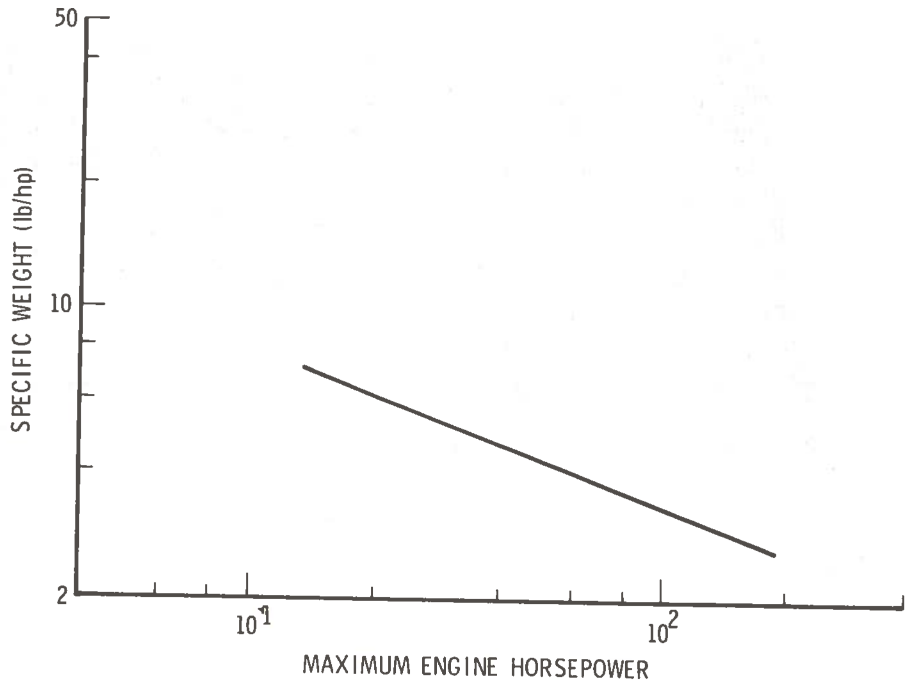

FIGURE 5-5. SPECIFIC WEIGHT OF SPARK IGNITION ENGINES

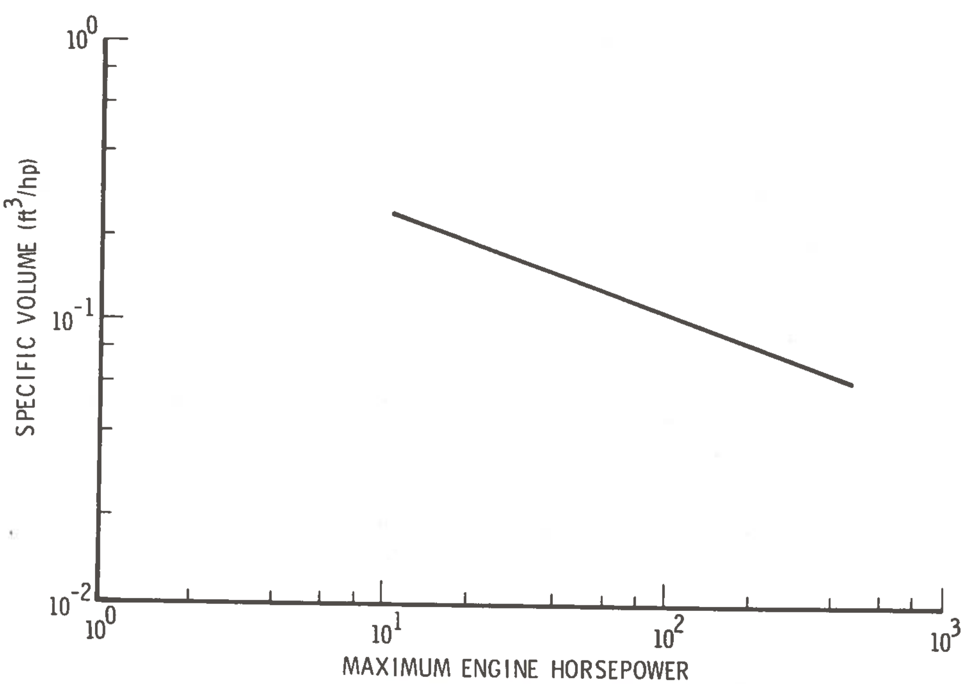

FIGURE 5-6. SPECIFIC VOLUME OF SPARK IGNITION ENGINES

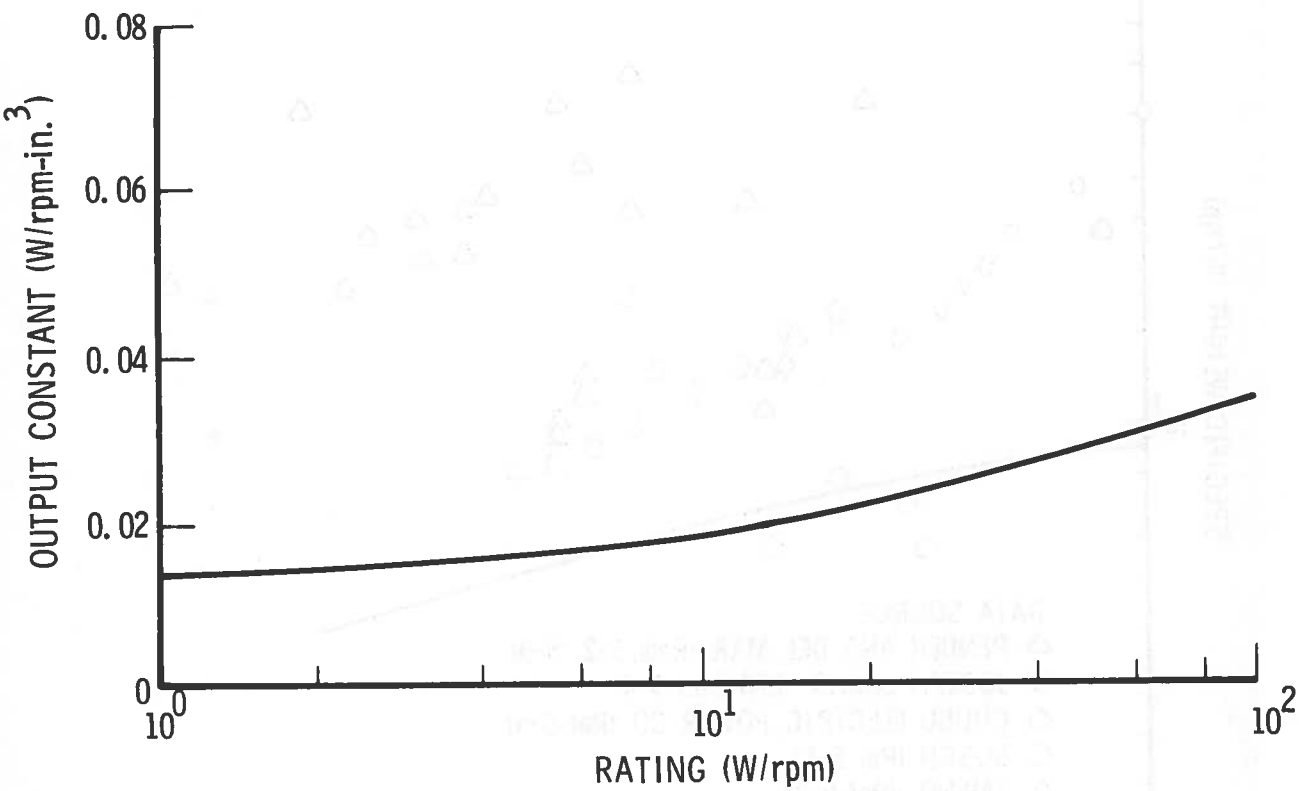

FIGURE 5-7. VARIATION OF DC MACHINE OUTPUT CONSTANT WITH MACHINE RATING

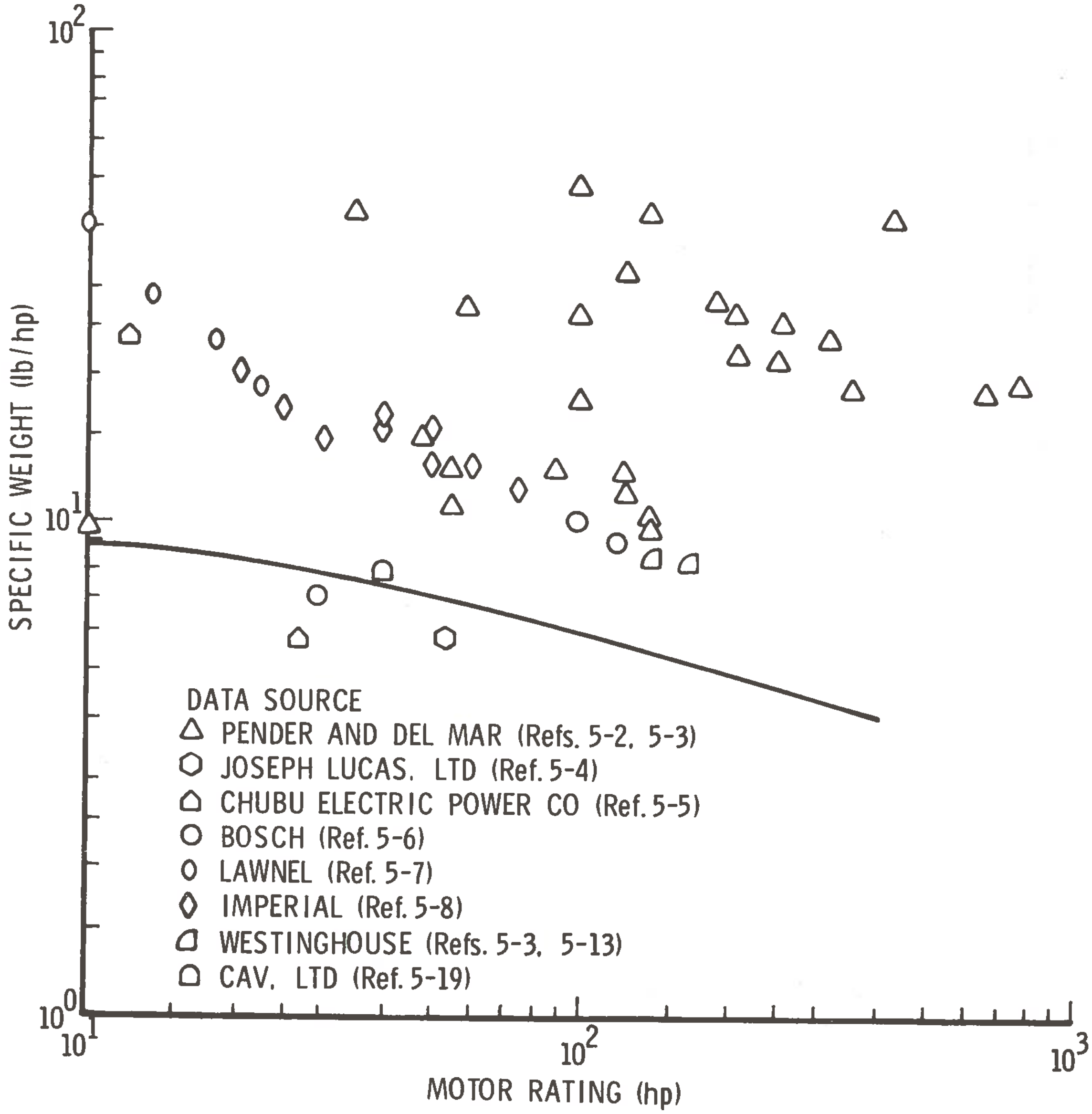

FIGURE 5-8. SPECIFIC WEIGHT CURVE FOR DC MOTORS

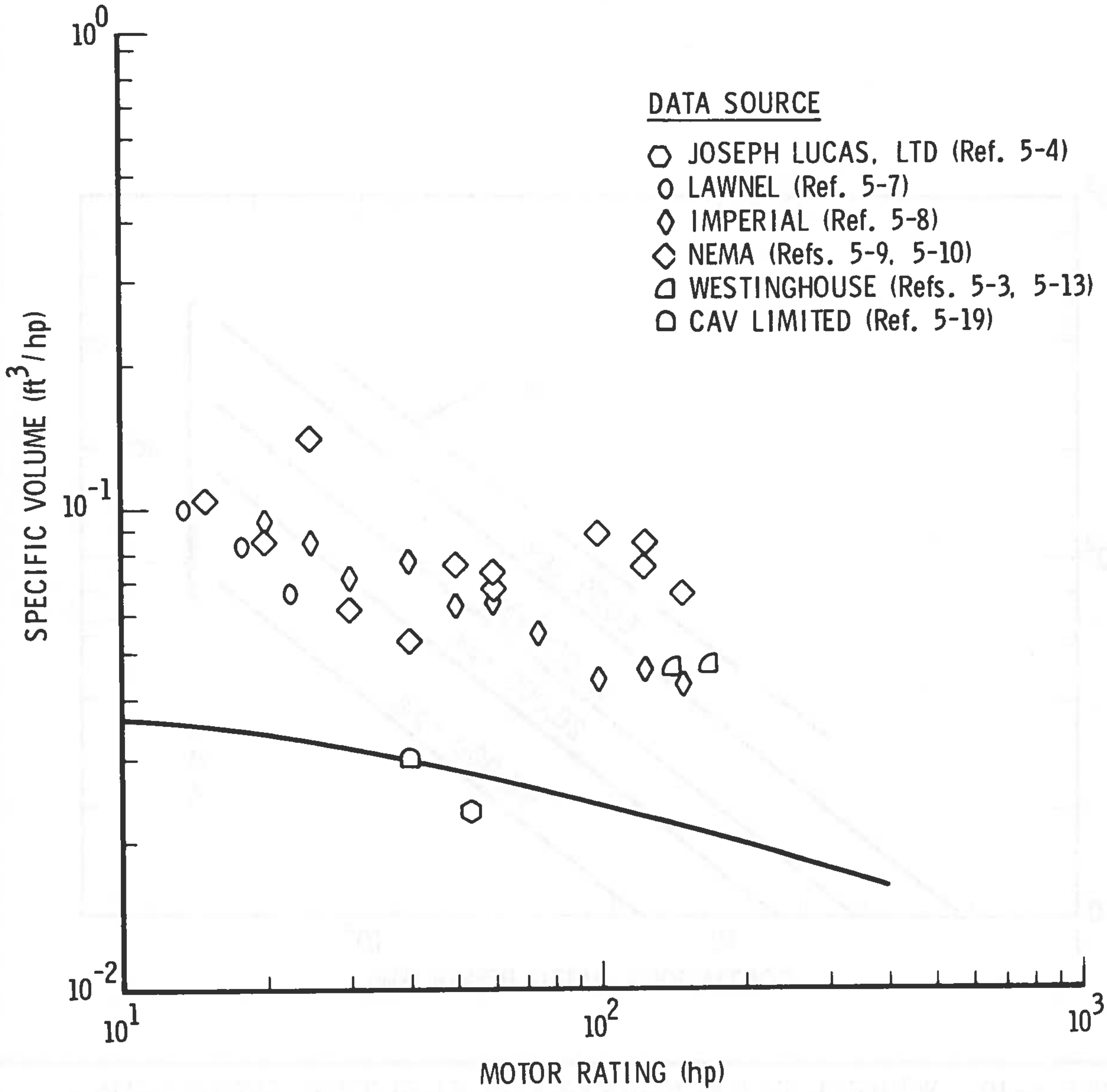

FIGURE 5-9. SPECIFIC VOLUME CURVE FOR DC MOTORS

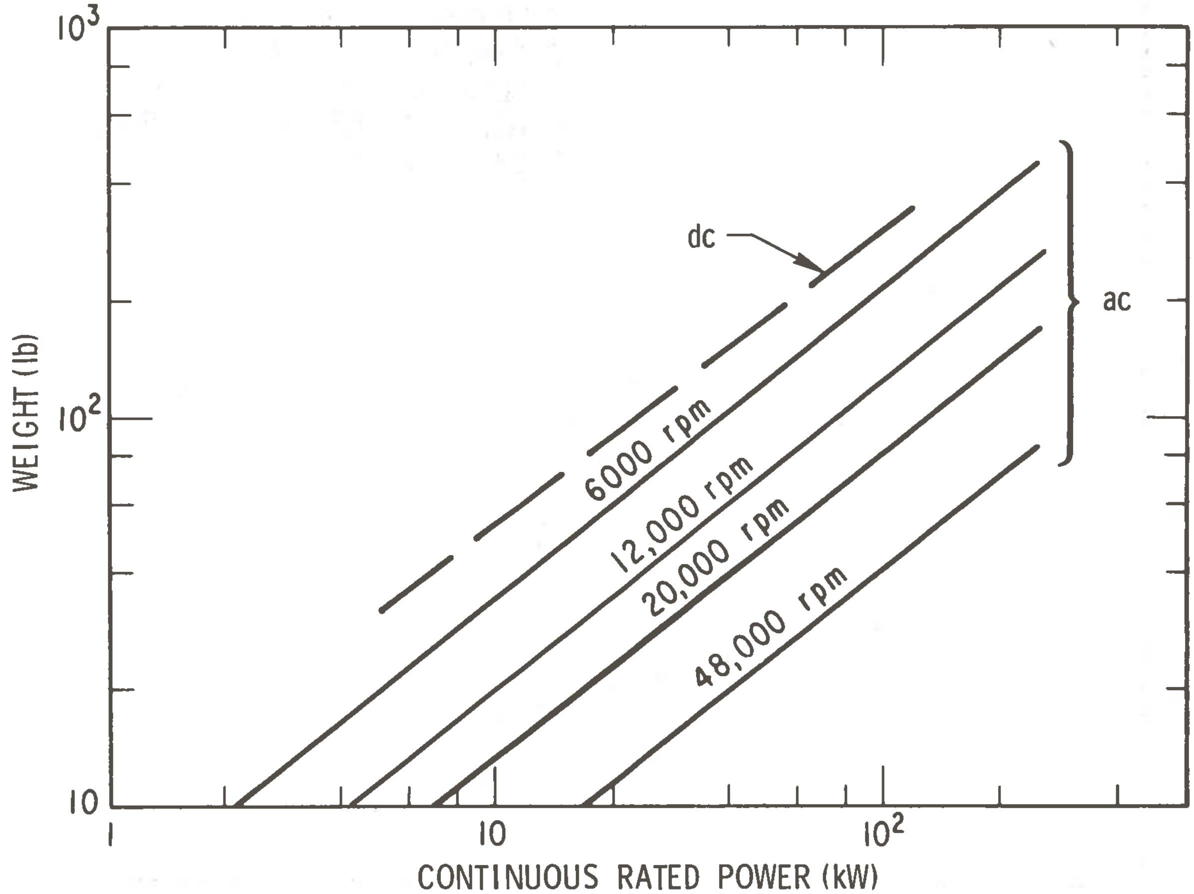

FIGURE 5-10. WEIGHT SIZING CURVES FOR ELECTRIC GENERATORS NOT DESIGNED FOR OVERLOAD (Ref. 5-21)

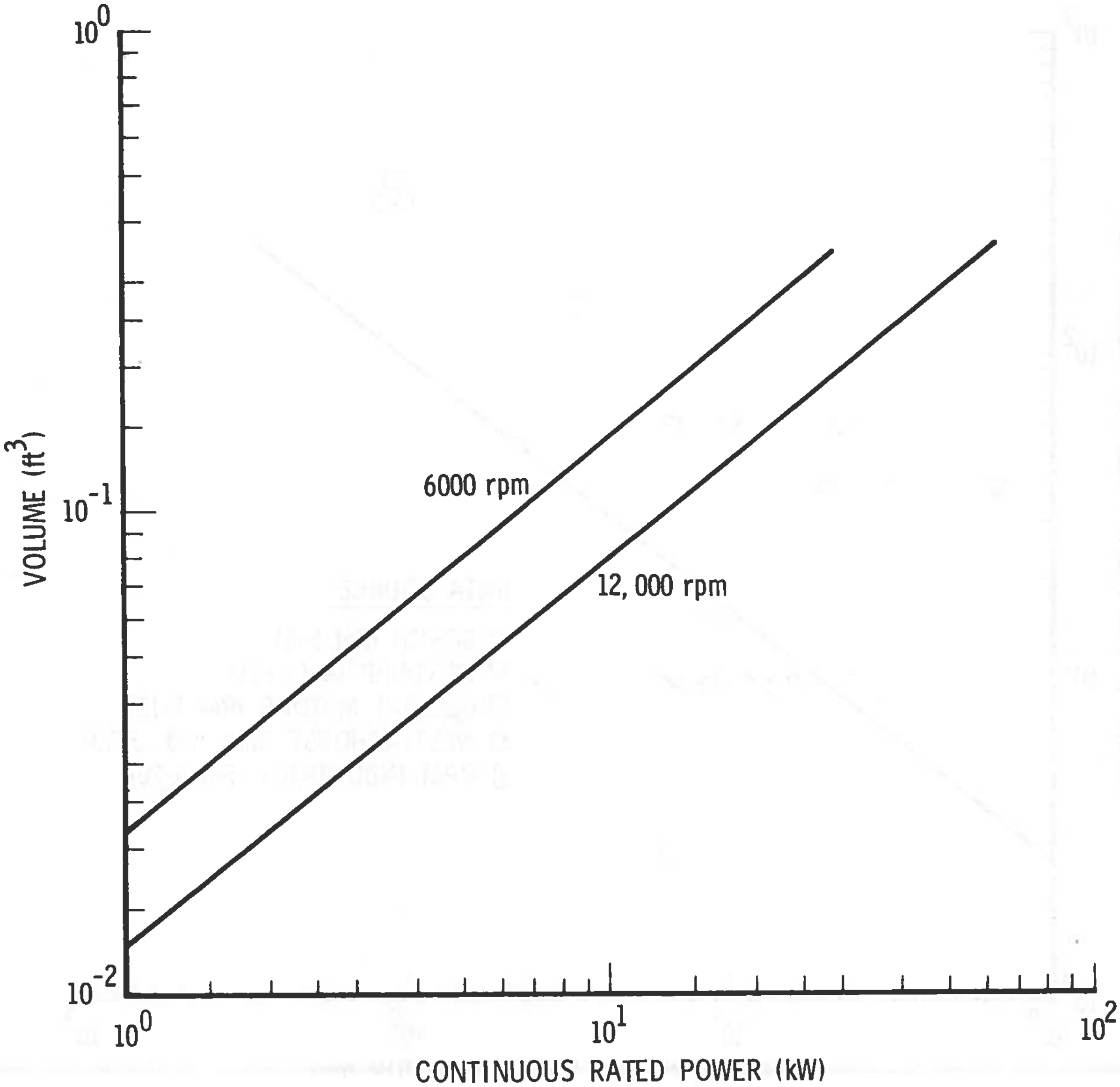

FIGURE 5-11. VOLUME SIZING CURVE FOR ELECTRIC GENERATORS

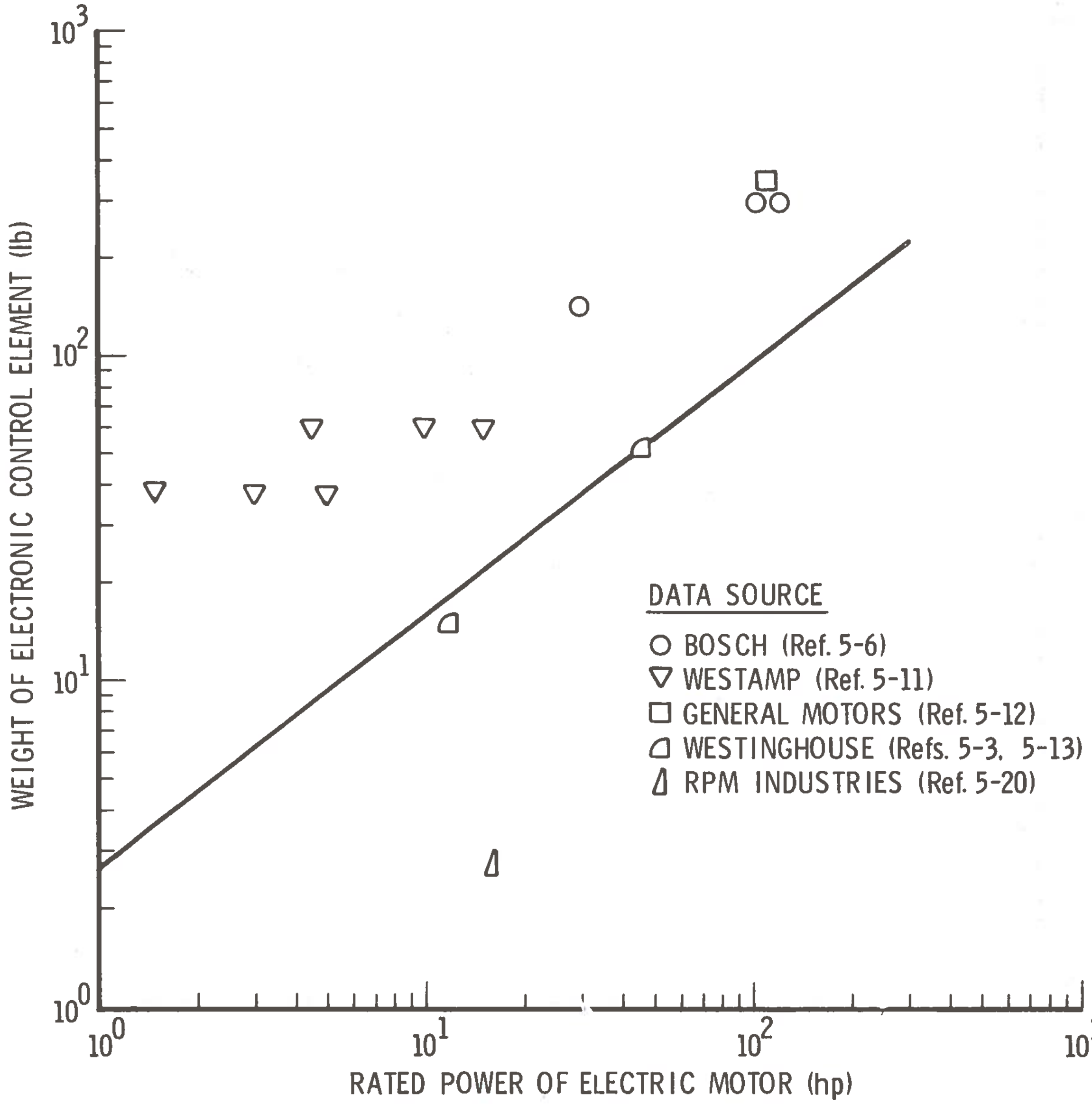

FIGURE 5-12. ELECTRONIC CONTROLLER WEIGHT SIZING CURVE

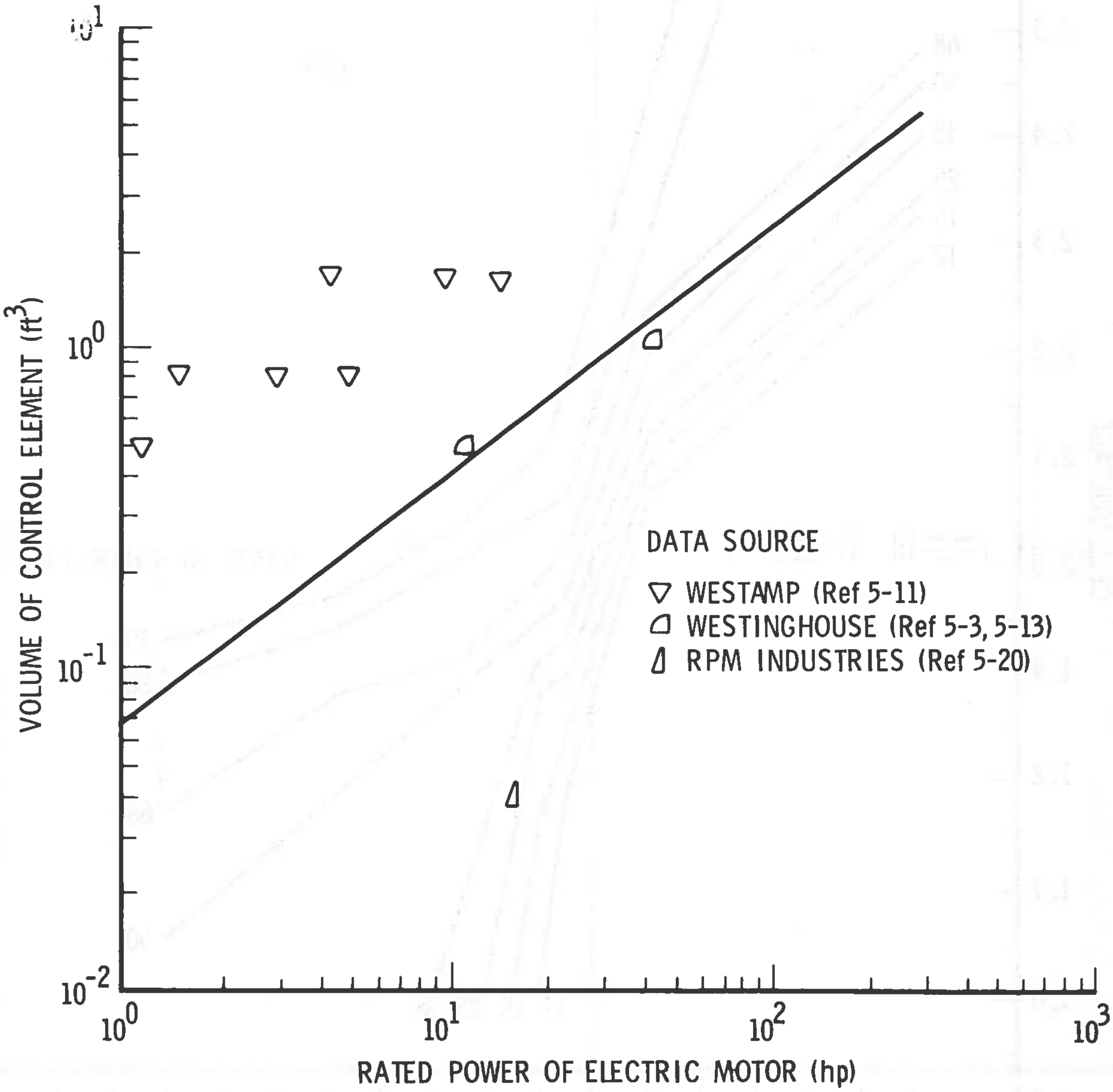

FIGURE 5-13. ELECTRONIC CONTROLLER VOLUME SIZING CURVE

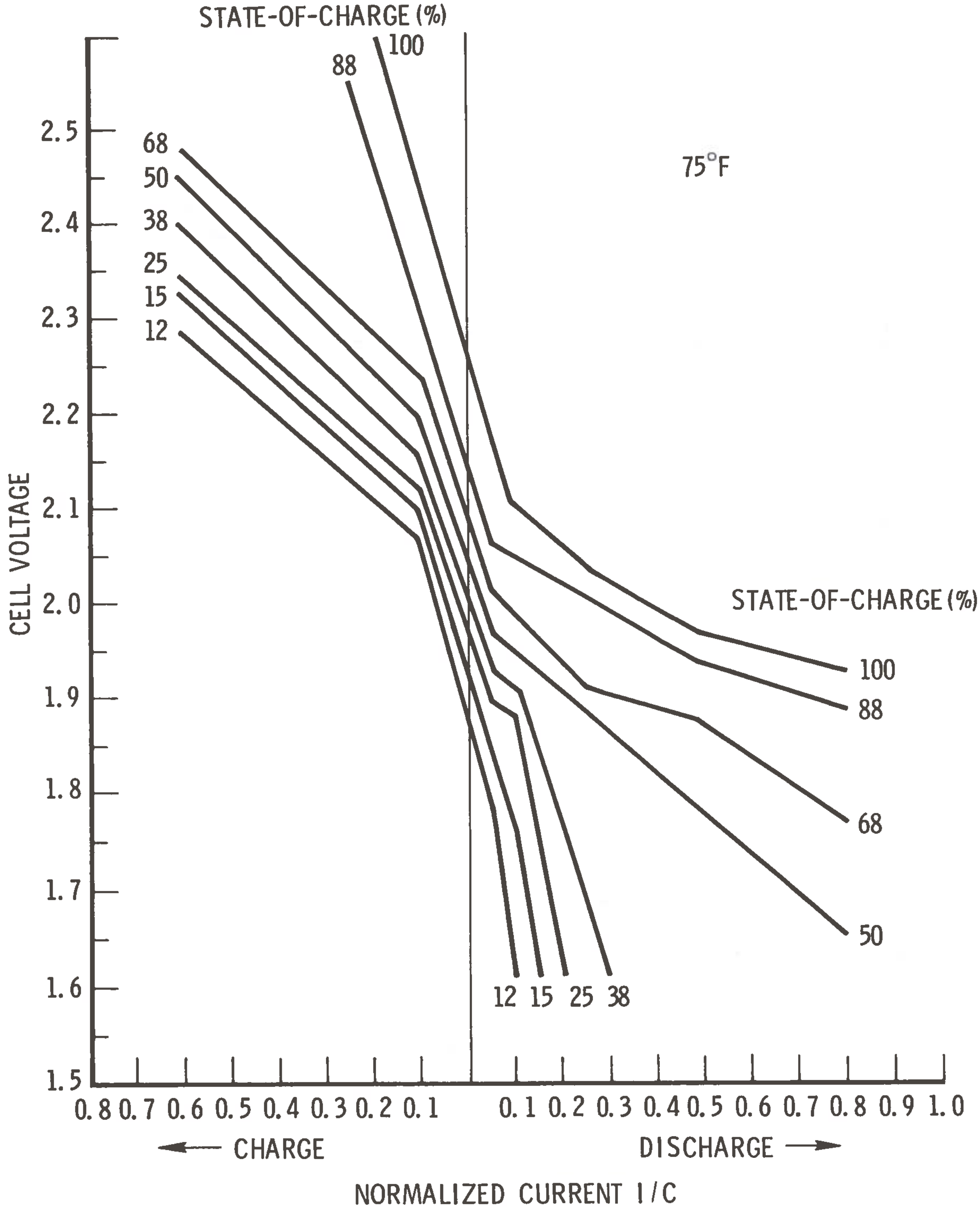

FIGURE 5-14. LEAD-ACID BATTERY CHARACTERISTICS

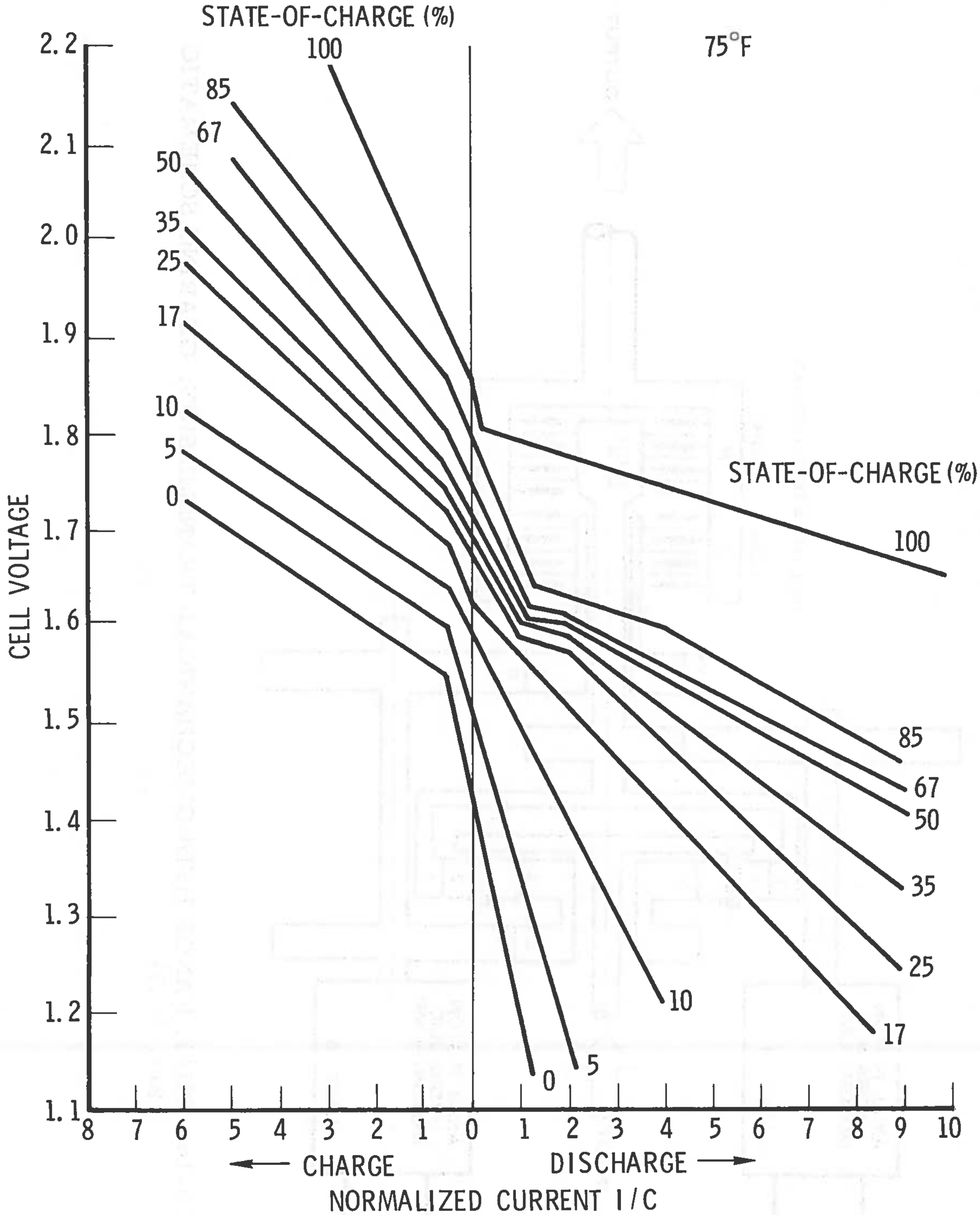

FIGURE 5-15. NICKEL-ZINC BATTERY CHARACTERISTICS

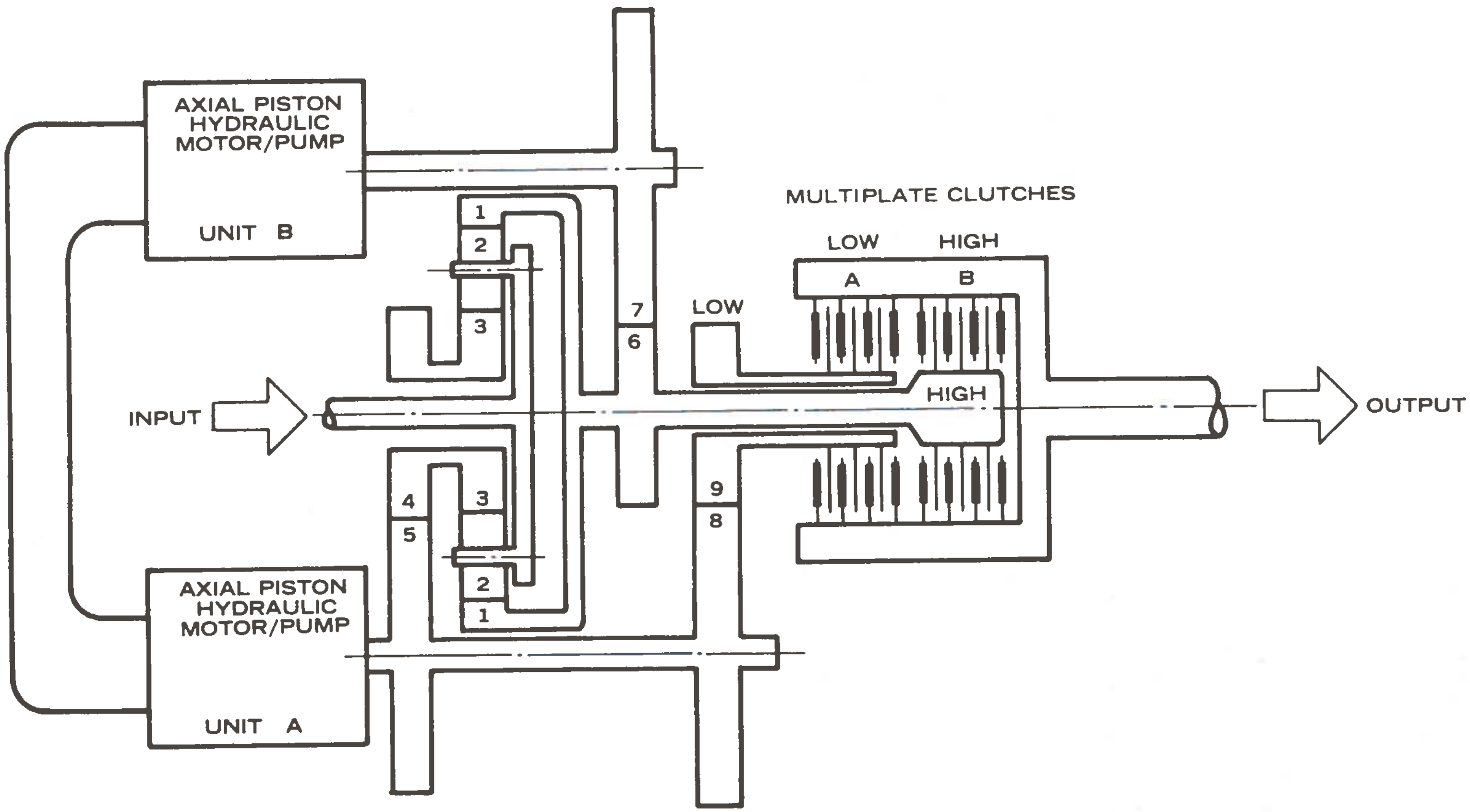

FIGURE 5-16. DUAL-RANGE HYDROMECHANICAL TRANSMISSION: GEARING SCHEMATIC (Ref. 5-29)

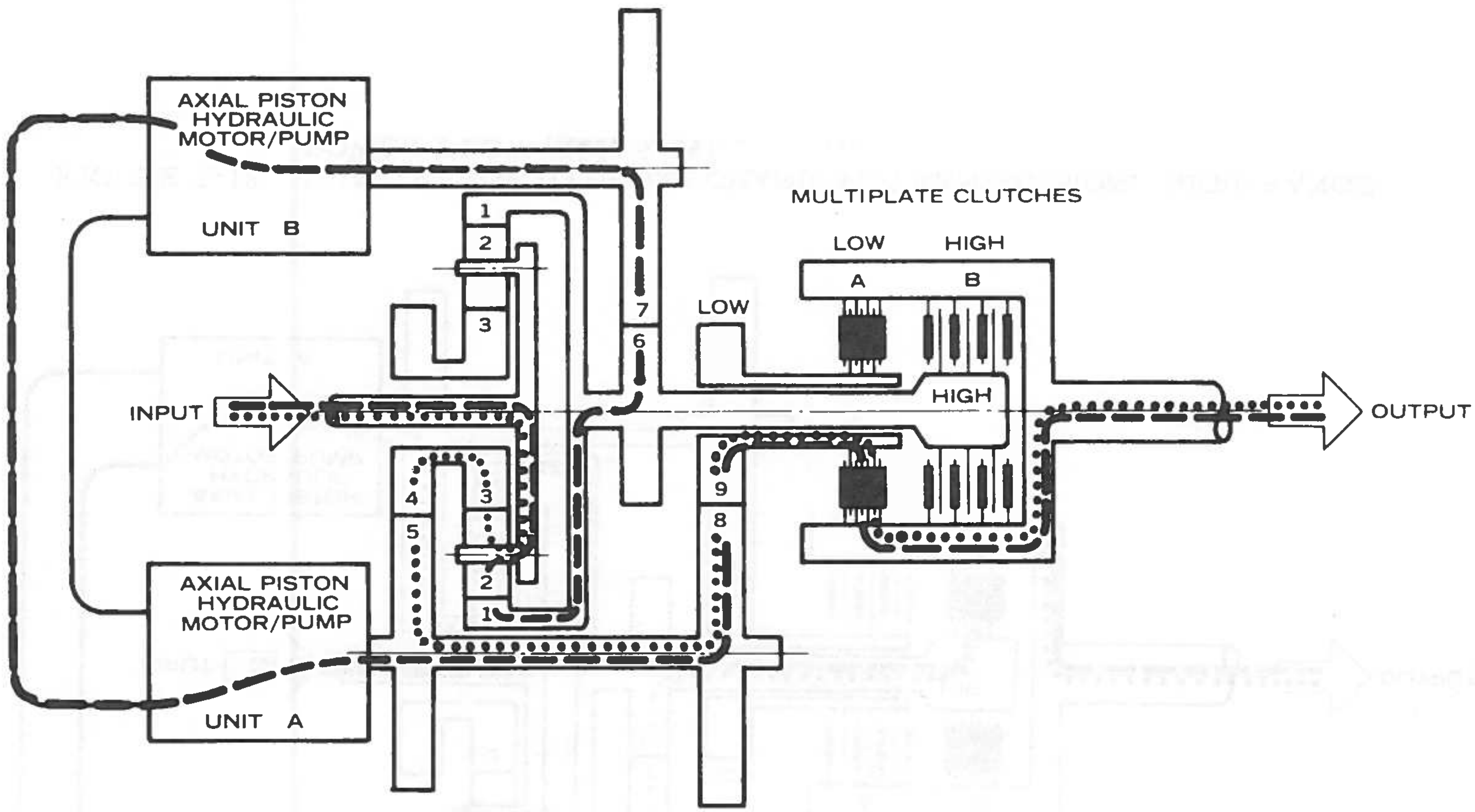

FIGURE 5-17. DUAL-RANGE HYDROMECHANICAL TRANSMISSION: LOW-RANGE POWER FLOW (Ref. 5-29)

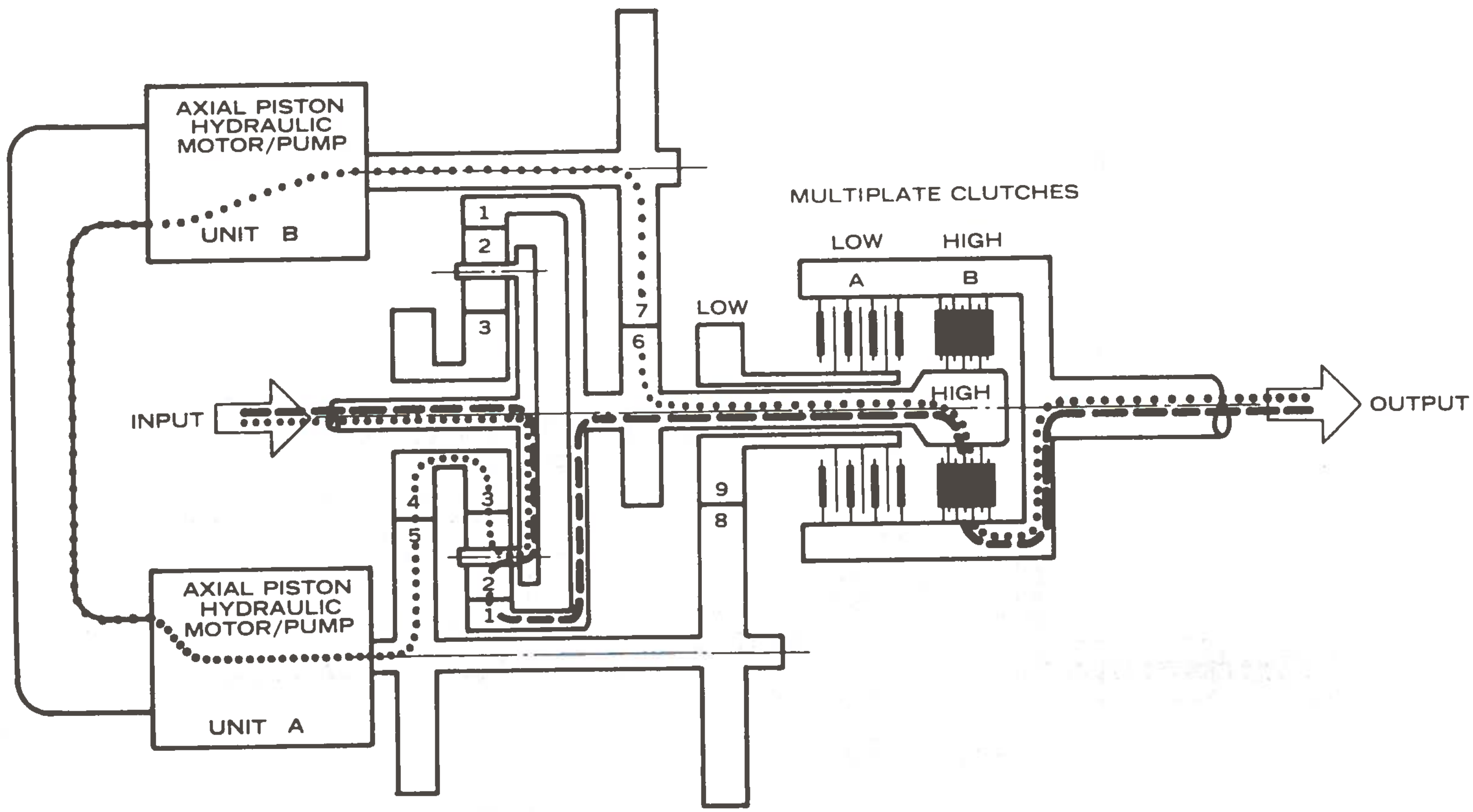

FIGURE 5-18. DUAL-RANGE HYDROMECHANICAL TRANSMISSION: HIGH-RANGE POWER FLOW (Ref. 5-29)

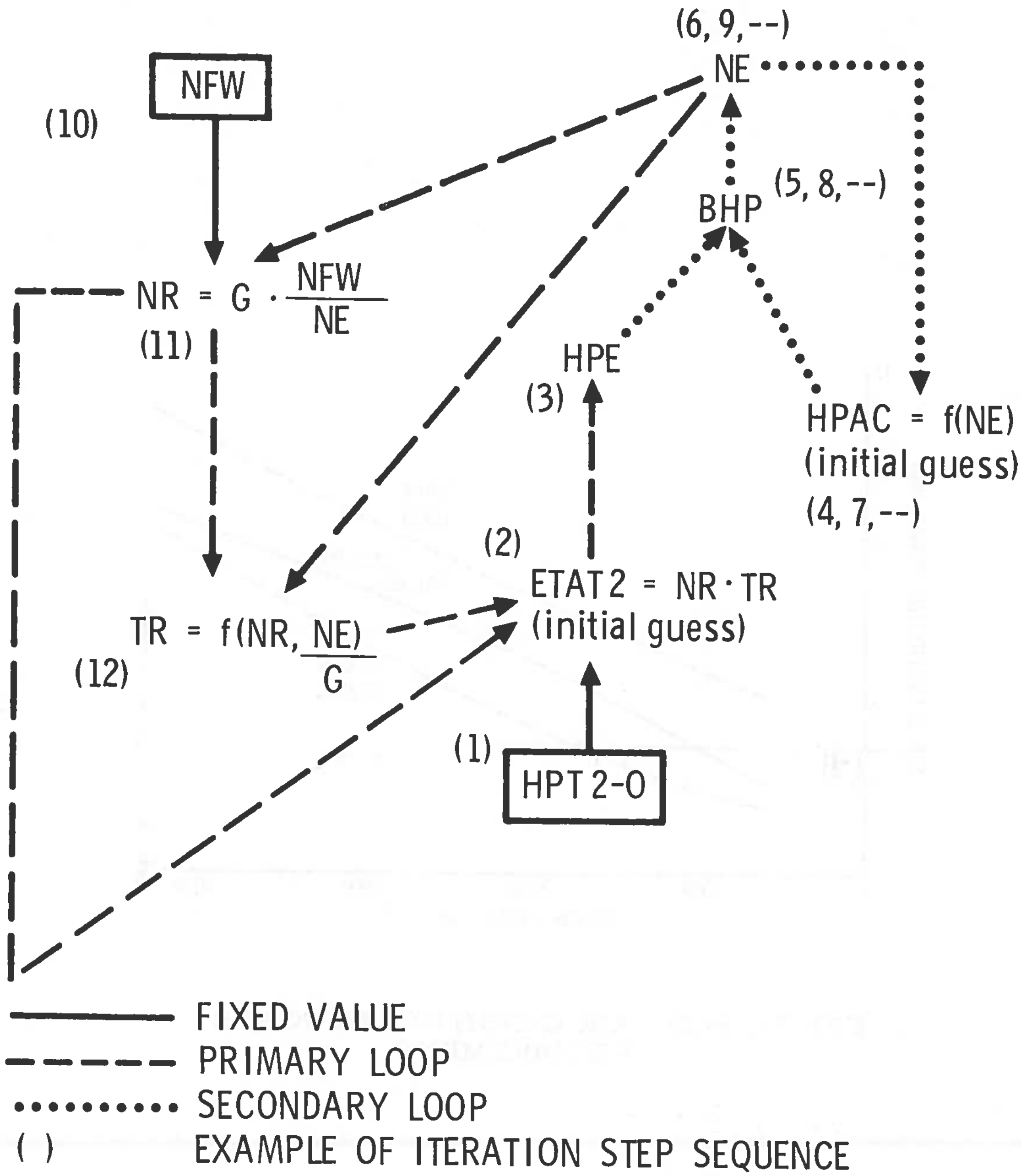

FIGURE 5-19. COMPUTER LOOPING PROCEDURE FOR THE TRANSMISSION LOCATED BETWEEN HEAT ENGINE AND FLYWHEEL

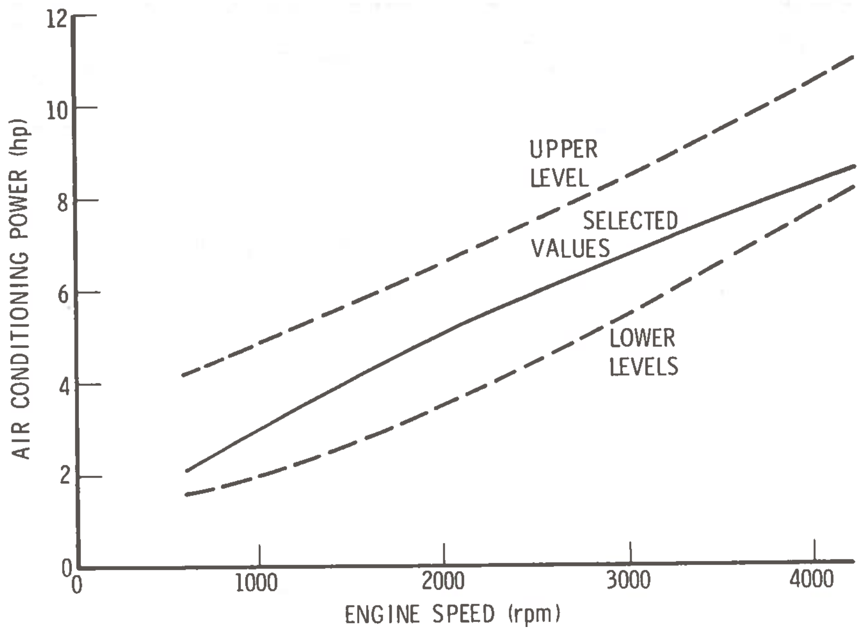

FIGURE 5-20. AIR CONDITIONING POWER REQUIREMENT

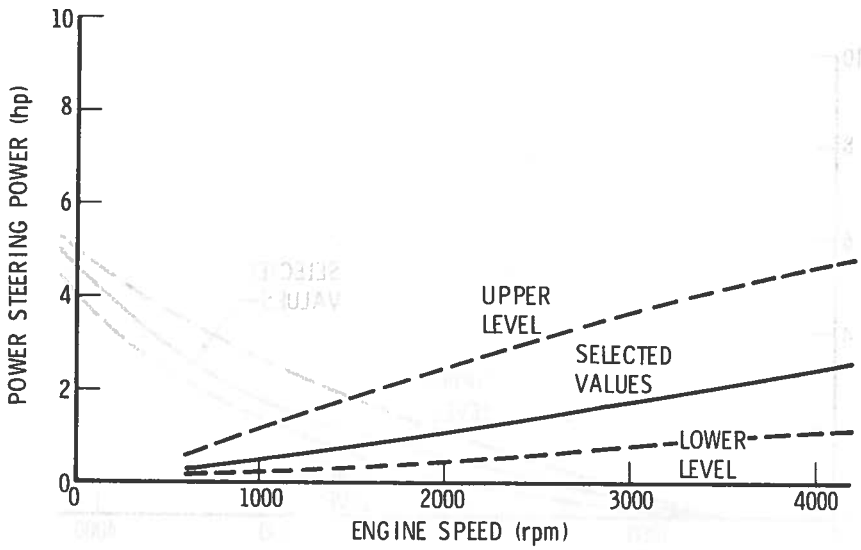

FIGURE 5-21. POWER STEERING POWER REQUIREMENT

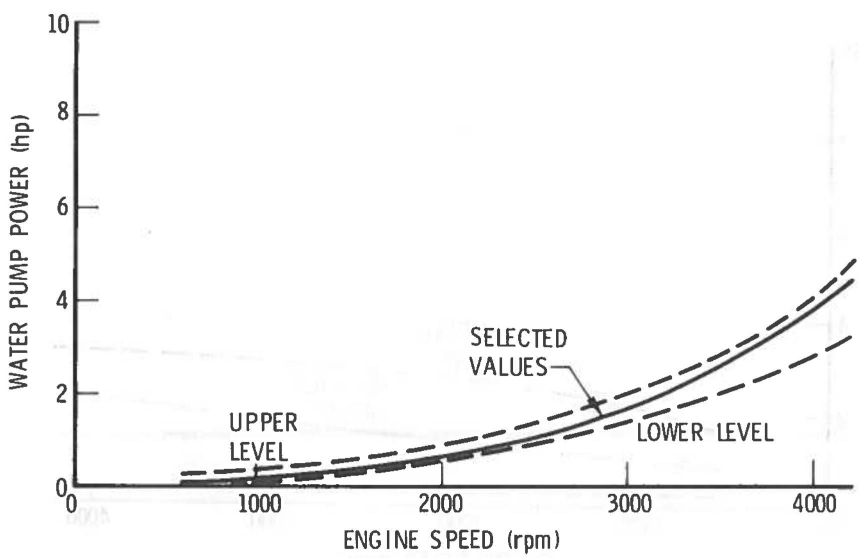

FIGURE 5-22. WATER PUMP POWER REQUIREMENT

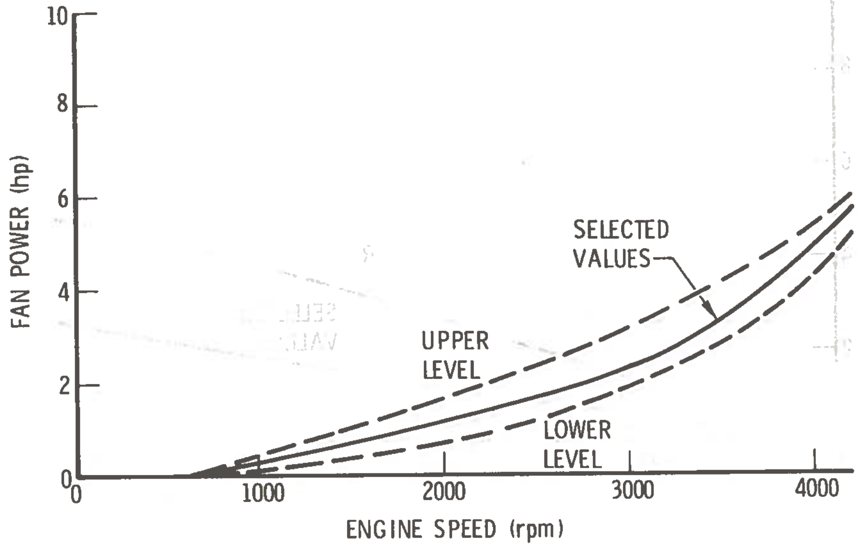

FIGURE 5-23. RADIATOR COOLING FAN POWER REQUIREMENT

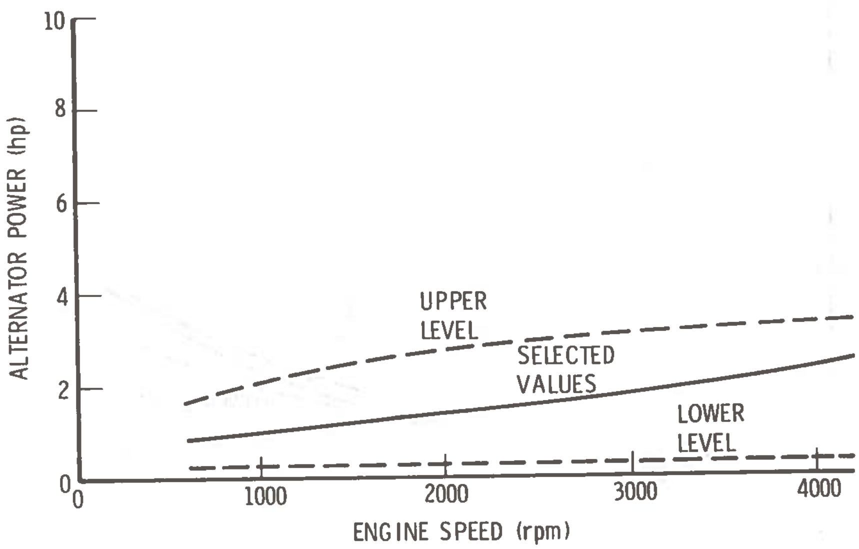

FIGURE 5-24. ALTERNATOR POWER REQUIREMENT

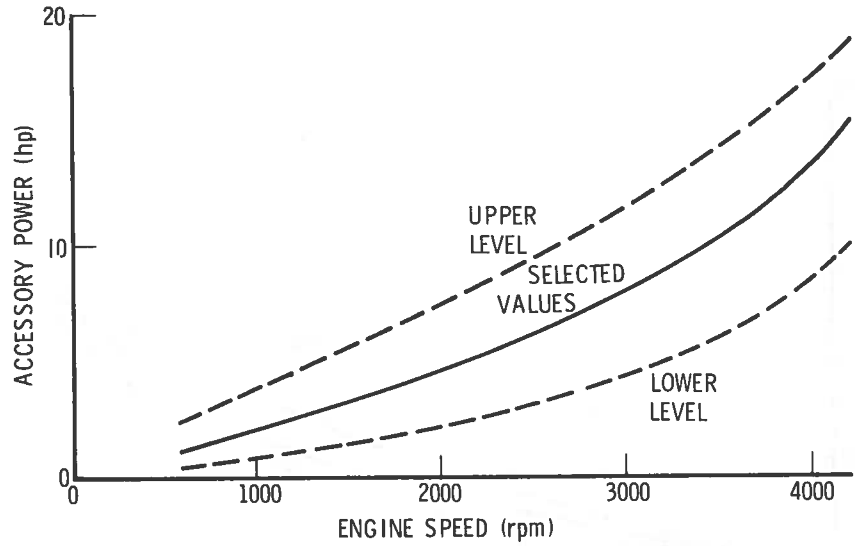

FIGURE 5-25. TOTAL VEHICLE ACCESSORY/ENGINE AUXILIARY POWER REQUIREMENT WITHOUT AIR CONDITIONING

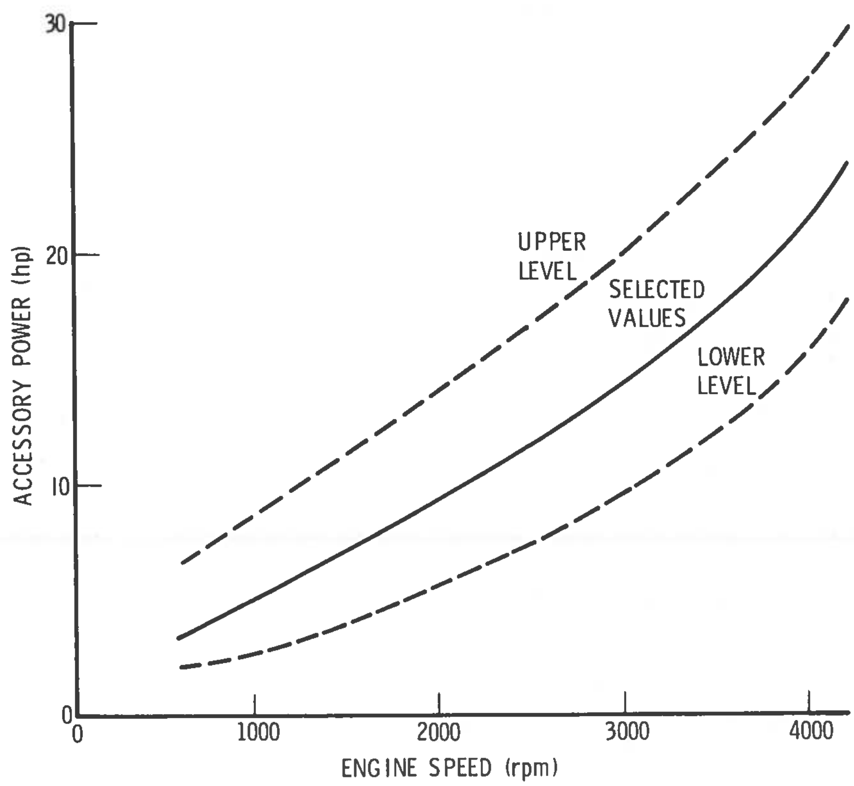

FIGURE 5-26. TOTAL VEHICLE ACCESSORY/ENGINE AUXILIARY POWER REQUIREMENT WITH AIR CONDITIONING

6. SELECTED CHARACTERISTICS FOR STATIONARY ELECTRIC GENERATING PLANTS

6.1 ENERGY SOURCES

In order to establish the geographic variation in percent utilization of the various types of fuels used by the United States electric utility industry, current data and future projections were summarized for different regions in the country. For example, almost 80 percent of the power generated in the east-north-central and east-south-central states is derived from burning coal, whereas west-south-central states rely about 87 percent on natural gas. For the Pacific states, hydropower provides about 60 percent of needs. These fuel usage data, along with generating plant efficiencies and emission factors, are given in the following discussion.

Data obtained on the utilization of various energy sources by the electric utility industry include both nationwide usage and a breakdown by geographic regions. One of the most comprehensive statistical compilations is found in Ref. 6-1.

Table 6-1 presents national data on total electric energy generated by prime mover and fuel usage. Data are for 1973, designated as preliminary in Ref. 6-1. The breakdown of electric energy generation by geographic region and prime mover is given in Table 6-2. Most notable is the significant hydropower contribution in the Mountain and Pacific Regions, particularly the almost total reliance on this source in the State of Washington. The thermally generated (total less hydropower) electric energy in 1973 is given in Table 6-3 by regions and type of fuel. Figure 6-1 and Table 6-4 show the regional composition by states as used in Tables 6-2 and 6-3.

The data presented to this point represent the contemporary situation in the electric utility industry. However, it is necessary to make some projection of the energy division in future years. One estimate through the year 2000 is shown in Table 6-5. Table 6-6 is a more recent projection of energy source utilization, but it extends only to 1979. Table 6-7 gives projections to 1979 for an eight-region division; the eight regions are specified in Table 6-8 and in Figure 6-2.

6.2 EFFICIENCY OF POWER PLANTS

In order to compute electric utility power plant fuel consumption and emissions, it is necessary to estimate electric power generation and powerline transmission efficiencies. With regard to the thermal efficiency of fossil fuel plants, the historical trend in average efficiency is shown in Figure 6-3. The figure shows that in the decade between 1951 and 1961 there was a steady increase in the overall thermal efficiency which has since remained relatively constant. In the future, the efficiency of fossil fuel plants is expected to increase again as new technology is incorporated in the mix of generating capacity.

Table 6-9 shows a 1972 projection of the expected efficiencies for several of these new technologies and the expected year of availability. The effect on average fossil-fueled electric power plant efficiency is depicted in Figure 6-4. The efficiency projection in Table 6-10 is slightly more optimistic, i.e., by about one percentage point in 1985. While coal-burning power plants are more efficient than oil and gas units by about one to two percentage points, the difference may not be significant in light of the uncertainty in projecting into the future.

Nuclear plants are somewhat less efficient than fossil-fuel units. Table 6-10 shows predicted efficiencies through 2000, based upon Atomic Energy Commission data for projected nuclear plant mixes. The nuclear plant efficiency remains constant at current values until 1985 when advanced high-temperature gas reactors and the liquid metal fast breeder reactor are introduced into the inventory. The current efficiency of 32 percent is less than that of the more efficient, modern fossil-fuel steam plants (~35 percent) but near the average for all fossil-fuel plants when older units, internal combustion engines, and gas turbines are included.

With regard to electric power transmission efficiency, a value of 91 percent was used in Ref. 6-4, which is based upon Southern California Edison Company data. Reference 6-1 data for 1973 indicate an efficiency of 91.5 percent.

6.3 EMISSION FACTORS

Electric power generating station emissions were based on the nationwide emission factors given in Refs. 6-5 through 6-8. These emission factors for oil, gas, and coal are shown in Table 6-11. The values for hydrocarbons (HC), carbon monoxide (CO), oxides of nitrogen (NO_x), and particulates were derived from data given in Refs. 6-5 and 6-6. For sulfur oxides (SO_x), the 1973 emission factors were EPA published data (Ref. 6-7) assuming an average of one percent sulfur by weight in coal and fuel oil and no control equipment. The 1980 SO_x emission factors are based on the assumption that all utility plants will meet the federal regulations for coal and oil firing (Ref. 6-8). The SO_x emission factor for natural gas in 1980 was taken to be the same as in 1973.

In deriving these data, emission factors based upon quantity of fuel burned were converted to pounds of pollutant per 1000 kW-hr of energy in the fuel on the assumption of 25×10^6 Btu/ton of coal, 142,800 Btu/gal of oil, 1050 Btu/ft^3 of gas, and a conversion factor of 3413 Btu/kW-hr. On the basis of the foregoing information, energy supplied by electric generating plants was assumed to be accomplished by nationwide reliance on the division of energy sources as given in Table 6-12. On a region-by-region basis, deviations from the nationwide average were selected for both 1975 and 1980 (Table 6-13).

For purposes of this study, it was sufficient to use a fixed value of 38 percent for generating plant efficiency and a fixed value of 92 percent for transmission/distribution line efficiency. The choice of operating efficiency is based on the expected growth in use of combined thermodynamic cycles for generating stations. This is in concert with the nationwide goal of conserving energy.

Emission factors for generating plants were used directly as given in Table 6-11. When performing analyses for 1975, the factors for 1975 were assumed to be the same as for 1973. The SO_x and particulate emissions were not included in any of the analyses.

6.4 REFERENCES

6-1. Statistical Year Book of the Electric Utility Industry for 1973, Publication No. 74-34, Edison Electric Institute, New York (November 1974).

6-2. W. G. Dupree, Jr. and J. A. West, United States Energy Through the Year 2000, U.S. Department of the Interior, Washington, DC (December 1972).

6-3. 56th Semi-Annual Electric Power Survey, Edison Electric Institute, New York (October 1974).

6-4. W. F. Hamilton, Impact of Future Use of Electric Cars in Los Angeles Region, EPA-460/3-74-020, U.S. Environmental Protection Agency, Research Triangle Park, N.C. (October 1974) (General Research Corporation; EPA Contract No. 68-01-2103).

6-5. O. W. Dykema, Analysis of Test Data for NO_x Control in Gas- and Oil-Fired Utility Boilers, EPA-650/2-75-012, U.S. Environmental Protection Agency, Research Triangle Park, N. C. (January 1975) (ATR-75(7487)-1, The Aerospace Corporation; EPA Grant No. R802366).

6-6. O. W. Dykema and V. E. Kemp, Inventory of Combustion-Related Emissions from Stationary Sources, EPA-600/7-76-012, U.S. Environmental Protection Agency, Research Triangle Park, N.C. (September 1976) (ATR-76(7549)-1, The Aerospace Corporation; EPA Grant No. R803283-01).

6-7. Compilation of Air Emission Factors, AP-42, U.S. Environmental Protection Agency, Research Triangle Park, N.C. (February 1972).

6-8. "Standards of Performance for New Stationary Sources," Federal Register, p. 24876 (23 December 1971).

TABLE 6-1. TOTAL ELECTRIC UTILITY INDUSTRY GENERATION, 1973 (Ref. 6-1)

Power Source	Electric Power Generated (kW-hr)
Prime Mover Driving Generator	
Hydro	271.053×10^9 (14.7%)
Conventional Steam	1488.713×10^9 (80.5%)
Nuclear Steam	83.292×10^9 (4.5%)
Internal Combustion	6.202×10^9 (0.3%)
Fuel	
Coal	845.986×10^9 (53.6%)
Oil	310.657×10^9 (19.7%)
Gas	336.001×10^9 (21.3%)
Nuclear	83.292×10^9 (5.3%)
Geothermal, Wood, and Waste	2.271×10^9 (0.1%)
Total	1849.260×10^9

TABLE 6-2. ELECTRIC POWER GENERATION BY GEOGRAPHIC REGIONS AND PRIME MOVER, 1973 (Ref. 6-1)

Region	Electric Power Generated [10^9 kW-hr (% of total)]				
	Total	Hydro	Conventional Steam	Nuclear Steam	Internal Combustion Engine
New England	72.180	5.354 (7.4)	52.145 (72.3)	14.372 (19.9)	0.309 (0.4)
Middle Atlantic	245.522	30.192 (12.3)	203.832 (83.0)	11.173 (4.6)	0.325 (0.1)
East North Central	344.693	3.854 (1.1)	310.686 (90.1)	28.837 (8.4)	1.316 (0.4)
West North Central	116.240	12.336 (10.6)	97.743 (84.1)	3.870 (3.3)	2.291 (2.0)
South Atlantic	331.283	19.313 (5.8)	293.730 (88.7)	17.704 (5.3)	0.536 (0.2)
East South Central	179.519	27.053 (15.0)	152.193 (84.8)	0.273 (0.2)	-
West South Central	217.043	9.799 (4.5)	206.395 (95.1)	-	0.849 (0.4)
Mountain	96.067	27.943 (29.1)	67.820 (70.6)	-	0.304 (0.3)
Pacific	239.960	134.913 (56.2)	97.969 (40.8)	7.063 (3.0)	0.015 (<0.1)
State of Washington	77.408	68.518 (88.5)	4.458 (5.8)	4.432 (5.7)	-
Alaska and Hawaii	6.753	0.296 (4.4)	6.200 (91.8)	-	0.257 (3.8)

TABLE 6-3. THERMALLY GENERATED ELECTRIC POWER BY GEOGRAPHIC REGIONS AND FUEL, 1973 (Ref. 6-1)

Region	Electric Power Generated [10^9 kW-hr (% of total)]				
	Total Thermal[a]	Coal	Oil	Gas	Nuclear
New England	66.826 (4.2)	2.888 (4.3)	49.084 (73.5)	0.482 (0.7)	14.372 (21.5)
Middle Atlantic	215.331 (13.7)	111.320 (51.7)	85.129 (39.5)	7.709 (3.6)	11.173 (5.2)
East North Central	340.835 (21.6)	287.119 (84.2)	14.160 (4.2)	10.719 (3.1)	28.837 (8.5)
West North Central	103.838 (6.6)	64.089 (61.7)	2.183 (2.1)	33.696 (32.5)	3.870 (3.7)
South Atlantic	311.970 (19.8)	185.380 (59.4)	87.522 (28.1)	21.364 (6.8)	17.704 (5.7)
East South Central	152.466 (9.7)	141.446 (92.8)	3.568 (2.3)	7.179 (4.7)	0.273 (0.2)
West South Central	207.143 (13.2)	6.530 (3.2)	12.287 (5.9)	188.326 (90.9)	-
Mountain	68.075 (4.3)	42.695 (62.7)	5.223 (7.7)	20.157 (29.6)	-
Pacific	102.995 (6.5)	4.275 (4.1)	46.244 (44.9)	45.413 (44.1)	7.063 (6.9)
Alaska and Hawaii	6.457 (0.4)	0.244 (3.8)	5.257 (81.4)	0.956 (14.8)	-
U.S. Total	1575.936 (100.0)				

[a]Excludes geothermal, wood, and waste.

TABLE 6-4. REGIONAL COMPOSITION BY STATES ACCORDING TO REF. 6-1

Region	State
New England	Maine New Hampshire Vermont Massachusetts Rhode Island Connecticut
Middle Atlantic	New York New Jersey Pennsylvania
East North Central	Ohio Indiana Illinois Michigan Wisconsin
West North Central	Minnesota Iowa Missouri North and South Dakota Nebraska Kansas
South Atlantic	Delaware Maryland District of Columbia Virginia West Virginia North and South Carolina Georgia Florida
East South Central	Kentucky Tennessee Alabama Mississippi
West South Central	Arkansas Louisiana Oklahoma Texas
Mountain	Montana Idaho Wyoming Colorado New Mexico

TABLE 6-4. CONTINUED

Region	State
Mountain	Arizona Utah Nevada
Pacific	Washington Oregon California
Alaska and Hawaii	

TABLE 6-5. PROJECTION OF PERCENTAGE ENERGY SOURCE CONTRIBUTION TO U.S. ELECTRIC POWER GENERATION (Ref. 6-2)

Energy Source	Electric Power Generation (%)				
	1971 (actual)	1975	1980	1985	2000
Coal	43.9	39.5	35.9	35.9	21.9
Oil	13.8	15.9	16.9	16.7	6.3
Gas	23.4	16.9	12.2	8.7	3.3
Nuclear	2.4	11.3	21.0	27.3	60.7
Hydro	16.5	16.4	14.0	11.4	7.8

TABLE 6-6. PROJECTION OF PERCENTAGE ENERGY SOURCE CONTRIBUTION TO TOTAL U.S. ELECTRIC POWER GENERATION (Ref. 6-3)

Energy Source	Electric Power Generation (%)[a]						
	1973 (actual	1974	1975	1976	1977	1978	1979
Coal	45.9	45.8	45.1	44.1	44.3	44.9	45.0
Oil	17.4	16.5	18.6	19.0	18.8	18.8	18.3
Gas	17.2	15.6	13.3	12.1	10.9	10.2	9.1
Nuclear	4.7	7.8	11.3	13.7	15.5	16.1	18.1
Hydro	14.5	14.0	11.4	10.8	10.1	9.6	9.1
Other	0.3	0.3	0.3	0.3	0.4	0.4	0.4

[a]Data does not include Alaska and Hawaii.

TABLE 6-7. PROJECTION OF PERCENTAGE ENERGY SOURCE CONTRIBUTION TO REGIONAL ELECTRIC POWER GENERATION (Ref. 6-3)

Source	1973 (actual)	1974	1975	1976	1977	1978	1979
Region I Electric Power Generation (%)							
Coal	30.3	31.6	28.6	26.3	25.1	24.8	25.4
Oil	47.0	41.8	40.8	41.9	40.5	41.2	39.4
Gas	2.4	1.5	0.4	0.3	0.6	0.5	0.5
Nuclear	7.5	13.1	19.2	21.2	24.1	24.2	25.9
Hydro	12.7	11.8	10.8	10.1	9.5	9.1	8.6
Other	0.1	0.2	0.2	0.2	0.2	0.2	0.2
Region II Electric Power Generation (%)							
Coal	92.4	89.0	87.9	85.3	84.3	83.9	79.7
Oil	3.3	3.5	3.5	3.3	3.1	2.9	2.7
Gas	1.8	1.7	1.5	1.4	1.3	1.2	1.2
Nuclear	1.3	4.0	5.4	8.4	9.7	10.5	14.8
Hydro	1.2	1.8	1.7	1.6	1.6	1.5	1.6
Other	0	0	0	0	0	0	0
Region III Electric Power Generation (%)							
Coal	60.4	58.9	57.5	54.9	53.0	50.6	48.5
Oil	17.7	16.9	17.3	15.8	15.2	14.9	15.1
Gas	6.1	4.9	3.4	2.9	2.5	2.2	1.7
Nuclear	4.7	9.6	14.5	19.5	22.8	26.2	28.8
Hydro	11.1	9.7	7.3	6.9	6.5	6.1	5.9
Other	0	0	0	0	0	0	0
Region IV Electric Power Generation (%)							
Coal	70.8	70.2	69.6	70.5	71.3	70.9	69.7
Oil	3.7	3.6	2.7	2.6	3.9	5.5	4.9
Gas	6.7	5.3	1.8	0.9	0.4	0.3	0.2
Nuclear	15.8	18.6	23.9	24.1	22.7	21.7	23.6
Hydro	2.3	1.9	1.7	1.6	1.5	1.4	1.3
Other	0.7	0.4	0.3	0.3	0.2	0.2	0.3

TABLE 6-7. CONTINUED

Source	1973 (actual)	1974	1975	1976	1977	1978	1979
Region V Electric Power Generation (%)							
Coal	7.9	8.9	10.0	11.6	16.2	22.9	29.4
Oil	8.3	9.0	11.2	14.1	14.8	13.8	13.2
Gas	83.4	80.2	75.7	71.8	64.9	59.5	52.3
Nuclear	-	0.7	2.0	1.5	3.2	2.9	4.3
Hydro	0.4	1.2	1.1	1.0	0.9	0.9	0.8
Other	0	0	0	0	0	0	0
Region VI Electric Power Generation (%)							
Coal	49.3	47.3	53.3	57.4	60.8	63.5	66.9
Oil	1.0	1.2	1.4	1.6	1.7	2.3	2.4
Gas	20.0	16.5	9.0	5.1	3.6	2.6	1.7
Nuclear	1.4	9.9	15.7	18.1	17.2	15.8	14.6
Hydro	28.1	25.0	20.6	17.8	16.7	15.8	14.4
Other	0.2	0.1	<0.1	-	-	-	-
Region VII Electric Power Generation (%)							
Coal	9.7	12.8	17.0	19.3	21.3	23.2	26.0
Oil	0.3	1.1	1.6	1.4	1.4	1.2	1.8
Gas	0.5	0.6	0.5	0.5	0.5	0.5	0.4
Nuclear	3.4	3.4	3.8	7.0	7.2	6.6	7.6
Hydro	86.1	82.1	77.1	71.8	69.6	68.5	64.2
Other	<0.1	<0.1	<0.1	<0.1	<0.1	<0.1	<0.1
Region VIII Electric Power Generation (%)							
Coal	11.8	14.0	15.3	17.5	18.5	19.5	20.9
Oil	29.3	33.6	53.0	54.9	53.6	53.7	53.2
Gas	31.0	17.9	9.1	3.7	1.8	1.2	0.8
Nuclear	1.5	2.5	5.9	8.1	10.3	10.4	10.6
Hydro	24.8	30.0	14.3	13.5	12.8	11.9	11.2
Other	1.6	2.0	2.4	2.3	3.0	3.3	3.3

TABLE 6-8. REGIONAL COMPOSITION BY STATES ACCORDING TO REF. 6-3

Region	State
I	Maine Vermont New Hampshire Massachusetts Rhode Island Connecticut New York New Jersey Delaware Portions of Pennsylvania and Maryland
II	Ohio Indiana Michigan Portions of Pennsylvania, Maryland, Kentucky, Virginia, and West Virginia
III	North and South Carolina Georgia Alabama Tennessee Florida Portions of Virginia, West Virginia, Kentucky, and Mississippi
IV	Wisconsin Illinois Iowa Portions of Minnesota, South Dakota, and Missouri
V	Texas Louisiana Arkansas Oklahoma Kansas Portions of New Mexico, Missouri, and Mississippi

TABLE 6-8. CONTINUED

Region	State
VI	North Dakota Nebraska Colorado Portions of South Dakota, Montana, Wyoming, New Mexico, and Minnesota
VII	Washington Oregon Idaho Utah Portions of Montana, Wyoming, Nevada, and California
VIII	Arizona Portions of California, Nevada, and New Mexico

TABLE 6-9. ESTIMATES ON AVAILABILITY OF COMMERCIAL TECHNOLOGY FOR ENERGY CONVERSION (Ref. 6-4)

Technology	Electrical Thermal Efficiency (%)	Year Available
Stand-Alone MHD	20-25	1980
MHD-Topped Power Plant	50-52	1985
MHD-Topped Power Plant	55-60	1995
Fuel Cells Using Reformed Methane	40-45	1976
Combined Cycle[a] Using Clean Fossil Fuels	40	1972
Combined Cycle[a] Using Clean Fossil Fuels	45	1978
Combined Cycle[a] Using Clean Fossil Fuels	48	1985
Fixed-Bed Gasification of Coal and Cymbined Cycle[a]	40	1975
Fixed-Bed Gasification of Coal and Combined Cycle[a]	45	1978
Fluid-Bed Gasification of Coal and Combined Cycle[a]	40	1982
Fluid-Bed Gasification of Coal and Combined Cycle[a]	45	1988
Fluid-Bed Gasification of Coal and Combined Cycle[a]	48	1992
Fluid-Bed Combustion Coal or Residual Oil: Rankine Cycle	38-41	1980
Thermionic Topping Fossil-Fuel Power Plants	45	1985
Gas Turbine-Brayton Cycle (Clean Fossil Fuels)	28	1972
Gas Turbine-Brayton Cycle (Clean Fossil Fuels	34	1978
Gas Turbine-Brayton Cycle (Clean Fossil Fuels)	38	1985

[a]Brayton-Rankine

TABLE 6-10. PROJECTED NUCLEAR AND FOSSIL-FUELED STEAM ELECTRIC PLANT THERMAL EFFICIENCIES (Ref. 6-2)

Year	Thermal Efficiency (%)	
	Nuclear	Fossil-Fueled
1971 (actual)	32	32.5
1975	32	33.5
1980	32	35.9
1985	32.8	37.0
2000	37.9	40.2

TABLE 6-11. POWER STATION EMISSION FACTORS (Refs. 6-5 through 6-8)

Emission	Oil	Gas	Coal
1973 Emission Factor (lb/1000 kW-hr)			
HC	0.048	0.003	0.041
CO	0.072	0.055	0.137
NO_x	2.030	2.040	3.140
SO_x	3.800	0.002	5.190
Particulates	0.287	0.078	2.590
1980 Emission Factor (lb/1000 kW-hr)			
HC	0.048	0.003	0.041
CO	0.072	0.055	0.137
NO_x	0.860	0.917	2.320
SO_x	2.720	0.002	4.100
Particulates	0.239	0.068	2.310

TABLE 6-12. ASSUMED DIVISION OF ENERGY SOURCES FOR STATIONARY ELECTRIC GENERATING PLANTS

Energy Source	Energy Source Division (%)	
	1975	1980
Coal	45.5	45.5
Oil	17.0	17.0
Gas	15.0	10.0
Nuclear and Hydroelectric	22.5	27.5

TABLE 6-13. ASSUMED DIVISION OF ENERGY SOURCES FOR STATIONARY ELECTRIC GENERATING PLANTS FOR FOUR GEOGRAPHIC REGIONS

Region	Energy Source Division (%)			
	Coal	Oil	Gas	Nuclear and Hydroelectric
Northern Pacific	10	0	0	90
East-North-Central	90	0	0	10
West-South-Central	15	10	75	0
New England and Middle Atlantic	25	45	0	30

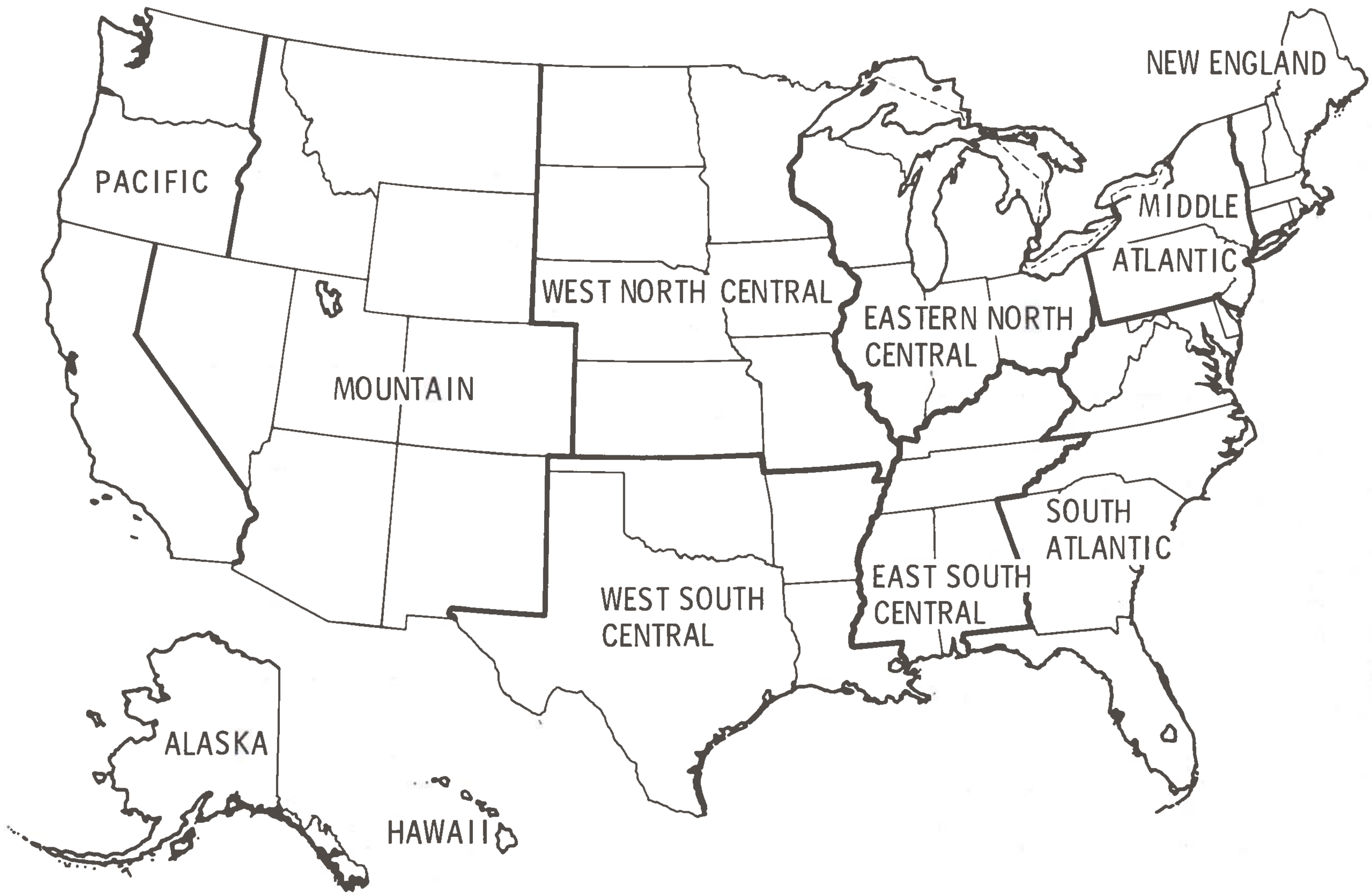

FIGURE 6-1. NINE-REGION DIVISION OF THE UNITED STATES (Ref. 6-1)

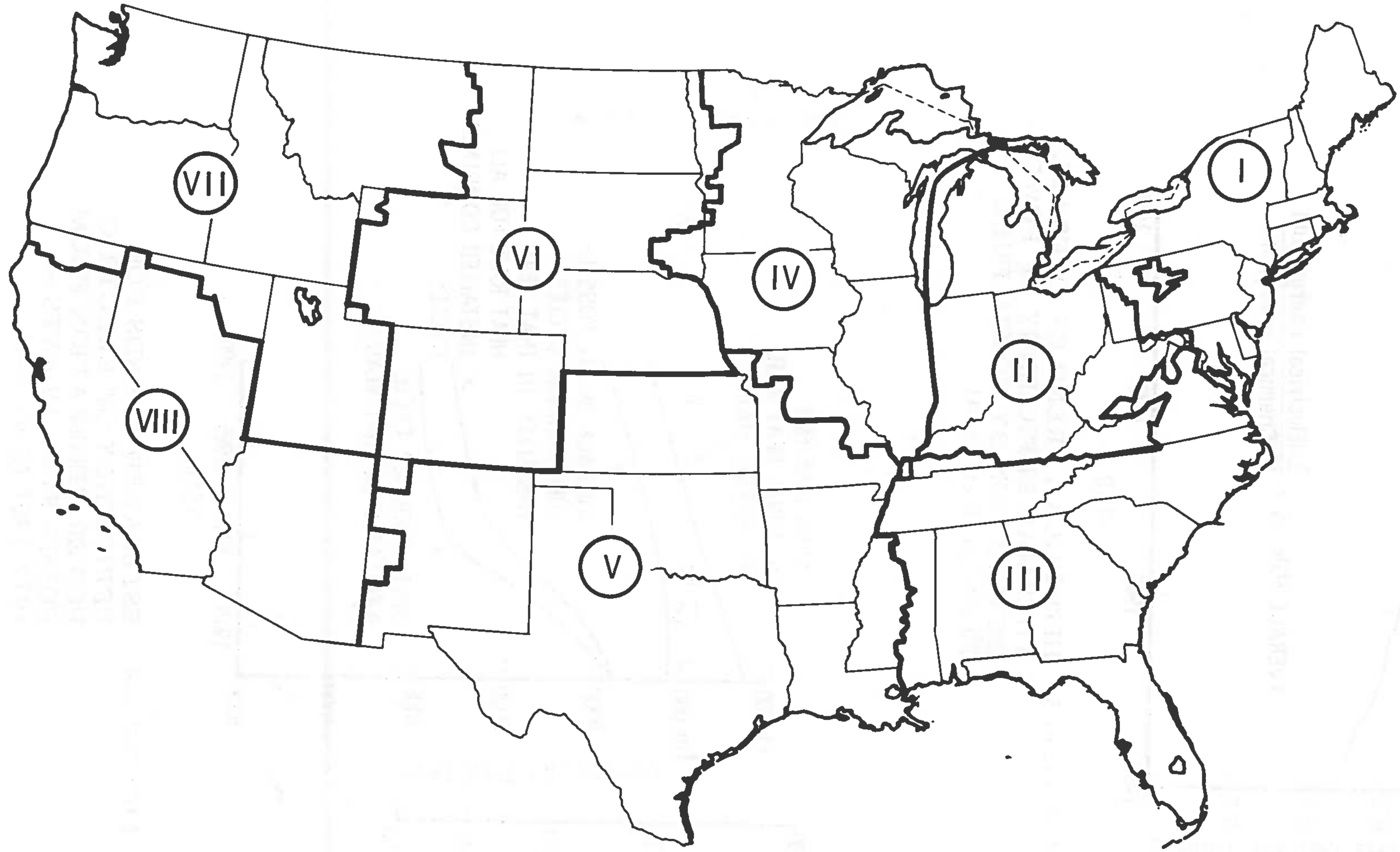

FIGURE 6-2. EIGHT-REGION DIVISION OF THE UNITED STATES (Ref. 6-3)

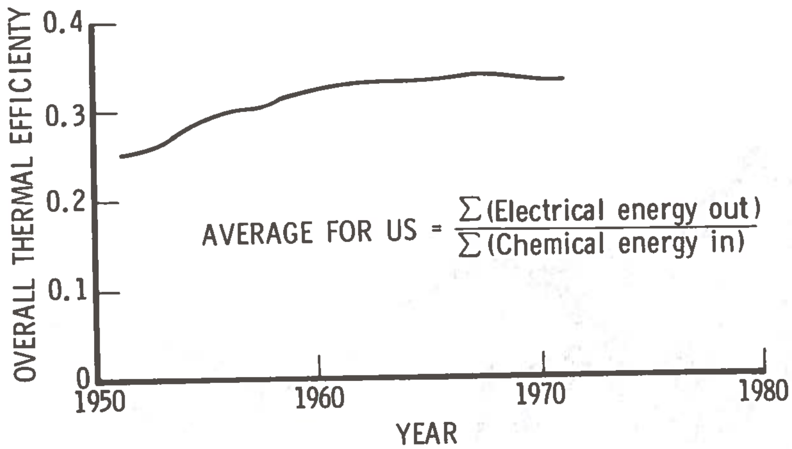

FIGURE 6-3. HISTORICAL TREND OF OVERALL THERMAL EFFICIENCY OF POWER GENERATION BY FOSSIL FUEL PLANTS (Ref. 6-4)

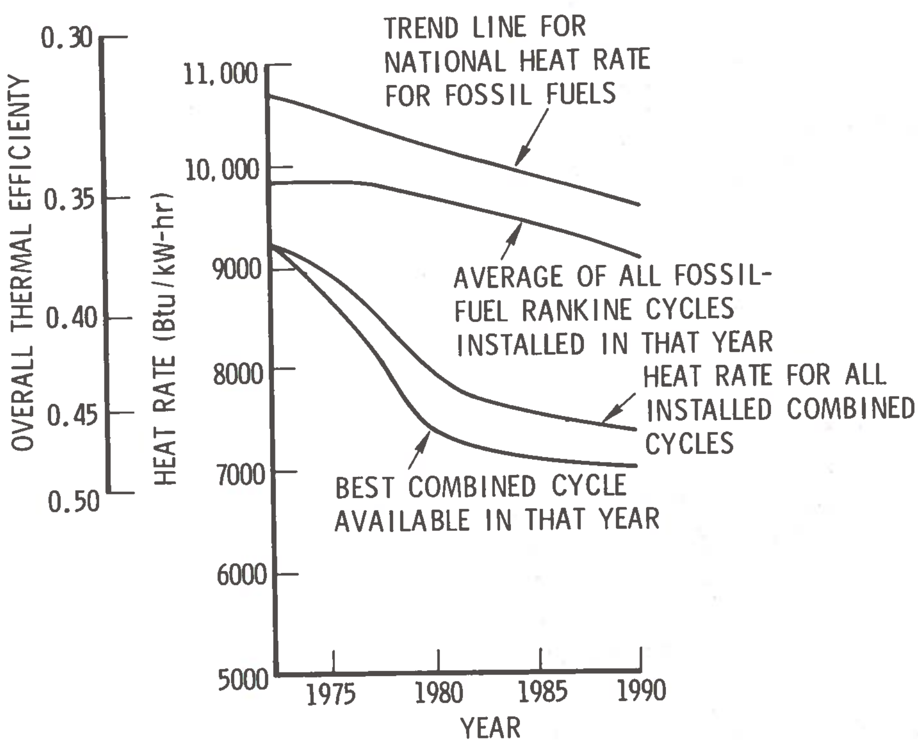

FIGURE 6-4. ESTIMATED TRENDS FOR EFFICIENCY OF ELECTRIC POWER GENERATION FROM FOSSIL FUEL PLANTS — 1972-1990 (Ref. 6-4)

7. SELECTED CHARACTERISTICS FOR HYBRID AND CONVENTIONALLY POWERED (BASELINE) VEHICLES

The vehicle characteristics discussed are of two types: performance and physical. The selected values are based both on figures for current conventional vehicles and on estimated figures for possible designs of the future that are required to meet increasingly stricter government regulations for fuel consumption and exhaust emissions. Such considerations dictate the inclusion of vehicle characteristics related to designs with lightweight bodies, reduced acceleration, and reduced maximum cruise speed.

7.1 HYBRID VEHICLE CHARACTERISTICS

Three vehicles were selected for evaluation: a 2500-lb car,* a 4000-lb car,* and a 6000-lb van.* Vehicle characteristics that are used to determine road load are given in Table 7-1.

Maximum performance of these vehicles is specified by design peak cruise speed and design peak acceleration, where the latter specification is given by the time to reach 60 mph from a stop. These figures are given in Table 7-2. It should be noted that the peak design cruise speed is based solely on the use of heat engine power to achieve this speed. Power augmentation from the energy storage system can permit a considerable increase in speed for short periods (e.g., passing another vehicle), subject to design speed limits for other elements in the powertrain (e.g., drive motor).

Within the guidelines established for this study, the design acceleration has very little effect on powertrain component efficiency** during vehicle operation over a given driving cycle. However, the design cruise speed does have a significant impact on the powertrain efficiency because, for example, it affects the size of the heat engine, which for a given power setting determines the fraction of full-load operation during a driving cycle, and this in turn affects fuel consumption and emissions.

---

*Loaded weight (includes 300 pounds for occupants and luggage in passenger cars and 1000 pounds for occupants and cargo in vans).

**Primarily the electric drive motor efficiency due to changes in power rating, speed rating, and size as design acceleration varies.

No specifications were set for gradeability or range; these factors are determined separately for each vehicle based on its design speed, design acceleration, and method of heat engine operation.

In regard to available weight and volume for the hybrid powertrain, specifications used in Ref. 7-1 were also used in this study, but with some variations. For a car with a loaded weight of 4000 pounds, a powertrain weight of 1500 pounds was initially assigned in Ref. 7-1. This is 40.5 percent of a curb weight of 3700 pounds and was recognized in Ref. 7-1 as possibly being a liberal figure for a conventional car. Indeed, a figure of 1210 pounds (32.7 percent of curb weight) was proposed later in the study, but too late to adjust the original guidelines. It is interesting to note, however, that for a curb weight of 2930 pounds for the General Motors Stir-Lec I hybrid car, 1189 pounds (or 40.5 percent) was contained in the powertrain (Ref. 7-2). Other data, given in Ref. 7-3, show a powertrain weight equal to 27 percent of a Ford Pinto curb weight of 2436 pounds and 31.7 percent of a Mercury Comet curb weight of 2926 pounds. Reference 7-4 notes that the powertrain consists of the following weight division for the Pinto:

Engine and cooling	400 lb
Driveline	14
Transmission	61
Clutch	27
Exhaust	30
Fuel	86
Electric power	39
Total	657 lb

Because of the difficulty in establishing a proper figure for allowable powertrain weight, a factor of 37.5 percent of vehicle loaded weight was used in all cases.

It is recognized that the weight allowance for the powertrain can impact on component design requirements. As noted in Section 2.4, the weight of all components, except the energy storage system, is subtracted from the allowable powertrain weight. The balance could then be used as a design requirement for the energy storage system in terms of specific power (watts per pound) and specific energy (watt-hours per pound). A similar approach could be used to evaluate the impact of allowable power-train volume on component design requirements.

7.2 CONVENTIONALLY POWERED (BASELINE) VEHICLE CHARACTERISTICS

The conventional vehicle is considered to be the domestic automotive product powered by a reciprocating piston, spark ignition engine fueled by gasoline. It is used in the analysis as a baseline vehicle for purposes of comparing energy consumption and exhaust emissions of the hybrid vehicle. For a given loaded weight, it was assumed that the physical characteristics of the conventional vehicle were identical to those of the hybrid vehicle (including passenger and luggage space), as specified in Table 7-1. With regard to performance characteristics, all conventional vehicles should be able to exceed the 80-mph peak cruise speed. Acceleration times are variable, depending on the installed engine power and vehicle weight; except for special performance vehicles, the times are certainly bracketed by the values given in Table 7-2.

For reference purposes, the two most important characteristics are energy consumption and exhaust emissions. With regard to the EPA Urban Driving Cycle (Ref. 7-5) and the EPA Highway Driving Cycle (Ref. 7-6), energy consumption data for each vehicle weight are based on the average, sales-weighted gasoline mileage figures given in Ref. 7-7 for 1975 model year vehicles tested on chassis dynamometers while operating over these cycles.

For the U.S. Postal Service Driving Cycle (Ref. 7-8), there are no well-documented figures for fuel consumption or emissions for conventionally powered vehicles, particularly as used in the present analysis where the cycle has been modified slightly by using the basic acceleration, deceleration, and loiter periods, but reducing the degree of repetition in order to avoid lengthy computer time. Hence, fuel consumption of conventionally powered vehicles operating on the U.S. Postal Driving Cycle was estimated by use of the vehicle simulation computer program described in Ref. 7-9. An order-of-magnitude comparison of results was afforded by the data given in Ref. 7-10, which shows fuel energy consumption of 5.1 kW-hr/mi for a 1/4-ton Jeep-type vehicle operating on mail delivery routes in Cupertino, California. No vehicle test weights or velocity histories were available for comparison with the cycle used in the present study.

Table 7-3 shows the mileage figures for the three vehicle weights analyzed in the present study. Also given in Table 7-3 is the conversion to equivalent energy in kilowatt-hours per mile of the fuel consumed by the engine. This conversion was accomplished by use of the equation

$$\frac{\text{kw-hr}}{\text{mi}} = \frac{6.2\,\frac{\text{lb}}{\text{gal fuel}} \times 18,600\,\frac{\text{Btu}}{\text{lb fuel}} \times 2.93 \times 10^{-4}\,\frac{\text{kw-hr}}{\text{Btu}}}{\text{mi/gal}} \qquad (7\text{-}1)$$

The reference exhaust emissions are the federally mandated interim standards for the 1975-76 model year, light-duty vehicles (Ref. 7-11). These are:

Hydrocarbons (HC)	1.5 gm/mi
Carbon monoxide (CO)	15.0 gm/mi
Oxides of nitrogen (NO_x)	3.1 gm/mi

These standards must be met by the 2500-lb, 4000-lb, and 6000-lb vehicles in a cold-start, constant volume sampling test procedure described in Ref. 7-5. They are applicable only to the EPA Urban Driving Cycle; no standards are given for the EPA Highway Driving Cycle or U.S. Postal Driving Cycle.

For determining vehicle operating range, the vehicle fuel economy in miles per gallon must be multiplied by the capacity of the fuel tank in gallons. Fuel tank capacities that were assumed for both hybrid and conventionally powered vehicles, along with the calculated range, are given in Table 7-4.

Of general interest is the energy that is expended at the vehicle drive wheels while traversing a given type of driving cycle. A curve showing this relationship with vehicle loaded weight is presented in Figure 7-1 for each of the driving cycles considered in this study. (The values shown are applicable to both hybrid and conventionally powered vehicles.) While the urban and highway cycles have similar energy requirements, the postal cycle requirements are considerably less. The large jump in energy needs for the 6000-lb van are due to the large aerodynamic drag for this vehicle compared to the lower profile (reduced frontal area) of the automobile. The cited increase is not apparent for the postal cycle because the low vehicle speeds preclude any significant aerodynamic effect; hence, a simple straight-line relationship with weight is the result. Evidently, drag coefficients and frontal areas used in the calculations for various size vehicles can have a noticeable effect on energy requirements, particularly for those driving cycles with higher average speeds.

7.3 REFERENCES

7-1. Hybrid Heat Engine/Electric Systems Study, Final Report, TOR-0059(6769-01)-2, The Aerospace Corporation, El Segundo, Calif. (1 June 1971).

7-2. P. Argarwal, R. Mooney, and R. Toepel, Stir-Lec I, A Stirling Electric Hybrid Car, GMR 840, General Motors Corporation, General Motors Research Laboratories, Detroit, Mich. (13 January 1969).

7-3. L. E. Unnewehr, et al., Electric Vehicle Systems Study, SR-73-132, Ford Motor Company, Dearborn, Mich. (October 1973).

7-4. L. E. Unnewehr, Electric Vehicle Systems Study, Ford Motor Company, Paper No. 7414, presented at the Third Electric Vehicle Symposium and Exposition, Washington, D.C., 19-21 February 1974.

7-5. "New Motor Vehicles and New Motor Vehicle Engines -- Control of Air Pollution," Federal Register, Vol. 37, No. 221, Part II, pp 24316-24318, 15 November 1972.

7-6. Federal Register, Vol. 39, No. 200, pp 36897-36898, 15 October 1974.

7-7. Factors Affecting Automotive Fuel Economy, Environmental Protection Agency, Office of Air and Waste Management, Mobile Source Air Pollution Control, Emission Control Technology Div., Ann Arbor, Mich. (September 1975).

7-8. Truck, Electric, Light Delivery, 500 Pound Payload, 50 Cubic Feet Cargo Compartment Capacity, USPS-PD-155 (DS), Purchase Description, U.S. Postal Service, Washington, D.C., 28 September 1973.

7-9. H. S. Porjes, C. Speisman, and P. H. Young, "An Advanced Computer Program For Determining Vehicle Emissions and Fuel Economy Under Road Traffic Conditions," The Aerospace Corporation, Paper presented at Transpo LA Symposium, Los Angeles, Calif., 12 November 1975.

7-10. "4 for 1 EV Comparison Data - a Report from Cupertino," Electric Vehicle News, The Porter Corporation, Westport, Conn., November 1973.

7-11. 40 C.F.R. 85.075 (1)* as revised by 38 FR. 17441 (7.2.73).**

*Code of Federal Regulations, Title 40, Part 85 (in Federal Register cited in Ref. 7-6).

**Federal Register, Vol. 38, p. 17441, 2 July 1973.

TABLE 7-1. PHYSICAL CHARACTERISTICS FOR HYBRID VEHICLES

Vehicle Loaded Weight (lb)	Tire Radius (ft)	Tire Pressure (psi)	Drag Area (ft^2)	Drag Coefficient (Dimensionless)
2500	0.98	25	19.0	0.45
4000	1.09	25	22.8	0.45
6000	1.215	40	35.0	0.76

TABLE 7-2. PERFORMANCE CHARACTERISTICS FOR HYBRID VEHICLES

Vehicle Loaded Weight (lb)	Design Peak Cruise Speed (mph)	Range of Design Peak Acceleration, Time from 0 to 60 mph (sec)
2500	65	11-20
4000	55	11-20
4000	65	11-20
4000	80	11-20
6000	65	21-30

TABLE 7-3. FUEL ENERGY EXPENDITURE OF CONVENTIONAL VEHICLES

Driving Cycle	Characteristic	Vehicle Loaded Weight (lb)		
		2500	4000	6000
Urban	Mileage (mpg)	21.7	14.2	9.3
	Energy Expended (kW-hr/mi)	1.56	2.38	3.64
Highway	Mileage (mpg)	31.0	19.4	14.1
	Energy Expended (kW-hr/mi)	1.09	1.74	2.40
Postal	Mileage (mpg)	12.4	8.1	5.3
	Energy Expended (kW-hr/mi)	2.72	4.15	6.34

TABLE 7-4. FUEL TANK CAPACITIES FOR STUDY VEHICLES AND RANGE FOR CONVENTIONALLY POWERED VEHICLES

Vehicle Loaded Weight (lb)	Assumed Fuel Tank Capacity (gal)	Conventionally Powered Vehicle Range (mi)		
		Urban Driving Cycle	Highway Driving Cycle	Postal Driving Cycle
2500	12.5	271	387	155
4000	20.0	284	388	163
6000	30.0	279	423	160

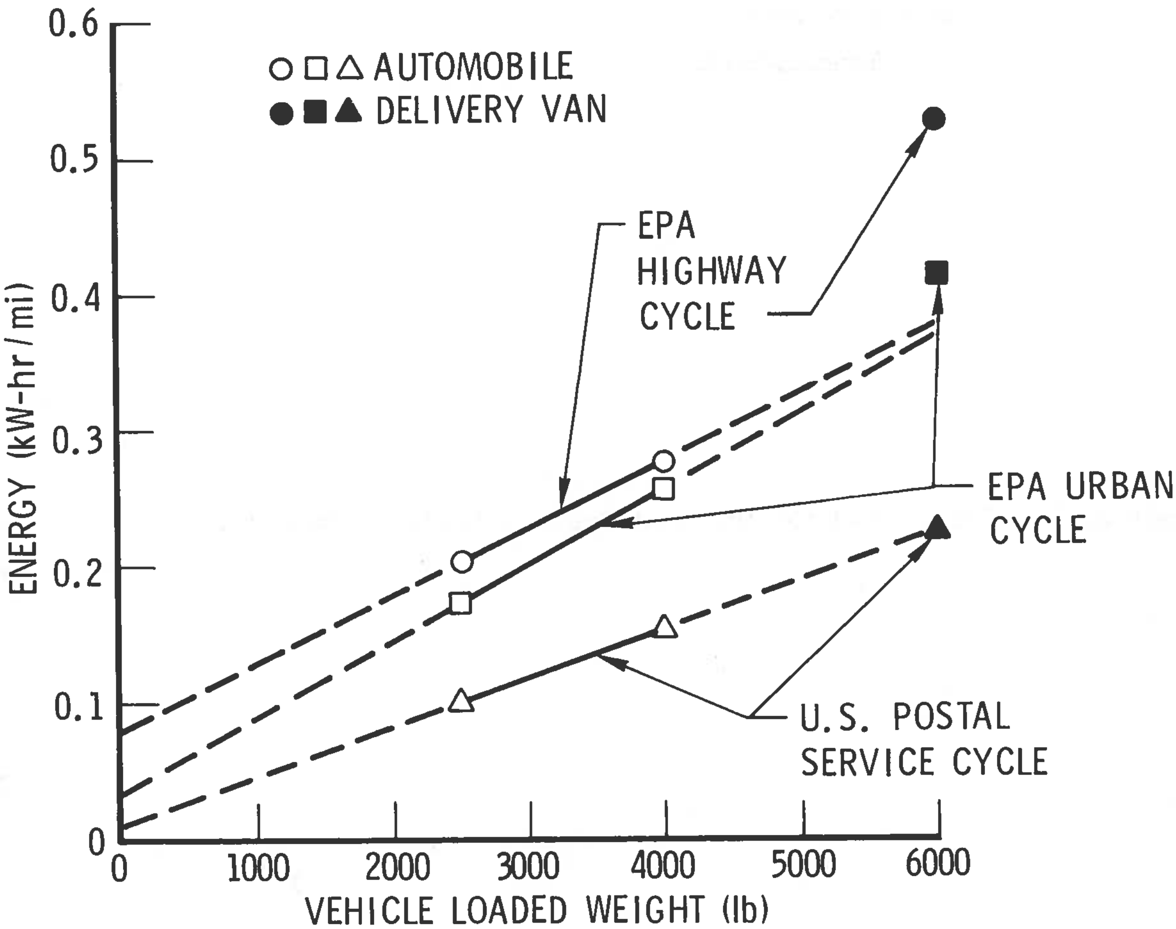

FIGURE 7-1. ENERGY EXPENDED AT VEHICLE DRIVE WHEELS FOR VARIOUS DRIVING CYCLES

8. HYBRID VEHICLE SIMULATION COMPUTER PROGRAM

8.1 SERIES CONFIGURATION

The overall computer program for the series configuration was constructed in stages and is divided into major elements which, in turn, are divided into subelements. The major elements comprise one program used for sizing the powertrain components and a second program used for determining vehicle energy consumption and related exhaust emissions. Each of these major programs is then made up of separate programs for heat engine/battery and heat engine/flywheel powertrains. These subelements were constructed from modules (termed subroutines), which may be combined, much as building blocks, to create any one of several possible structures. A typical subroutine is used to calculate the power required at the drive wheels for vehicle propulsion; this subroutine also provides calculations of wheel torque and axle speed.

Given the power, torque, and speed requirements at the drive wheels, along with gear ratios in various parts of the powertrain, the program is designed to permit calculations of power, torque, and speed at various points in the powertrain. Such calculations required modeling of all power-transmitting and energy-storing elements. Unless scaling considerations dictated otherwise, these simulation models were unaffected by variations in the size of a particular component. For example, the battery characteristics are not revised for different-size batteries, but the engine auxiliaries and the vehicle accessories are scaled according to engine rated power and vehicle weight.

The Powertrain Component Sizing Program relies on two factors in performing calculations: (a) a specified variation in vehicle speed history for accelerations from 0 to 60 mph, and (b) a peak cruise speed for the vehicle. A series of design acceleration curves was coded into the program; access to an individual curve is accomplished by simply stating which curve is desired. The design peak cruise speed is stated as an input quantity. For illustrative purposes, Figure 8-1 presents a summary plot of all acceleration curves for automobiles and vans. (Detailed acceleration profiles are tabulated in Section 9.)

For a given vehicle, the sizing computer program determines power flow throughout the powertrain at intervals of one second, while the vehicle follows the acceleration profile. Power flow is also calculated at the selected peak cruise speed. Component sizing is then carried out according to the methods and sizing curves discussed in Section 9. A flow diagram for the sizing program is shown in Figure 8-2.

The Energy Consumption and Emissions Program is larger and much more complex than the Powertrain Component Sizing Program. For the selected means of vehicle simulation, the battery and flywheel energy storage systems, for example, required more extensive modeling of performance characteristics, along with characteristics for the stationary electric generating station fuel consumption and exhaust emissions. Furthermore, the system logic for control of power flow from the heat engine and energy storage device introduces additional complexities to the program algorithms. Logical flow diagrams and subroutines are presented in Figure 8-3 for the heat engine/battery powertrain and in Figure 8-4 for the heat engine/flywheel powertrain.

From the discussion of hybrid vehicle powertrains given in Section 2 and the discussion of characteristics of powertrain elements and power sources given in Sections 5 and 6, a complete simulation model was constructed for the computer program. Schematic drawings illustrating the direction of power flow and the type of component modeling to be found in the computer program are presented in Figures 8-5 and 8-6 for the heat engine/battery and heat engine/flywheel systems, respectively.

8.2 PARALLEL CONFIGURATION AND REGENERATIVE BRAKING

The effects of a parallel configuration and of regenerative braking were determined separately by modifying in discrete steps the series configuration distribution of heat engine power to the drive wheels and to the energy storage system, respectively. (See Section 2 for schematic of powertrain concepts). For the heat engine/battery parallel configuration, it was estimated that the heat engine output shaft energy (exclusive of battery recharge energy and vehicle accessory/engine auxiliary drive energy) would be 70 percent of that required in the series configuration, regardless of driving cycle. This figure was based on the improved efficiency of an automatic transmission compared with the combined efficiencies of the generator/drive motor set. For the heat engine/flywheel parallel configuration, the automatic transmission efficiency was fixed at 90 percent, and this was reflected in a variable impact on series configuration drive shaft energy ranging from 63 to 84 percent, depending on the particular driving cycle being considered. In both the battery and flywheel systems, it was assumed that engine effeciency (or brake specific fuel consumption) was equivalent to that determined for the series configuration.

Regenerative braking was treated parametrically. Various percent energy recovery values were used for comparative purposes for each of the vehicle driving cycles. The percent energy recovery refers to the percent of total driving cycle energy expended at the vehicle wheels that is recovered and delivered into the energy storage system by the regenerative braking system. This energy recovery amount was then used to reduce the energy required from the heat engine for recharging the energy storage system.

The vehicle-related energy consumption and exhaust emissions were calculated as a function of γ, the fraction of recharge energy that is provided by the on-board heat engine (or heat engine plus regenerative braking). When $\gamma = 0$, all recharging is accomplished by power from an electric wall out (supplied by a stationary electric generating plant); when $\gamma = 1.0$, all recharging is accomplished by power from the engine on board the vehicle. Intermediate values designate the division of recharging between these two energy sources.

To illustrate the above effects, Figure 8-7 shows the split of heat engine shaft output energy over the EPA Urban Driving Cycle for the 4000-lb heat engine/battery hybrid car with the series configuration powertrain. Figure 8-8 depicts the effect on heat engine energy required as the configuration is changed to parallel, and as regenerative braking is added to both series and parallel powertrain configurations of the same 4000-lb car over the same EPA Urban Driving Cycle. In the case of regenerative braking, a γ of 0 is not possible, of course, because regeneratively stored energy always assures $\gamma > 0$, even if the heat engine portion of battery recharge energy is reduced to zero.

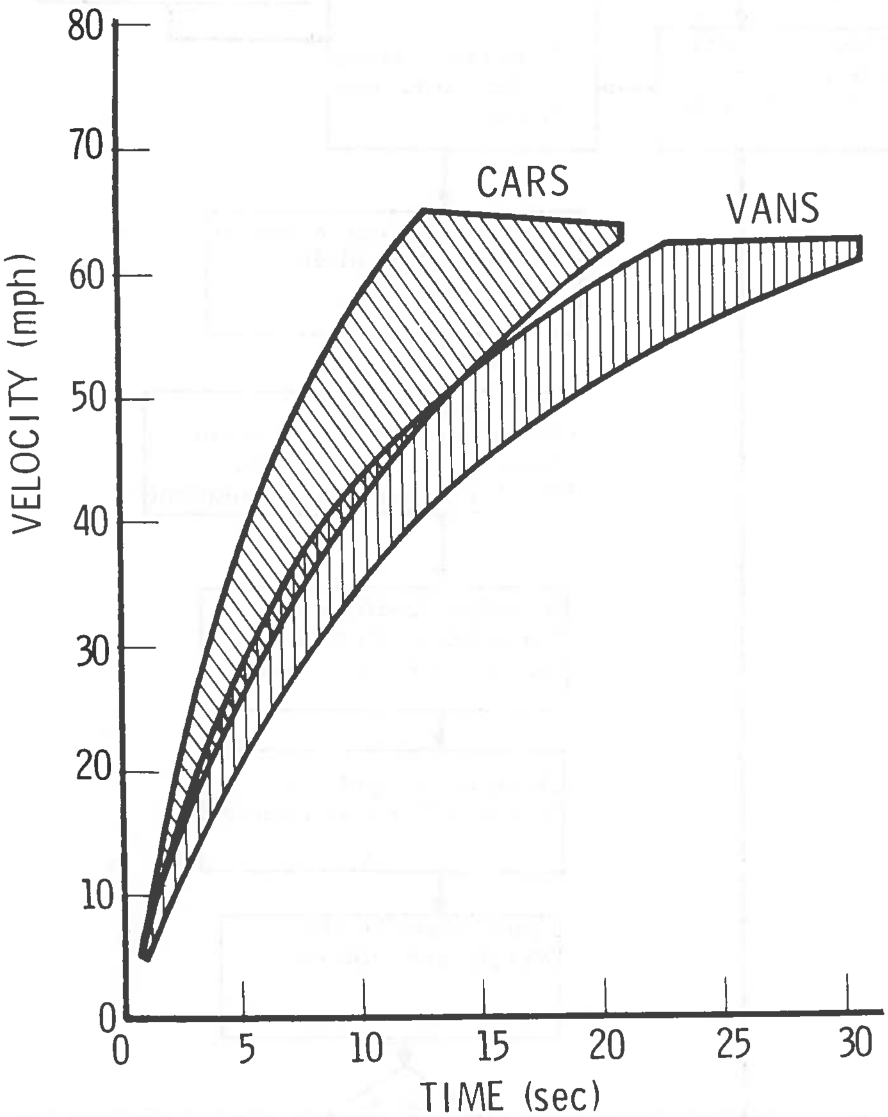

FIGURE 8-1. VEHICLE ACCELERATION PROFILES

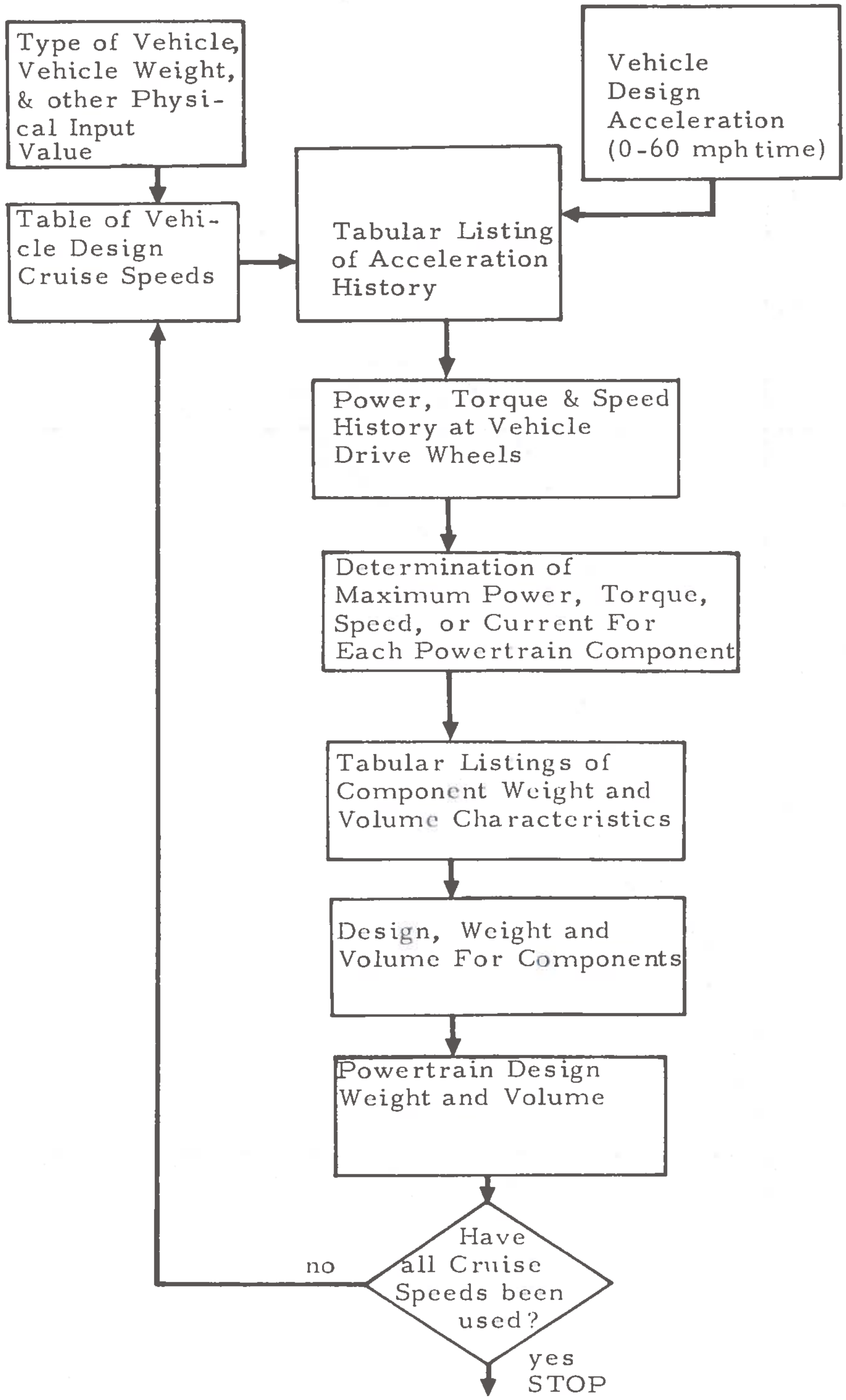

FIGURE 8-2. FLOW DIAGRAM FOR POWERTRAIN COMPONENT SIZING COMPUTER PROGRAM

I. Main Program

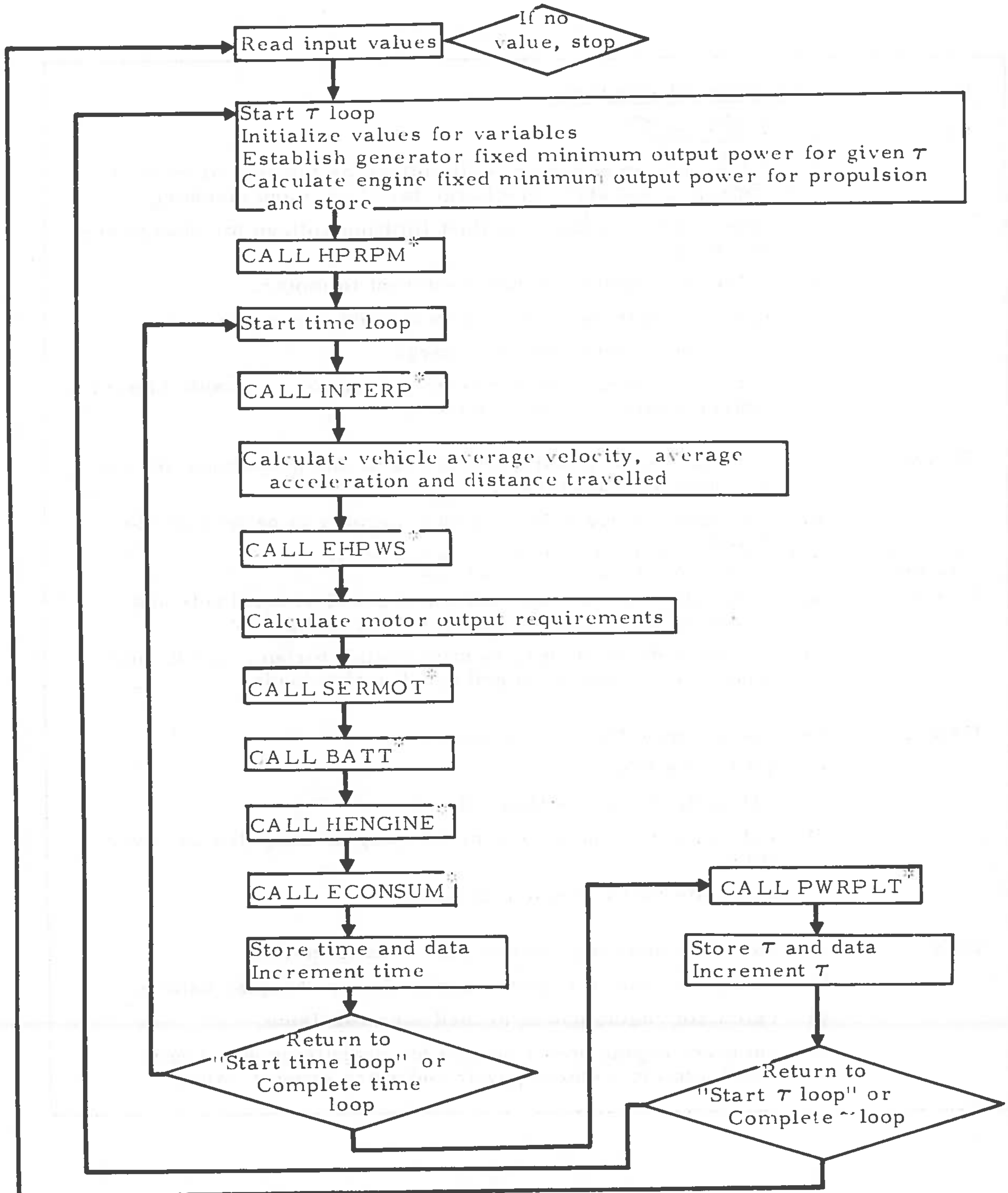

* Caps refer to Execution Sub-routines

FIGURE 8-3. FLOW DIAGRAM FOR ENERGY CONSUMPTION AND EMISSIONS COMPUTER PROGRAM, HYBRID HEAT ENGINE/BATTERY VEHICLE SIMULATION, SERIES CONFIGURATION

II.	Execution Sub-Routines
BATT	a) CALL GEN
	b) table look-up of battery cell voltage as function of current, capacity, and state-of-charge for charge and discharge.
	c) check battery voltage against limiting voltage for charge and discharge.
	d) calculate battery discharge current to motor.
	e) calculate battery charge current from generator.
	f) calculate battery state-of-charge
	g) calculate charging power from generator, allowable battery charge power and power wasted.
ECONSUM	a) calculate energy delivered by engine for propulsion and for accessories/auxiliaries.
	b) calculate energy delivered by generator to battery and to motor.
EHPWS	a) calculate vehicle road cruise and acceleration loads and resulting drive wheel torque, speed, and power.
	b) calculate drive shaft (into differential) torque, speed, and power for vehicle road and acceleration loads.
GASCLC	a) scale engine brake horsepower
	b) CALL TABNEW
	c) calculate fuel mass flow rate
	d) calculate fuel mass consumed by engine and integrate over time.
	e) calculate fuel remaining in tank
GEN	a) calculate generator power delivered to motor.
	b) calculate generator power available for charging battery.
	c) calculate engine power needed for propulsion.
	d) compare engine power needed for propulsion with engine fixed minimum output power and store greater value.

FIGURE 8-3. CONTINUED

II. <u>Execution Sub-Routines (continued)</u>

HENGINE

a) when required engine propulsion power is less than engine fixed minimum power level, use previously calculated brake horsepower and rpm established at CALL HPRPM before "start time loop", or

a') when required engine propulsion power is greater than engine fixed minimum power level, CALL HPRPM.

b) calculate engine brake mean effective pressure.

c) CALL SMOGCLC

d) CALL GASCLC

HPRPM

a) <u>USE HORSPWR</u>* (initial estimate for brake horsepower is engine propulsion power)

b) calculate speed of accessories/auxiliaries power shaft

c) <u>USE DRIVLIN</u>*

d) start loop

e) add accessories/auxiliaries power to engine propulsion power to get engine brake horsepower.

f) <u>USE HORSPWR</u>*

g) calculate speed of accessories/auxiliaries power shaft

h) <u>USE DRIVLIN</u>*

i) store value for accessories/auxiliaries power and engine power

j) return to "start loop" or

j') complete loop when case-to-case variation in engine brake horsepower doesn't exceed given delta horsepower.

INTDBL

a) table look-up of engine brake specific emissions as function of brake mean effective pressure and rpm.

INTERP

a) table look-up of vehicle velocity as function of time.

PWRPLT

a) calculate fuel energy used by vehicle engine and divide by reference energy.

b) calculate energy needed to recharge battery

---

* Underline and caps refers to Block Data Sub-Routine.

FIGURE 8-3. CONTINUED

II.		Execution Sub-Routines (continued)
PWRPLT	c)	calculate fuel energy used by electric generating plant.
	d)	calculate combined fuel energy used by vehicle and powerplant and divide by reference energy.
	e)	divide vehicle emissions by reference emissions.
	f)	USE SUMTBL*
	g)	calculate electric generating plant emissions.
	h)	calculate emissions combined from vehicle and powerplant and divide by reference emissions.
	i)	calculate vehicle range based on either vehicle fuel tank or on energy in battery whichever gives lesser range value.
SERMOT	a)	calculate motor voltage, current and power input.
SMOGCLC	a)	CALL INTDBL
	b)	calculate mass emissions and integrate with time.
TABNEW	a)	table look-up of engine brake specific fuel consumption as function of scaled brake horsepower and rpm.

* Underline and caps refers to Block Data Sub-Routine.

III.	Block Data Sub-Routine
DRIVLIN -	table of accessories/auxiliaries power as function of shaft speed.
HORSPWR -	table of engine speed as function of brake horsepower.
SUMTBL -	table of electric generating powerplant specific emissions factors as function of type of fuel used.

FIGURE 8-3. CONTINUED

IV. Input Values

A. Physical

a) vehicle weight

b) vehicle frontal area and drag coefficient

c) vehicle tire pressure and radius

d) vehicle fuel tank fluid mass

e) number of battery cells

f) baseline engine piston displacement

g) design engine piston displacement

B. Performance

a) vehicle design peak cruise speed

b) vehicle design peak acceleration

c) vehicle reference energy consumption

d) vehicle accessories/auxiliary power and scaling factors

e) baseline engine rated power

f) design engine rated power

g) generator rated current, voltage, power, speed, and efficiency.

h) motor rated current, voltage, torque, speed, power, and loss factors.

i) electrical system rated voltage

j) battery rated current, voltage, and capacity

k) battery charge/discharge efficiency for on-board generator charge and for off-board stationary charge.

l) control systems efficiencies

m) gear systems gear ratios and efficiencies

C. External Environment

a) vehicle velocity history

b) road grade

D. Program Control

a) initial and increment values for time and τ.

b) number of time and τ values.

FIGURE 8-3. CONTINUED

I. Main Program

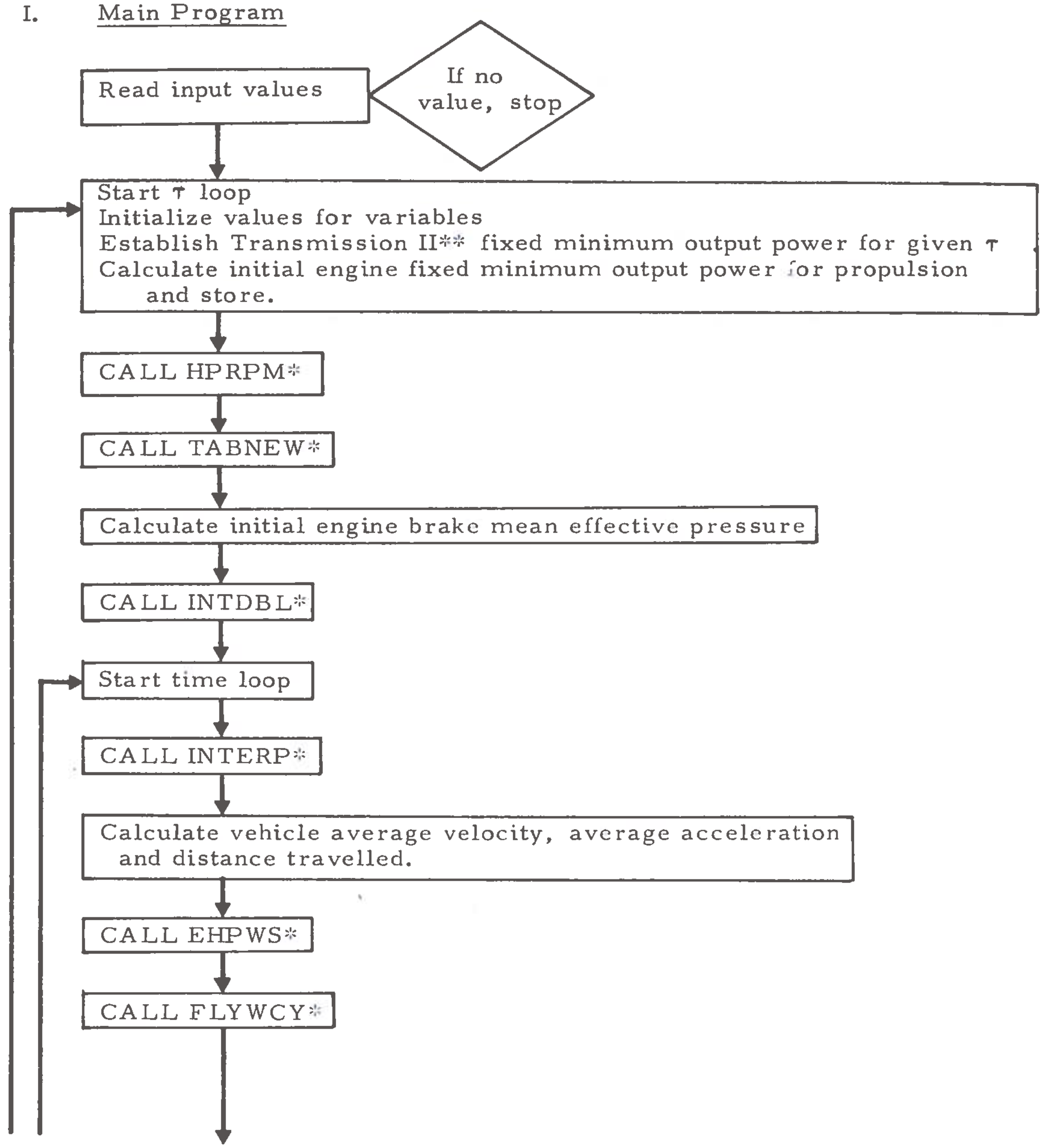

* Caps refer to Execution Sub-routines

** Transmission I is in Parallel Configuration

FIGURE 8-4. FLOW DIAGRAM FOR ENERGY CONSUMPTION AND EMISSIONS COMPUTER PROGRAM, HYBRID HEAT ENGINE/FLYWHEEL VEHICLE SIMULATION, SERIES CONFIGURATION

I. Main Program (continued)

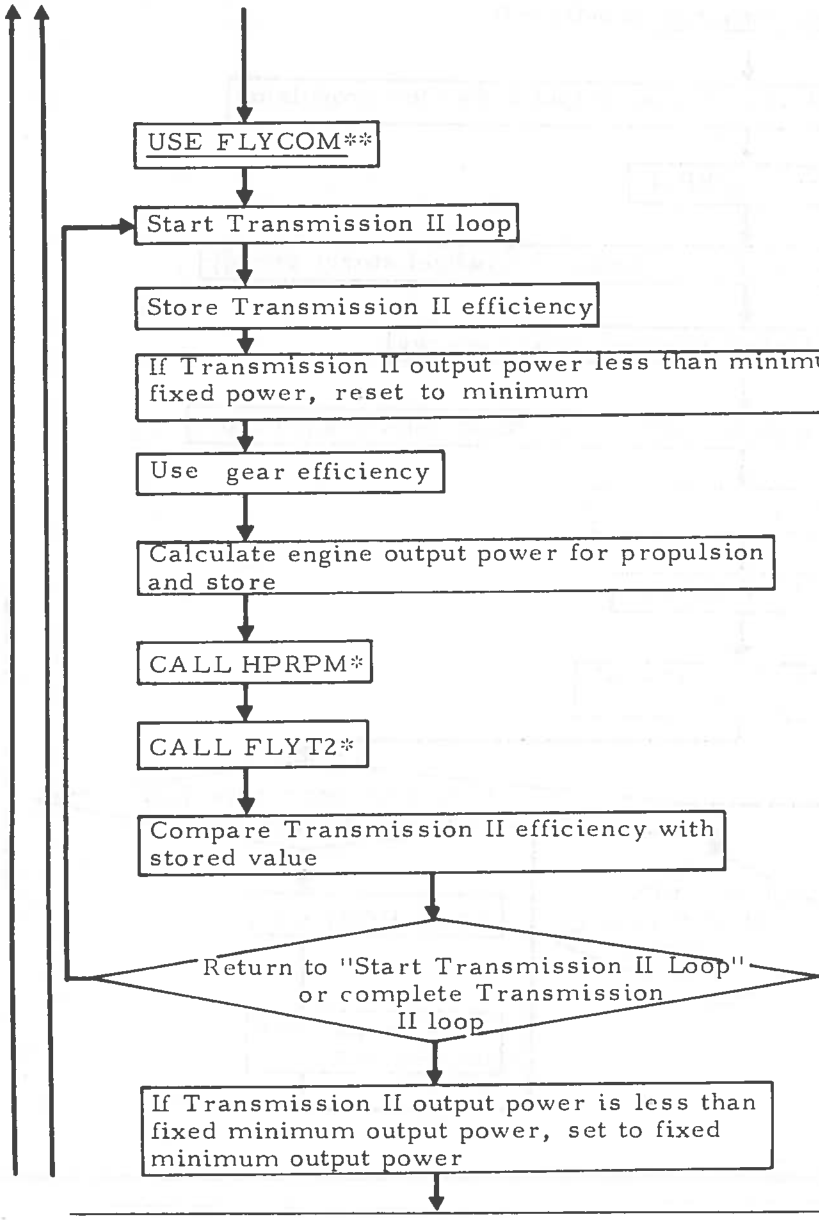

* Caps refer to Execution Sub-routines

** Underline and Caps Refer to Block Data Sub-routine

FIGURE 8-4. CONTINUED

I. Main Program (continued)

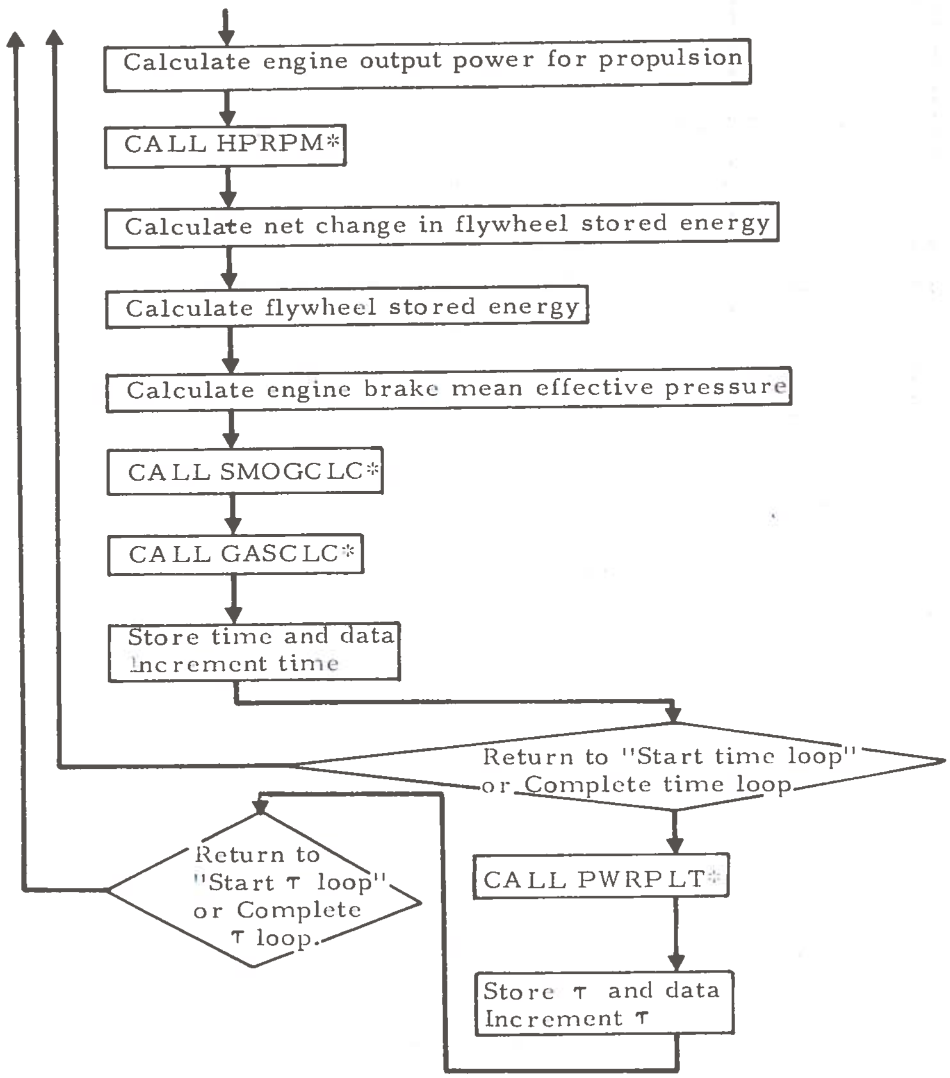

---

* Caps refer to Execution Sub-routine

FIGURE 8-4. CONTINUED

II.	Execution Sub-Routines	
EHPWS	a)	calculate vehicle road cruise and acceleration loads and resulting drive wheel torque, speed, and power.
	b)	calculate driveline torque, speed, and power output (into differential) for vehicle road and acceleration loads.
FLYT2	a)	use gear ratios, engine speed and flywheel speed to calculate Transmission II output speed and Transmission II input speed
	b)	calculate Transmission II output-input speed ratio
	c)	CALL FTRANS
	d)	multiply speed and torque ratios to get Transmission II efficiency
FLYWCY	a)	use gear ratio and driveline speed to calculate Transmission III output speed and torque
	b)	use gear ratio and flywheel speed to calculate Transmission III input speed
	c)	calculate Transmission III output-input speed ratio (set = 1.0 when vehicle stationary)
	d)	CALL FTRANS
	e)	multiply speed ratio and torque ratio to get Transmission III efficiency
	f)	calculate Transmission III input torque
	g)	use gear ratio and gear efficiency to calculate flywheel output power
	h)	calculate flywheel parasitic power loss
	i)	calculate flywheel input power
	j)	use gear efficiency to calculate Transmission II output power
FTRANS	a)	table look-up of transmission output-input torque ratio as function of input speed and output-input speed ratio

FIGURE 8-4. CONTINUED

II.		<u>Execution Sub-Routines (continued)</u>
GASCLC	a)	scale engine brake horsepower
	b)	CALL TABNEW
	c)	calculate fuel mass flow rate
	d)	calculate fuel mass consumed by engine and integrate over time.
	e)	calculate fuel remaining in tank
HPRPM	a)	<u>USE HORSPWR</u>* (initial estimate for brake horsepower is engine propulsion power)
	b)	calculate speed of accessories/auxiliaries power shaft
	c)	<u>USE DRIVLIN</u>*
	d)	add accessories/auxiliaries power to engine propulsion power to get engine brake horsepower.
	c)	<u>USE HORSPWR</u>*
	f)	calculate speed of accessories/auxiliaries power shaft
	g)	<u>USE DRIVLIN</u>*
	h)	store value for accessories/auxiliaries power
INTDBL	a)	table look-up of engine brake specific emissions as function of brake mean effective pressure and rpm
INTERP	a)	table look-up of vehicle velocity as function of time
PWRPLT	a)	calculate fuel energy used by vehicle engine and divide by reference energy
	b)	calculate energy needed to recharge flywheel
	c)	calculate fuel energy used by electric generating plant
	d)	calculate combined fuel energy used by vehicle and power-plant and divide by reference energy
	e)	divide vehicle emissions by reference emissions
	f)	<u>USE SUMTBL</u>*
	g)	calculate electric generating plant emissions

* Underline and caps refers to Block Data Sub-Routine

FIGURE 8-4. CONTINUED

II.	Execution Sub-Routines (continued)	
PWRPLT	h)	calculate emissions combined from vehicle and power-plant and divide by reference emissions
	i)	calculate vehicle range based either on vehicle fuel tank or on energy in flywheel whichever gives lesser range value
SMOGCLC	a)	CALL INTDBL
	b)	calculate mass emissions and integrate with time
TABNEW	a)	table look-up of engine brake specific fuel consumption as function of scaled brake horsepower and rpm
III.	Block Data Sub-Routine	
DRIVLIN	-	table of accessories/auxiliaries power as function of shaft speed
FLYCOM	-	initial value for efficiency of Transmission II
HORSPWR	-	table of engine speed as function of brake horsepower
SUMTBL	-	table of electric generating powerplant specific emission factors as function of type of fuel used.

FIGURE 8-4. CONTINUED

IV. Input Values

A. Physical

a) vehicle weight

b) vehicle frontal area and drag coefficient

c) vehicle tire pressure and radius

d) vehicle fuel tank fluid mass

e) baseline engine piston displacement

f) design engine piston displacement

g) flywheel thickness, diameter, mass, and moment of inertia

B. Performance

a) vehicle design peak cruise speed

b) vehicle design peak acceleration

c) vehicle reference energy consumption

d) vehicle accessories/auxiliary power and scaling factors

e) baseline engine rated power

f) design engine rated power

g) generator efficiency for recharging flywheel from stationary power source

h) flywheel rated speed and energy storage capability

i) control systems efficiencies

j) gear systems gear ratios and efficiencies

C. External Environment

a) vehicle velocity history

b) road grade

D. Program Control

a) initial and increment values for time and τ .

b) number of time and τ values.

FIGURE 8-4. CONTINUED

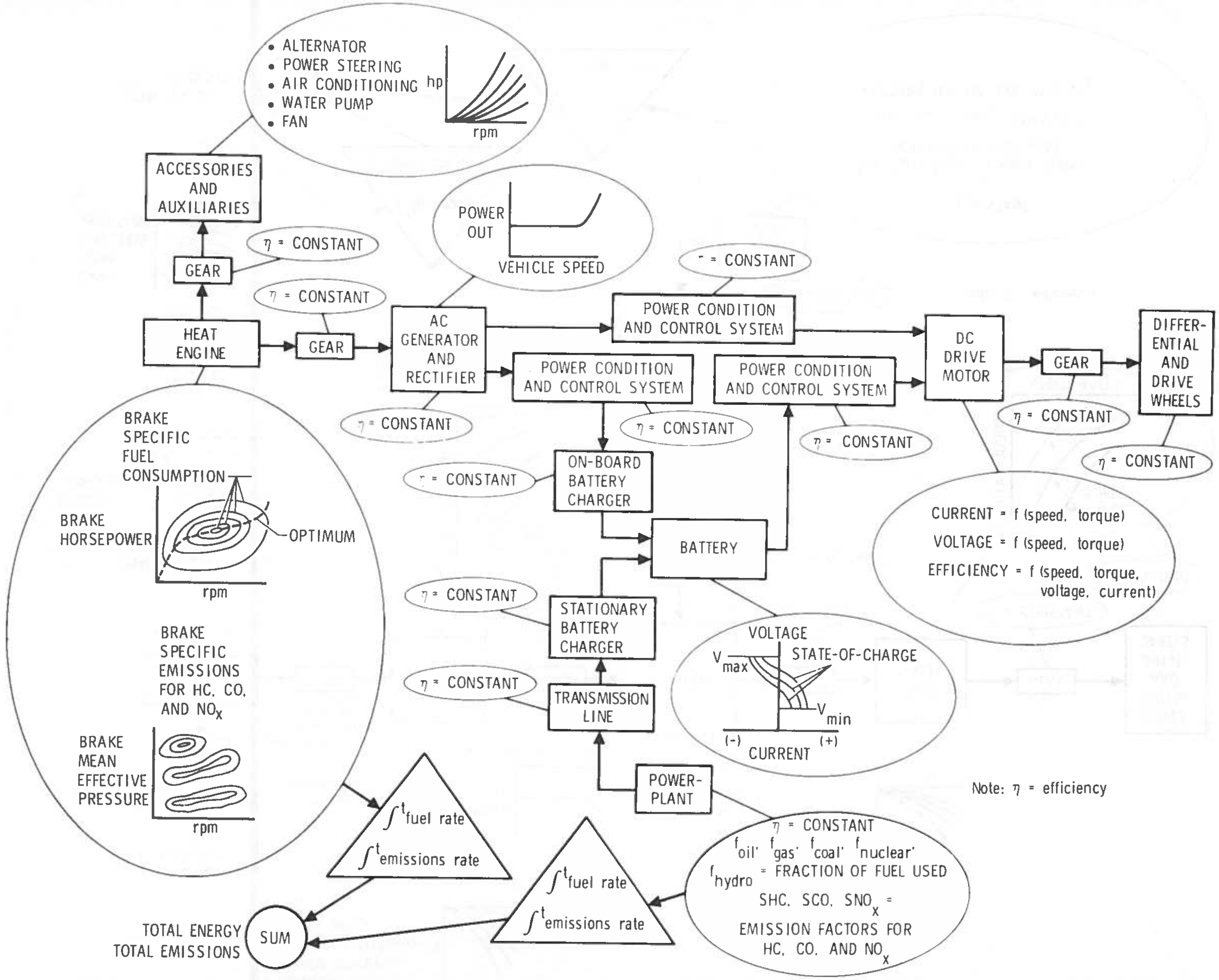

FIGURE 8-5. SCHEMATIC FOR COMPUTER MODELING, HEAT ENGINE/BATTERY HYBRID POWERTRAIN, SERIES CONFIGURATION

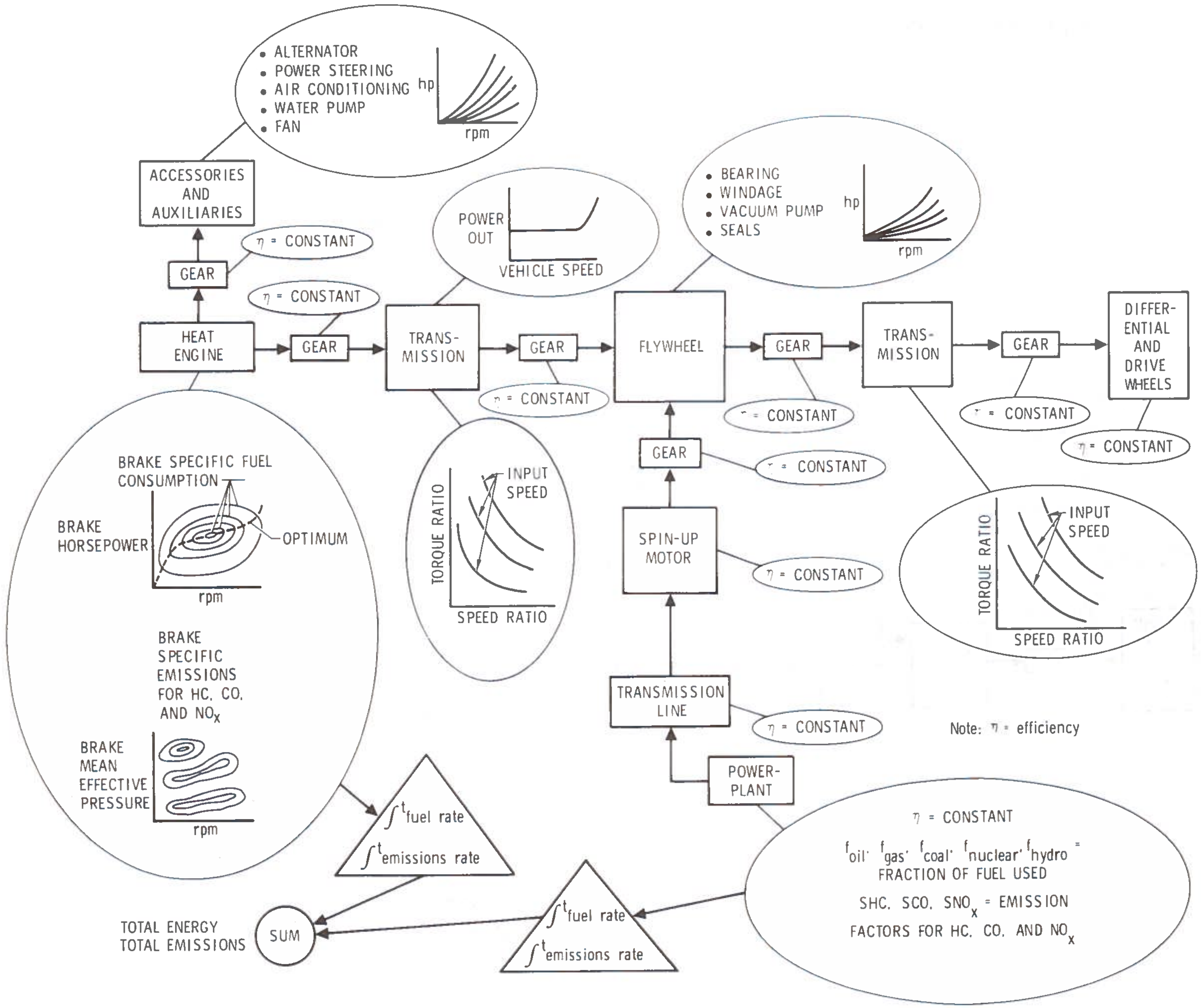

FIGURE 8-6. SCHEMATIC FOR COMPUTER MODELING, HEAT ENGINE/FLYWHEEL

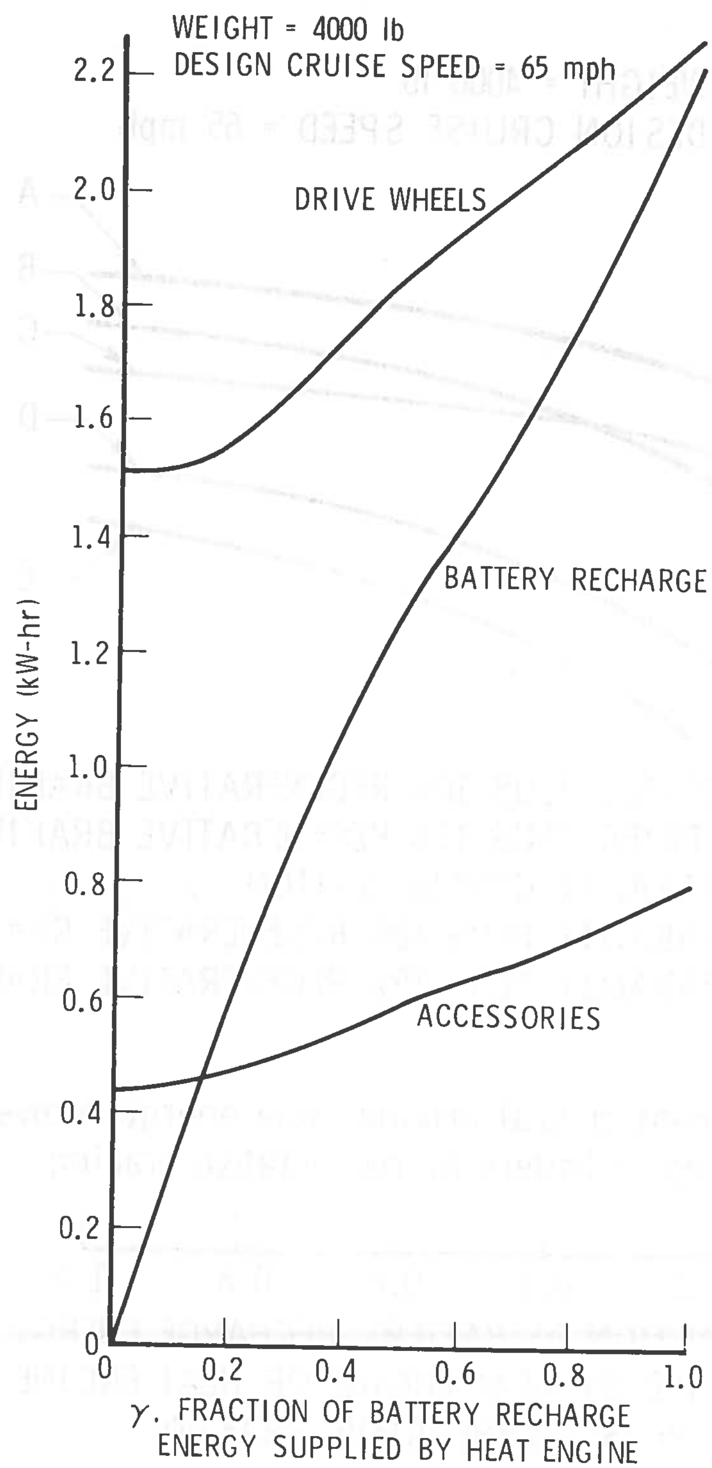

FIGURE 8-7. HEAT ENGINE ENERGY DISTRIBUTION FOR HEAT ENGINE/BATTERY HYBRID VEHICLE: EPA URBAN DRIVING CYCLE, SERIES CONFIGURATION

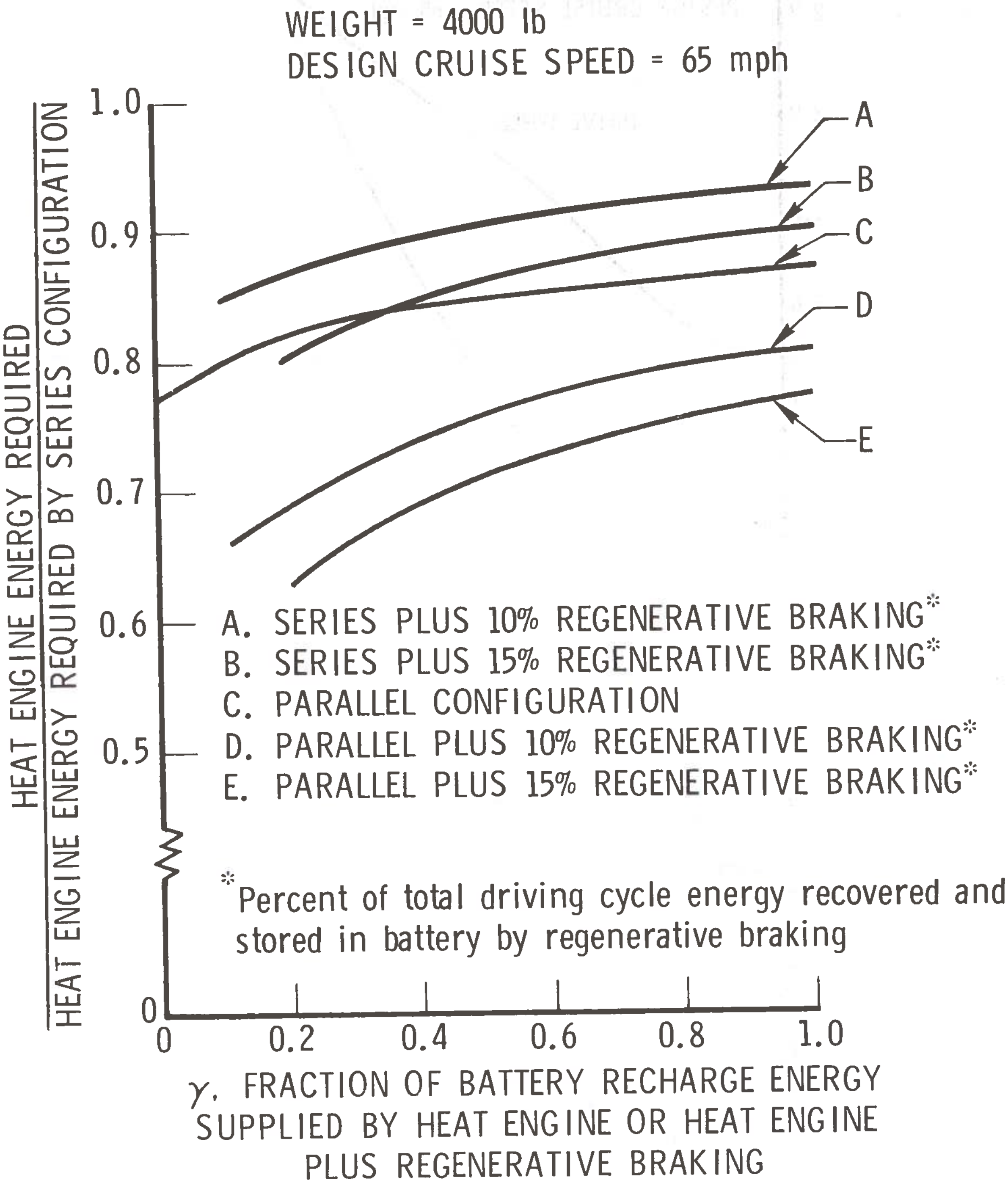

FIGURE 8-8. IMPACT OF PARALLEL OPERATION AND REGENERATIVE BRAKING ON HEAT ENGINE ENERGY REQUIREMENTS FOR HEAT ENGINE/BATTERY HYBRID VEHICLE: EPA RUBAN DRIVING CYCLE

9. SIZING ANALYSIS FOR POWERTRAIN COMPONENTS

The equations and rationale used in sizing powertrain components are discussed. Computational results are presented for the series powertrain configuration to illustrate the impact of vehicle design requirements (peak acceleration and peak cruise speed) on component weight and power rating. Similar effects can be expected for the parallel configuration powertrain; the most significant change would be a marked reduction in weight and power rating for the electric drive motor, as noted in Section 2.

9.1 POWERTRAIN PERFORMANCE REQUIREMENTS FOR HYBRID VEHICLES

The range in performance requirements imposed on the vehicle powertrain must be defined in order to select and size components for each system being investigated. Accordingly, power, torque, and axle speed were computed at the vehicle drive wheels for passenger cars (1800 to 6300 pounds) and delivery vans (3000 to 6000 pounds). Differential gear losses were not included in these calculations, but were included in calculations used to establish power ratings for electric drive motors or transmissions.

The equations used to compute power, torque, and speed at the drive wheels are as follows:

$$HPW = HPR + HPD + HPA$$

$$TOW = HPW \times 5252 \div NO$$

$$NO = V \times 14 \div R$$

$$HPR = \frac{V}{375} \times \frac{W}{2000} \times \left(10 + \frac{300}{P} + \frac{0.07V^2}{P}\right)$$

$$HPD = \frac{V}{375} \times 0.0027 \times C_D \times S \times V^2$$

$$HPA = K \times W \times A \times V \div 375$$

$$A = ACC \times 5280 \div (32.174 \times 3600)$$

Each term is defined in Table 9-1. The values used for each term concerned with cruise road load are given in Table 9-2. An acceleration schedule for passenger cars and vans is given in Table 9-3 and Table 9-4, respectively.

The results of the calculations are presented in Figures 9-1 through 9-5 for passenger cars and in Figures 9-6 through 9-10 for vans. Apparent discontinuities in passenger car torque and axle speed curves are caused by discrete changes in tire size as vehicle weight is varied. (Results of calculations for the van were faired in a continuous curve.)

9.2 RATIONALE FOR POWERTRAIN COMPONENT SIZING

The basis for sizing each of the major elements in the hybrid vehicle powertrain is reviewed. The particular design requirements and scaling factors discussed herein were included in the applicable hybrid vehicle powertrain simulation computer program, along with the equations necessary to define the power, torque, speed, current, or voltage transmitted into or out of each component.

9.2.1 Electric Drive Motor and Control System

For the series configuration hybrid heat engine/battery vehicle analyzed in this study, the drive motor is required to continuously provide tractive power as long as the vehicle is in motion (except for unpowered decelerations). The vehicle tractive power design requirements are of two types: maximum acceleration and steady cruise at maximum speed. These requirements are sketched in Figure 9-11.

Let η_{gr} and GR be the efficiency and the gear ratio between the motor and the wheels (see Table 9-5 for nomenclature). Then the motor power P_m is related to the vehicle tractive power P_t,

$$P_m \geq \frac{P_t}{\eta_{gr}} \qquad (9\text{-}1)$$

The maximum tractive torque at the wheels is related to the motor torque by

$$T_m^t \geq \frac{T_t^{max}}{GR\ \eta_{gr}} \qquad (9\text{-}2)$$

This value of motor torque is the constant of proportionality between power and speed. The maximum torque condition is shown in Figure 9-12. The maximum power condition is

$$P_m^p \geq \frac{P_t^p}{\eta_{gr}} \tag{9-3}$$

The speed at which the maximum power occurs is N_m^p. The motor speed is related to the wheel speed by

$$N_m^p = GR\ N_{wh}^p \tag{9-4}$$

The maximum power condition is shown as the horizontal line in Figure 9-12. The corresponding motor speed is at the vertical line denoted as N_m^p.

The maximum wheel speed, N_{wh}^s, is related to the maximum vehicle speed as follows:

$$N_{wh}^s = \frac{60}{2\pi} \frac{V^s}{R_{wh}} \tag{9-5}$$

The maximum motor speed is related to the maximum wheel speed by the gear ratio:

$$N_m^s = GR\ N_{wh}^s \tag{9-6}$$

Maximum motor speed was limited to 12,000 rpm. The vehicle power requirement at the wheels for the maximum speed condition is P_t^s. The corresponding motor power requirement is P_m^s and is related to the vehicle power requirement by the efficiency of the gears:

$$P_m^s \geq \frac{P_t^s}{\eta_{gr}} \tag{9-7}$$

The motor speed and power requirement at the maximum vehicle speed is shown in Figure 9-12.

The continuous duty power rating of a motor is determined by the ability of the motor to dissipate heat. For constant operation of the vehicle at its maximum speed, the continuous duty rating for the motor must equal or exceed the tractive power requirement P_t^s at that speed, N_m^s;

$$\therefore \; P_{continuous} = P_m^s \geq \frac{P_t^s}{\eta_{gr}} \text{ at } N_m^s \tag{9-8}$$

The overload capability of a dc motor depends on the duration of the overload condition and the frequency of repetition of the overload condition. For conditions where the overload condition is frequently repeated, the continuous duty rating of the motor may be exceeded by 300 percent for speeds above the motor base speed, as shown in Figure 9-13. This means that the maximum motor power required should not exceed three times the continuous duty rating of the motor:

$$P_{continuous} \geq \frac{P_m^p}{300\%} \qquad N_m^p > N_m^{bs} \tag{9-9}$$

The continuous power rating of the motor is determined by the more restrictive of the criteria given by Eqs. (9-8) and (9-9).

The gear ratio between the motor and the wheels is chosen such that the motor torque in the constant torque regime, i.e., at motor speeds below the base speed illustrated in Figure 9-13, is sufficient to match the maximum tractive torque requirement which occurs at zero velocity in Figure 9-11. The constant torque output from the motor as estimated from the characteristic shown in Figure 9-13 is

$$T_m^t = \frac{P_{continuous}}{N_m^{bs}} \tag{9-10}$$

Then, the gear ratio may be expressed as

$$GR \geq \frac{T_t^{max} N_m^{bs}}{\eta_{gr} P_{continuous}} \quad (9\text{-}11)$$

Once the motor power rating is established, the curves presented in Section 5.2 can be used to determine motor weight and volume. Similar curves are also given for determining weight and volume of the control system.

9.2.2 Electric Generator

The power demand on the generator is independent of vehicle acceleration and depends solely on the electric motor power needs at vehicle maximum crusing speed (the battery provides the electric motor power needs in excess of those needed for meeting vehicle cruise speed). Therefore, once the motor power and efficiency at peak cruise speed are determined, along with control system and power conditioning efficiencies, the generator rated power is established. The weight and volume are then calculated by use of the curves presented in Section 5.2.

9.2.3 Battery System

Design of the battery system is most dependent on the motor power requirements that it must meet. First, the peak motor input power required P_{IM} is determined during vehicle acceleration. Then, accounting for the power conditioning and control system efficiencies η_c, the battery power P_B is set. This value is then divided by a maximum motor rated current I_{MMR} of 1600/3 amperes to establish the system voltage V_{BS}. With the cell voltage V_{BC} known for a given battery system, the number of cells N_{BC} is determined. In equation form, this is expressed as

$$P_B = \frac{P_{IMR}}{\eta_c} \quad , \quad \text{watts} \quad (9\text{-}12)$$

$$V_{BS} = \frac{P_B}{I_{MMR}} \quad , \quad \text{volts} \tag{9-13}$$

$$NBC = \frac{V_{BS}}{V_{BC}} \tag{9-14}$$

Next, all other powertrain component weights WPC are subtracted from the allowable powertrain weight WTDT fcr the hybrid heat engine/battery vehicle. This gives the weight available for the battery system WBB. Dividing the system weight by the number of cells and a cell packaging factor F_C gives the allowable cell weight WBC. Finally, dividing the cell weight by the cell capacity unit weight C_u in pounds per ampere-hour gives the capacity of the system CR. In equation form, this is expressed as

$$WBB = WTDT - WPC \quad , \quad \text{lb} \tag{9-15}$$

$$WBC = \frac{WBB}{NBC \times F_C} \quad , \quad \text{lb} \tag{9-16}$$

$$CR = \frac{WBC}{C_u} \quad , \quad \text{amp-hr} \tag{9-17}$$

Values for C_u are given in Section 5.3 for nickel-zinc and lead-acid battery cells. F_C was taken to be 1.1.

9.2.4 Continuously Variable Transmissions

Two transmissions are in the heat engine/flywheel hybrid powertrain. One transmission links the flywheel output to the vehicle drive wheels through additional intermediate gearing and the differential. The other transmission links the heat engine output to the flywheel input. The design power output for the former transmission is established by the peak power output required during vehicle maximum acceleration. The latter transmission power output is determined by the power requirement at vehicle maximum cruise speed. With the output power levels established, weight and volume for each transmission can be calculated from the design sizing factors given in Section 5.5.

9.2.5 Flywheel System

Because of the low energy densities of steel flywheel systems, the sizing is restricted by allowable volume in a given vehicle,* not by weight By assuming that the allowable volume can be proportioned to vehicle weight, the following equation for rotor radius was derived from data in Ref. 9-1 for vehicle volume-weight relationships and from rotor size data in Ref. 9-2 for a 4000-lb vehicle.

$$R_{FW} = 0.544\left(\frac{W}{4000}\right)^{0.21}, \quad \text{feet} \qquad (9\text{-}18)$$

where W is the vehicle loaded weight. With the rotor radius established, the equations given in Section 5.4 will permit the calculation of the rotor design speed and energy storage capability. This calculation is for a maximum possible speed that loads the rotor material to its maximum working stress. Additional equations in Section 5.4 then give the weight and volume of other parts of the flywheel system, as well as the rotor parasitic power losses.

The maximum energy storage capability essentially determines the number of repetitive maximum accelerations that are available to a given vehicle weight class before the flywheel energy is depleted. If either the number of accelerations or the rate of acceleration is relaxed, a smaller, lower speed rotor could be designed. In either case, the parasitic losses would be reduced, and a more efficient powertrain would result. Investigation of this advantage was beyond the scope of this study.

9.2.6 Heat Engine

Because the heat engine is designed to provide steady propulsion power just to meet vehicle cruising power needs, sizing is accomplished at the peak cruise speed and is independent of vehicle acceleration. The peak

---

*Actually, by space available for accepting rotor housing diameter.

cruise power at the wheels is combined with the powertrain component efficiencies and gear efficiencies to yield the propulsion power output at the engine shaft.

An iterative looping process is required to determine engine total (brake) horsepower and shaft speed because the engine auxiliaries/ vehicle accessories power requirements are dependent on engine speed, and they must be added to the propulsion power in order to arrive at the total power, which in turn determines engine speed in accordance with the power-speed profile given in Section 5.1. For the heat engine/flywheel system, an additional iterative loop is necessary because the efficiency of the transmission linking the engine to the flywheel is a function of engine output torque and speed (Section 5.5).

With the engine total rated power established, the weight and volume are found by using the sizing curves given in Section 5.1.

9.2.7 Engine Auxiliaries/Vehicle Accessories

Engine auxiliary and vehicle accessory power requirements given in Section 5.6 were developed largely on the basis of data for a nominal 4000-lb conventionally power vehicle with a 350-CID, 145-hp engine (rated net brake horsepower). For the various vehicles and engine sizes analyzed in this study, the power levels must be adjusted by appropriate scaling factors. The majority of these factors were derived from the earlier hybrid study conducted by Aerospace (Ref. 9-1).

The fan and water pump are scaled with rated engine power. The alternator/generator load is set for each class of vehicle according to the values given in Ref. 9-2 for matching overall vehicle electrical loads. Power steering is scaled with vehicle weight (it is not used on the compact car). Air conditioning is set for the 4000-lb car according to the curves in Section 5.6. It is not used on the delivery van and is reduced to 68 percent of the 4000-lb car value when applied to the compact car. The foregoing scaling factors are summarized in Table 9-6.

9.2.8 Miscellaneous Drive Train Elements

Sizing factors for items such as fuel tank, radiator, and differential were taken from Ref. 9-1. They are given as a function of vehicle loaded weight W_V or rated engine horsepower P_E.

Differential and other gearing weight and volume are given by

$$W_D = 0.023\ W_V$$
$$V_D = 0.0001\ W_V \qquad (9\text{-}19)$$

Engine-generator gear system weight and volume are given by

$$W_{EG} = 0.003\ W_V$$
$$V_{EG} = 2 \times 10^{-5}\ W_V \qquad (9\text{-}20)$$

Radiator weight and volume are given by

$$WR = 0.3318\ P_E$$
$$V_R = 0.0042\ P_E \qquad (9\text{-}21)$$

Exhaust system weight and volume are given by

$$W_{EX} = 0.3308\ P_E$$
$$V_{EX} = 0.0054\ P_E \qquad (9\text{-}22)$$

Starter weight and volume are given by

$$W_S = 0.1193\ P_E$$
$$V_S = 0.001038\ P_E \qquad (9\text{-}23)$$

Fuel tank weight and volume are given by

$$W_{FT} = 0.04\ W_V$$
$$V_{FT} = 0.0008\ W_V \qquad (9\text{-}24)$$

9.3 RESULTS OF SIZING ANALYSIS FOR POWERTRAIN COMPONENTS

9.3.1 Powertrain Component Weights

Hybrid heat engine/battery powertrain component weights of primary interest are illustrated in Figures 9-14 through 9-33 for vehicle weights of 2500 and 4000 pounds. Component weight is plotted versus time-to-accelerate-to-60-mph for different vehicle design peak cruise speeds (VC). A similar set of curves is given in Figures 9-34 through 9-45 for the hybrid heat engine/flywheel powertrain. (A nomenclature for these figures can be found in Table 9-7.) Results for the 4000-lb vehicle for each type of hybrid are briefly discussed.

9.3.1.1 Heat Engine/Battery Powertrain

Figures 9-24 and 9-25 give the heat engine and generator weights, respectively. As noted previously in Sections 9.2.2 and 9.2.6, these weights are invariant with vehicle acceleration. A decline with decreasing cruise speed is seen.

The motor weight is given in Figure 9-26. It is unaffected by vehicle acceleration for an 80-mph design cruise speed but is mostly controlled by acceleration at the lower cruise speeds. The 65-mph cruise speed shows that cruise speed dominates at the longer acceleration times, whereas acceleration dominates at the shorter acceleration times. Because the motor controller is sized by motor-rated power, its characteristics, as seen in Figure 9-27, are identical. Both the controller and motor weights show a marked decrease as design cruise speed is decreased from 80 to 65 mph.

Figures 9-28 shows the total powertrain weight except for batteries, and Figure 9-29 shows the allowable powertrain weight of 1500 pounds for this vehicle weight. The difference between these two curves is the weight available for batteries, and this is plotted in Figure 9-30. The effect of the major decrease in component weights as design cruise speed is decreased from 80 to 65 mph is apparent in its effect on weight available for batteries.

Figures 9-31 and 9-32 show battery cell weight and capacity (ampere-hours), respectively. Lastly, the battery specific power (watts per pound) is given in Figure 9-33. There is a very marked impact on specific power as cruise speed and acceleration are decreased. Problems formerly encountered in designing high-power batteries can largely be relieved by relaxation of vehicle performance requirements. However, it should be pointed out that if the allowable powertrain weight were to slip to 1210 pounds as discussed in Section 7, then a large increase in specific power would result. For example, with a design cruise speed of 65 mph, the specific power at an 11-second acceleration time would increase from 135 to 278 W/lb, and at a 20-second acceleration it would increase from 71 to 138 W/lb. Therefore, vehicle design performance is expected to be strongly connected with the allowable powertrain weight for battery systems having limited performance.

9.3.1.2 Heat Engine/Flywheel Powertrain

Heat engine weights are given in Figure 9-40 for the 4000-lb car. These weights are very close to the values required for the heat engine/battery powertrain.

Transmission weights are given in Figures 9-41 and 9-42. The former set of curves shows weights for the transmission linking the heat engine and the flywheel; it is insensitive to acceleration as discussed in Section 9.2.4. The latter set of curves is for the transmission linking the flywheel to the drive wheels, and it is decidedly affected by acceleration.

Figure 9-43 shows the flywheel system weight (rotor, housing, containment ring, etc.); it being solely a function of the size of the vehicle, there is no effect seen of acceleration or design cruise speed.

The total powertrain component weights are summarized in Figure 9-44. There is clearly no problem with this installation if the allowable powertrain weight is 1500 pounds. If this weight should decrease to 1210 pounds, then some compromise must be introduced into the design for almost all acceleration times with the 80-mph design cruise speed. This would likely involve reducing the size of the rotor and result in some decrease in energy storage capacity.

Finally, the total powertrain component volume given in Figure 9-45 shows that this type of vehicle is not volume-limited because Ref. 9-1 assigned a volume of 28 ft^3 to a vehicle of this weight. The nearly 20 ft^3

required at the highest acceleration for 80-mph design cruise speed still leaves considerable additional space for component design growth, if needed.

9.3.2 Powertrain Component Power Ratings

The most pertinent component power ratings are summarized in Tables 9-8 through 9-12 for various combinations of vehicle weight, design peak cruise speed, and design acceleration time from 0 to 60 mph. (Data regarding flywheel characteristics may be found in Section 5.4.) Major differences between engine rated power and generator rated power are due to engine power absorption by the vehicle accessory/engine auxiliary units. Reduced differences in these relative power levels are seen for the van because of the removal of air conditioning as a design requirement.

9.4 REFERENCES

9-1 Hybrid Heat Engine/Electric Systems Study, Final Report, Vol. I, TOR-0059(6769-01)-2, The Aerospace Corporation, El Segundo, Calif. (1 June 1971).

9-2 Flywheel Feasibility Study and Demonstration, LMSC-DOO7915, Lockheed Missiles and Space Company, Sunnyvale, Calif. (30 April 1971).

TABLE 9-1. NOMENCLATURE FOR VEHICLE POWER REQUIREMENT EQUATIONS

A	vehicle acceleration (g's)
ACC	vehicle acceleration (mph/sec)
C_D	drag coefficient
HPA	power at wheels needed to accelerate the vehicle (hp)
HPD	power loss due to vehicle drag (hp)
HPR	power loss due to vehicle road friction (hp)
HPW	power required at wheels (hp)
K	rotational inertia factor
NO	wheel speed (rpm)
P	tire pressure (psi)
R	tire equivalent radius (ft)
S	vehicle equivalent cross-section area (ft^2)
TOW	torque required at vehicle wheels (ft-lb)
V	vehicle speed (mph)
W	vehicle loaded weight (lb): the weight of the passenger cars includes 300-lb allowance for passenger and luggage; the weight of the vans includes 1000 lb for passenger and cargo.

TABLE 9-2. VEHICLE PHYSICAL CHARACTERISTICS

W	R	P	S	C_D
PASSENGER CARS				
1800	0.95	25	17	0.45
2300	0.98	25	18	0.45
2800	0.98	25	19	0.45
3300	0.99	25	20.5	0.45
3800	0.99	25	21.6	0.45
4300	1.09	25	22.8	0.45
4800	1.12	25	23.7	0.45
5300	1.17	25	24.4	0.45
5800	1.23	25	24.8	0.45
6300	1.23	25	25.2	0.45
VANS				
3000	0.93	30	29.4	0.76
4000	1.12	30	35	0.76
5000	1.18	30	35	0.76
6000	1.215	40	35	0.76

TABLE 9-3. ACCELERATION SCHEDULE FOR PASSENGER CARS: TIME FROM 0 to 60 MPH

Time (sec)	11 sec V (mph)	14 sec V (mph)	17 sec V (mph)	20 sec V (mph)
0	0	0	0	0
1	8.6	7.6	6.2	5.
2	16.6	14.5	12.1	9.8
3	24.2	20.8	17.6	14.4
4	31.1	26.3	22.5	18.7
5	37.1	31.	26.8	22.7
6	42.1	35.2	30.7	26.4
7	46.6	39.	34.3	29.9
8	50.5	42.5	37.6	33.2
9	54.	45.8	40.6	36.3
10	57.2	48.9	43.4	39.2
11	60.	51.9	46.1	41.9
12		54.8	48.7	44.4
13		57.5	51.2	46.7
14		60.	53.6	48.9
15			55.9	51.
16			58.	53.
17			60.	54.9
18				56.7
19				58.4
20				60.

TABLE 9-4. ACCELERATION SCHEDULE FOR VANS: TIME FROM 0 TO 60 MPH

Time (sec)	21 sec V (mph)	24 sec V (mph)	27 sec V (mph)	30 sec V (mph)
0	0	0	0	0
1	7.4	6.3	5.5	4.7
2	13.9	12.0	10.5	9.
3	19.6	17.2	15.1	13.
4	24.5	21.9	19.3	16.7
5	28.7	26.1	23.2	20.1
6	32.3	29.8	26.8	23.3
7	35.5	33.1	30.1	26.4
8	38.4	36.	33.1	29.3
9	41.	38.6	35.8	32.0
10	43.3	40.9	38.2	34.5
11	45.4	43.	40.4	36.8
12	47.3	44.9	42.4	38.9
13	49.1	46.7	44.2	40.8
14	50.8	48.4	45.8	42.6
15	52.4	50.	47.3	44.3
16	53.9	51.5	48.7	45.9
17	55.3	52.9	50.	47.4
18	56.6	54.2	51.3	48.8
19	57.8	55.4	52.2	50.1
20	58.9	56.5	53.6	51.3
21	60.0	57.5	54.6	52.4
22		58.4	55.6	53.4
23		59.2	56.6	54.3
24		60.	57.6	55.2
25			58.5	56.1
26			59.3	56.9
27			60.0	57.7
28				58.5
29				59.3
30				60.0

TABLE 9-5. NOMENCLATURE FOR MOTOR SIZING EQUATIONS

GR	gear ratio between motor and wheels
N_m^{bs}	base speed of motor
N_m^p	motor speed at peak tractive power
N_m^s	motor speed at maximum vehicle speed
N_{wh}^p	wheel speed at maximum tractive power
N_{wh}^s	wheel speed at maximum vehicle speed
P_m^p	peak motor power
P_m^s	motor power at maximum vehicle speed
P_t^p	peak tractive power required
P_t^s	tractive power required at maximum vehicle speed
$P_{continuous}$	continuous power rating of motor
R_{wh}	radius of wheel
T_A	time to accelerate to 60 mph
T_m^t	motor torque
T_t^{max}	maximum tractive torque required at wheels
V_m	volume of motor
V^s	maximum vehicle speed
W_m	weight of motor
η_{gr}	efficiency of gear

TABLE 9-6. ENGINE AUXILIARY AND VEHICLE ACCESSORY SCALING FACTORS

Accessory	Family Car (FC) (>3200 lb)	Compact Car (<3200 lb)	Van
Air Conditioning	1.0	$0.68 \times FC$	0.0
Power Steering	$1.0 \times \frac{WFC}{4000}$	0.0	1.0
Alternator/Generator	1.0	$0.75 \times FC$	$0.5 \times FC$
Water Pump	$1.0 \times \frac{HP_{FC}}{145}$	$1.0 \times \frac{HP_C}{145}$	$1.0 \times \frac{HP_V}{145}$
Fan	$1.0 \times \frac{HP_{FC}}{145}$	$1.0 \times \frac{HP_C}{145}$	$1.0 \times \frac{HP_V}{145}$

Note: WFC = loaded weight of hybrid family car, lb

FC = value of accessory power determined for family car, hp

HP_{FC} = engine rated power for hybrid family car, hp

HP_C = engine rated power for hybrid compact car, hp

HP_V = engine rated power for hybrid van, hp

TABLE 9-7. NOMENCLATURE FOR POWERTRAIN COMPONENT WEIGHT SUMMARY

CR	battery capacity in ampere-hours
SPBAT	battery specific power, W/lb
Time to 60 mph	time to reach 60 mph (design acceleration), sec
VC	vehicle design cruise speed, mph
VTDT	total volume of all powertrain components, ft^3
WBB	battery system weight, lb
WBC	battery cell weight, lb
WFW	weight of flywheel system (rotor, housing, etc.), lb
WG	generator weight, lb
WHE	heat engine weight, lb
WM	motor weight, lb
WMC	motor power conditioning and control weight, lb
WPC	total weight of all powertrain components except the battery, lb
WTDT	total weight of all powertrain components, lb
WT2	weight of transmission linking engine to flywheel, lb
WT3	weight of transmission linking flywheel to vehicle drive wheels, lb

TABLE 9-8. HEAT ENGINE RATED BRAKE HORSEPOWER

ACCELERATION TIME, 0-60 mph (sec)

		2500 lb					4000 lb					6000 lb				
	PEAK CRUISE SPEED (mph)	11	13	16	18	20	11	13	16	18	20	21	23	26	28	30
HEAT ENGINE/BATTERY SYSTEM	45	23.9					36.6					38.9				
	55	33.1					48.5					63.1				
	65	45.3					63.7					96.9				
	80	71.1					96.3					169.5				
HEAT ENGINE/FLYWHEEL SYSTEM	45	25.0					36.6					40.7				
	55	34.2					48.2					65.0				
	65	47.3					64.2					99.4				
	80	76.9					100.6					178.4				

VEHICLE LOADED WEIGHT

TABLE 9-9. ELECTRIC GENERATOR RATED HORSEPOWER

ACCELERATION TIME, 0-60 mph (sec)

PEAK CRUISE SPEED (mph)	2500 lb					4000 lb					6000 lb				
	11	13	16	18	20	11	13	16	18	20	21	23	26	28	30
45	12.2					16.7					30.7				
55	19.8					26.5					50.6				
65	29.8					38.9					78.4				
80	51.0					65.8					137.9				

VEHICLE LOADED WEIGHT

TABLE 9-10. ELECTRIC DRIVE MOTOR RATED HORSEPOWER

ACCELERATION TIME, 0-60 mph (sec)

Vehicle Loaded Weight	2500 lb					4000 lb					6000 lb				
Peak Cruise Speed (mph)	11	13	16	18	20	11	13	16	18	20	21	23	26	28	30
45	24.5	20.7	17.9	16.1	14.6	38.3	32.2	27.8	24.9	22.5	41.6	31.0	29.4	27.0	27.0
55	24.5	22.4	19.2	18.0	16.5	38.3	34.2	29.4	27.4	24.6	43.6	→	→	→	→
65	25.2	→	→	→	→	38.3	34.5	33.3	→	→	68.2	→	→	→	→
80	43.9	→	→	→	→	57.1	→	→	→	→	121.2	→	→	→	→

TABLE 9-11. RATED HORSEPOWER OF TRANSMISSION LINKING HEAT ENGINE TO FLYWHEEL

ACCELERATION TIME, 0-60 mph (sec)

PEAK CRUISE SPEED (mph)	2500 lb: 11	13	16	18	20	4000 lb: 11	13	16	18	20	6000 lb: 21	23	26	28	30
45	12					17					31				
55	19					26					50				
65	29					38					77				
80	51					66					139				

VEHICLE LOADED WEIGHT

TABLE 9-12. RATED HORSEPOWER OF TRANSMISSION LINKING FLYWHEEL TO VEHICLE DRIVE WHEELS

ACCELERATION TIME, 0-60 mph (sec)

2500 lb

PEAK CRUISE SPEED (mph)	11	13	16	18	20
45	72	61	53	47	43
55		66	57	53	48
65					
80					

4000 lb

PEAK CRUISE SPEED (mph)	11	13	16	18	20
45	113	95	82	73	66
55		101	86	81	72
65					
80					

6000 lb

PEAK CRUISE SPEED (mph)	21	23	26	28	30
45	122	91	86	79	79
55		94	89	84	81
65				89	86
80				89	86

VEHICLE LOADED WEIGHT

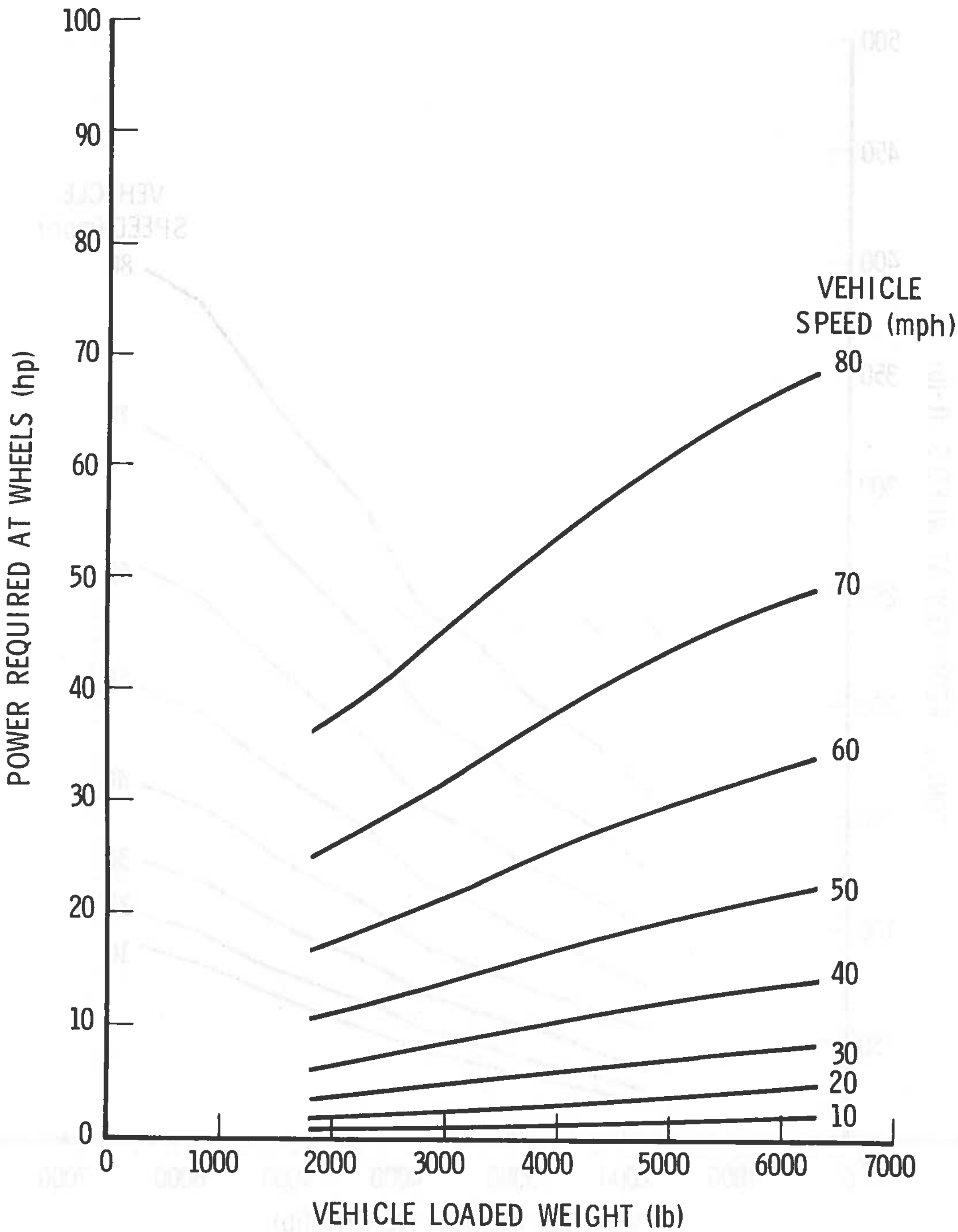

FIGURE 9-1. POWER REQUIRED AT WHEELS DURING CRUISE FOR PASSENGER CARS (ZERO ACCELERATION)

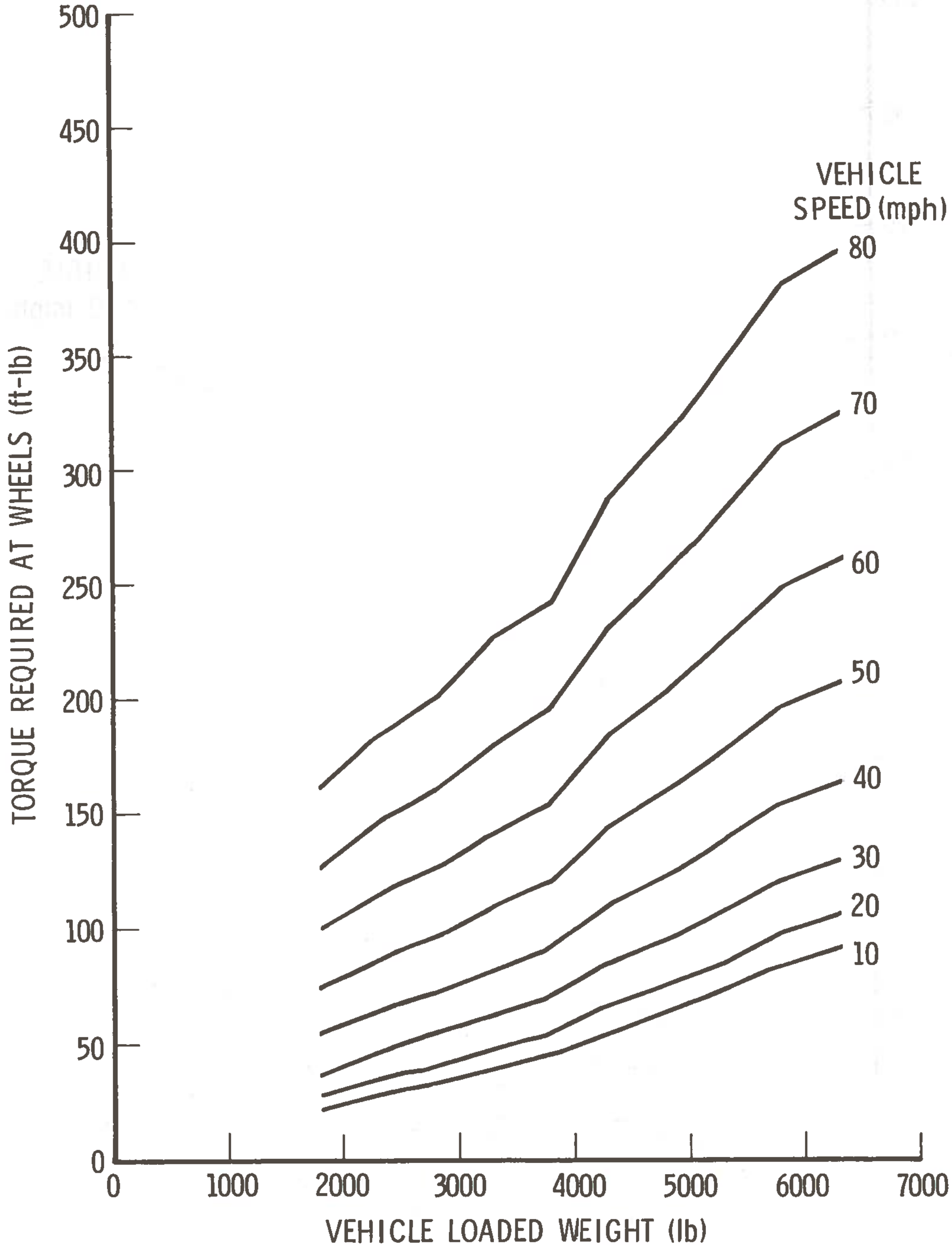

FIGURE 9-2. TORQUE REQUIRED AT WHEELS DURING CRUISE FOR PASSENGER CARS

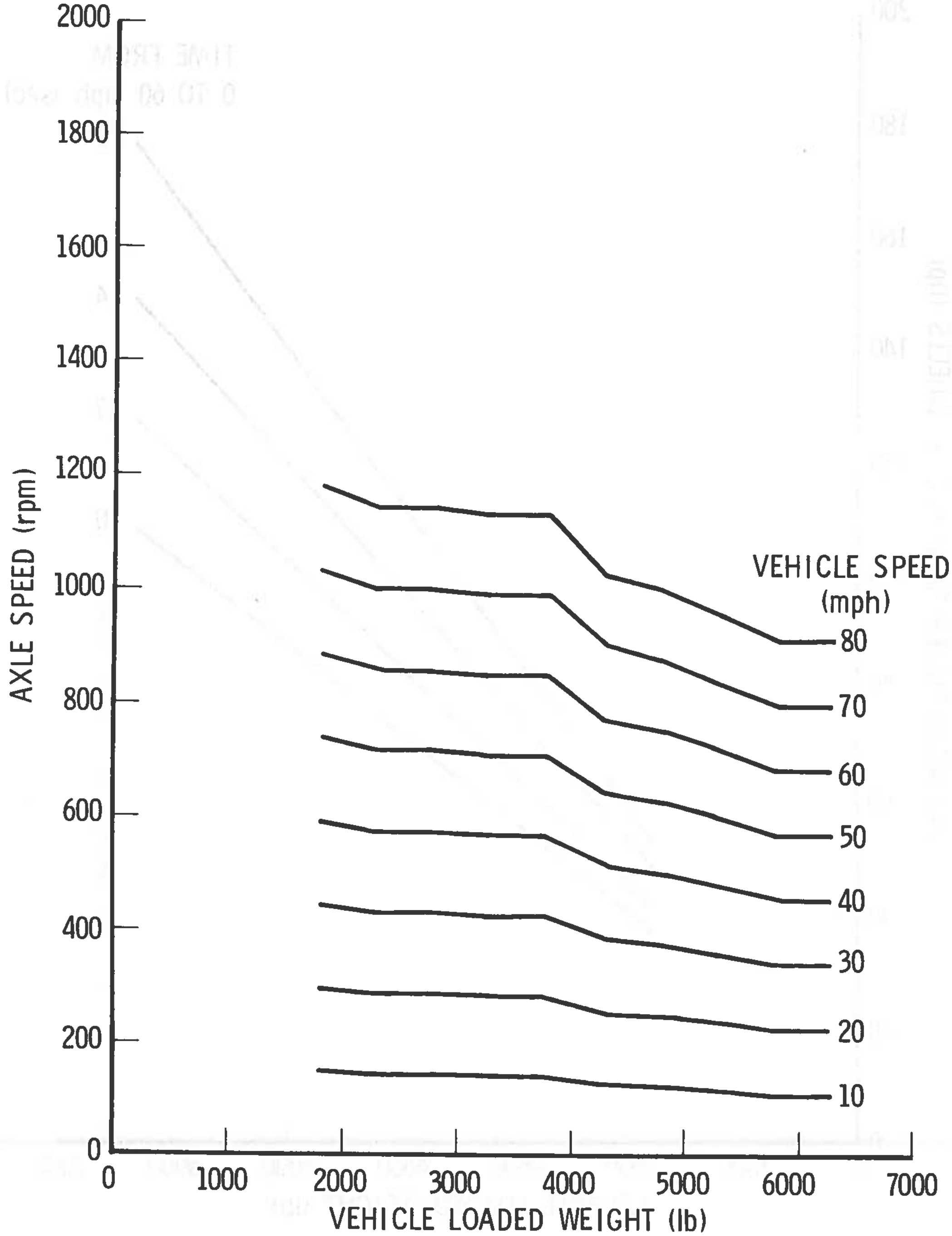

FIGURE 9-3. AXLE SPEED DURING CRUISE FOR PASSENGER CARS

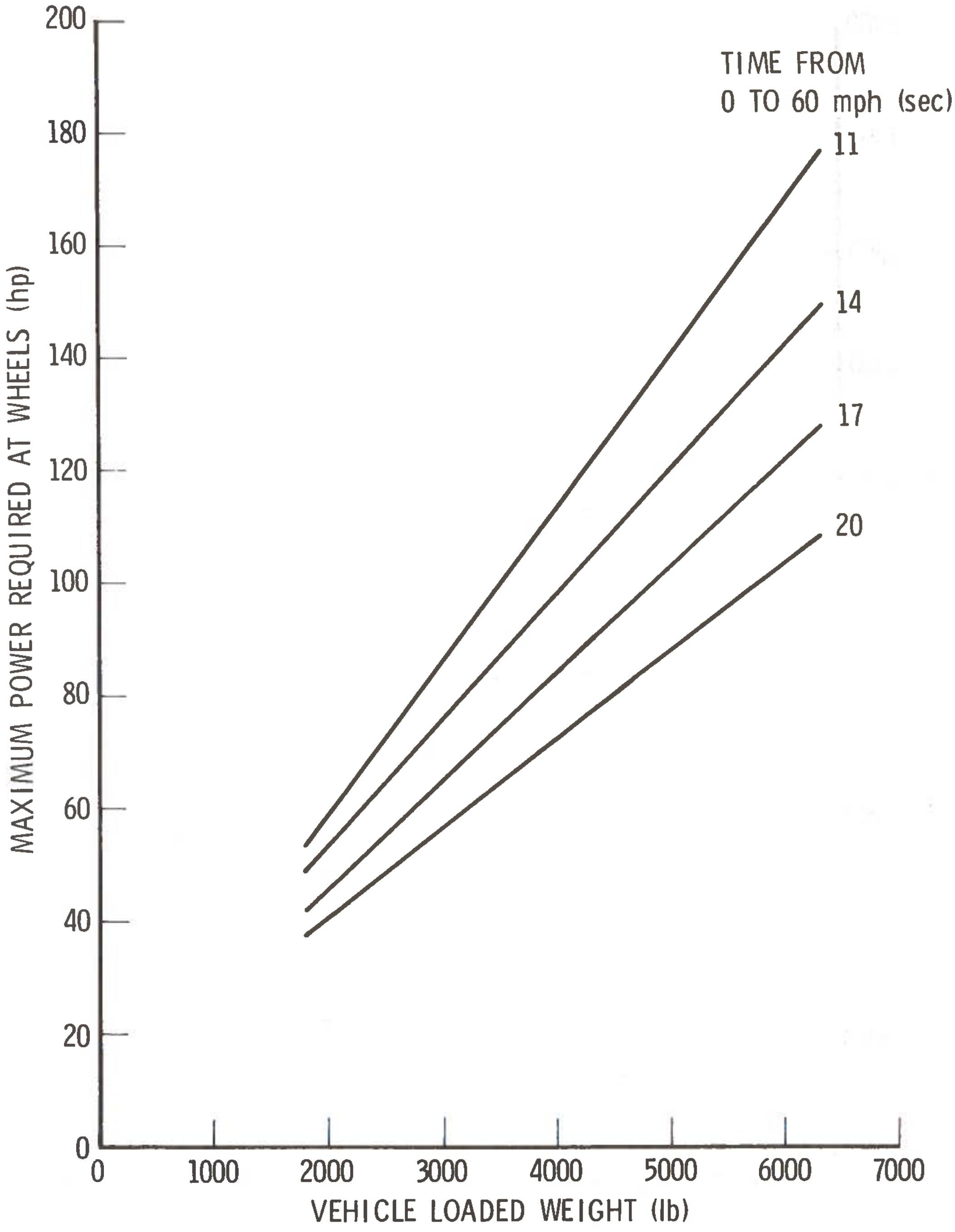

FIGURE 9-4. MAXIMUM POWER REQUIRED AT WHEELS FOR PASSENGER CARS (VARIED ACCELERATION)

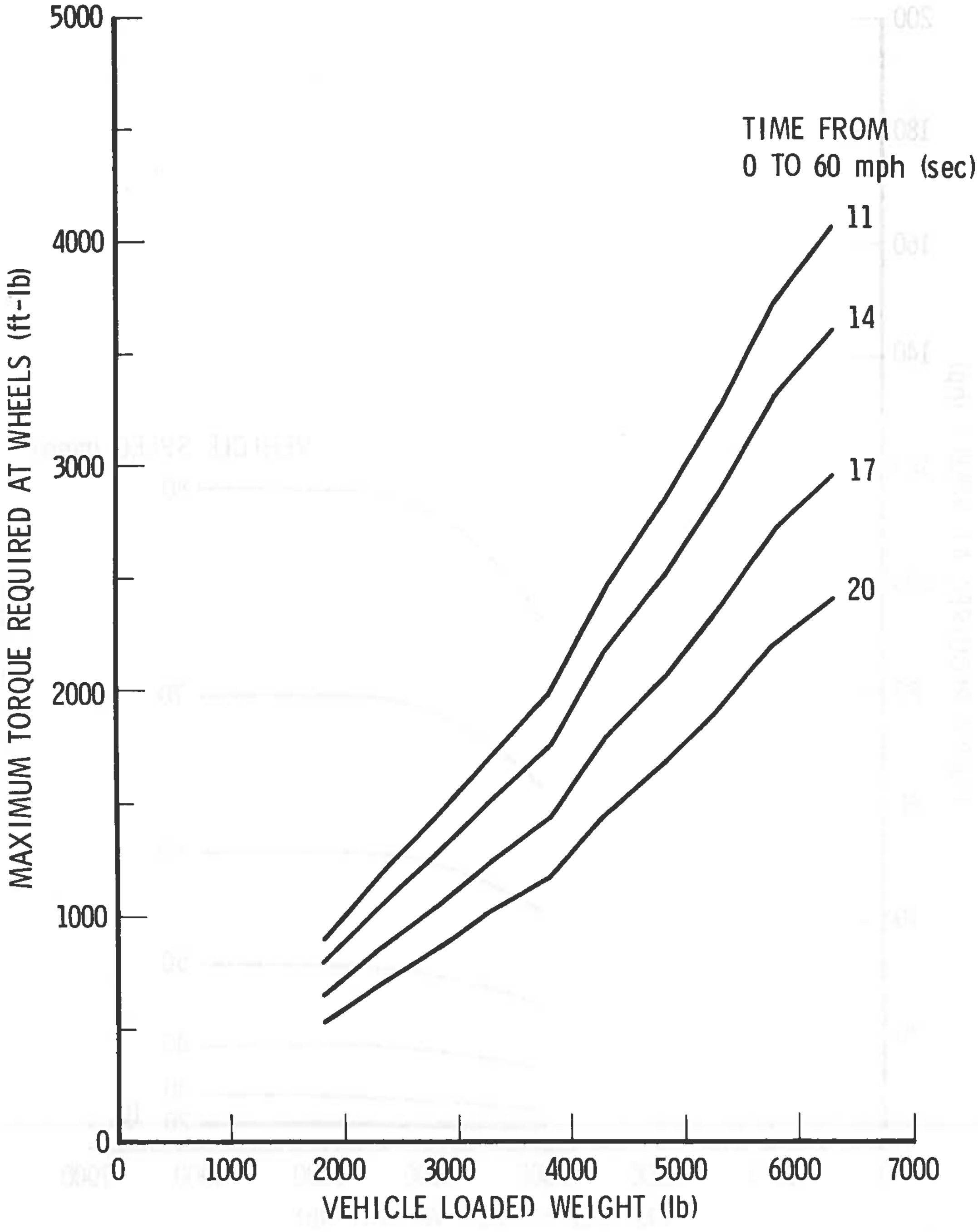

FIGURE 9-5. MAXIMUM TORQUE REQUIRED AT WHEELS FOR PASSENGER CARS (VARIED ACCELERATION)

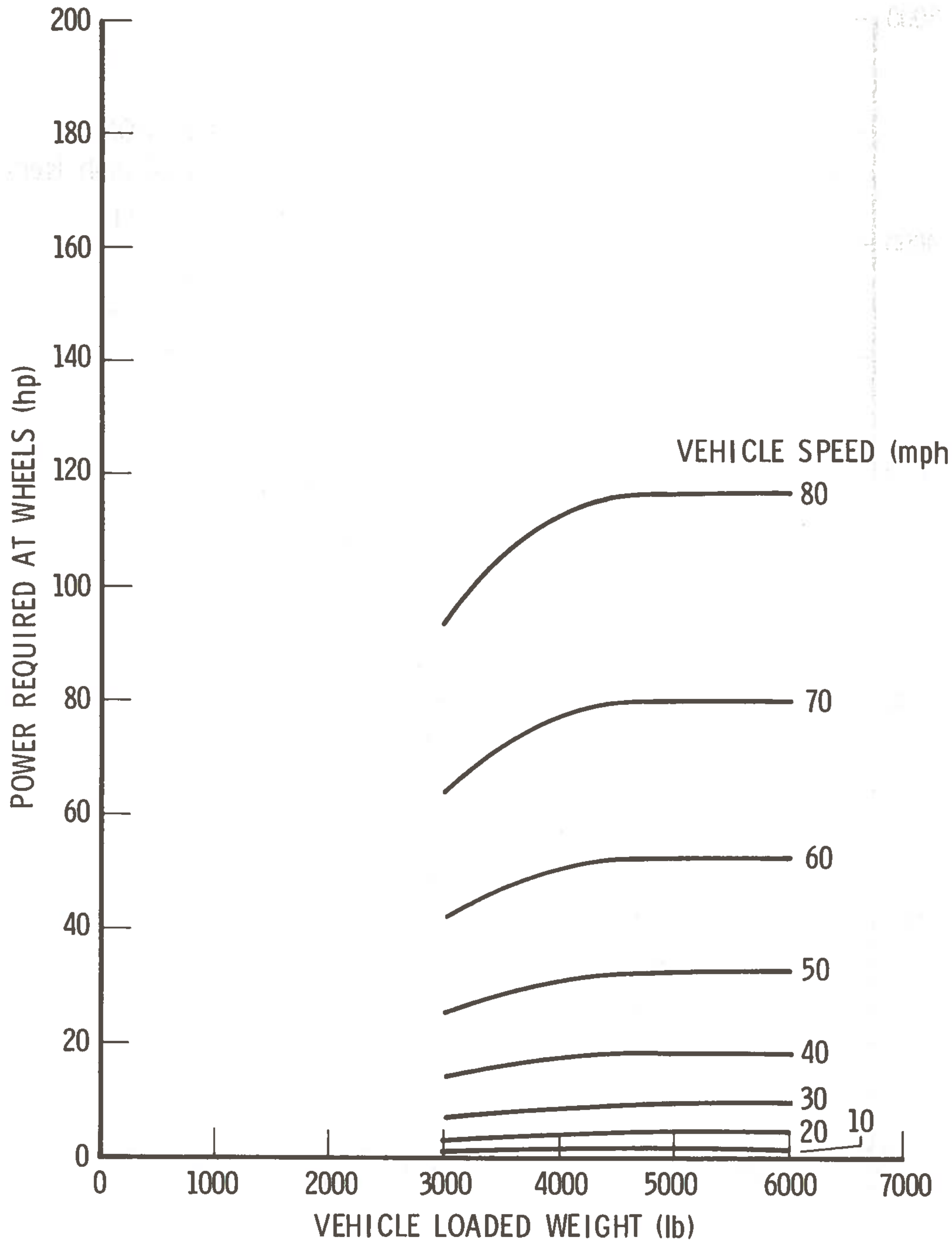

FIGURE 9-6. POWER REQUIRED AT WHEELS DURING CRUISE FOR VANS (ZERO ACCELERATION)

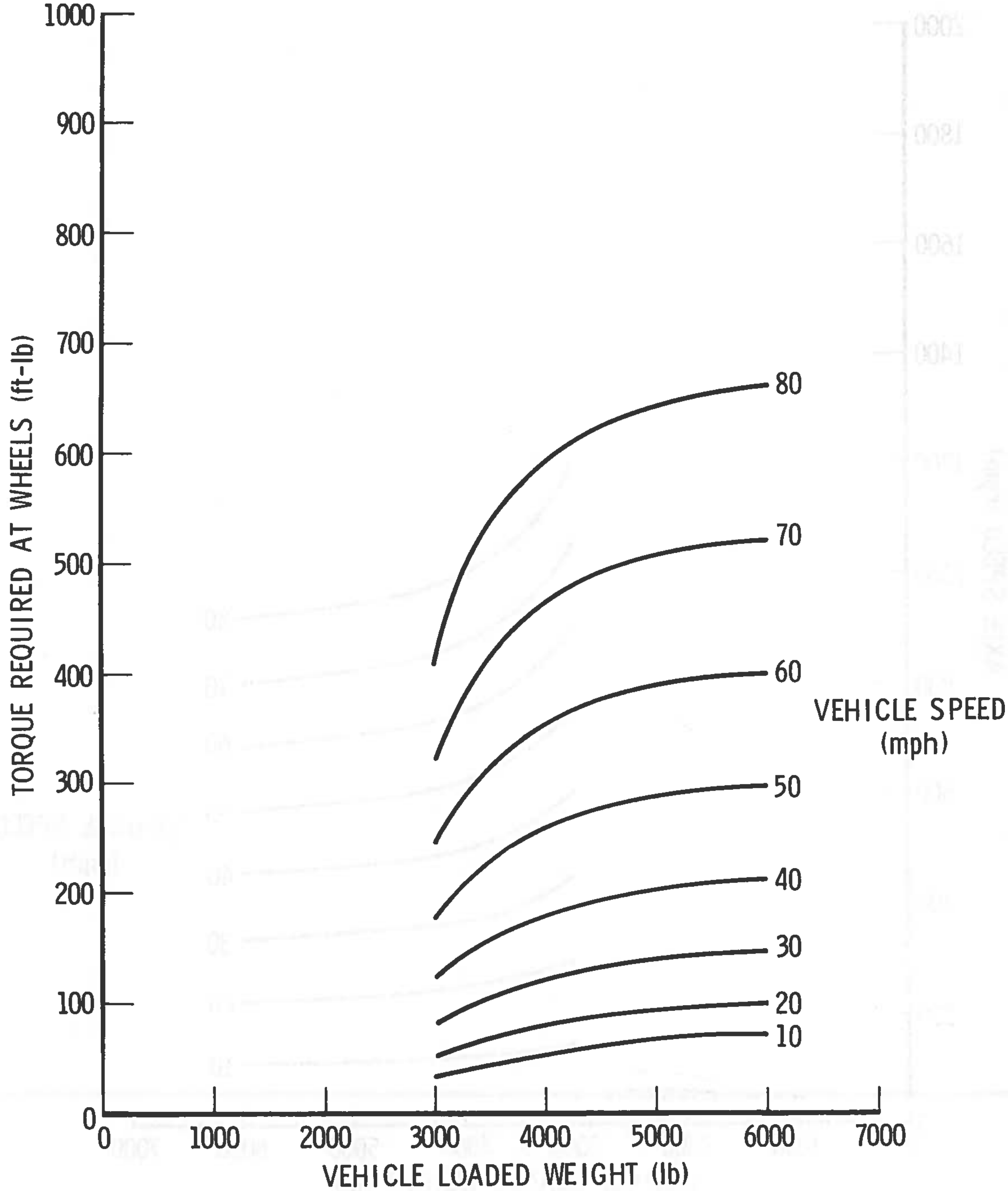

FIGURE 9-7. TORQUE REQUIRED AT WHEELS DURING CRUISE FOR VANS (ZERO ACCELERATION)

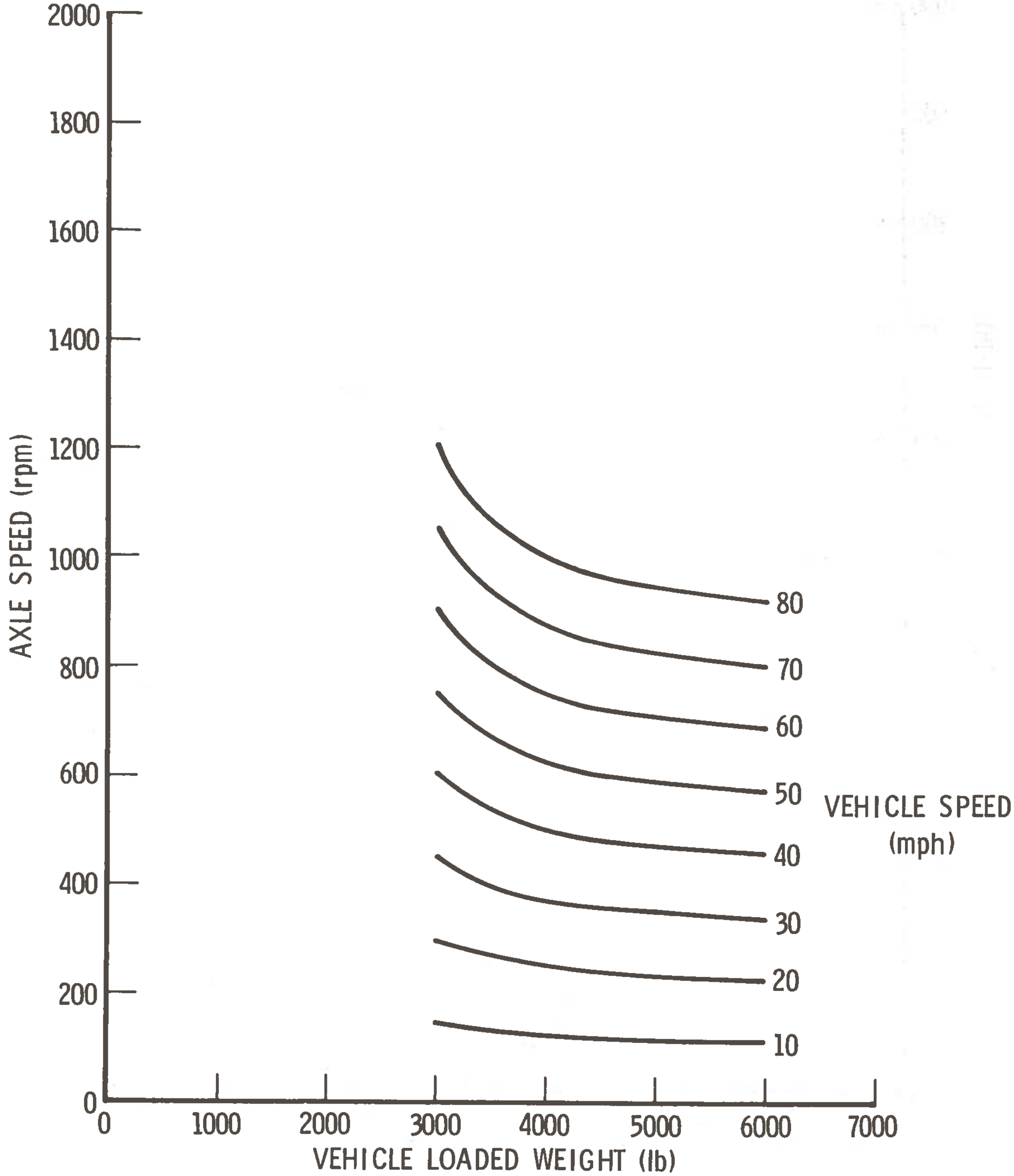

FIGURE 9-8. AXLE SPEED DURING CRUISE FOR VANS

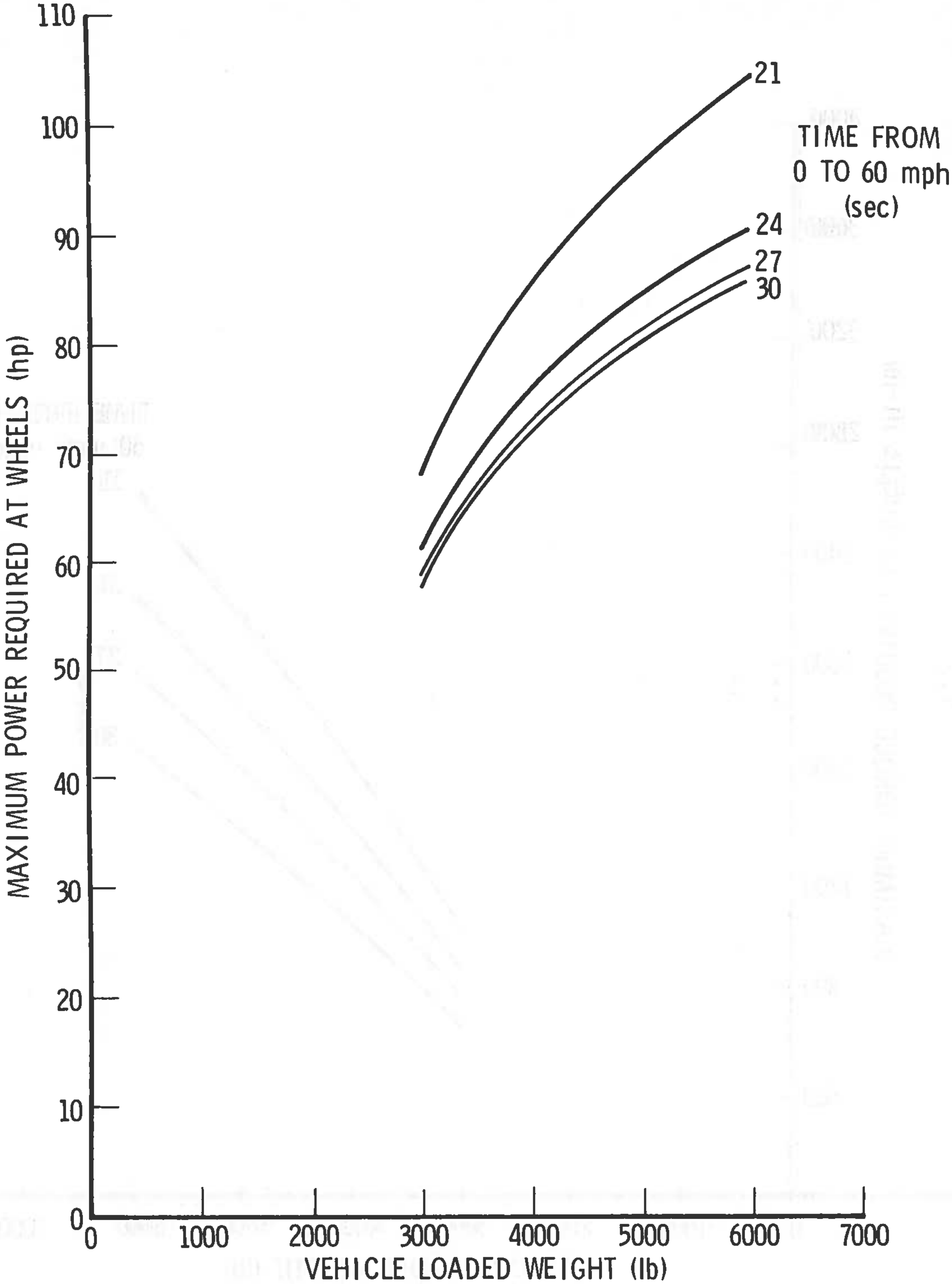

FIGURE 9-9. MAXIMUM POWER REQUIRED AT WHEELS FOR VANS (VARIED ACCELERATION)

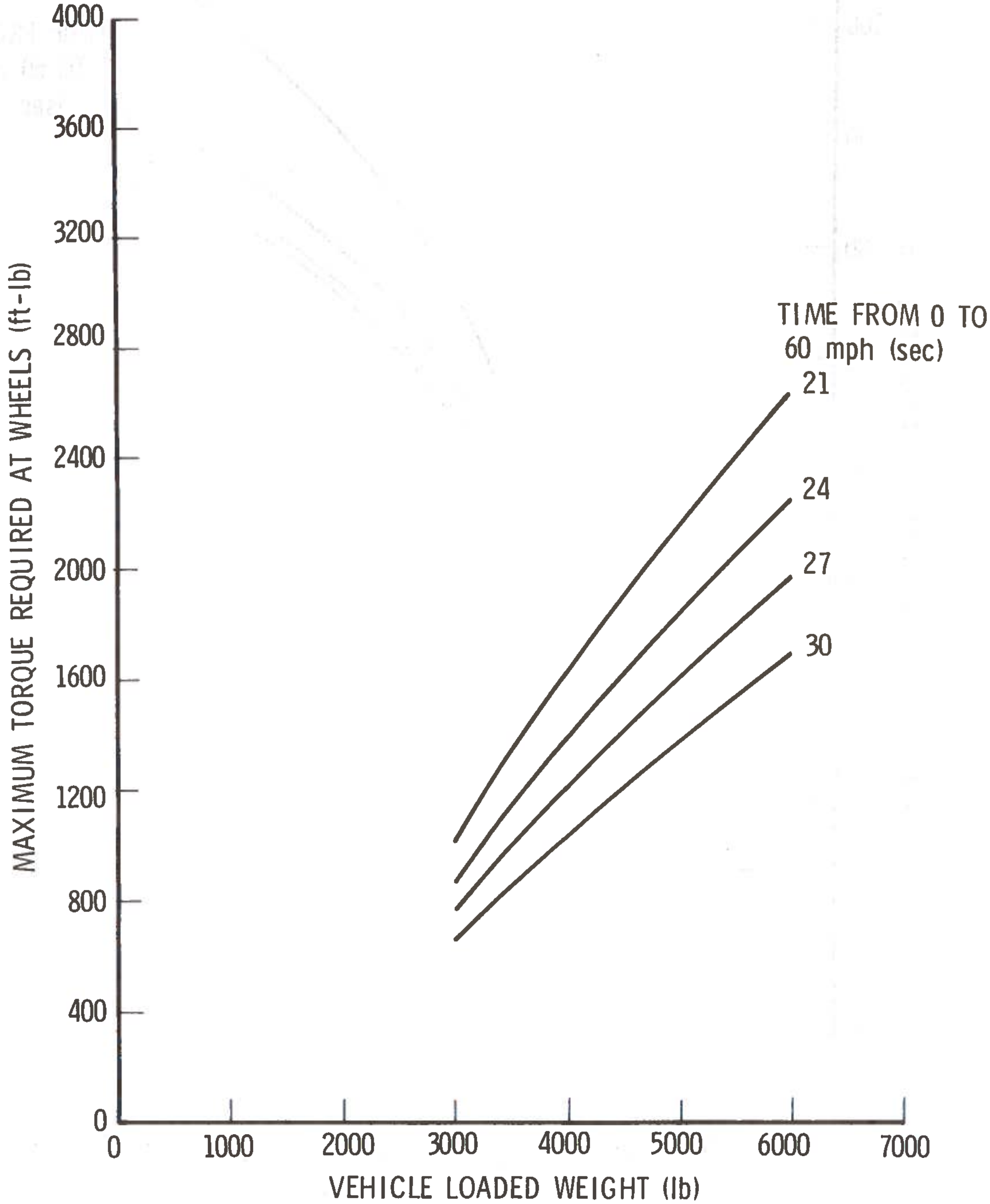

FIGURE 9-10. MAXIMUM TORQUE REQUIRED AT WHEELS FOR VANS (VARIED ACCELERATION)

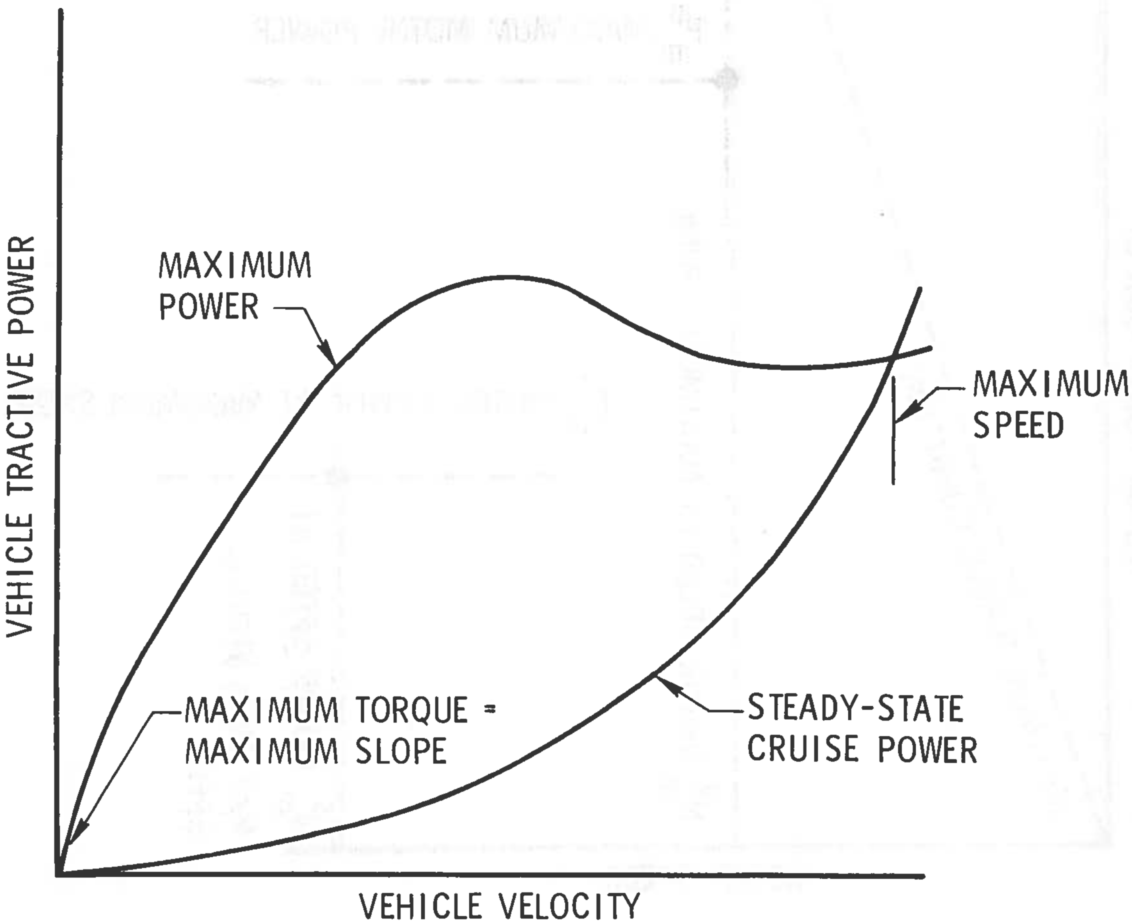

FIGURE 9-11. VEHICLE TRACTIVE POWER VERSUS VELOCITY

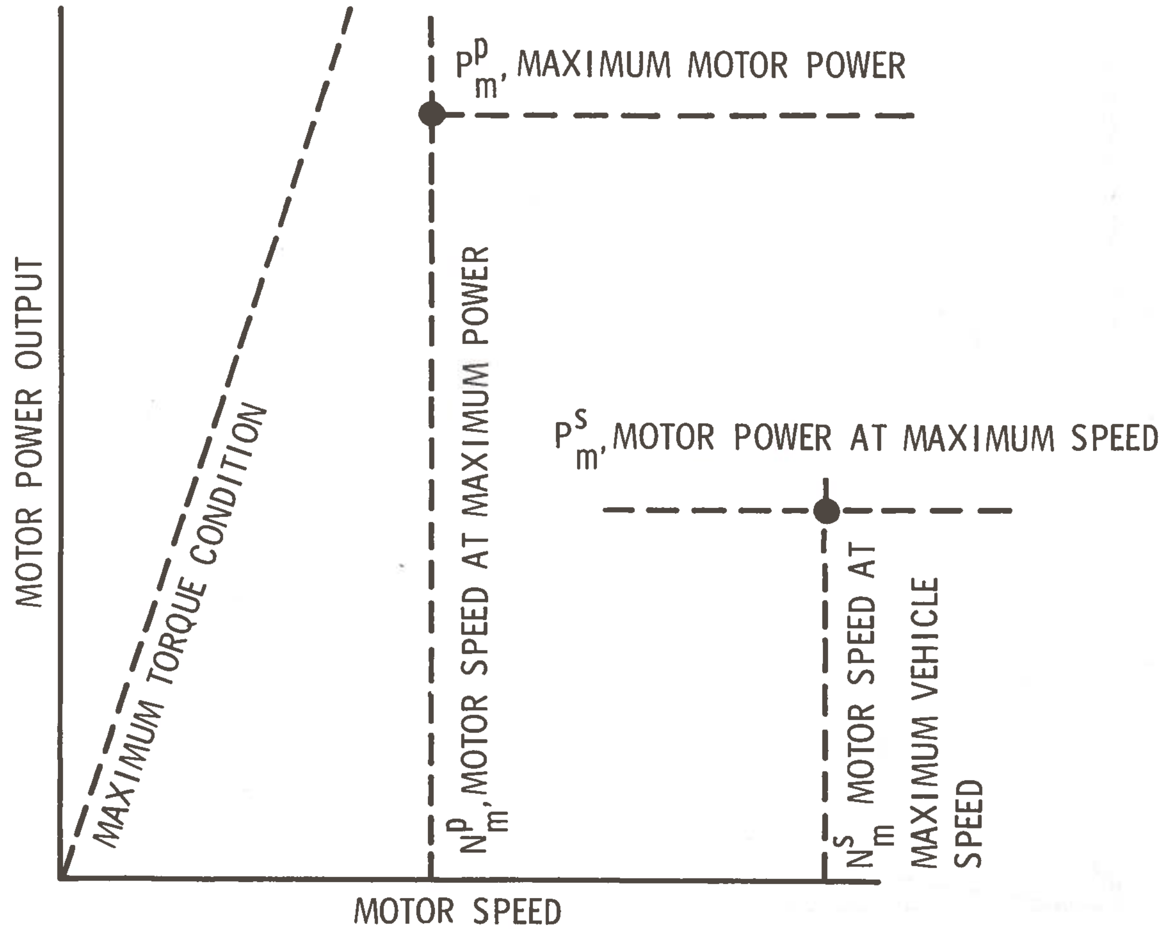

FIGURE 9-12. MOTOR POWER REQUIRED VERSUS SPEED

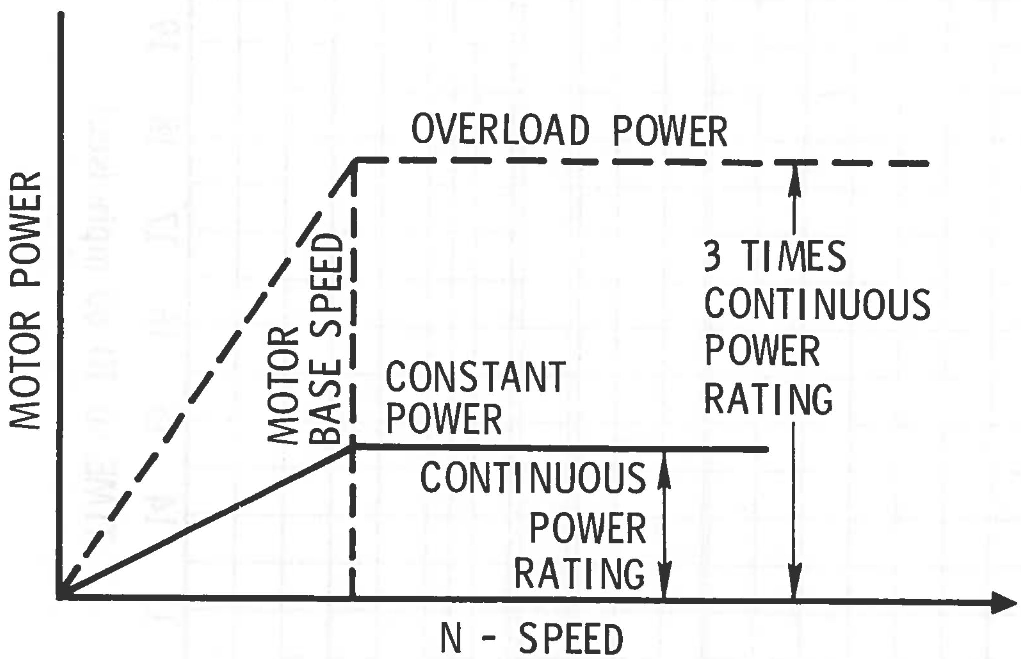

FIGURE 9-13. DC MOTOR POWER VERSUS SPEED (CHARACTERISTICS FOR SIZING)

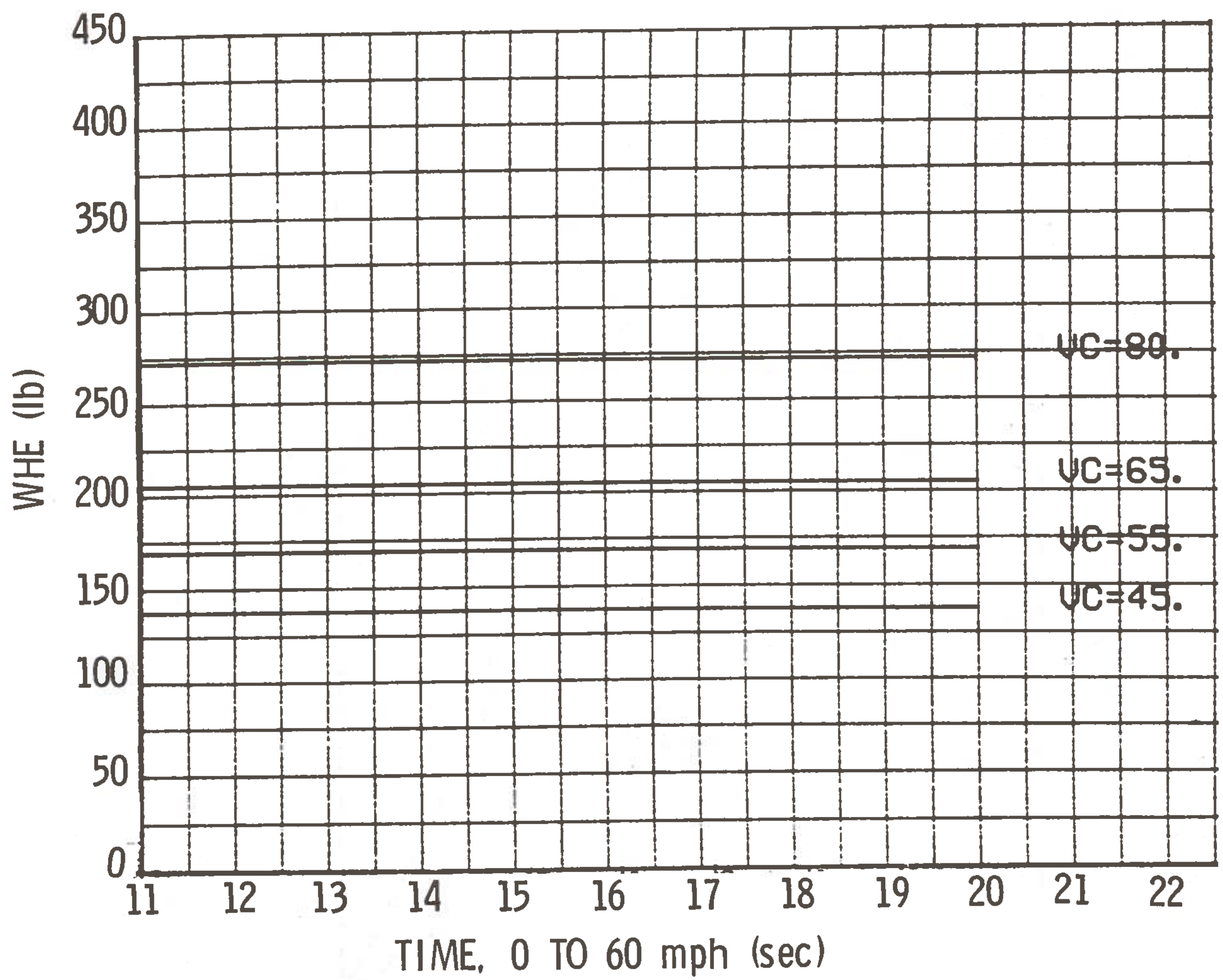

FIGURE 9-14. HEAT ENGINE WEIGHT (WHE) FOR 2500-LB VEHICLE: HYBRID HEAT ENGINE/BATTERY SYSTEM, SERIES CONFIGURATION

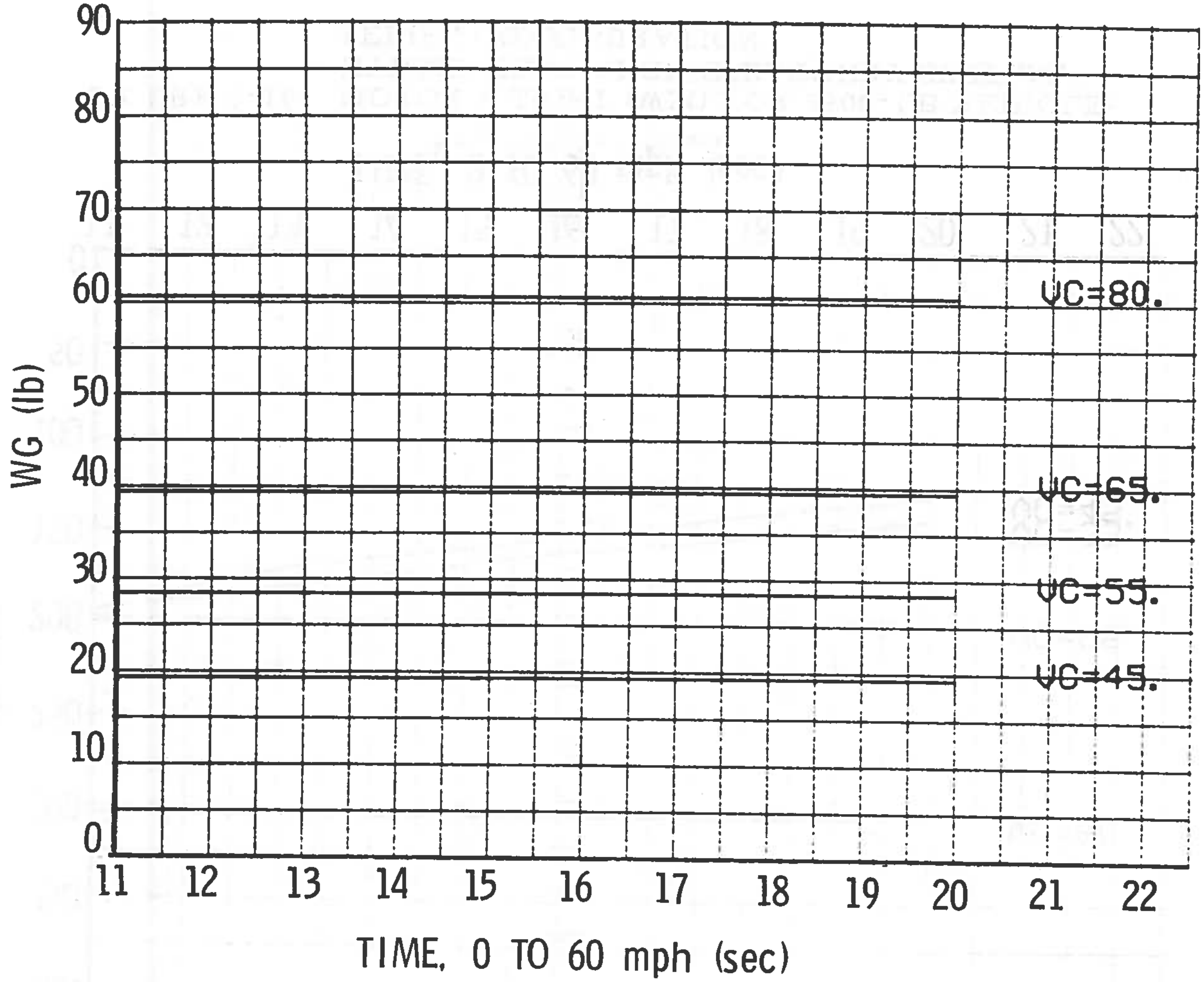

FIGURE 9-15. GENERATOR WEIGHT (WG) FOR 2500-LB VEHICLE: HYBRID HEAT ENGINE/BATTERY SYSTEM, SERIES CONFIGURATION

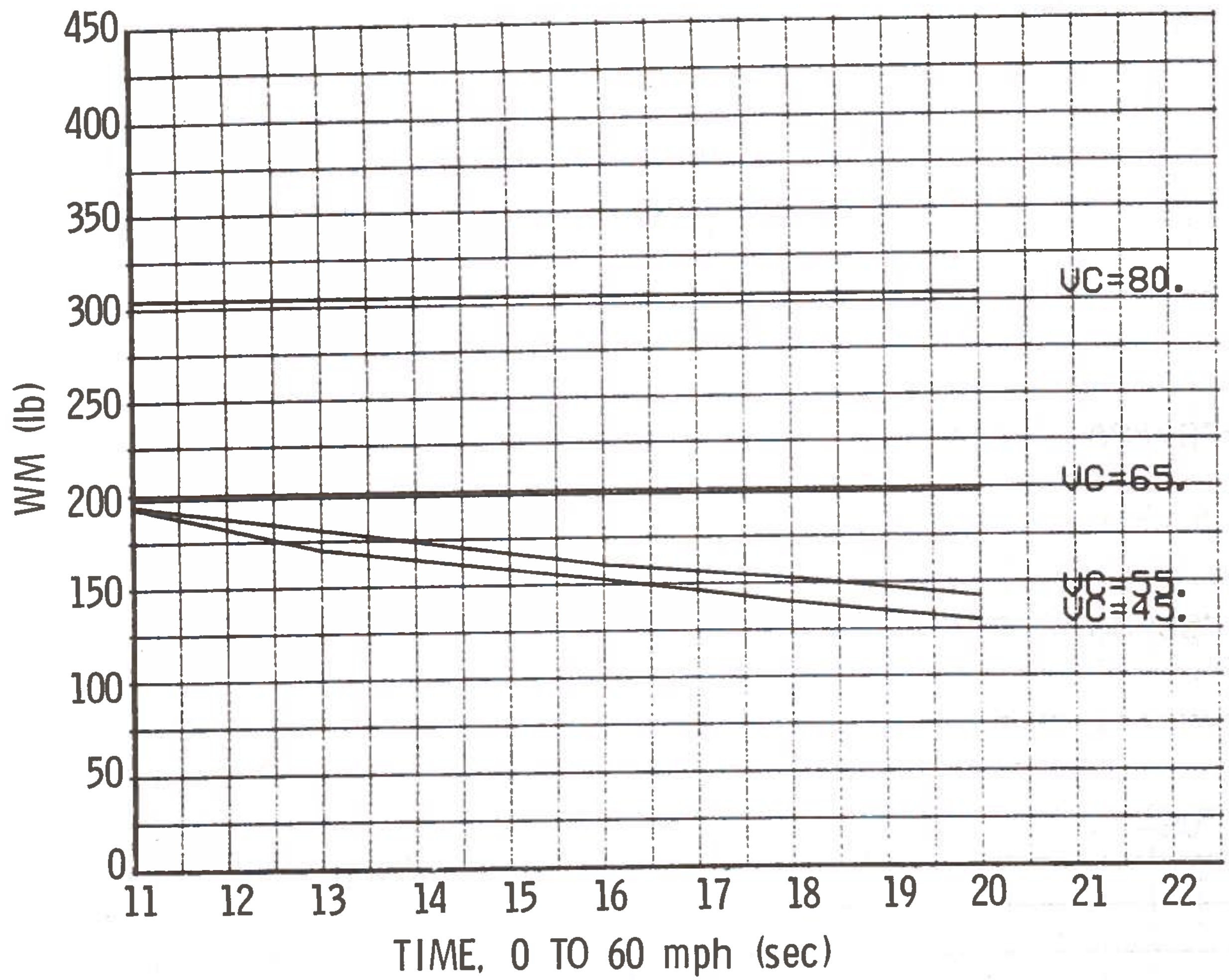

FIGURE 9-16. MOTOR WEIGHT (WM) FOR 2500-LB VEHICLE: HYBRID HEAT ENGINE/BATTERY SYSTEM, SERIES CONFIGURATION

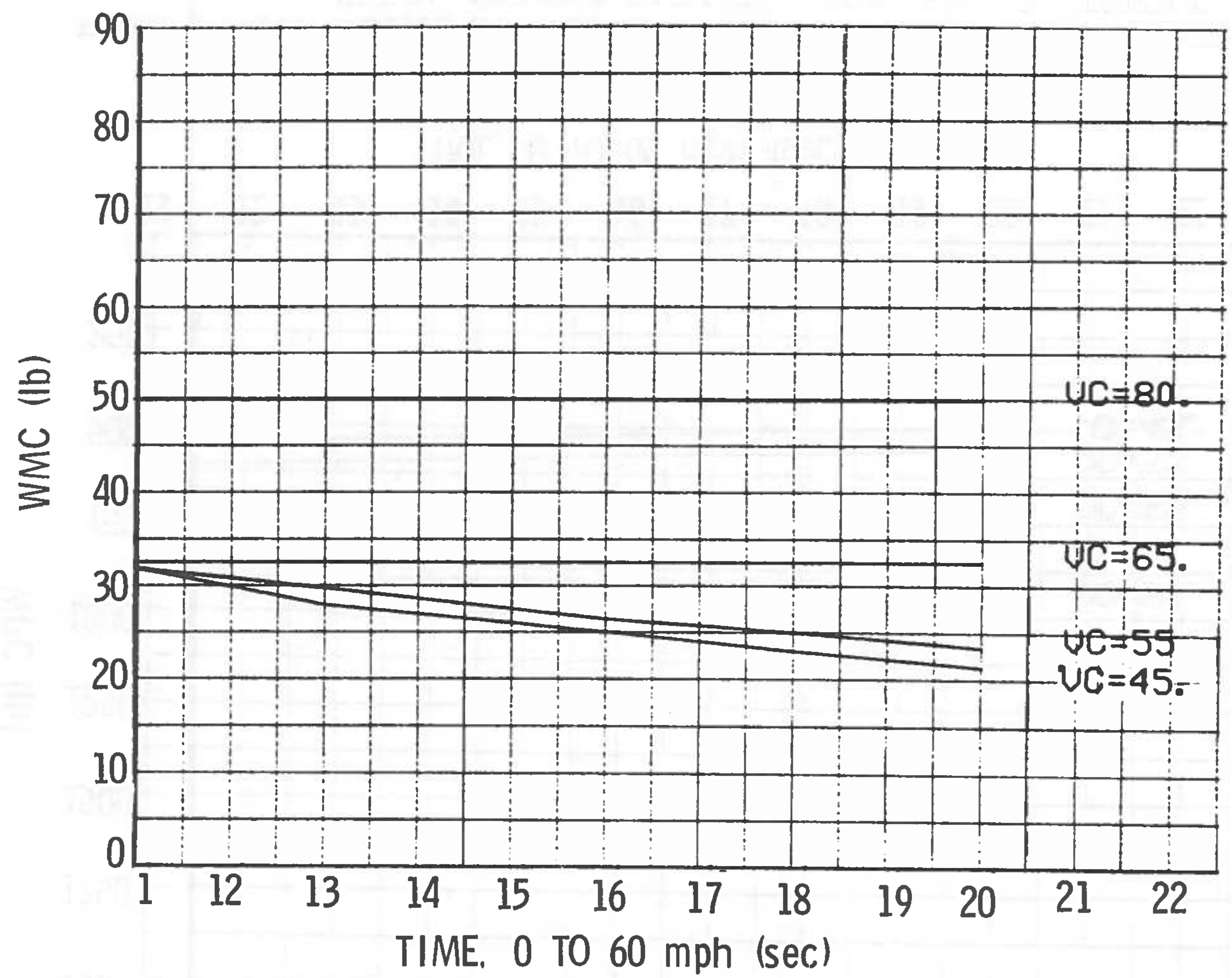

FIGURE 9-17. MOTOR POWER CONDITIONING AND CONTROL WEIGHT (WMC) FOR 2500-LB VEHICLE: HYBRID HEAT ENGINE/ BATTERY SYSTEM, SERIES CONFIGURATION

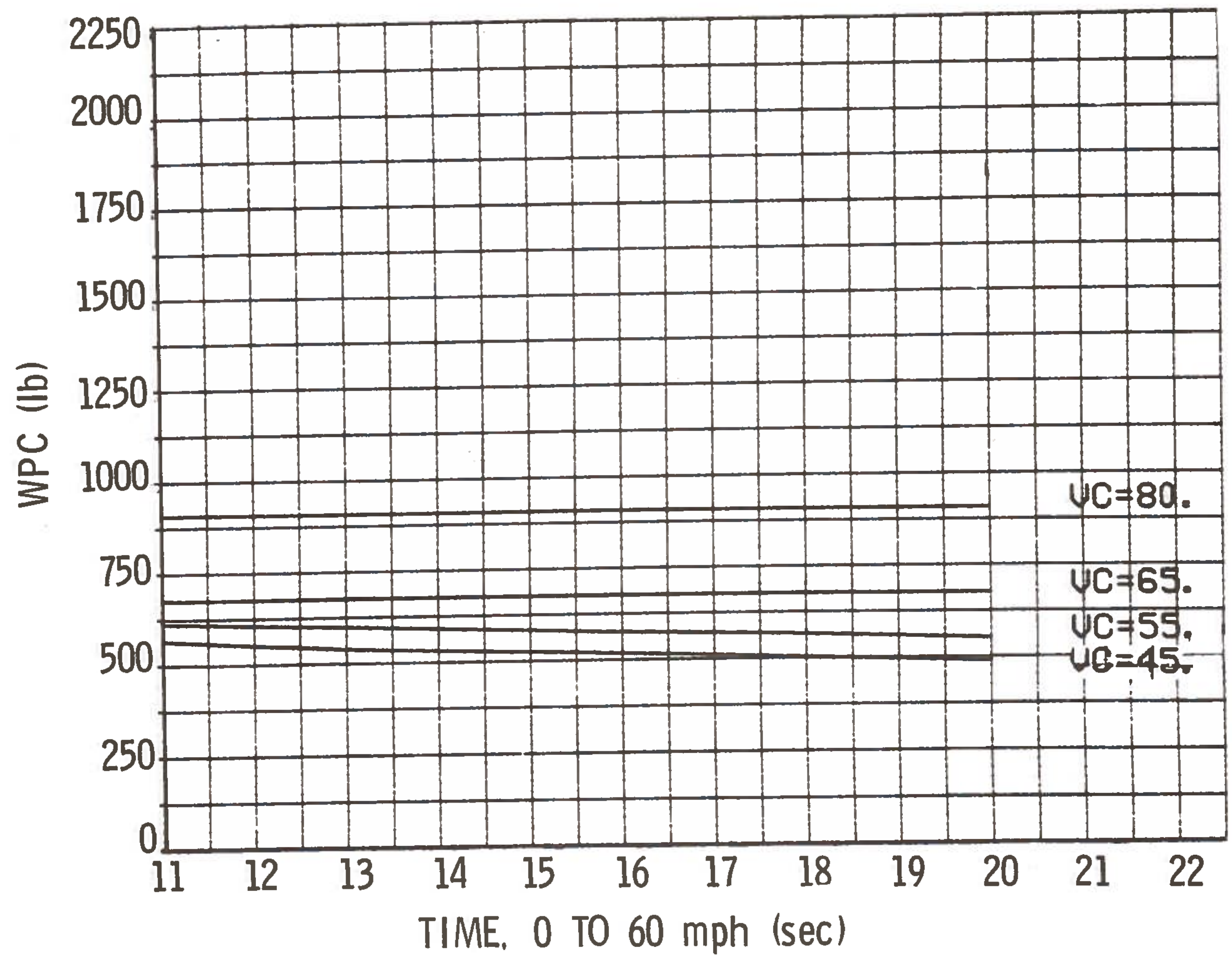

FIGURE 9-18. TOTAL WEIGHT OF ALL POWERTRAIN COMPONENTS (WPC), EXCEPT BATTERY, FOR 2500-LB VEHICLE: HYBRID HEAT ENGINE/BATTERY SYSTEM, SERIES CONFIGURATION

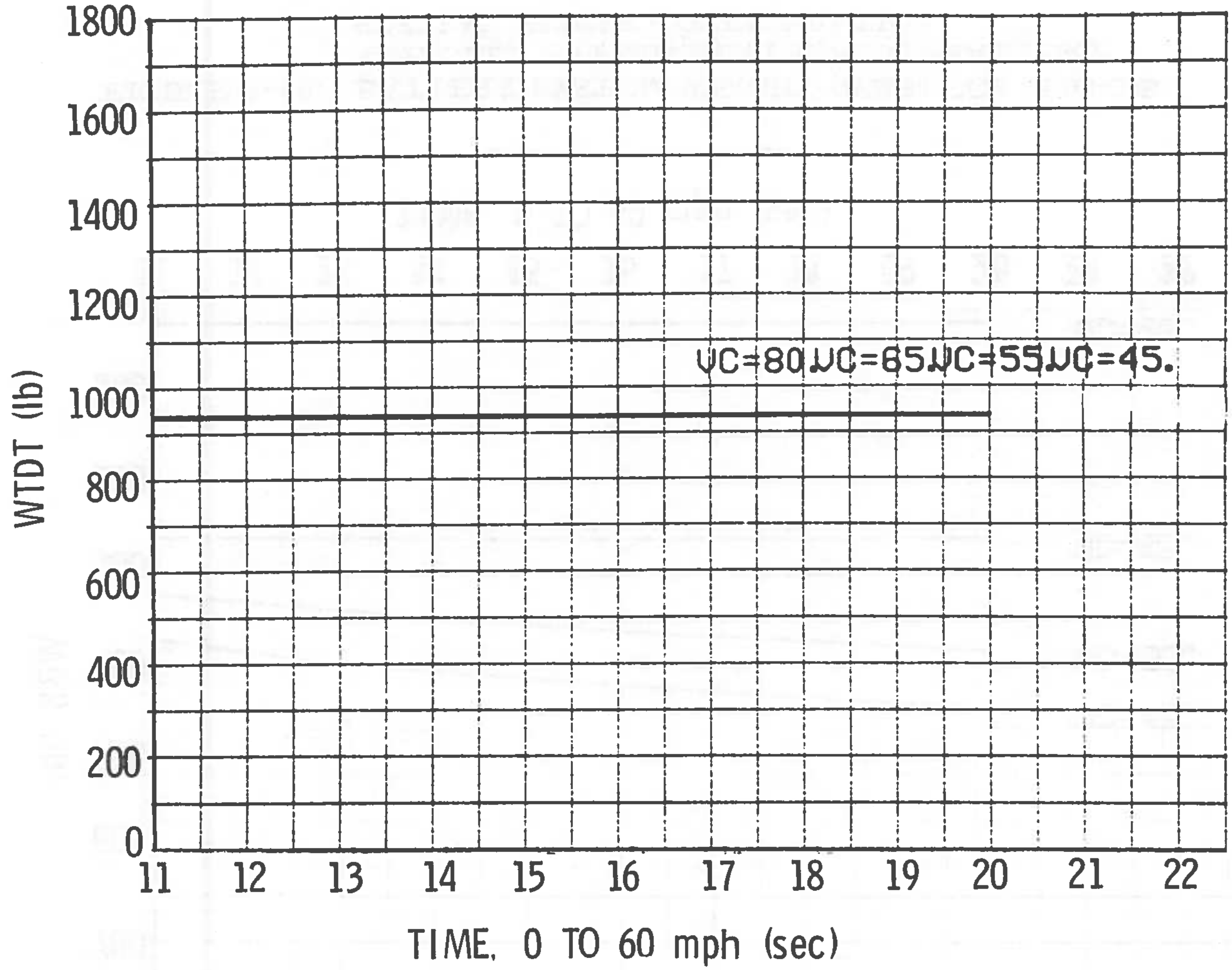

FIGURE 9-19. TOTAL WEIGHT OF ALL POWERTRAIN COMPONENTS (WTDT) FOR 2500-LB VEHICLE: HYBRID HEAT ENGINE/BATTERY SYSTEM, SERIES CONFIGURATION

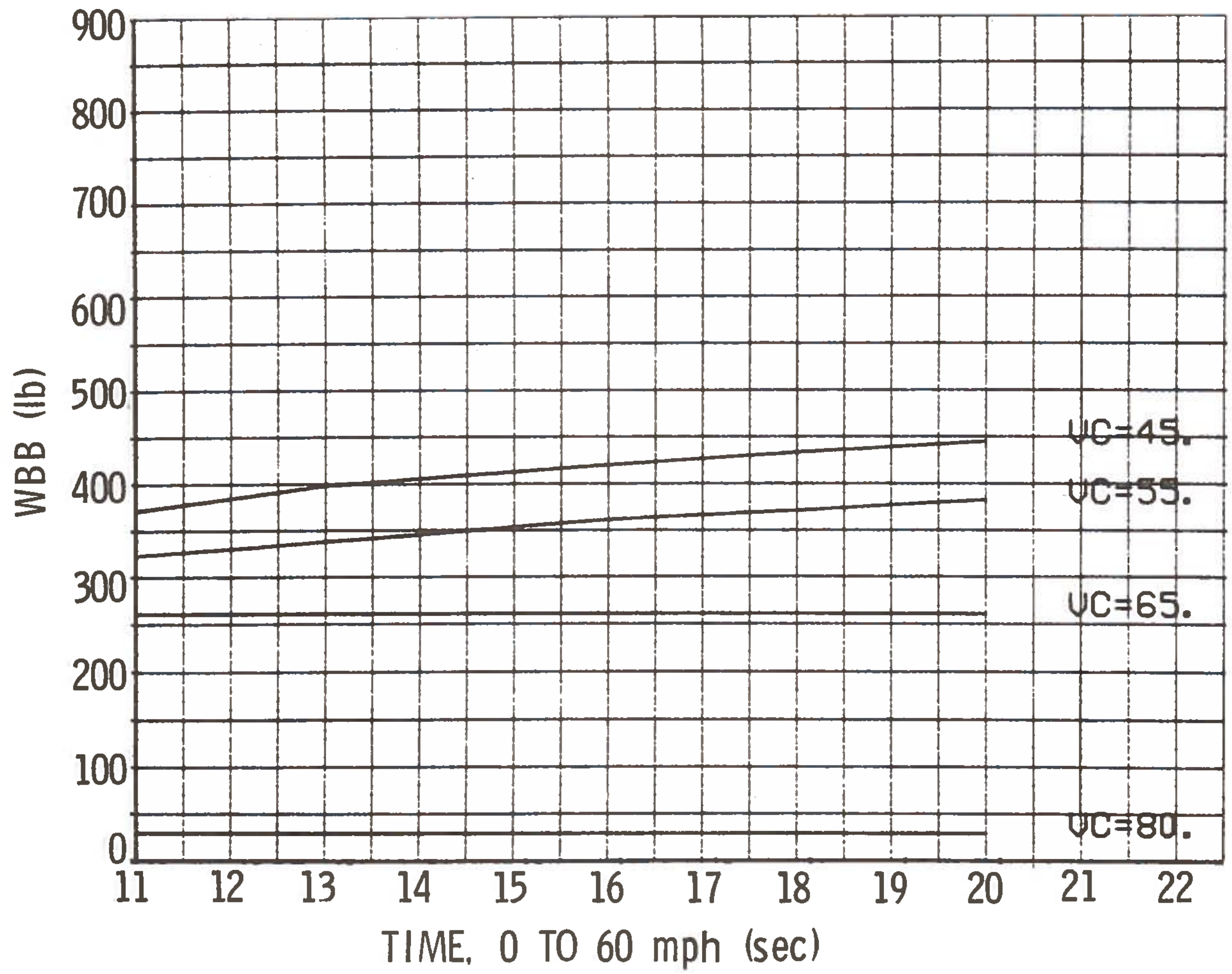

FIGURE 9-20. BATTERY SYSTEM WEIGHT (WBB) FOR 2500-LB VEHICLE: HYBRID HEAT ENGINE/BATTERY SYSTEM, SERIES CONFIGURATION

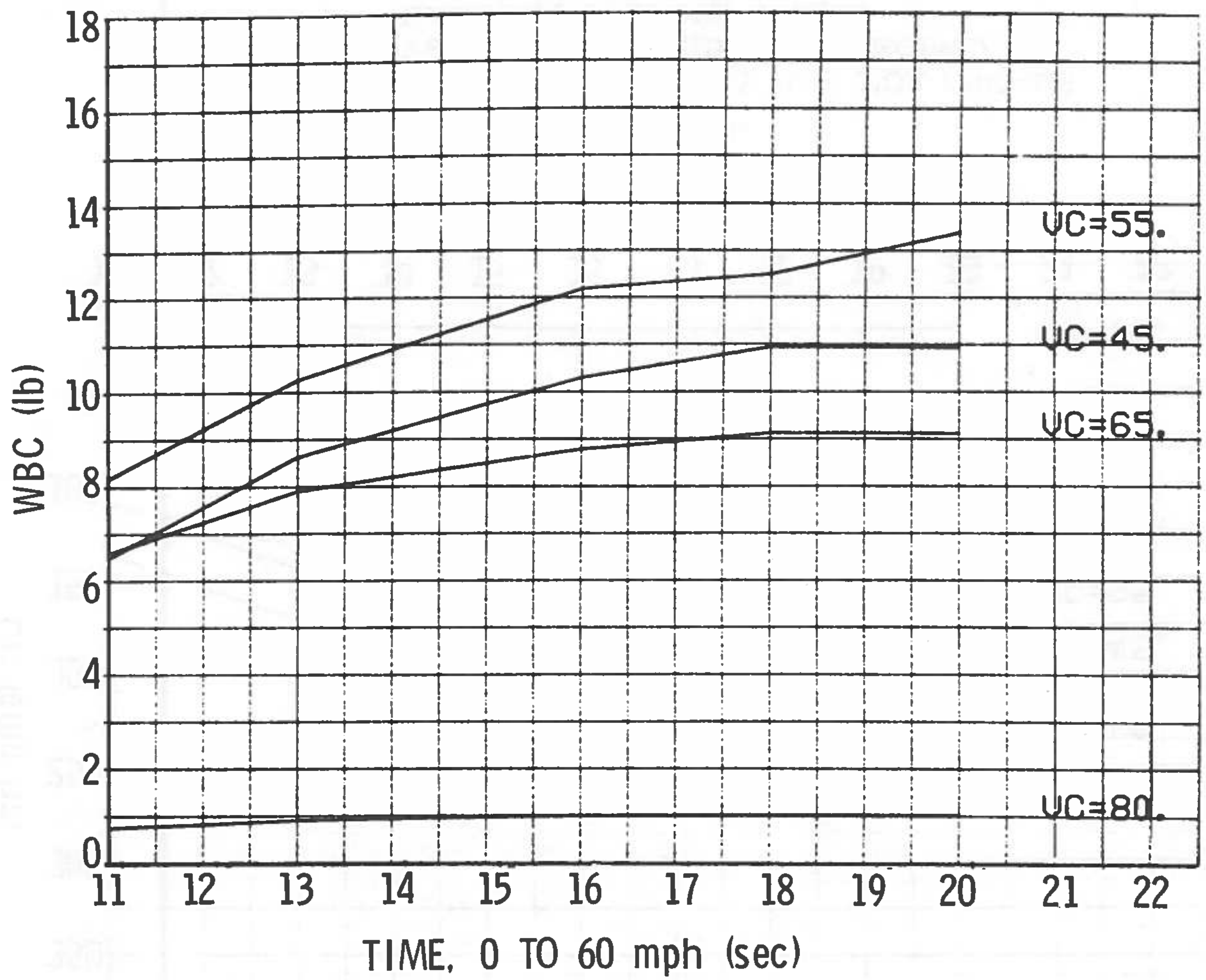

FIGURE 9-21. BATTERY CELL WEIGHT (WBC) FOR 2500-LB VEHICLE: HYBRID HEAT ENGINE/BATTERY SYSTEM, SERIES CONFIGURATION

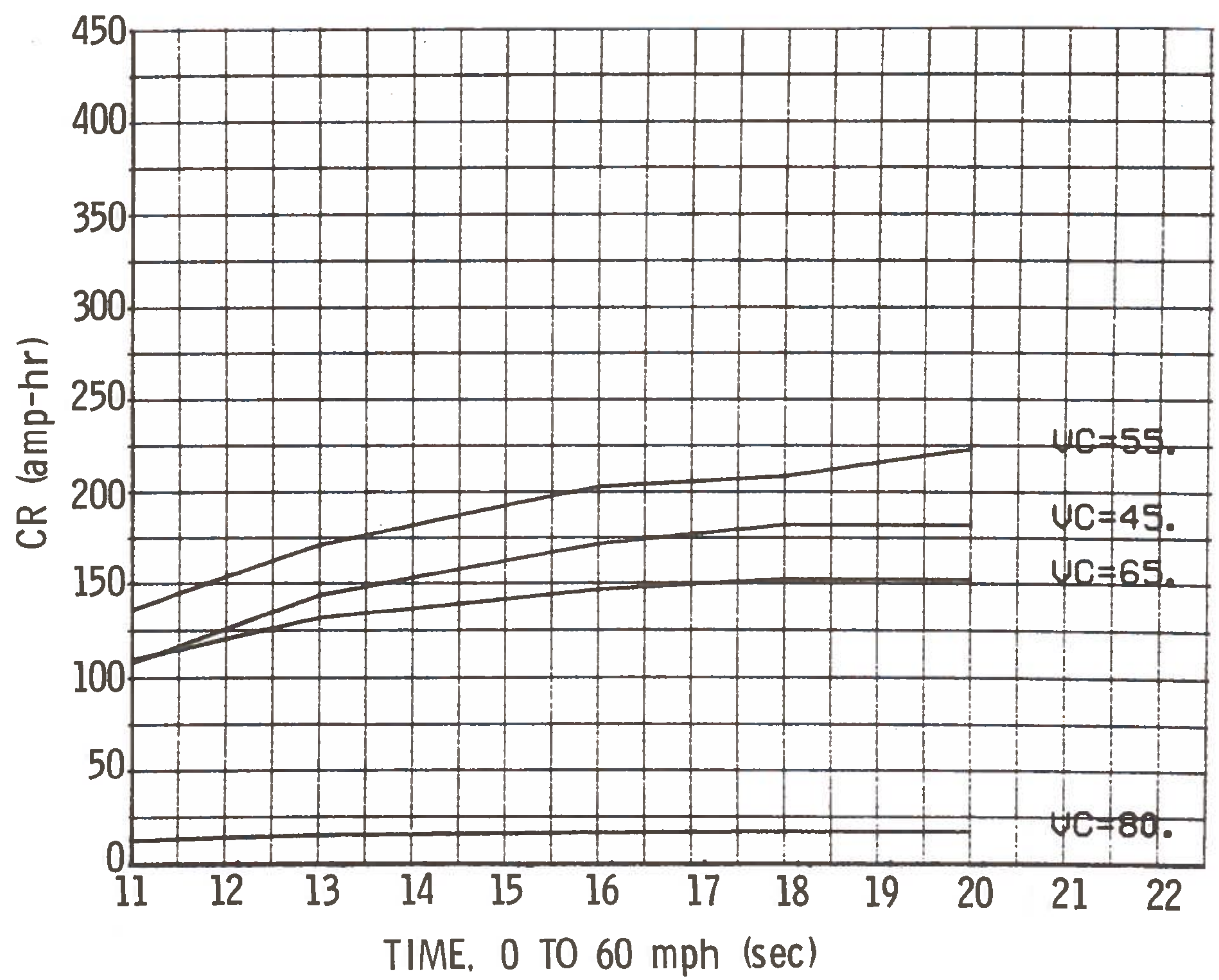

FIGURE 9-22. BATTERY CAPACITY (CR) FOR 2500-LB VEHICLE: HYBRID HEAT ENGINE/ BATTERY SYSTEM, SERIES CONFIGURATION

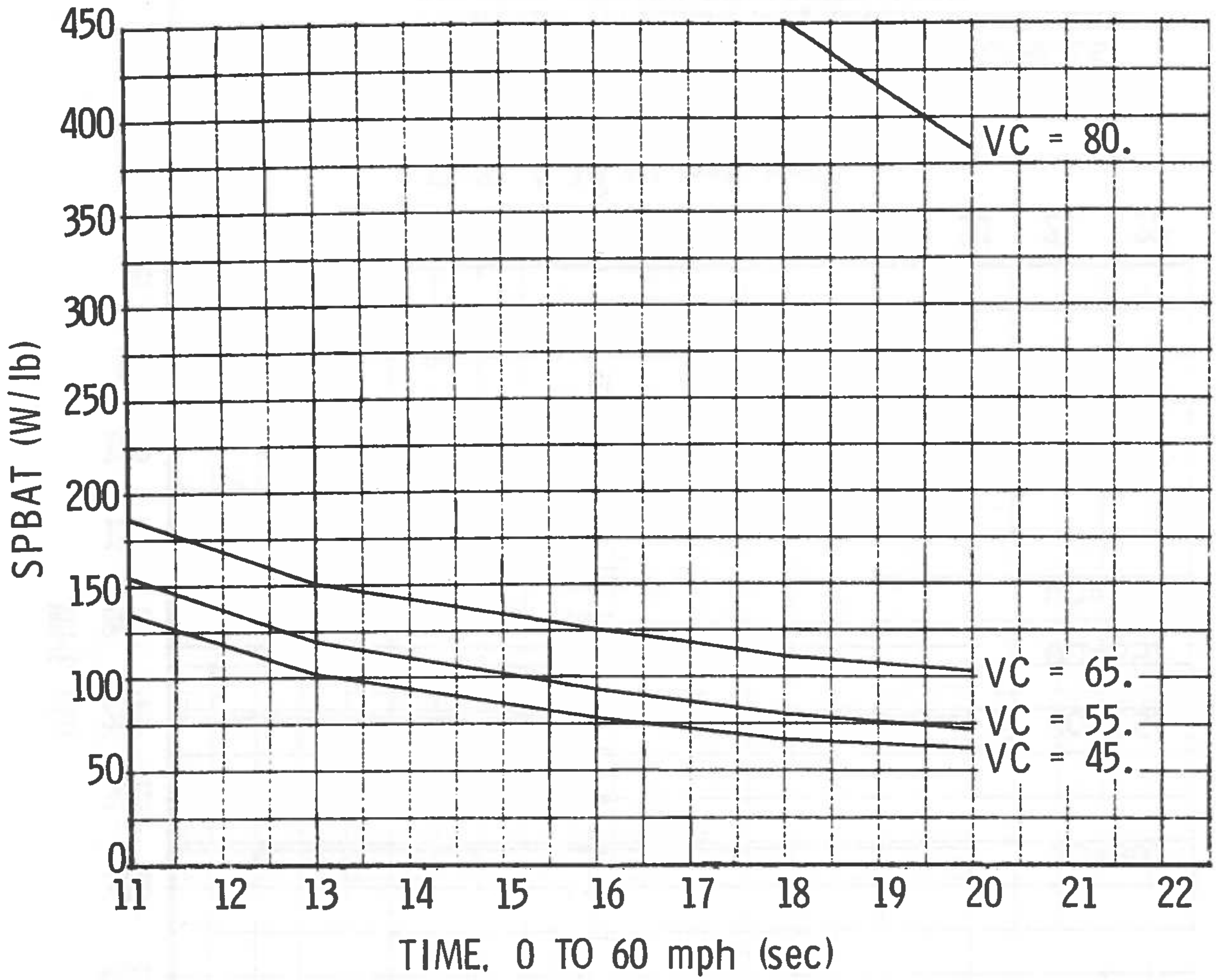

FIGURE 9-23. BATTERY SPECIFIC POWER (SPBAT) FOR 2500-LB VEHICLE: HYBRID HEAT ENGINE/BATTERY SYSTEM, SERIES CONFIGURATION

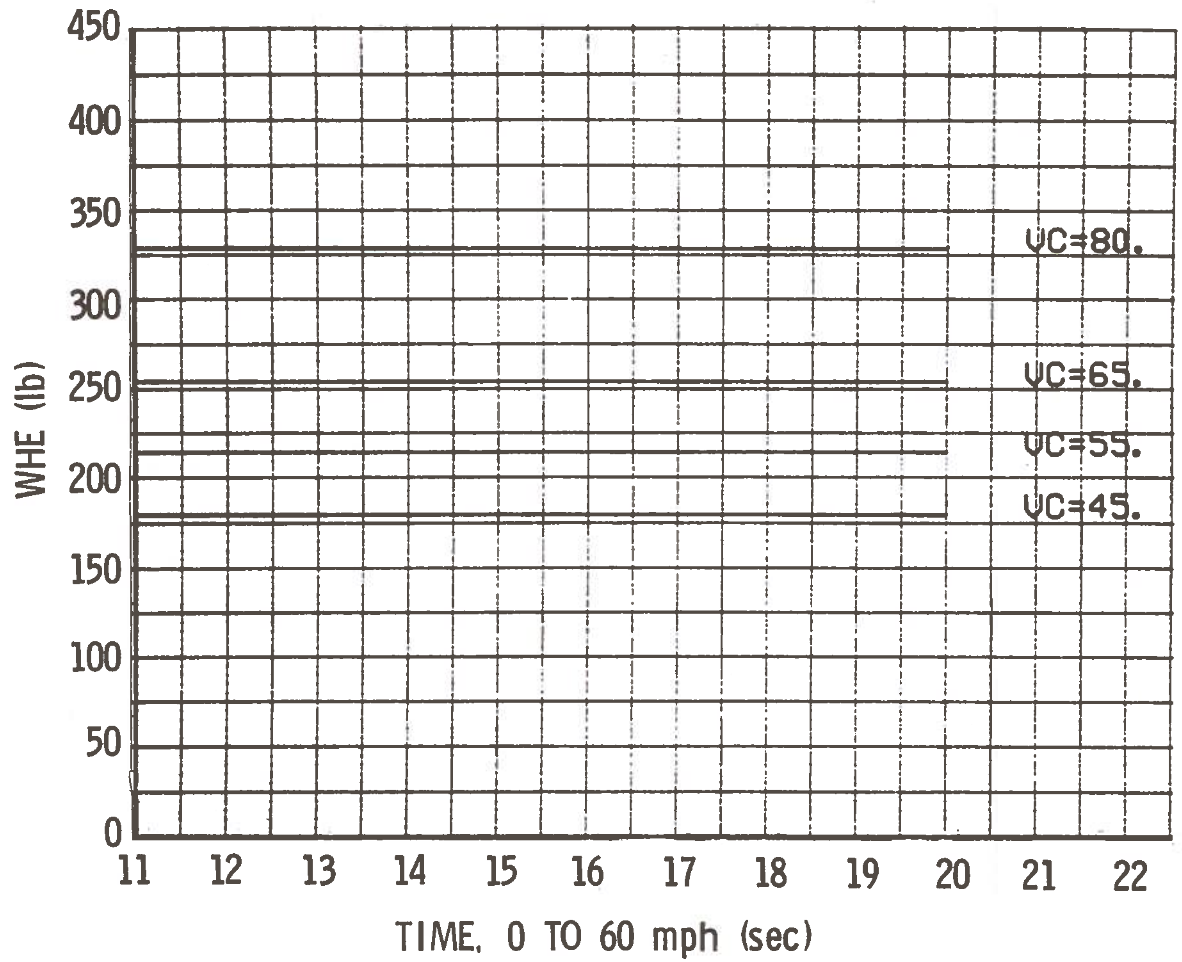

FIGURE 9-24. HEAT ENGINE WEIGHT (WHE) FOR 4000-LB VEHICLE: HYBRID HEAT ENGINE/BATTERY SYSTEM, SERIES CONFIGURATION

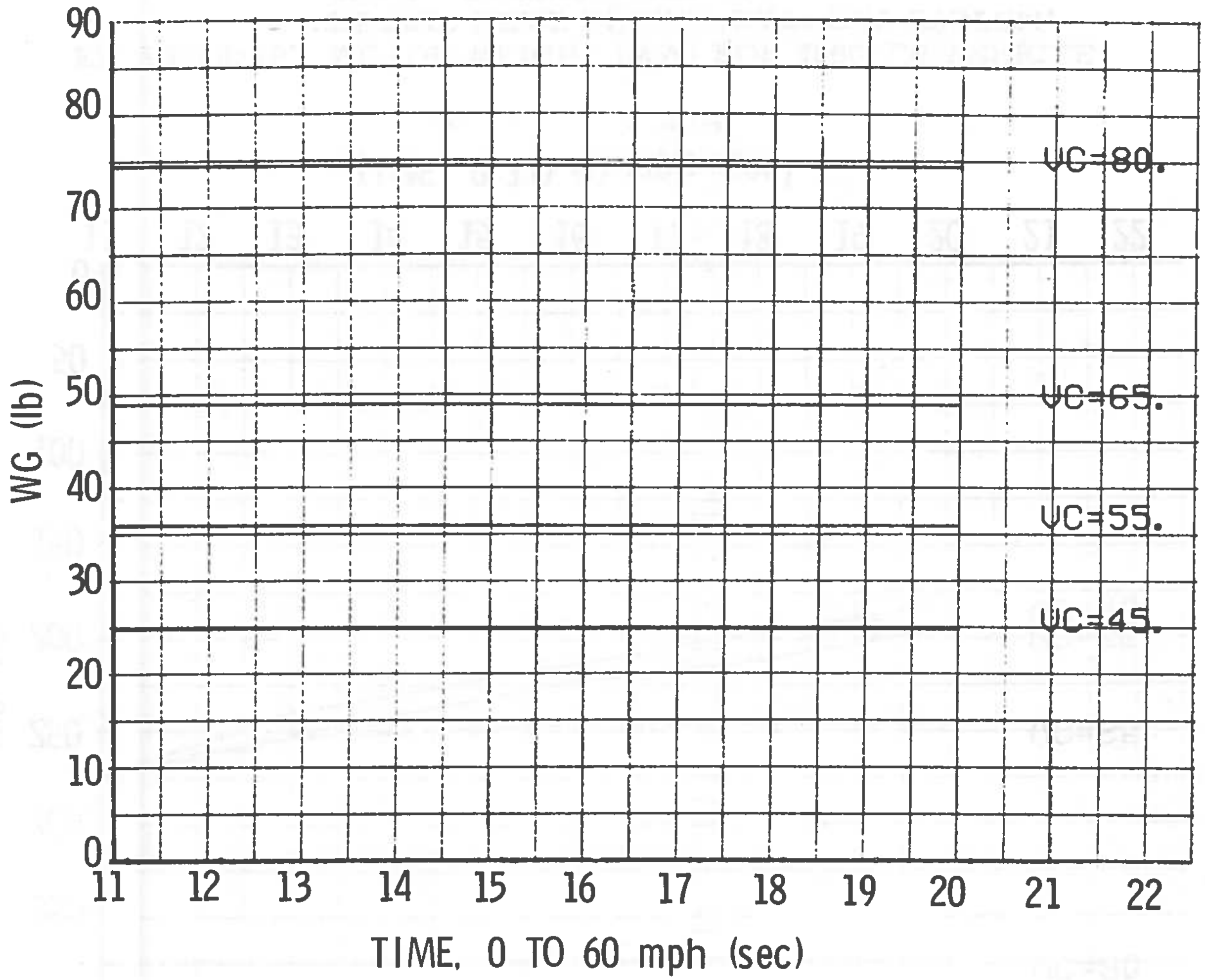

FIGURE 9-25. GENERATOR WEIGHT (WG) FOR 4000-LB VEHICLE: HYBRID HEAT ENGINE/ BATTERY SYSTEM, SERIES CONFIGURATION

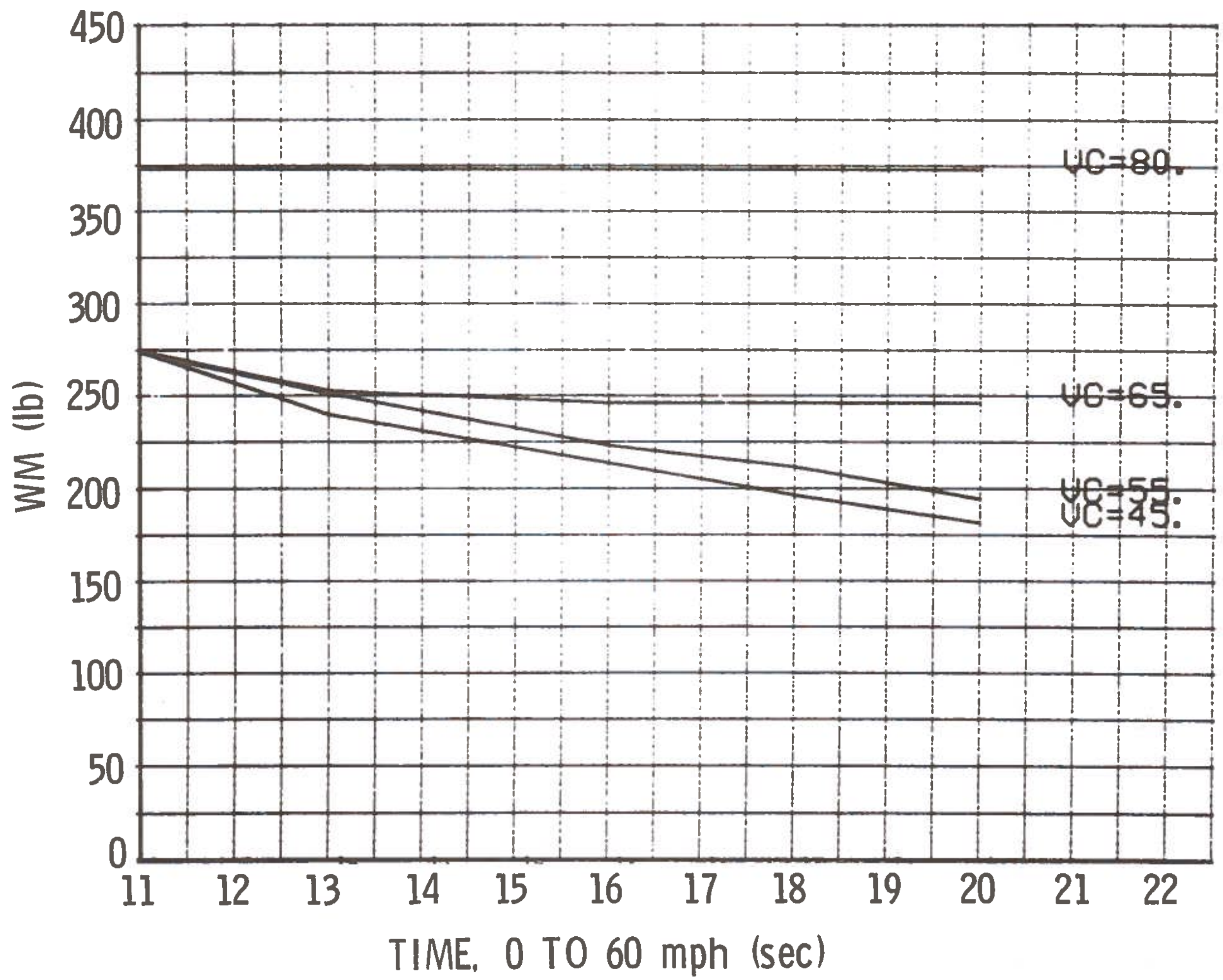

FIGURE 9-26. MOTOR WEIGHT (WM) FOR 4000-LB VEHICLE: HYBRID HEAT ENGINE/BATTERY SYSTEM, SERIES CONFIGURATION

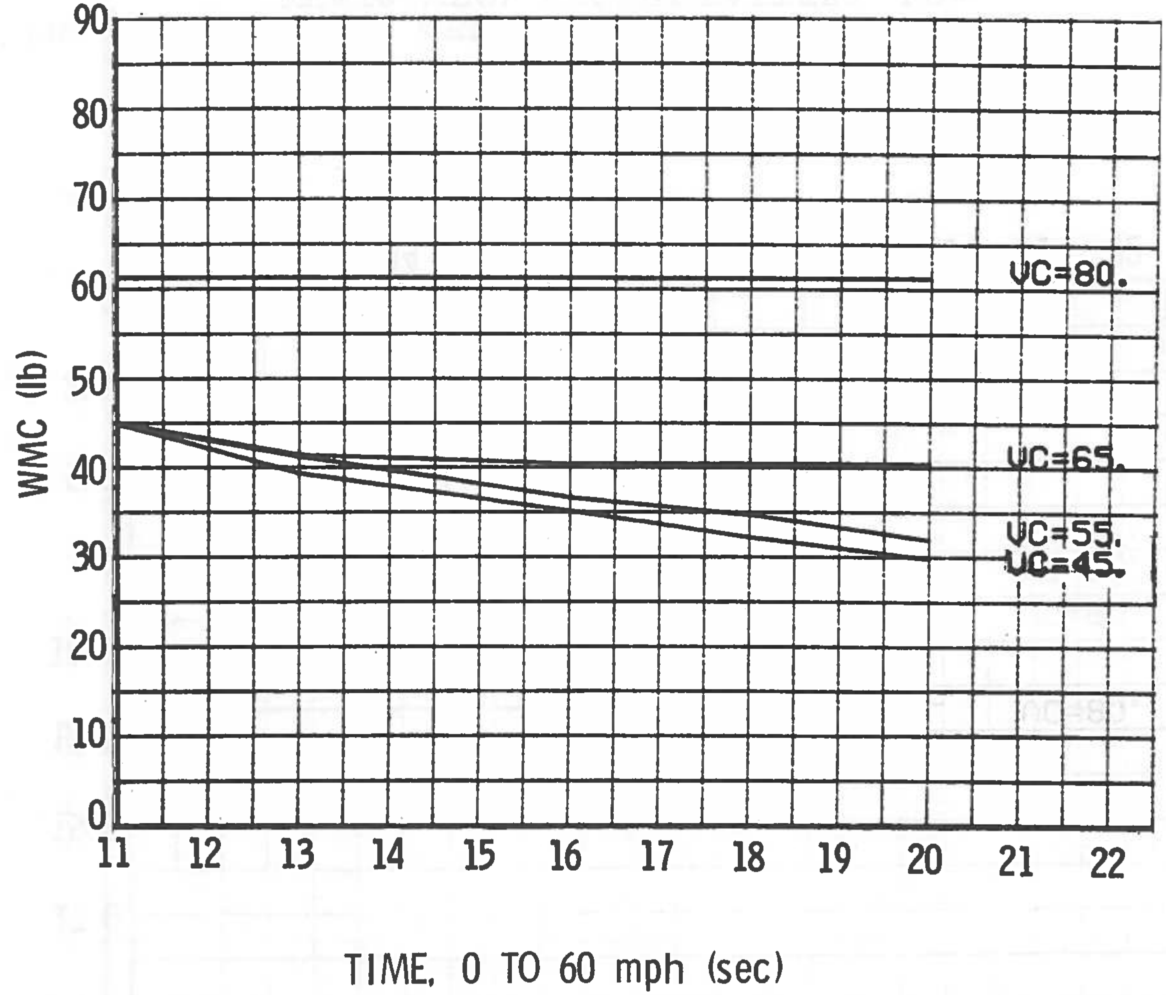

FIGURE 9-27. MOTOR POWER CONDITIONING AND CONTROL WEIGHT (WMC) FOR 4000-LB VEHICLE: HYBRID HEAT ENGINE/BATTERY SYSTEM, SERIES CONFIGURATION

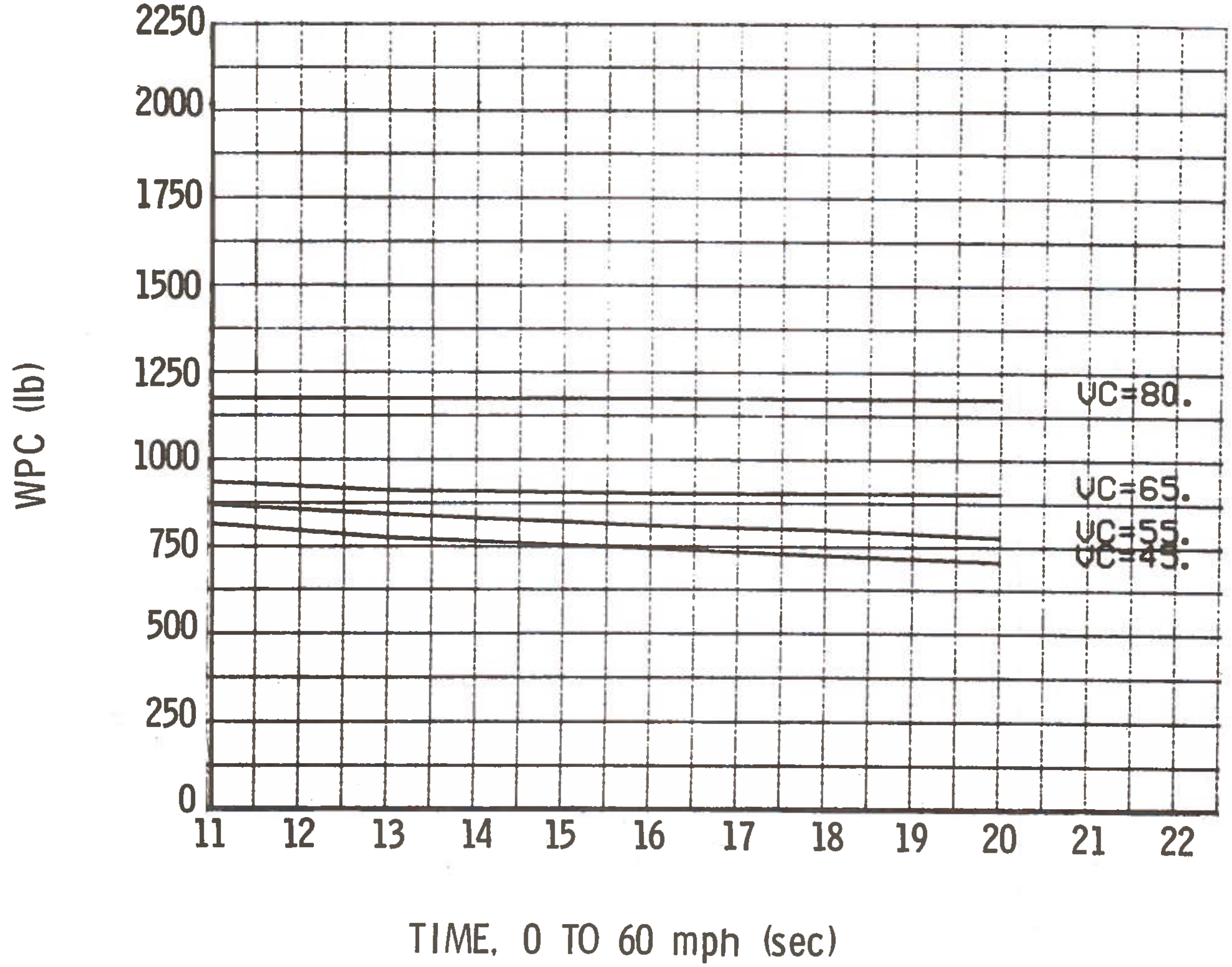

FIGURE 9-28. TOTAL WEIGHT OF ALL POWERTRAIN COMPONENTS (WPC), EXCEPT BATTERY, FOR 4000-LB VEHICLE: HYBRID HEAT ENGINE/ BATTERY SYSTEM, SERIES CONFIGURATION

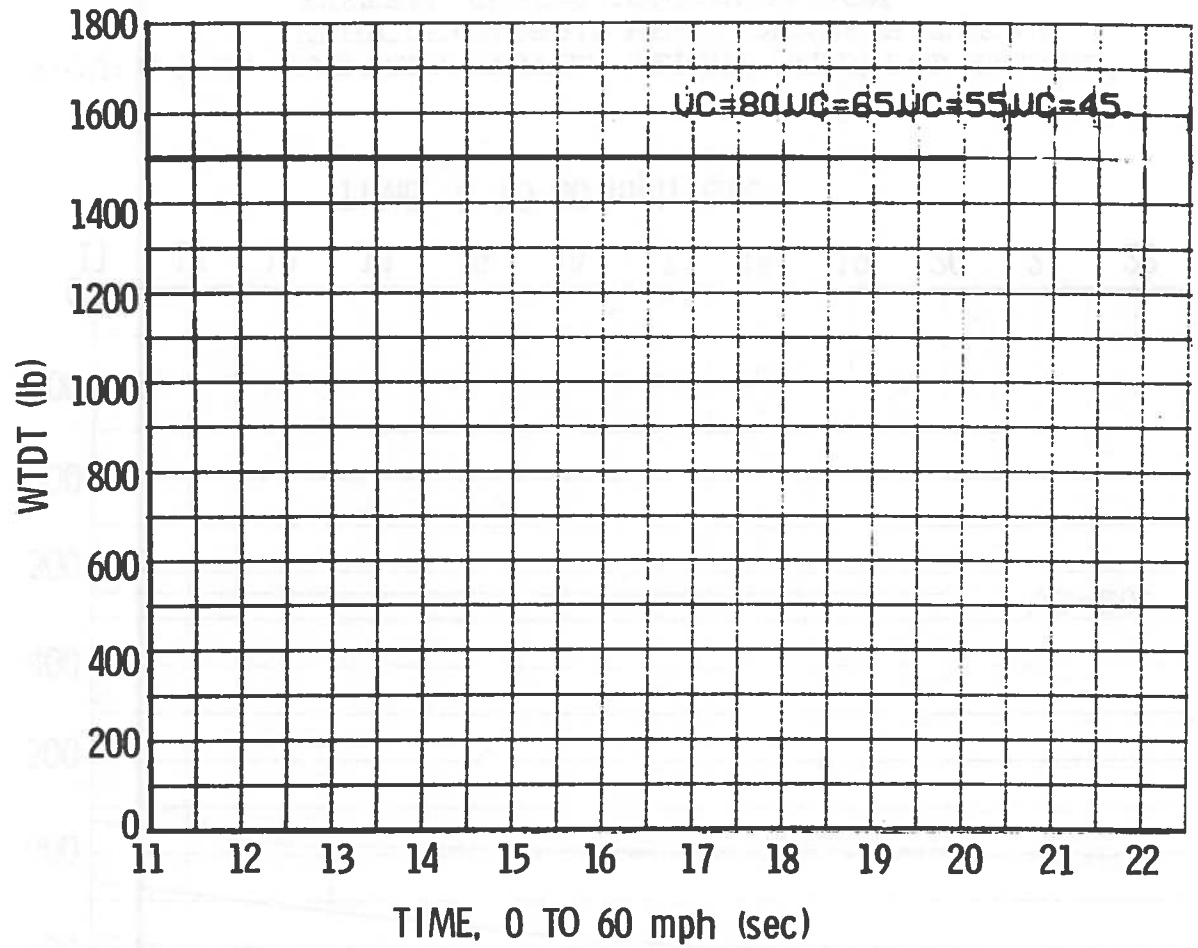

FIGURE 9-29. TOTAL WEIGHT OF ALL POWERTRAIN COMPONENTS (WTDT) FOR 4000-LB VEHICLE: HYBRID HEAT ENGINE/BATTERY SYSTEM, SERIES CONFIGURATION

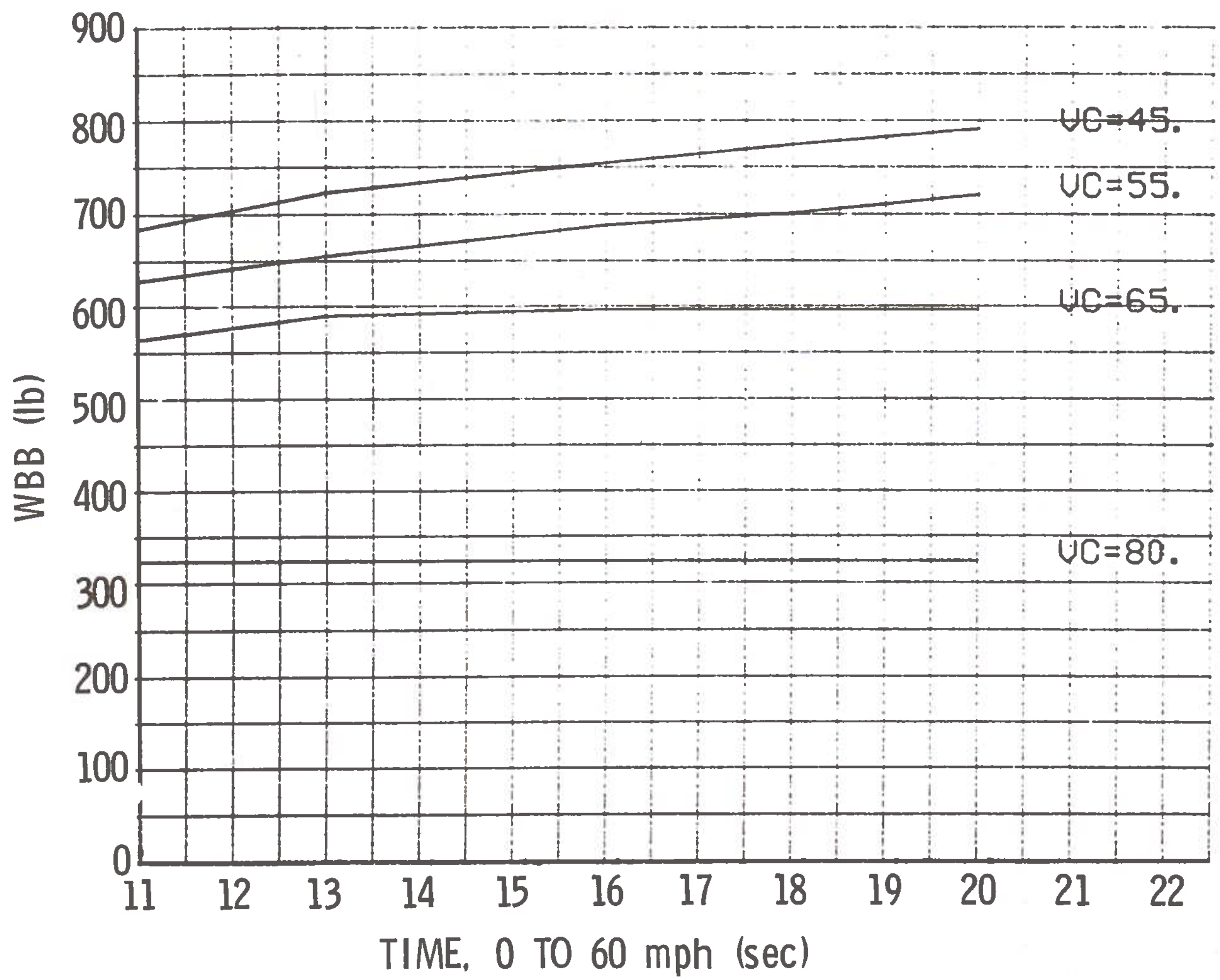

FIGURE 9-30. BATTERY SYSTEM WEIGHT (WBB) FOR 4000-LB VEHICLE: HYBRID HEAT ENGINE/BATTERY SYSTEM, SERIES CONFIGURATION

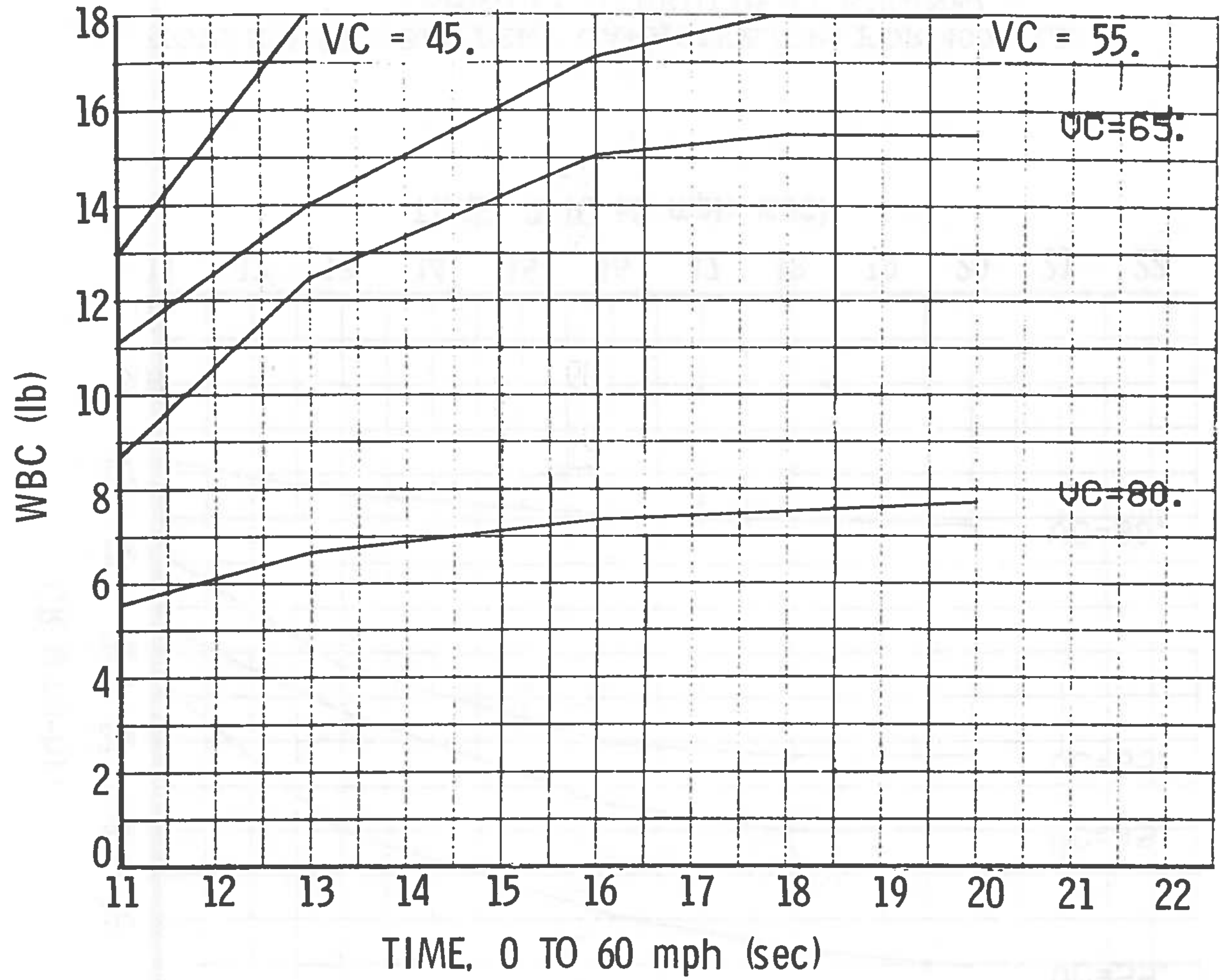

FIGURE 9-31. BATTERY CELL WEIGHT (WBC) FOR 4000-LB VEHICLE: HYBRID HEAT ENGINE/BATTERY SYSTEM, SERIES CONFIGURATION

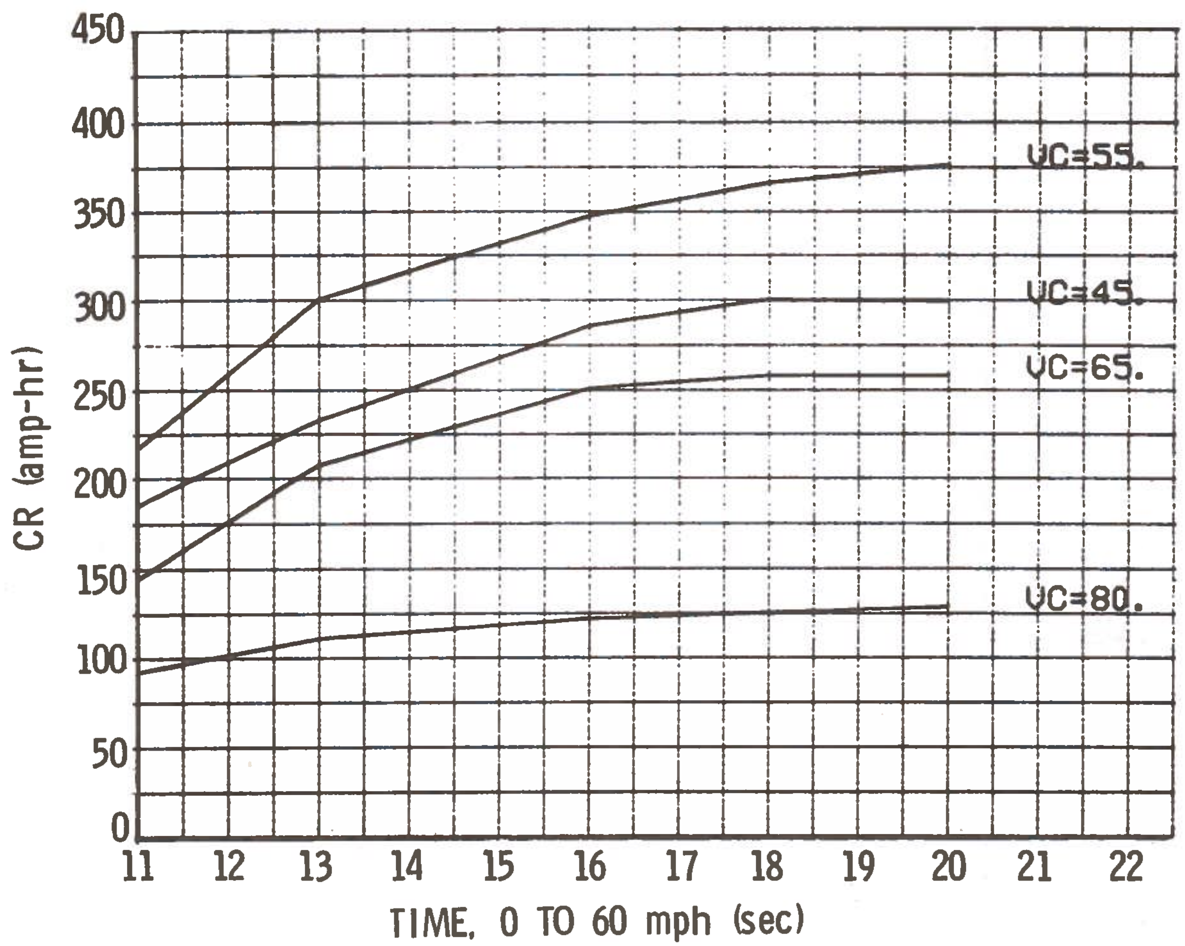

FIGURE 9-32. BATTERY CAPACITY (CR) FOR 4000-LB VEHICLE: HYBRID HEAT ENGINE/ BATTERY SYSTEM, SERIES CONFIGURATION

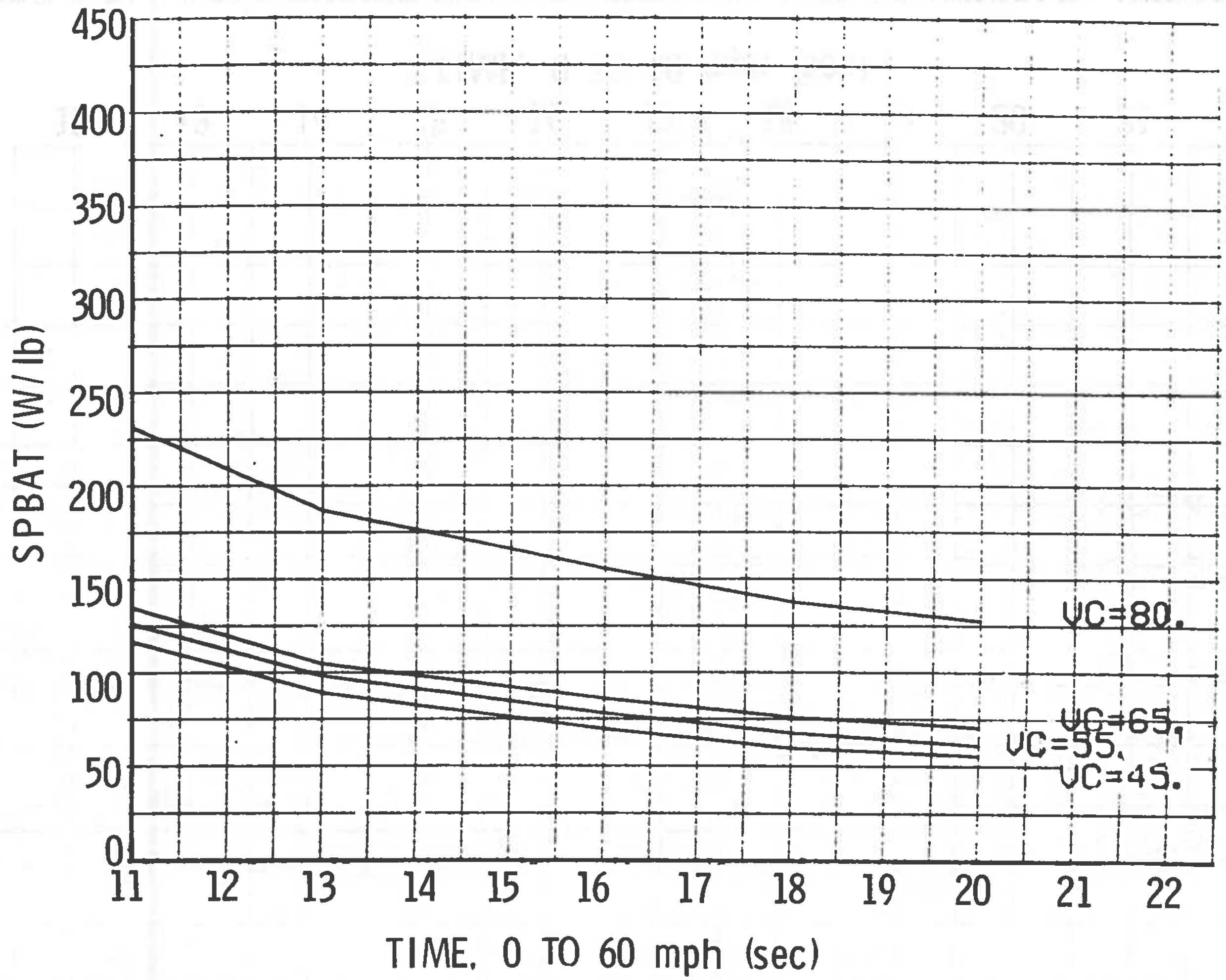

FIGURE 9-33. BATTERY SPECIFIC POWER (SPBAT) FOR 4000-LB VEHICLE: HYBRID HEAT ENGINE/BATTERY SYSTEM, SERIES CONFIGURATION

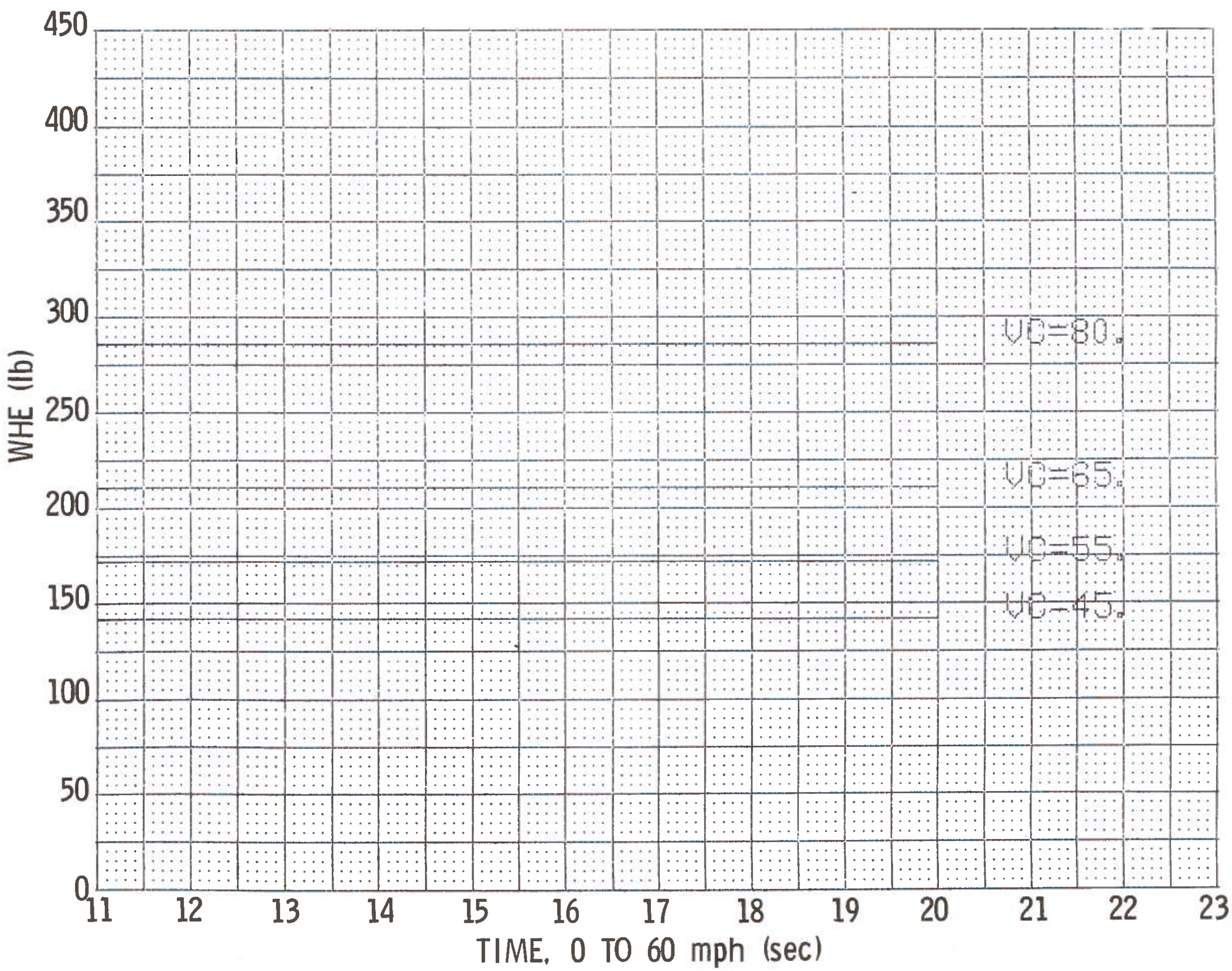

FIGURE 9-34. HEAT ENGINE WEIGHT (WHE) FOR 2500-LB VEHICLE: HYBRID HEAT ENGINE/FLYWHEEL SYSTEM, SERIES CONFIGURATION

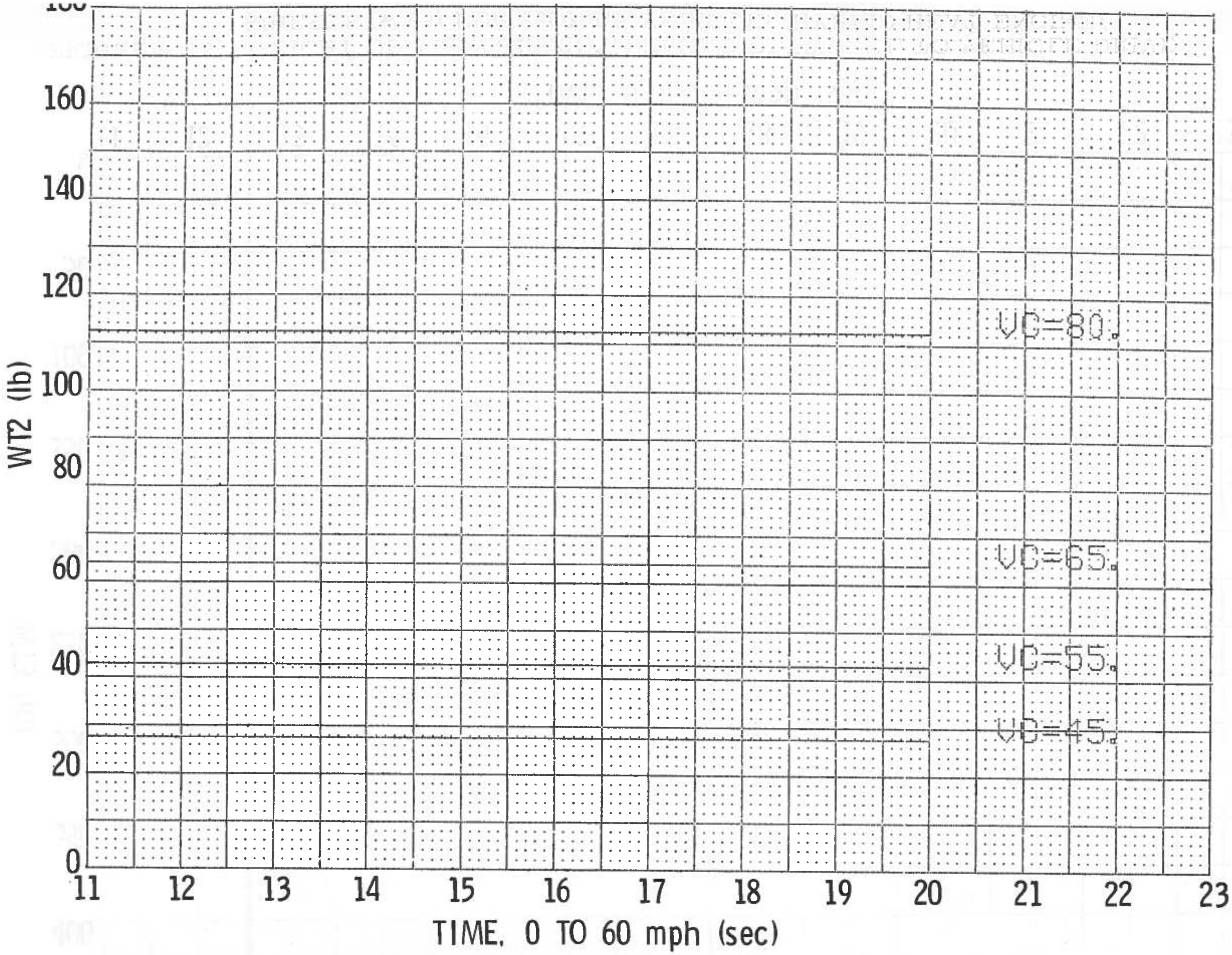

FIGURE 9-35. WEIGHT OF TRANSMISSION LINKING ENGINE TO FLYWHEEL (WT2) FOR 2500-LB VEHICLE: HYBRID HEAT ENGINE/FLYWHEEL SYSTEM, SERIES CONFIGURATION

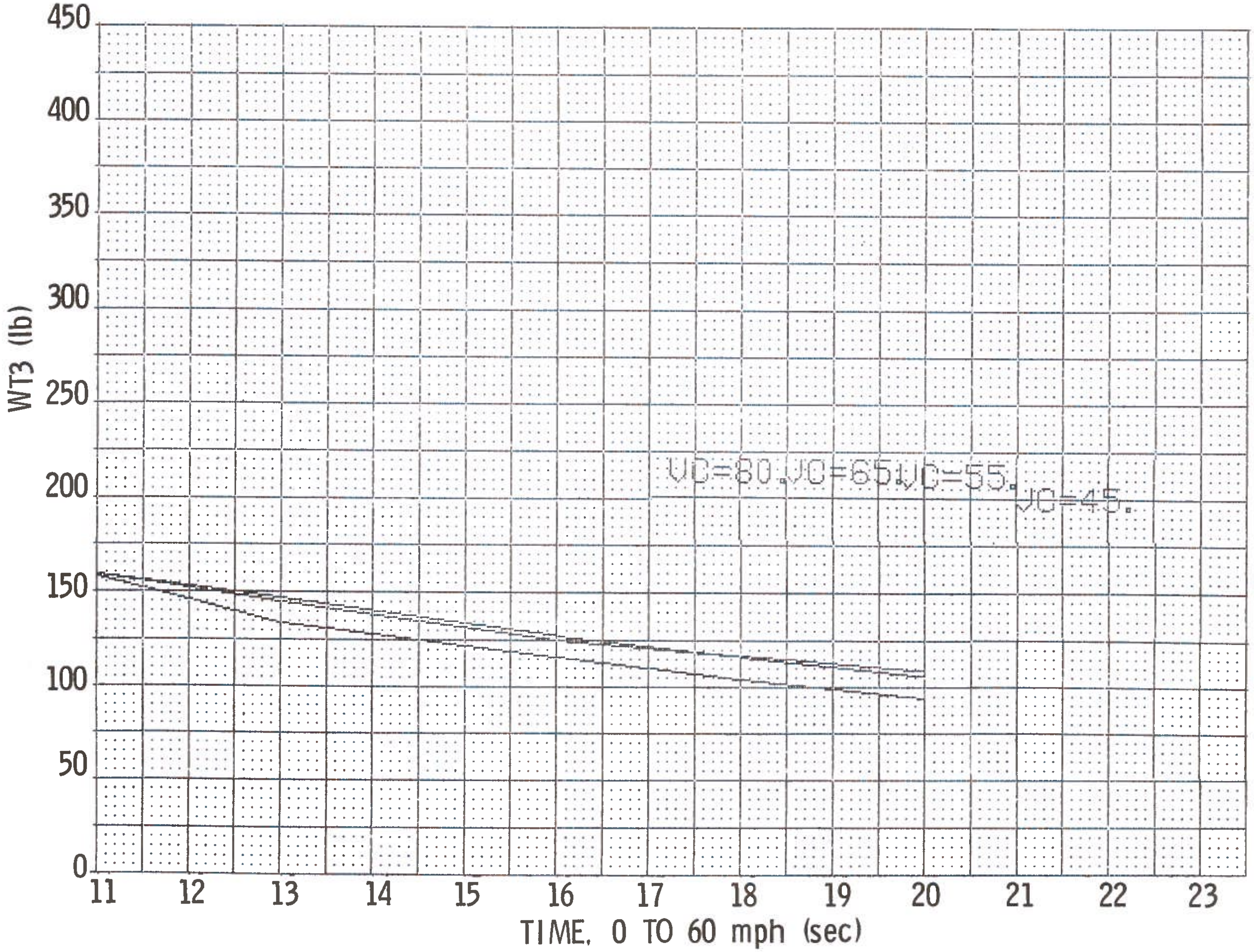

FIGURE 9-36. WEIGHT OF TRANSMISSION LINKING FLYWHEEL TO VEHICLE DRIVE WHEELS (WT3) FOR 2500-LB VEHICLE: HYBRID HEAT ENGINE/

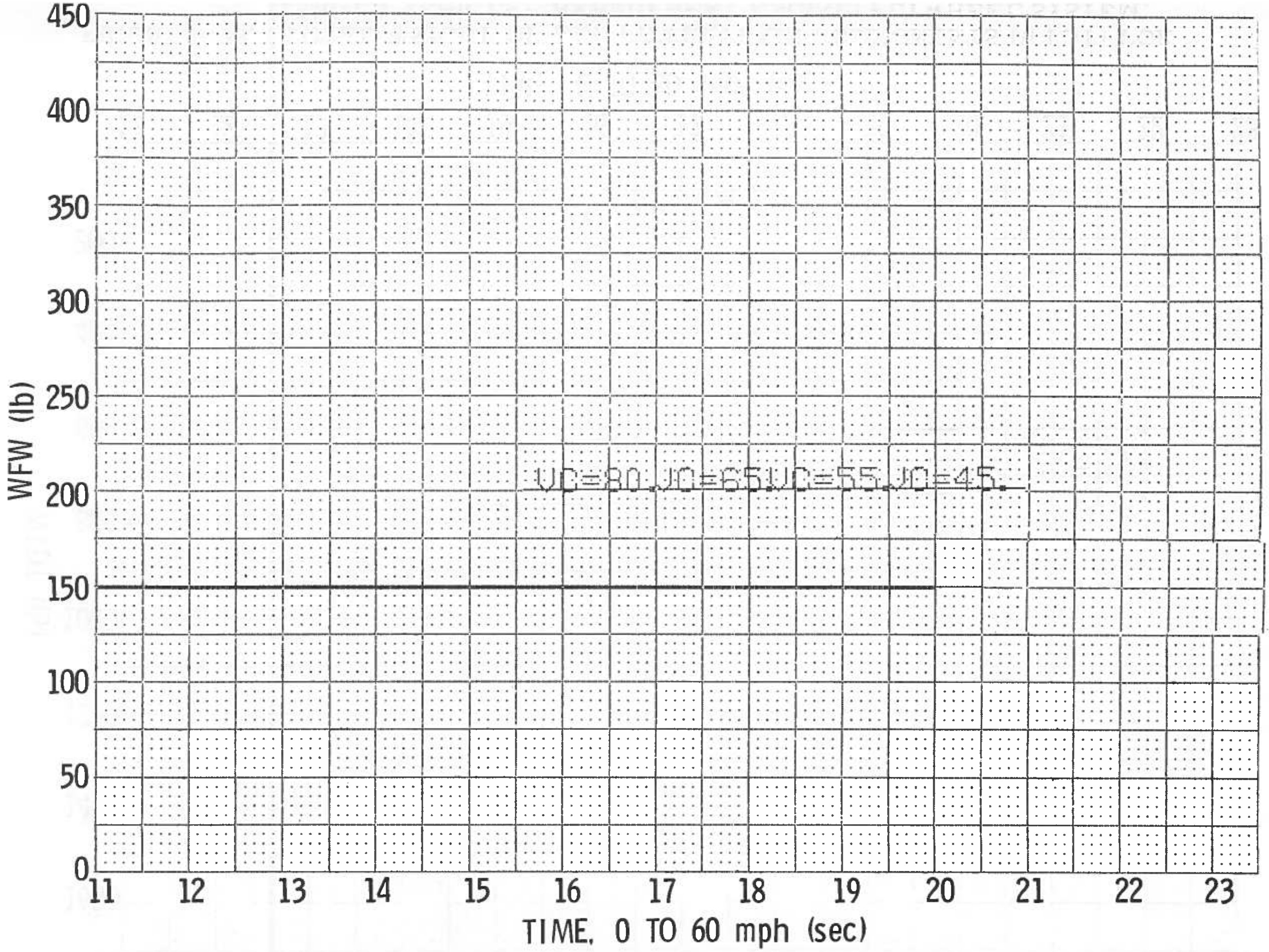

FIGURE 9-37. WEIGHT OF FLYWHEEL SYSTEM (WFW) FOR 2500-LB VEHICLE: HYBRID HEAT ENGINE/FLYWHEEL SYSTEM, SERIES CONFIGURATION

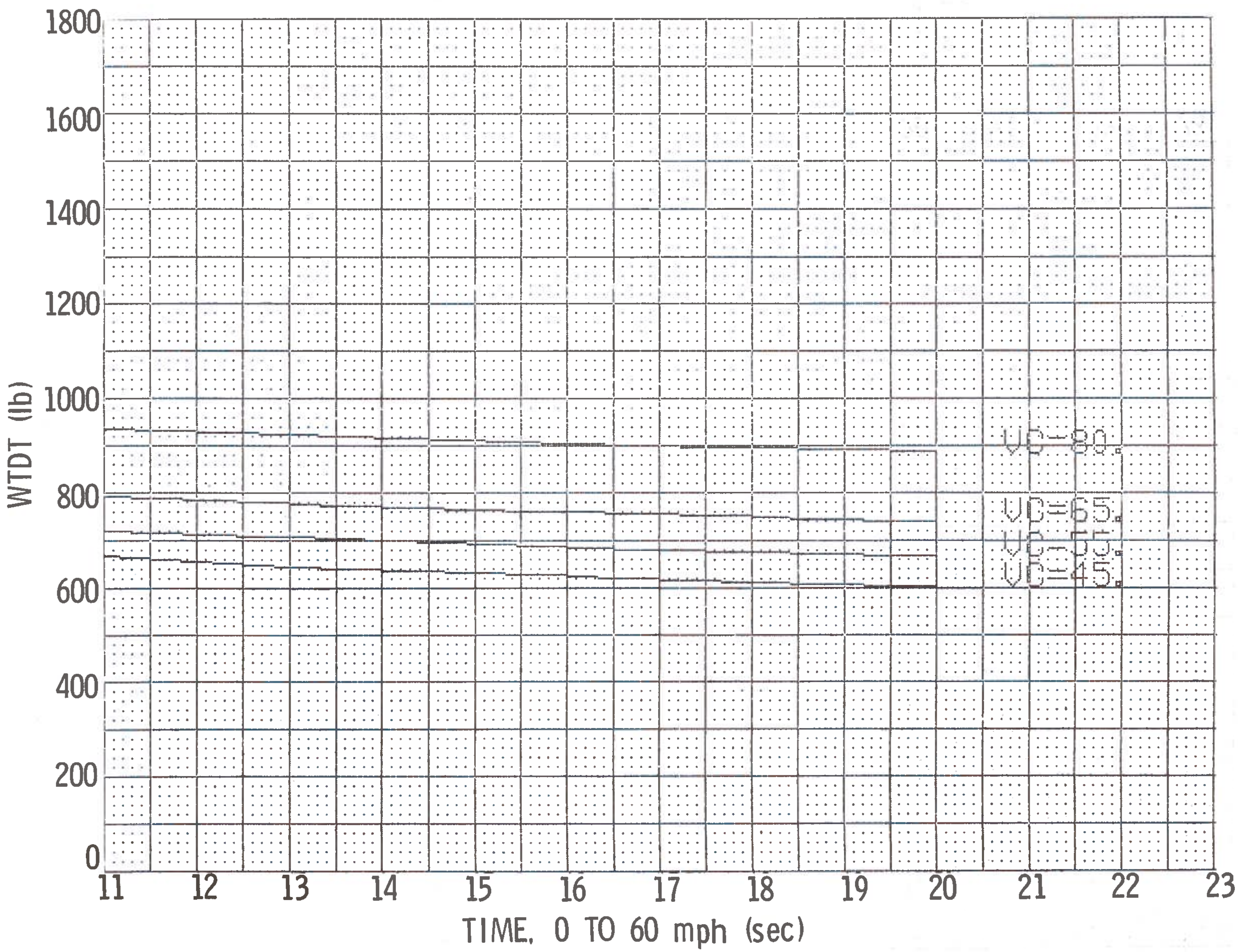

FIGURE 9-38. TOTAL WEIGHT OF ALL POWERTRAIN COMPONENTS (WTDT) FOR 2500-LB VEHICLE: HYBRID HEAT ENGINE/FLYWHEEL SYSTEM.

FIGURE 9-39. TOTAL VOLUME OF ALL POWERTRAIN COMPONENTS (VTDT) FOR 2500-LB VEHICLE: HYBRID HEAT ENGINE/FLYWHEEL SYSTEM, SERIES CONFIGURATION

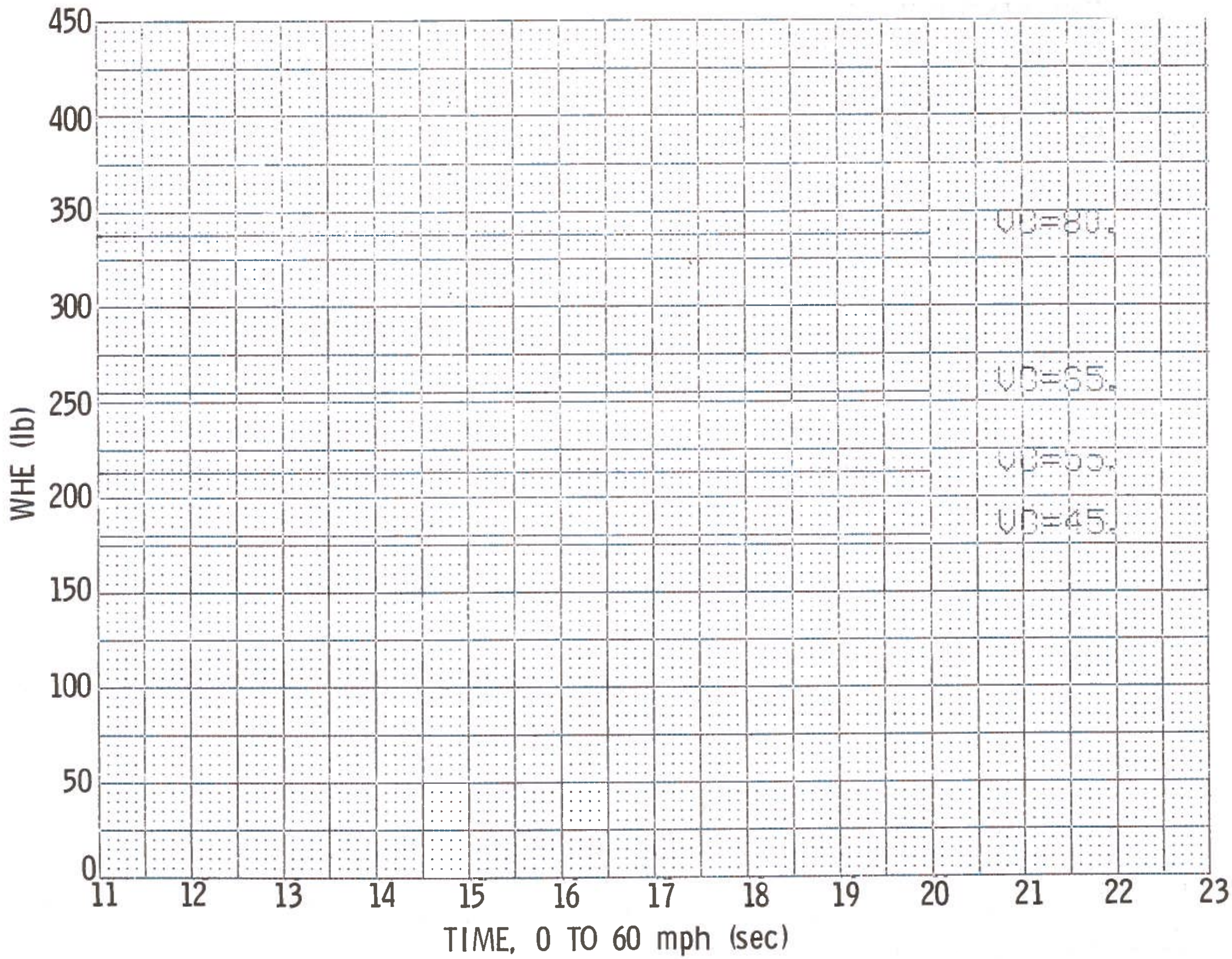

FIGURE 9-40. HEAT ENGINE WEIGHT (WHE) FOR 4000-LB VEHICLE: HYBRID HEAT ENGINE/FLYWHEEL SYSTEM. SERIES CONFIGURATION

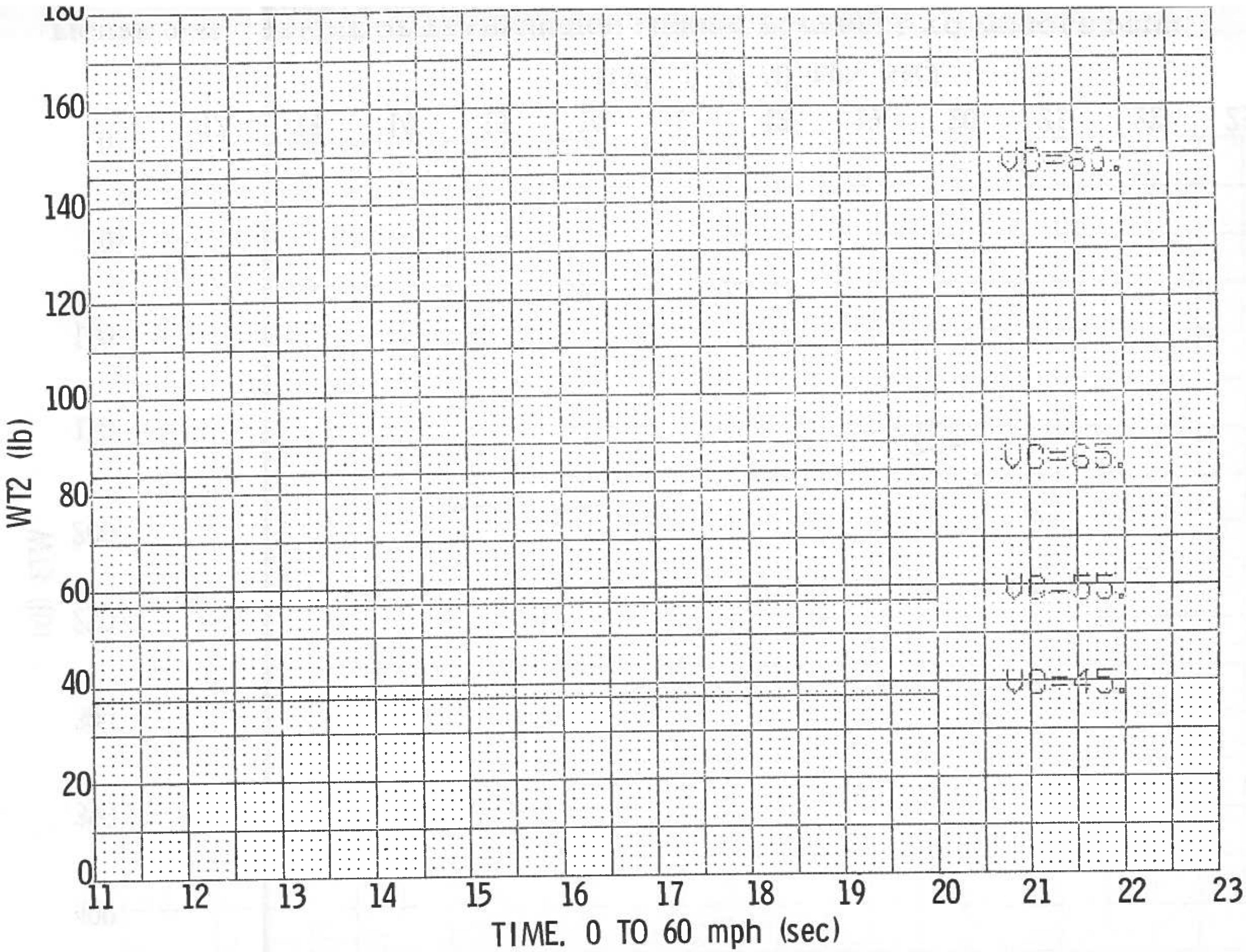

FIGURE 9-41. WEIGHT OF TRANSMISSION LINKING ENGINE TO FLYWHEEL (WT2) FOR 4000-LB VEHICLE: HYBRID HEAT ENGINE/FLYWHEEL SYSTEM, SERIES CONFIGURATION

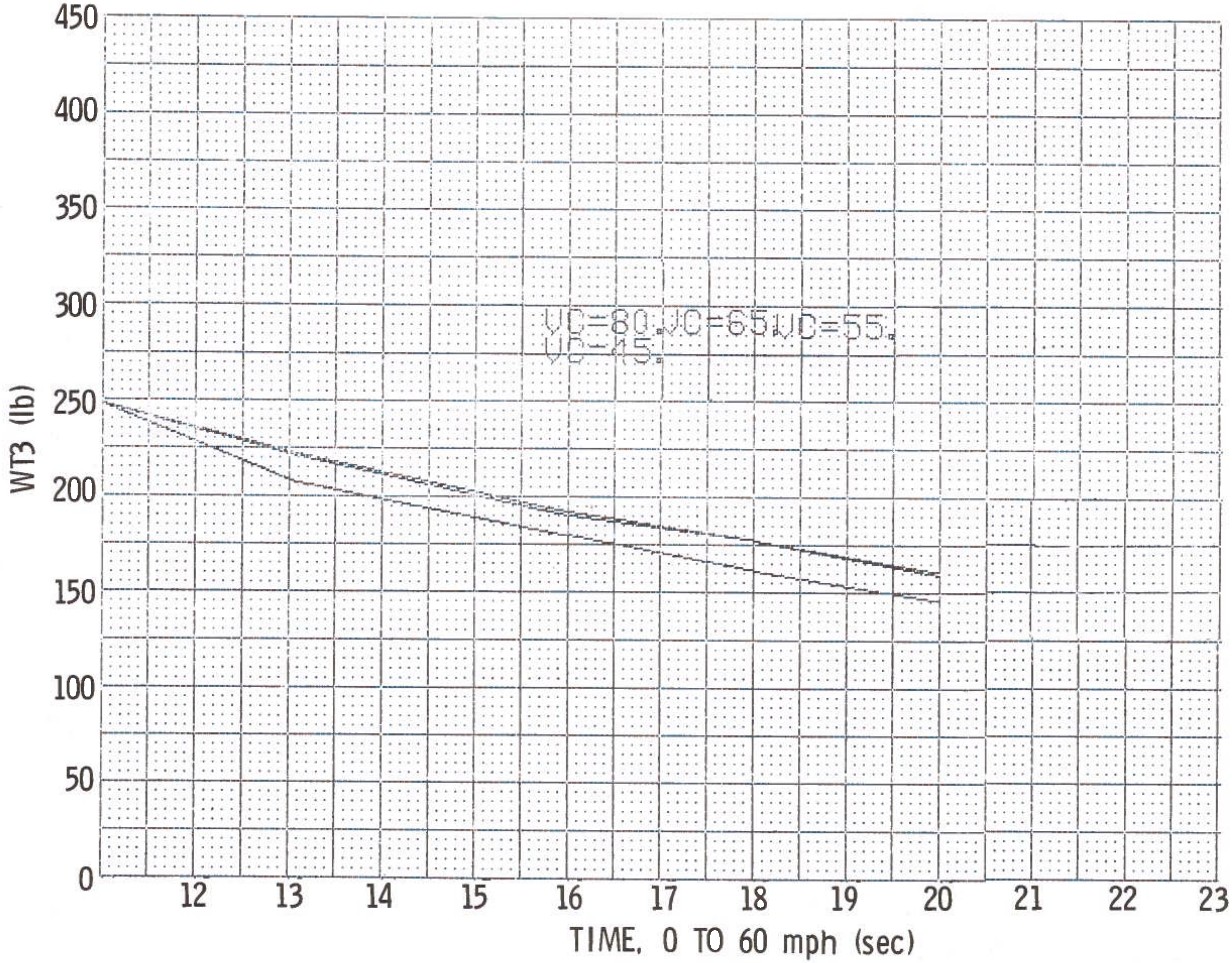

FIGURE 9-42. WEIGHT OF TRANSMISSION LINKING FLYWHEEL TO VEHICLE DRIVE

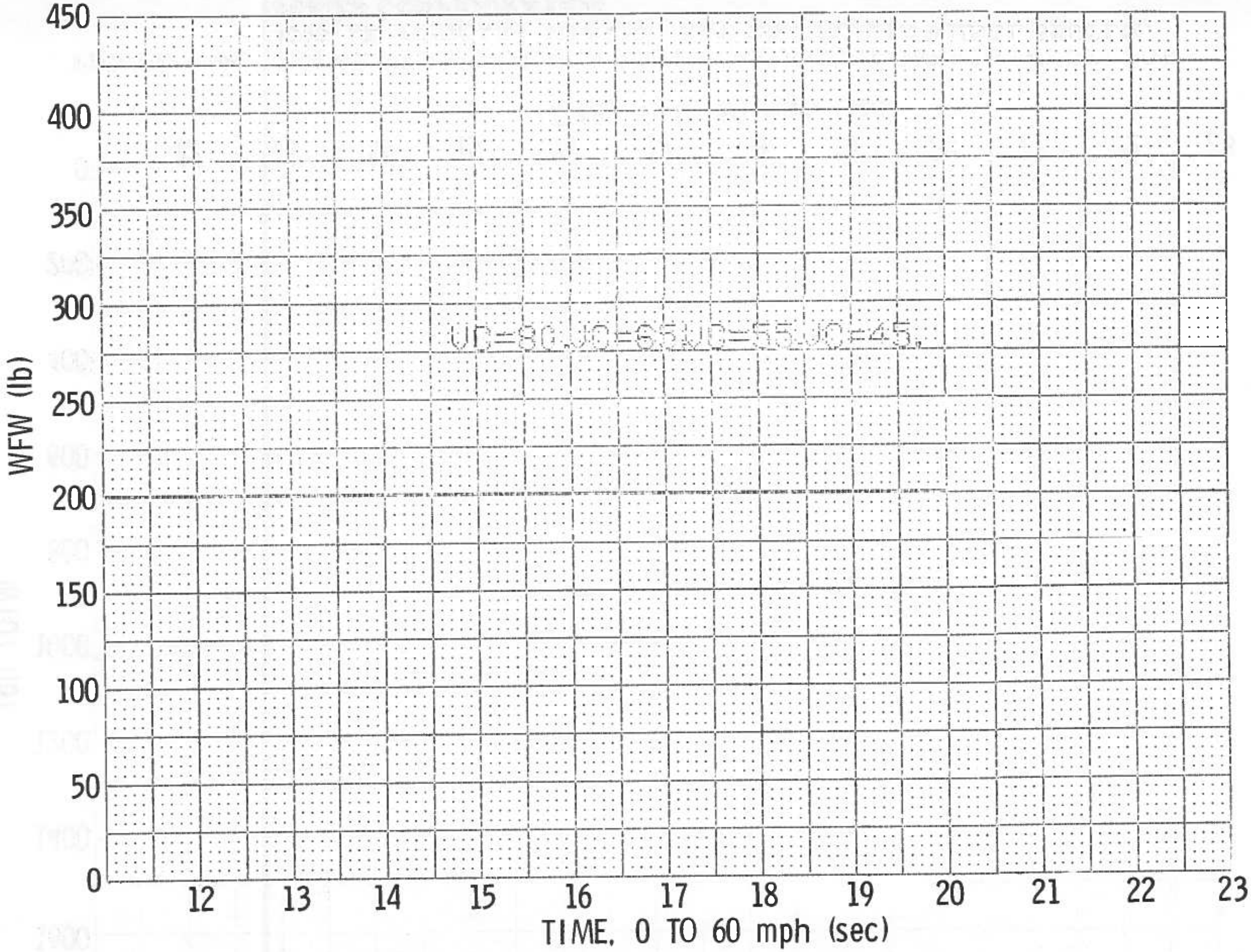

FIGURE 9-43. WEIGHT OF FLYWHEEL SYSTEM (WFW) FOR 4000-LB VEHICLE: HYBRID HEAT ENGINE/FLYWHEEL SYSTEM, SERIES CONFIGURATION

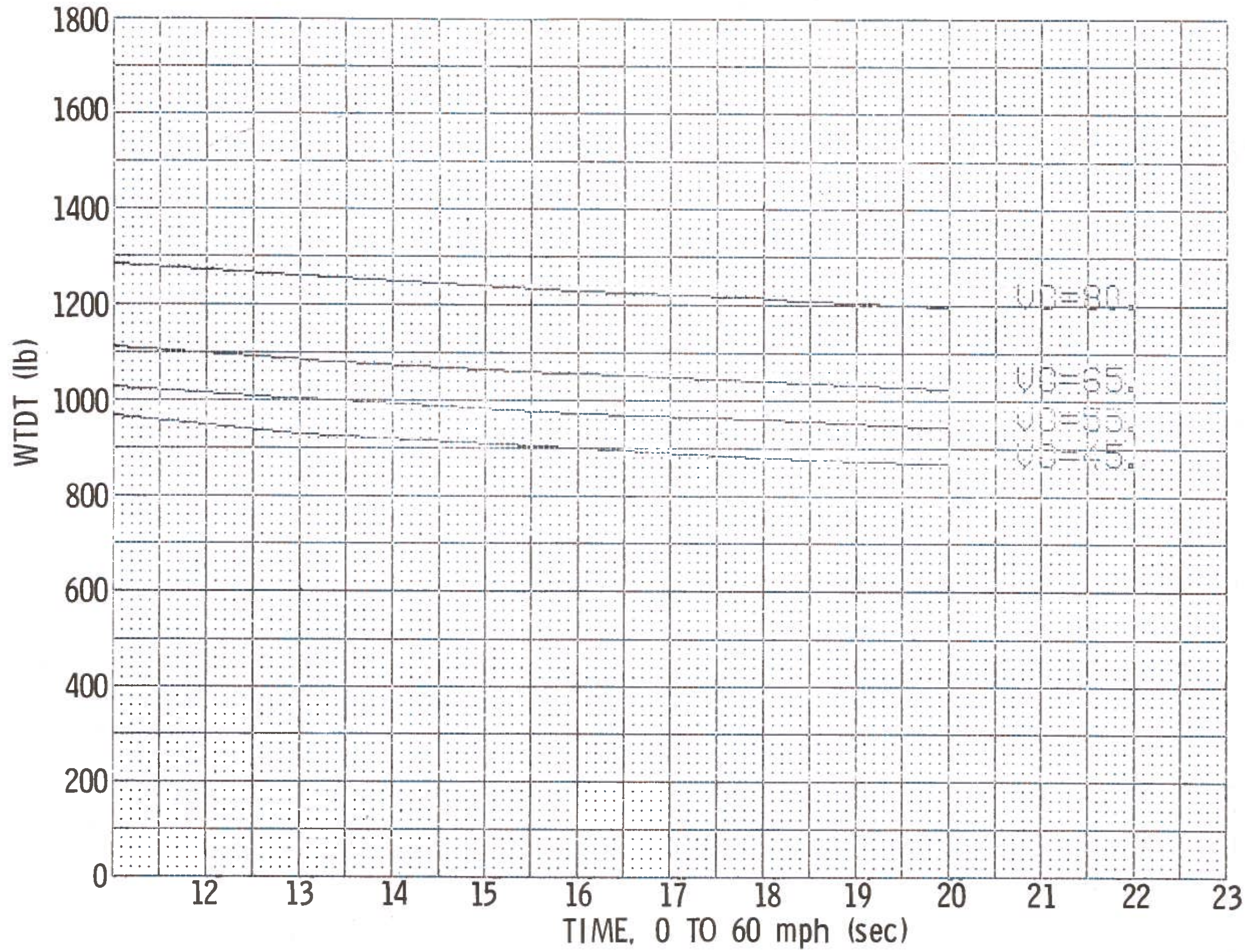

FIGURE 9-44. TOTAL WEIGHT OF ALL POWERTRAIN COMPONENTS (WTDT) FOR 4000-LB VEHICLE: HYBRID HEAT ENGINE/FLYWHEEL SYSTEM, SERIES CONFIGURATION

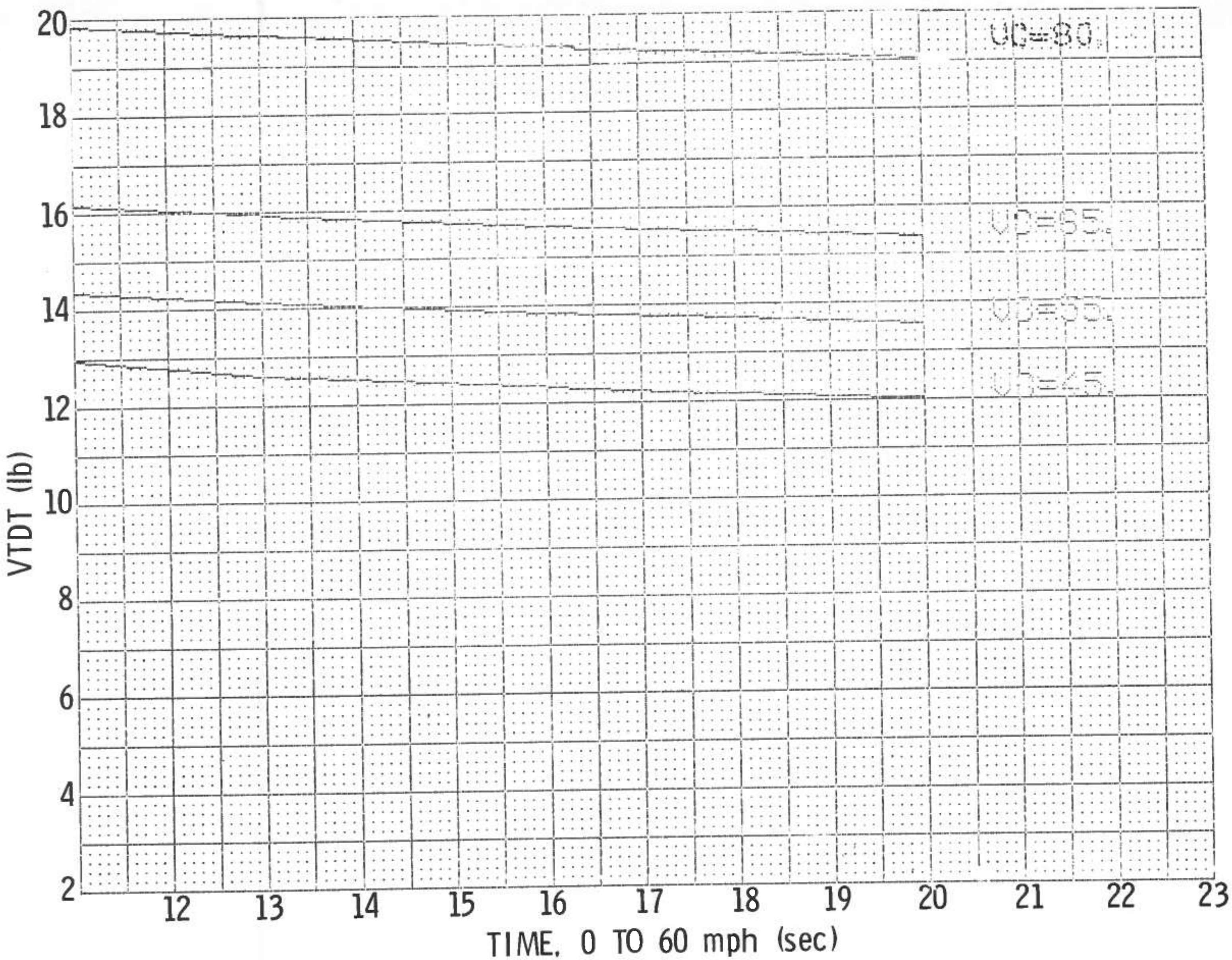

FIGURE 9-45. TOTAL VOLUME OF ALL POWERTRAIN COMPONENTS (VTDT) FOR 4000-LB VEHICLE: HYBRID HEAT ENGINE/FLYWHEEL SYSTEM, SERIES CONFIGURATION